

# RESEARCH PERFORMANCE FINAL TECHNICAL REPORT

Submitted to:

**US Department of Energy  
Office of Energy Efficiency and Renewable Energy  
Advanced Manufacturing Office**

Award no:

**DE-EE00008412**

Project title:

**Converter-Interfaced CHP Plant for Improved Grid-  
Integration, Flexibility and Resiliency**

Principal Investigator:

**Dr. Ibrahima Ndiaye**

Technology Manager,  
GE Research

One Research Circle, Niskayuna NY 12309

Email: [ndiaye@ge.com](mailto:ndiaye@ge.com), Phone: 518-387-6796

Submission date:

**August 2, 2022**

DUNS number:

**086188401**

Recipient organizations:

**GE Research**

One Research Circle, Niskayuna, NY 12309

Project performance period:

**10/1/2018 through 5/31/2021**

Reporting period:

**10/1/2018 to 5/31/2021**

Report Term:

**Final**

DOE Project Team:

Program Manager: **Bob Gemmer**

Technical Project Officer: **John Tabacchi**

Contract Specialist: **Carla Winaught**

Contracting Officer: **Susan Miltenberger**

**Acknowledgement:** "This material is based upon work supported by the Department of Energy under Award Number DE-EE00008412"

**Disclaimer:** "This report was prepared as an account of work sponsored by an agency of the United States Government. Neither the United States Government nor any agency thereof, nor any of their employees, makes any warranty, express or implied, or assumes any legal liability or responsibility for the accuracy, completeness, or usefulness of any information, apparatus, product, or process disclosed, or represents that its use would not infringe privately owned rights. Reference herein to any specific commercial product, process, or service by trade name, trademark, manufacturer, or otherwise does not necessarily constitute or imply its endorsement, recommendation, or favoring by the United States Government or any agency thereof. The views and opinions of authors expressed herein do not necessarily state or reflect those of the United States Government or any agency thereof."

## Table of Contents

<b>EXECUTIVE SUMMARY</b>	10
<b>1. INTRODUCTION</b>	12
<b>1.1 Project objectives</b>	13
<b>1.2 Anticipated results and benefits</b>	13
<b>2. THE CONCEPT OF CONVERTER-INTERFACED CHP</b>	14
<b>3. TECHNICAL FEASIBILITY AND SPECIFICATIONS OF CONVERTER-INTERFACED CHP</b>	16
<b>3.1 Technical evaluation of potential solutions for the interface converter design</b>	18
<b>3.1.1 Harmonics analysis</b>	19
<b>3.1.2 Cost trade-off analysis of the interface converter</b>	23
<b>3.1.3 Stability assessment of the back-to-back VSC system</b>	24
<b>3.2 Review of distributed energy resources (DER) interconnection standards</b>	25
<b>3.2.1 Steady-state performance requirements</b>	26
<b>3.2.2 Dynamic performance requirements</b>	27
<b>3.2.3 Microgrid operation and controller functions</b>	28
<b>4. ECONOMIC FEASIBILITY ANALYSIS OF CONVERTER-INTERFACED CHP</b>	29
<b>4.1 Analysis of the U.S Technical Potential of CHP</b>	30
<b>4.1.1 Analysis of the population of small to medium sized CHP installed in the U.S.</b>	31
<b>4.1.2 The U.S technical potential of small to medium-sized CHP</b>	36
<b>4.1.3 User cases selected for the feasibility analysis of converter-interfaced CHP</b>	40
<b>4.1.4 Challenges facing the interconnection of CHP systems in the distribution grid</b>	41
<b>4.1.5 Federal and States incentives for CHPs</b>	43
<b>4.2 Evaluation of the economic benefits of interface converter for CHP coupling</b>	45
<b>4.2.1 Return of Investment (ROI) calculations for CHP applications</b>	45
<b>4.2.2 Time-series simulations for the evaluation of revenue generation of CHP plants</b>	48
<b>4.2.3 Results of the ROI calculations for the different user cases</b>	53
<b>4.3 Sensitivity analysis on the ROI of converter-interfaced CHP</b>	57
<b>4.3.1 Automatic toolkit for CHP ROI evaluation</b>	58
<b>4.3.2 Approach for the sensitivity analysis</b>	58
<b>4.3.3 Impact of the CHP sizing scenario</b>	61
<b>4.3.4 Evaluation of the most critical parameters impacting the economic feasibility of converter-interfaced CHP</b>	63
<b>4.4 Analysis of the U.S Technical Potential of converter-interfaced CHP</b>	68
<b>4.4.1 Basic comparison model</b>	69

<b>4.4.2 Comparison model with MVA demand charge .....</b>	74
<b>4.4.3 Estimation of the U.S technical potential of converter-interfaced CHP .....</b>	77
<b>4.5 Evaluation of the economic benefits of converter-interfaced CHP combined with battery energy system (BESS) .....</b>	81
<b>4.6 Evaluation of CHP coupled with BESS and solar photovoltaic (PV) system .....</b>	86
<b>5. DEVELOPMENT AND VALIDATION OF THE CONVERTER-INTERFACED CHP CONTROLS PLATFORM .....</b>	88
<b>5.1 Grid integration study of converter-interfaced CHP plants.....</b>	88
<b>5.1.1 Details of the system model .....</b>	89
<b>5.1.2 Results of the grid integration study.....</b>	93
<b>5.2 Development of the hardware-in-the-loop simulation platform .....</b>	97
<b>5.2.1 Performance objectives of the HIL simulations .....</b>	101
<b>5.2.2 Validation of the converter-interfaced CHP RTDS model .....</b>	104
<b>5.3 Validation of the control performance of converter-interfaced CHP .....</b>	109
<b>6. VALIDATION OF THE PERFORMANCE OF CONVERTER-INTERFACED CHP .....</b>	114
<b>6.1 Power hardware-in-the-loop test setup.....</b>	114
<b>6.1.1 Development of the PHIL testbed communication architecture .....</b>	116
<b>6.1.2 Validation of the functionality of the PHIL testbed.....</b>	120
<b>6.2 Power hardware test performance objectives .....</b>	124
<b>6.3 Performance validation test results .....</b>	127
<b>7. CONCLUSION.....</b>	134
<b>8. CERTIFICATE OF COMPLIANCE .....</b>	136

## List of Figures

<b>Figure 1:</b> Converter-interfaced CHP.....	14
<b>Figure 2:</b> Block-diagram of a converter-interfaced CHP system .....	16
<b>Figure 3:</b> Circuit and control block diagrams of the grid-side inverter.....	18
<b>Figure 4:</b> Time-domain waveforms(upper) and frequency-domain spectrum (lower) of generator output voltage and current with 6-pulse diode rectifier.....	20
<b>Figure 5:</b> Time-domain waveforms(upper) and frequency-domain spectrum (lower) of generator output voltage and current with 12-pulse diode rectifier.....	21
<b>Figure 6:</b> Time-domain waveforms(upper) and frequency-domain spectrum (lower) of generator output voltage and current with 6-pulse diode rectifier and active harmonic filter .....	22
<b>Figure 7:</b> Time-domain waveforms(upper) and frequency-domain spectrum (lower) of generator output voltage and current with VSC rectifier.....	22
<b>Figure 8:</b> Schematics of directly-coupled and converter-interfaced CHP .....	23
<b>Figure 9:</b> Small-signal impedance representation of VSC back-to-back system. ....	24
<b>Figure 10:</b> Impedance responses of grid side inverter $Z_{inv}(s)$ and generator side rectifier $Z_{rec}(s)$ . Solid lines: $Z_{inv}(s)$ ; dashed lines: $Z_{rec}(s)$ with slow AVR; dot-dashed lines: $Z_{rec}(s)$ with fast AVR	25
<b>Figure 11:</b> Time-domain responses of dc link bus voltage when the active power command steps from 1.6 MW to 2.0 MW. Dashed lines: dc voltage with slow AVR; dot-dashed lines: dc voltage with fast AVR. ....	25
<b>Figure 12:</b> Comparison of minimum reactive power requirements for Categories A and B DER. ....	26
<b>Figure 13:</b> Decision-tree for steady-state performance category assignment of DER .....	26
<b>Figure 14:</b> Transient performance category assignment for DER .....	27
<b>Figure 15:</b> Comparison of category I and II transient performance requirements.....	28
<b>Figure 16:</b> Minimum functional requirements of microgrid controllers.....	29
<b>Figure 17:</b> Geographic distribution of the small to medium-sized CHP in the U.S.....	32
<b>Figure 18:</b> Distribution of the small to medium-sized CHP in the U.S per state.....	32
<b>Figure 19:</b> Small to medium-sized CHP installed capacity by state .....	33
<b>Figure 20:</b> Distribution of the small to medium-sized CHP in the U.S per MW size .....	33
<b>Figure 21:</b> Distribution of the small to medium-sized CHP across the U.S by application .....	34
<b>Figure 22:</b> Repartition of small to medium-sized CHP applications by installed capacity .....	34
<b>Figure 23:</b> Repartition of prime movers used in small to medium-sized CHP U.S installations..	35
<b>Figure 24:</b> Distribution of the small to medium-sized technical potential CHP by state capacity	36
<b>Figure 25:</b> Distribution of the technical potential of small to medium-sized CHP for industrial applications in California .....	37
<b>Figure 26:</b> Distribution of the technical potential of small to medium-sized CHP for commercial applications in California .....	37
<b>Figure 27:</b> Distribution of the technical potential of small to medium-sized CHP for industrial applications in Texas.....	37
<b>Figure 28:</b> Distribution of the technical potential of small to medium-sized CHP for commercial applications in Texas.....	38
<b>Figure 29:</b> Distribution of the technical potential of small to medium-sized CHP for industrial applications in New York.....	38
<b>Figure 30:</b> Distribution of the technical potential of small to medium-sized CHP for commercial applications in New York.....	38

<b>Figure 31:</b> Distribution of the technical potential of small to medium-sized CHP for industrial applications in Pennsylvania.....	39
<b>Figure 32:</b> Distribution of the technical potential of small to medium-sized CHP for commercial applications in Pennsylvania.....	39
<b>Figure 33:</b> Distribution of the technical potential of small to medium-sized CHP for industrial applications in Illinois.....	39
<b>Figure 34:</b> Distribution of the technical potential of small to medium-sized CHP for commercial applications in Illinois.....	40
<b>Figure 35:</b> Typical interconnection process of DER.....	41
<b>Figure 36:</b> Typical interconnection equipment required for DER (National Grid).....	42
<b>Figure 37:</b> Proforma calculation of yearly net cash flow of CHP investment.....	46
<b>Figure 38:</b> Summary of the approach for the evaluation of the economic performance of CHP systems.....	48
<b>Figure 39:</b> Operating regions of a CHP system used as DER .....	49
<b>Figure 40:</b> Fact sheet of a college user case in CAISO .....	54
<b>Figure 41:</b> Fact sheet of a water reclamation plant user case in ERCOT.....	55
<b>Figure 42:</b> Fact sheet of a large office building user case in ERCOT .....	55
<b>Figure 43:</b> Fact sheet of a hotel user case in MISO .....	56
<b>Figure 44:</b> Automated simulation toolkit for CHP ROI evaluation.....	58
<b>Figure 45:</b> Power to thermal loads ratio in the investigated user cases.....	59
<b>Figure 46:</b> Box plot for hourly LMP in different ISO territories (2018 data).....	60
<b>Figure 47:</b> $\Delta ROI$ for each use case by different CHP sizing scenarios .....	62
<b>Figure 48:</b> Converter-interfaced CHP winning rate by location, application and user case .....	68
<b>Figure 49:</b> Cost of generator and interconnection for CHP applications.....	72
<b>Figure 50:</b> Portrait of the U.S technical potential of industrial converter-interfaced CHP.....	77
<b>Figure 51:</b> Portrait of the U.S technical potential of commercial converter-interfaced CHP.....	77
<b>Figure 52:</b> Nationwide technical potential of converter-interfaced CHP ranging from 1MWe to 5MWe.....	78
<b>Figure 53:</b> Nationwide technical potential of converter-interfaced CHP ranging from 5MWe to 20MWe .....	78
<b>Figure 54:</b> Estimation of U.S technical potential sites favorable to the converter-interfaced solution .....	80
<b>Figure 55:</b> Estimation of U.S technical potential sites favorable to the converter-interfaced solution if MVA demand charge applies .....	81
<b>Figure 56:</b> System architecture of BESS combined with converter-interfaced CHP .....	82
<b>Figure 57:</b> ROI of converter-interfaced CHP coupled with BESS for a hospital case in CAISO: BESS installed cost 400\$/kWh .....	84
<b>Figure 58:</b> ROI of converter-interfaced CHP coupled with BESS for a water reclamation plant case in CAISO: BESS installed cost 400\$/kWh.....	85
<b>Figure 59:</b> ROI of converter-interfaced CHP coupled with BESS for a hospital case in CAISO: BESS installed cost 250\$/kWh .....	85
<b>Figure 60:</b> ROI of converter-interfaced CHP coupled with BESS for a water reclamation plant case in CAISO: BESS installed cost 250\$/kWh.....	86
<b>Figure 61:</b> Architecture of a hybrid CHP system with PV and BESS coupling .....	86
<b>Figure 62:</b> ROI evaluation of hybrid CHP using the hospital in CAISO user case .....	87
<b>Figure 63:</b> One-line diagram of the system for grid integration studies .....	89

<b>Figure 64:</b> Different interconnection scenarios for grid-tied CHP system .....	89
<b>Figure 65:</b> Power factor control logic of the AVR .....	90
<b>Figure 66:</b> Governor and engine controls .....	91
<b>Figure 67:</b> Diagram of the interface converter with its control loops .....	92
<b>Figure 68:</b> Power factor at the POI with directly-coupled CHP .....	95
<b>Figure 69:</b> Power factor at the POI with converter-interfaced CHP .....	96
<b>Figure 70:</b> Conceptual diagram of the simulated microgrid with converter-interfaced CHP .....	98
<b>Figure 71:</b> Functional blocks of the converter-interfaced CHP system built in the hardware-in-the-loop (HIL) simulation platform .....	98
<b>Figure 72:</b> Specifications of the Jenbacher engine used as reference for the engine emulator and for the relationship between power and heat .....	99
<b>Figure 73:</b> One-line diagram of the simulation model built in RTDS .....	99
<b>Figure 74:</b> Example of the GE's C90+ communication with IEC61850/GOOSE messaging .....	100
<b>Figure 75:</b> Overview of the RTDS model of the CHP system implemented with the interface converter .....	104
<b>Figure 76:</b> Overview of the protection logic implemented with the CHP system .....	105
<b>Figure 77:</b> Validation of the voltage and frequency ride-through settings .....	106
<b>Figure 78:</b> Simulation results of the integrated converter-interfaced CHP .....	107
<b>Figure 79:</b> Validation of the communication of the HIL simulation platform .....	108
<b>Figure 80:</b> An overview of the C90+ logic editor for algorithms implementation .....	108
<b>Figure 81:</b> Summary of the voltage ride-through simulation results for the converter-interfaced CHP (category II DER per IEEE 1547-2018) .....	109
<b>Figure 82:</b> Summary of the frequency ride-through simulation results for the converter-interfaced CHP (category II DER per IEEE 1547-2018) .....	110
<b>Figure 83:</b> Simulation results for transition from grid-tie mode to island .....	111
<b>Figure 84:</b> Simulation results for reconnection to utility grid .....	112
<b>Figure 85:</b> Simulation results for active power dispatch with increase of grid-export .....	112
<b>Figure 86:</b> Simulation results for power factor control at PCC .....	113
<b>Figure 87:</b> Simulation results for temporary L-G fault inside the plant .....	113
<b>Figure 88:</b> Simulation results for black-start in islanding operation .....	114
<b>Figure 89:</b> Schematic diagram of the power hardware-in-the loop (PHIL) testbed .....	115
<b>Figure 90:</b> Single Line Diagram of the test layout .....	115
<b>Figure 91:</b> Installation of the two GE Brilliance inverters used as back-to-back VSC for the validation of the performance of the converter-interfaced CHP .....	116
<b>Figure 92:</b> Control and communication architecture of the PHIL testbed .....	116
<b>Figure 93:</b> Load meter <--> RTDS <--> Microgrid controller .....	117
<b>Figure 94:</b> Requests intervals during communication RTDS and Brilliance controllers .....	118
<b>Figure 95:</b> Test results of the communication between RTDS and the Brilliance controller .....	119
<b>Figure 96:</b> Evaluation of the impact of the communication delay between the Brilliance controller and RTDS .....	119
<b>Figure 97:</b> Fully installed and configured PHIL testbed .....	120
<b>Figure 98:</b> Details of the engine emulator model as implemented in the RTDS Novacor rack .....	120
<b>Figure 99:</b> Confirmation of the inverters readiness to operate .....	121
<b>Figure 100:</b> Steady-state operation following a power step change from 24kW to 48kW .....	121
<b>Figure 101:</b> Algorithms implemented for the power and heat dispatch .....	122
<b>Figure 102:</b> Algorithms implemented for the power factor control .....	123

<b>Figure 103:</b> Tests results on the performance of the dispatch algorithms.....	123
<b>Figure 104:</b> Snapshot of electric facilities loads measurement collected by the microgrid controller.....	126
<b>Figure 105:</b> Planned disconnection at 250kW.....	128
<b>Figure 106:</b> Transients captured at the Brilliance inverter control interface during a 250kW planned disconnection.....	128
<b>Figure 107:</b> Emergency disconnection at 250kW.....	129
<b>Figure 108:</b> Transients captured at the converter during 250kW emergency disconnection....	129
<b>Figure 109:</b> Reconnection and power ramp up at 1000kW/min. ....	130
<b>Figure 110:</b> Voltage regulation at point of interconnection (building main breaker). .....	130
<b>Figure 111:</b> Power following dispatch while a pf = 1 is maintained at POC (inverter).....	131
<b>Figure 112:</b> Power following dispatch while a pf = 0.9 is maintained at POC (inverter).....	132
<b>Figure 113:</b> Heat following dispatch while a pf = 1 is maintained at POC (inverter).....	132
<b>Figure 114:</b> Varying command between heat and electric load following.....	133

## List of Tables

<b>Table 1:</b> Parameters of the baseline generator for the harmonic evaluation .....	19
<b>Table 2:</b> Current Distortion Limits for system rated 120 V Through 69 kV and $I_{sc}/IL < 20$ .....	20
<b>Table 3:</b> Electrical System Cost Analysis of Four Different Rectifier Units .....	23
<b>Table 4:</b> Repartition of system sizes in leading small to medium-sized CHP applications.....	35
<b>Table 5:</b> Selected five user cases for the economic feasibility analysis .....	40
<b>Table 6:</b> Federal government clean energy program.....	43
<b>Table 7:</b> State incentives for CHP Systems.....	44
<b>Table 8:</b> Financial parameters for the ROI calculations .....	46
<b>Table 9:</b> Capex and Opex parameters .....	47
<b>Table 10:</b> Summary CHP eligibility for ancillary services in different ISO territories .....	48
<b>Table 11:</b> Results of the timeseries simulations and ROI calculations for the hospital in NYISO .....	54
<b>Table 12:</b> Summary of the factsheets of the CAISO, ERCOT, PJM and MISO user cases .....	56
<b>Table 13:</b> Summary of the ROI results for the five user cases analyzed .....	56
<b>Table 14:</b> Parameter settings for the baseline case.....	60
<b>Table 15:</b> ROI evaluation results for the extended 25 user cases .....	61
<b>Table 16:</b> ROI evaluation results ("AvrgElec") .....	61
<b>Table 17:</b> ROI evaluation results ("PeakElec") .....	62
<b>Table 18:</b> Critical parameters and varying scenarios .....	63
<b>Table 19:</b> Impact of critical parameters on the profitability of converter-interfaced CHP .....	64
<b>Table 20:</b> Example of the water reclamation user case in NYISO .....	65
<b>Table 21:</b> Example of the water reclamation user case in ERCOT .....	66
<b>Table 22:</b> Known parameters for the U.S technical potential estimation.....	70
<b>Table 23:</b> Average cost of electricity and price for reactive power in different ISO .....	71
<b>Table 24:</b> CHP interconnection costs as function of the generator size .....	72
<b>Table 25:</b> New York state industrial and commercial technical potential for CHP <sup>47</sup> .....	73
<b>Table 26:</b> Average demand charge across the U.S states .....	76
<b>Table 27:</b> ROI calculations of converter-interfaced CHP combined with BESS .....	83

<b>Table 28:</b> Parameters of the CHP generator for the grid study.....	89
<b>Table 29:</b> Typical distribution feeder configuration in the U.S.....	91
<b>Table 30:</b> Different grid strengths at POI as function of the feeder length .....	91
<b>Table 31:</b> Selected ride-through settings for the grid integration study .....	92
<b>Table 32:</b> Fault simulation results for the directly-coupled CHP .....	93
<b>Table 33:</b> Fault simulation results for the converter-interfaced CHP .....	93
<b>Table 34:</b> Simulated CHP loading levels.....	94
<b>Table 35:</b> Power output of directly-coupled CHP in PV mode.....	95
<b>Table 36:</b> Power output of the converter-interfaced CHP with pf control .....	96
<b>Table 37:</b> Results of transient simulations in islanding .....	97
<b>Table 38:</b> Performance objectives of the microgrid controller and integrated control system of converter-interfaced CHP .....	101
<b>Table 39:</b> DER synchronization parameters as per IEEE Std 1547-2018.....	103
<b>Table 40:</b> Technical data of the ~1MW generator used as a reference for the generator model .....	105
<b>Table 41:</b> Summary of the HIL simulation results.....	110
<b>Table 42:</b> Summary results of the dispatch and pf control algorithms testing .....	124
<b>Table 43:</b> Performance objectives of converter-interfaced CHP testbed .....	124
<b>Table 44:</b> Summary of the PHIL tests results .....	127

## EXECUTIVE SUMMARY

GE Research and its partner GE Renewables have proposed the use of an interface converter as a solution to increase the penetration of small to medium-sized CHP (1MWe to 20MWe) into distribution grids and improve their flexibility and grid support capability. Indeed, the proposed interface converter solution thanks to the presence of the grid-side inverter, allows to streamline the compliance to grid codes requirements, and reduce the costs and delays of interconnection, which ultimately lowers one of the main barriers for CHP adoption by commercial and industrial facilities. An additional benefit provided by the interface converter is the use of the grid-ready inverter for reactive power which eliminates the need of sizing the generator for that capability. The reduction of the generator size and interconnection costs and delays highly favor the economic feasibility of converter-interfaced CHP.

Five user cases, each in one of the leading U.S states for CHP potential reported by the DOE, were selected to compare the economic performances of converter-interfaced CHP relative to directly-coupled. They include a college campus in California, a hospital in New York, a water reclamation plant in Texas, a hotel in Minnesota, and a large office building in Pennsylvania. Results showed that, the presence of the interface converter allows to increase the return on investment (ROI) by 0.5 to 2 percentage points in most of the cases (4 of 5). Indeed, by shortening the interconnection process the interface converter allows to accelerate revenues while reducing interconnection costs. Added to the reduced cost of the required generator these savings trade in favorably the capital cost of the converter. The analysis also showed that the profitability of the converter-interfaced CHP is highly sensitive to some parameters including the energy price, interconnection delay, and converter cost. However, it appears that if the interface converter can shorten the interconnection process by at least 6 months, this solution will be more economically viable than directly-coupled configuration in almost all the +23,000 potential CHP sites forecasted in the DOE's U.S Technical Potential CHP. The evaluation of the benefits of a converter-interfaced CHP also showed that it enables higher ROI when coupled with other distributed energy resources (DER) such as battery energy systems (BESS) or solar photovoltaic (PV). Indeed, in those scenario, the grid-ready inverter included in the interface converter eliminates the need of separate inverters if DC-coupling is used.

On the technical performance, it has been verified that the presence of the interface converter allows to reduce by 70% to 80% the CHP short-circuit contribution to grid faults. This not only reduces the mechanical and thermal stresses exposed to the CHP electrical components but also increases the grid hosting capacity which ultimately enables higher penetrations CHP. Another key benefit of the interface converter validated with control and power hardware-in-the-loop testing is its superior capability for reactive power support. Indeed, using a power hardware testbed with two +700kW inverters configured in back-to-back, a microgrid controller and actual facilities loads, it was demonstrated that

the presence of the interface converter can help maintain a power factor of  $\sim 1$  or regulate the voltage to  $\sim 1.0\text{pu}$  at the point of common coupling. This benefit can be highly valuable if in the future, due to higher penetration of renewable distributed energy resources (DER), utilities start billing demand charge based on kVA instead of kW as currently. It was also validated that converter-interfaced CHP can dispatch heat and power commands and seamlessly switch between the two modes while consistently controlling the power factor or voltage at PCC. Indeed, the power hardware testing showed that grid-connected converter-interfaced CHP can follow either the power or heat demand while maintaining a unity power factor at the converter output.

This research proved that the adoption of an interface converter as the solution for interconnection of CHP systems into the distribution grid can greatly improve the economic feasibility of small to medium-sized CHP as well as the plant power quality, flexibility and resiliency. Additionally, it allows increased penetrations of CHP into the distribution grid, extends their grid support capability, and facilitates the integration of BESS and solar photovoltaic (PV) DER by streamlining their collocation within the same facilities. This ultimately provides an opportunity for commercial and small industrial facilities in the U.S to accelerate their energy transition thanks to the high energy efficiency of CHP systems and its reliable, flexible, and resilient microgrid operation when interconnected with an interface converter.

## 1. INTRODUCTION

Combined Heat and Power (CHP) plants are one of the most efficient ways to produce heat and electricity. The technology can achieve an overall energy efficiency greater than 90% and yield energy savings ranging between 15% and 40% when compared to separate supply of electricity and heat<sup>1</sup>. However, the unmatched efficiency claimed by the industry and reduced energy footprint advocates is only possible if the heat is directly used or stored for later dispatch. To generate heat, which is a byproduct of the electricity production, the engine needs to be in operation. Thus, the higher the utilization, the better are the energy savings for the facility. CHP plant owners have therefore a vested interest to continuously generate electric power, either for local use or for export into the grid. To maximize the utilization of the CHP engine and improve the economic feasibility of small- and medium-sized CHP plants, innovative ways to maintain high production rates of electricity that do not rely on the hosting facility load demand are critical.

Combined heat and power (CHP) systems have been used by the industry for decades. While large CHP systems i.e., greater than 20MWe, so-called cogeneration plants, are well adopted and proven to be cost-effective, small- to medium-sized CHP penetration in the distribution lags far behind<sup>2</sup>. One of the reasons highlighted are the high initial cost and the lengthy interconnection process involved in meeting the utility grid code requirements<sup>3</sup>. Although, the technical advancement in reciprocating gas engines have reduced costs and emissions to the level where small- to medium-sized CHP systems have become very competitive in many applications<sup>4</sup>, the complexity of grid integration procedures and associated costs have continued to prevent the potential emergence of small- to medium-sized commercial and industrial CHP systems in a manner that achieves full economic value for the facility, while improving power quality and providing grid support services<sup>2</sup>. Indeed, these CHP systems typically interconnect at distribution voltage levels and therefore are subject to interconnection standards for distributed energy resources (DER) such as IEEE 1547<sup>5</sup> and IEEE 2030.7<sup>6</sup>. This difficulty can be resolved by introducing a power electronics interface between the generator and the distribution system. The fast and flexible control of grid-side voltage source converters (VSC) will help the conventional CHP

---

<sup>1</sup> Power Mag; “Gaining steam: Combined Heat and Power. Available online <https://www.powermag.com/gaining-steam-combined-heat-and-power/>

<sup>2</sup> DOE, “CHP Technical Potential in the United States”, March 2016. Available online: <https://www.energy.gov/sites/default/files/2016/04/f30/CHP%20Technical%20Potential%20Study%203-31-2016%20Final.pdf>

<sup>3</sup> DOE, “CHP Financing Primer”, June 2017: Available online [https://betterbuildingssolutioncenter.energy.gov/sites/default/files/attachments/CHP\\_Financing\\_Primer.pdf](https://betterbuildingssolutioncenter.energy.gov/sites/default/files/attachments/CHP_Financing_Primer.pdf)

<sup>4</sup> U.S. Department of Energy, Office of Energy Efficiency and Renewable Energy –Flexible Combined Heat and Power for Grid Reliability and Resiliency. Available online: <https://eere-exchange.energy.gov/Default.aspx?Search=621&SearchType#Foald584ea317-c588-4b85-bf33-6d21e94f1464>

<sup>5</sup> IEEE 1547-2018 - IEEE Standard for Interconnection and Interoperability of Distributed Energy Resources with Associated Electric Power Systems Interfaces <https://standards.ieee.org/standard/1547-2018.html>

<sup>6</sup> IEEE 2030.7-2017 - IEEE Standard for the Specification of Microgrid Controllers [https://standards.ieee.org/standard/2030\\_7-2017.html](https://standards.ieee.org/standard/2030_7-2017.html)

generators to meet different grid codes and to be adaptive to stricter requirements. This can shorten the interconnection process which contributes to de-risking the economic viability.

### **1.1 Project objectives**

The overall objective of the project is to develop and validate a cost-effective interface converter that will allow to streamline the interconnection of small-to medium sized CHP plants into utility distribution grids. This includes: 1) specification and design of an interface converter for +1MWe CHP applications with a total installed cost <\$1600/kWe; 2) demonstration of the economic feasibility of small to medium-sized converter-interfaced CHP (1MWe to 20MWe) as compared to conventional directly-coupled CHP; 3) the validation of the control performance of converter-interfaced CHP for compliance with IEEE standards 1547<sup>5</sup>, IEEE 2030.7<sup>6</sup>; and 4) the demonstration of the grid benefits of converter-interfaced CHP through system simulations and power hardware testing.

Section 2 describes in more details the concept of interface converter for CHP and Section 3 provides the technical specifications guidelines for sizing the converter-interfaced CHP components. In section 4 the U.S Technical Potential of CHP is analyzed to specify five user cases for the economic feasibility evaluation of the converter-interfaced CHP. The five user cases include one typical CHP application in each of the five leading grid interconnection territories for total capacity of CHP potential. This section also details the sensitivity analysis performed on Return on Investment (ROI) of converter-interfaced CHP as well as an estimation of the US Technical Potential of converter-interfaced CHP and the economic feasibility for CHP coupled with battery energy systems (BESS) or solar photovoltaic (PV) DER. Section 5 presents the development of the control platform and its validation using hardware-in-the-loop (HIL) simulations while Section 6 details the system performance validation tests using power hardware equipment and facilities live data. Section 7 closes the report with summary of the conclusions and findings.

### **1.2 Anticipated results and benefits**

The proposed technology allows to streamline the interconnection process of small-to medium sized CHP plants by reducing the barrier for compliance to grid codes and interconnection standards which in turn will enable higher return of investment (ROI) by reducing interconnection costs, delays, and loss of production. Furthermore, the presence of the interface converter will quantifiably improve the power quality and grid-support capability of CHP plants which increase their ability to participate in different energy markets including ancillary services. This adds new revenue streams that can boost the ROI despite an inevitable increase in Capex due to the converter. However, it is anticipated that an installed cost of \$1600/kWe for the proposed solution is attainable. Ultimately the proposed solution will make CHP more attractive for broader adoption as distributed energy resources (DER) in commercial and industrial applications plants. In addition, the

solution will improve resiliency and reliability for local loads, saving the facility owner considerable expenses and energy production losses.

## 2. THE CONCEPT OF CONVERTER-INTERFACED CHP

Figure 1 shows the schematic of a converter-interfaced CHP in a plant microgrid. Compared to directly-connected CHP, the converter-interfaced CHP, is a CHP connected to the grid through a two-stage converter constituted of a rectifier, the “AC to DC” block and a grid-ready inverter, the “DC to AC” block. The rectifier is responsible of transforming the AC output of the generator into DC for the input of the inverter. The grid-ready inverter is responsible for the power quality at the point of interconnection, mainly the reactive power support for voltage and power factor control. The converter-interfaced CHP also includes an integrated control system which allows coordination between the inverter, the engine, and the generator to optimally dispatch the active and reactive power as well as the recoverable heat both in grid-tied and islanding modes. The microgrid controller also allows to implement the control and protection requirements for the system to meet grid code requirements and grid support services entitlements.

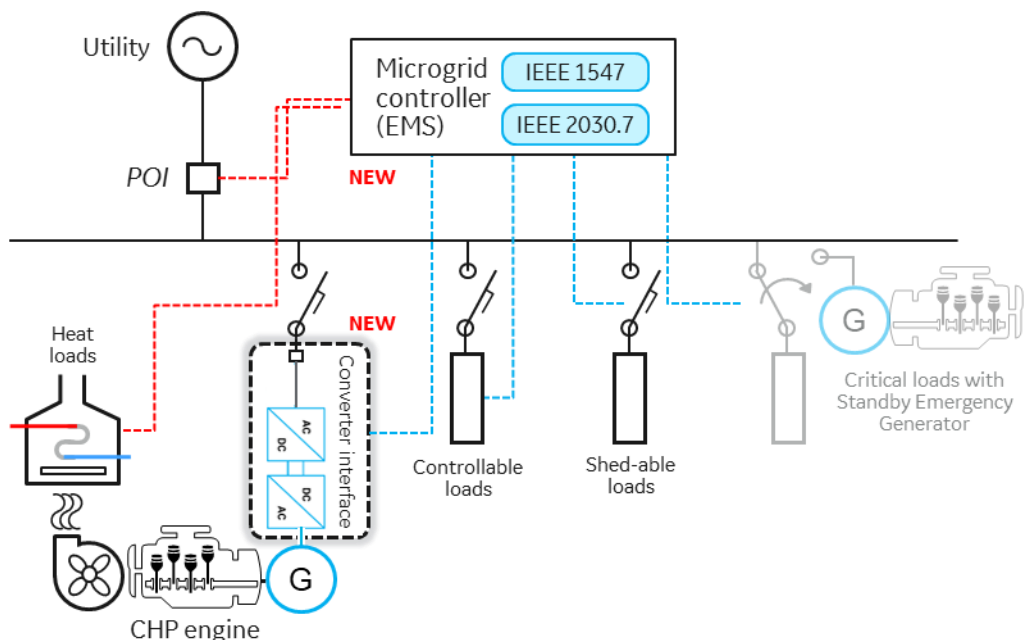


**Figure 1:** Converter-interfaced CHP.

The most salient characteristic of the interface converter is it allows to effectively decouple the engine speed and generator voltage from the grid frequency and voltage so that the engine operation and generator voltage are independent from the grid frequency and voltage. This allows to operate or design the engine at any optimal speed but also to reduce the impact of the frequency dynamics which increases the system stability particularly during islanding operation. However, the most direct consequence of the presence of the interface converter for the CHP operation is the decoupling of the active and reactive

power. By enabling that, the generator can operate at unity power factor ( $pf = 1$ ) regardless of the load or the grid condition which improves its efficiency. Indeed, it is known that the higher the load power factor the greater is generators efficiency. Not only decoupling active and reactive power allows the generator efficiency to be improved but also reduces its size, therefore its cost. For instance, the generator which is traditionally designed to operate up to 0.8 power factor at full load in directly-coupled CHP leading to is no longer required to provide reactive power. The grid-ready inverter can now provide such a support with much more flexibility and capability. Therefore, oversizing the generator to 1.25pu of the engine power for operation at non-unity power factor is not necessary. In such a case the generator can remain at 1.0 pu of the engine size which reduces its cost. It is important to note that depending on the size, generator kVA can be very expensive as compared to converter kVA. And hence trading generator capacity for converter can be economically viable and lead to higher return of investment (ROI) as compared to conventional CHP systems<sup>7</sup>. Additionally, unlike in directly-coupled, the converter-interfaced CHP will be able to operate with the full range of power factor in the inductive and capacitive quadrant. This allows to improve potential revenue stream from extended reactive power support.

A critical benefit provided by the interface converter is its impact on the short-circuit contribution of the CHP system. Indeed, connecting a traditional generator of multi-MW rating is challenging because of its potentially significant impact on a distribution circuit operation (load shedding, generator trip) and on the short-circuit current levels. As an example, a single typical reciprocating engine rated at 1.5MWe can generate a continuous short-circuit current of up to 2.7kA at 4.16kV, which may be the same order of magnitude as that of the grid short circuit contribution at the point of common coupling (PCC). Staging engines to reach higher capacity almost linearly increases the short-circuit current, leading to short-circuit levels that can significantly affect neighboring customers to an extent that can require modifications to the utility equipment and protection devices or installation of more sophisticated equipment at the CHP plant. It is important to note that all these modifications will be at the expense of the plant owner. Therefore, such a high short-circuit contribution not only substantially increases the initial investment costs but can also delay the interconnection process to a point that the overall project would not become profitable. Additionally, it can limit the hosting capacity of the grid i.e., the size of parallel generation that the grid can accept at this location. The presence of the interface converter helps overcomes these challenges by making the generator “invisible” to the grid as the inverter short-circuit current is limited to 1.25p.u. of its rated current. Furthermore, the presence of the converter allows a great interchangeability between different CHP generators and the staging of multiple engines while allowing to maintain the short-circuit contribution level of the CHP units at a relatively low level which significantly increases the

---

<sup>7</sup> Xian Guo, Ibrahima Ndiaye, Martin Yan, Ahmed Elasser, Yazhou Jiang, and Hanchao Liu, “Feasibility Analysis of Converter-Interfaced Combined Heat and Power System” 2020 IEEE Power & Energy Society General Meeting <https://ieeexplore.ieee.org/document/9282141>

grid hosting capacity and eventually penetration of the small to medium-sized CHP systems in the distribution grid.

Another critical benefit of the presence of the interface converter is the simplicity if provides to comply to grid code standards. It is important to highlight that as most small and medium sized commercial and industrial facilities typically interconnect to the grid at distribution voltage levels, CHP in those facilities must comply with DER interconnection standards such as UL 1741<sup>8</sup>, IEEE 1547, and IEEE 2030.7<sup>9</sup>. These standards are the minimum requirements in most utility grid codes for DER interconnection and can become difficult for a grid-integrated, line-connected generator to meet, especially in scenarios with high DER penetration<sup>10</sup>. The converter interface with its grid-side inverter will allow to accelerate the interconnection process of the CHP system as most today's commercially available grid-ready inverters are designed with grid support functions and typically comply with DER interconnection standards<sup>11</sup>.

### 3. TECHNICAL FEASIBILITY AND SPECIFICATIONS OF CONVERTER-INTERFACED CHP

Figure 2 depicts the block diagram of a converter-interfaced CHP system. It shows that the interface converter has a two-stage of power conversion. Indeed, instead of connecting the CHP generator directly to the utility grid, the generator AC output is first converted into DC through a rectifier and then back to AC using a grid-ready inverter to connect to grid.

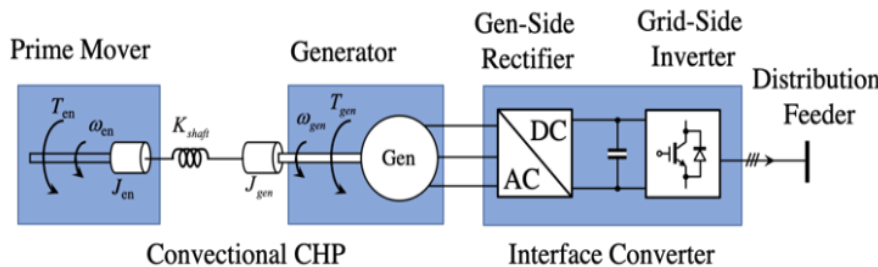


**Figure 2:** Block-diagram of a converter-interfaced CHP system

If for the grid-side inverter a voltage source converter (VSC) design is the only viable option, there are a few options for generator-side rectifier. The harmonics distortion induced by the ac-dc rectification will be one of the major system design considerations. Indeed, the rectifier harmonics determine not only the size of generators but also overall system

<sup>8</sup> UL 1741, UL standard Inverters, Converters, Controllers and Interconnection System Equipment for Use With Distributed Energy Resources <https://standardscatalog.ul.com/ProductDetail.aspx?productId=UL1741>

<sup>9</sup> [https://standards.ieee.org/standard/2030\\_7-2017.html](https://standards.ieee.org/standard/2030_7-2017.html)

<sup>10</sup> PJM Manual for Generation and Transmission Interconnection Planning -- Manual M-14A; Prepared by Planning Division Generation Interconnection Department; 2014. Available online:

<https://www.pjm.com/~/media/documents/manuals/m14a.ashx>

<sup>11</sup> LV 5+ Series, GE Energy Connections. Available online:

<https://www.gepowerconversion.com/sites/gepc/files/downloads/GEA32647%20%20GEPC%20LV5%2B%20Series%20Solar%20Inverter%20and%20Solar%20eHouse%20Solutions%20%28Web%29.pdf>

performance<sup>12</sup>. Diode rectifiers of six-pulse or twelve-pulse typically produce significant current harmonics which increase losses and impose extra insulation and thermal stress onto the generator windings. Typical solutions proposed to mitigate the effects of current harmonics are to oversize the generator. Generator manufactures normally recommend oversizing to 1.4 or 1.6 times for twelve-pulse or six-pulse rectifiers respectively or equivalently maintain the sub-transient reactance below 0.12 p.u<sup>13,14</sup>. However, oversizing the generator leads to a not a cost-effective solution and does not guarantee that the generator impedance excited by the harmonics (sub-transient reactance) will be reduced. Indeed, if the over-sized generator has a larger frame size, sub-transient reactance may increase and provide no help in voltage harmonics mitigation<sup>15</sup>. Customizing the generator design to reduce sub-transient reactance is not a practical solution neither cost-effective. Adding passive filters to reduce current harmonics injection to the generator might be more practical however, the large capacitor bank coming with the filter will make the generator operate at leading power factor and cause instability to automatic voltage regulator (AVR). Also, significant amount of generator rating will be wasted to absorb extra reactive power generated by filter capacitors and significantly penalize the capital expenditure as compared to directly-coupled CHP.

Different potential solutions that can be adopted for the generator-side rectifier have been analyzed and a trade-off analysis performed to select the most technically and economically viable solution for the interface converter architecture. They include:

- six-pulse diode rectifier,
- twelve-pulse diode rectifier,
- six-pulse diode rectifier with active harmonics filter and
- two-level VSC rectifier.

The twelve-pulse rectifier includes a three-winding phase-shift transformer at its ac terminal and two six-pulse diode rectifiers connected in series at the dc link. Such dc series connection avoids additional interphase transformer (IPT) which is normally used with dc parallel connection to reduce circulating currents. The active harmonic filters is a two-level VSC with instantaneous active and reactive components based hysteretic current control<sup>16</sup>. The VSC rectifier is a 3 kHz switching frequency converter that has the circuit and a current control structure as was shown in Figure 3. A generic *dq* reference frame current

---

<sup>12</sup> A. Elsebaay, M. A. Abuadma and M. Ramadan, "Analyzing the Effect of Motor Loads and Introducing a Method for Selection of Electric Generator Power Rating," 2018 Twentieth International Middle East Power Systems Conference (MEPCON), Cairo, Egypt, 2018, pp. 7-12.

<sup>13</sup> Engineering Bulletin CTV-PRB011-EN (2002). Available online: <http://www.trane.com>.

<sup>14</sup> Jim Iverson (2007) Power topic #7007: How to size a genset. Available online: <http://power.cummins.com/>

<sup>15</sup> Nhut-Quang Dinh and J. Arrillaga, "A salient-pole generator model for harmonic analysis," in IEEE Transactions on Power Systems, vol. 16, no. 4, pp. 609-615, Nov. 2001

<sup>16</sup> V. Soares, P. Verdelho and G. D. Marques, "An instantaneous active and reactive current component method for active filters," in IEEE Transactions on Power Electronics, vol. 15, no. 4, pp. 660-669, July 2000.

controller where d-axis current reference is provided by the dc bus voltage regulator is used. The system detailed circuit model is implemented and simulated in PSCAD<sup>17</sup>, an industry standard software for power system analysis.

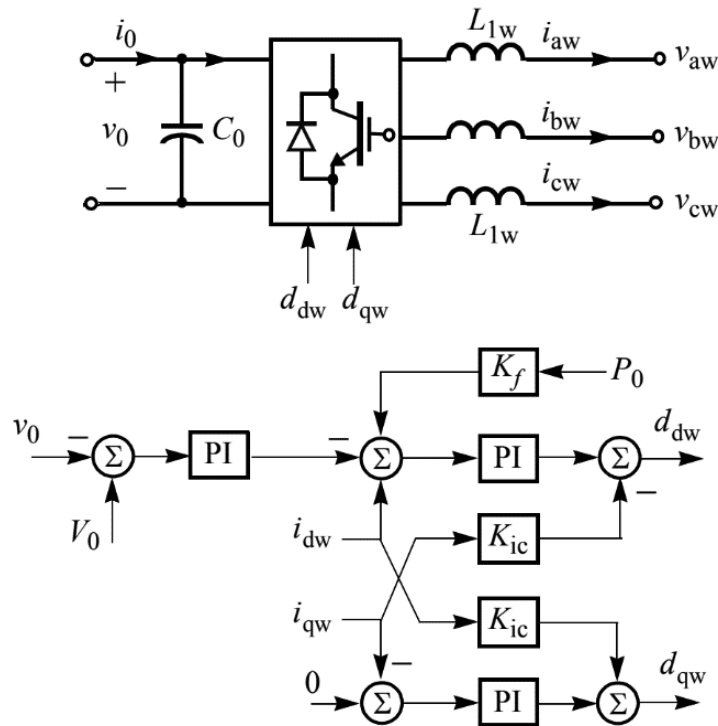


**Figure 3:** Circuit and control block diagrams of the grid-side inverter.

The analysis focused on the harmonic distortion level at the generator side and its impact on sizing the generator. The IEEE standard 519-2014<sup>18</sup> recommends practices and requirements for harmonics mitigation in power system and has been widely accepted by utilities. The harmonic spectrum at the generator terminal is compared against this standard. Another important aspect is the control stability of converter-interfaced CHP system. The DC link voltage stability of the interface converter is studied through impedance-based stability analysis which compares the dc terminal impedances of the interconnected rectifier and inverter<sup>19</sup>. This can help to provide design guidelines for system integration to avoid potential control interaction issues

### 3.1 Technical evaluation of potential solutions for the interface converter design

A 2MW medium-sized CHP system is selected as a benchmark to evaluate the different solutions for interface converter design. The generator is assumed to be a solid round rotor

<sup>17</sup> Power System Computer Aid Design <https://www.pscad.com/software/pscad/overview>

<sup>18</sup> IEEE Recommended Practice and Requirements for Harmonic Control in Electric Power Systems - Redline, in IEEE Std 519-2014 (Revision of IEEE Std 519-1992) - Redline , vol., no., pp.1-213, 11 June 2014

<sup>19</sup> H. Liu, H. Guo, J. Liang and L. Qi, "Impedance-Based Stability Analysis of MVDC Systems Using Generator Thyristor Units and DTC Motor Drives," in IEEE Journal of Emerging and Selected Topics in Power Electronics, vol. 5, no. 1, pp. 5-13, March 2017.

synchronous generator and modeled by IEEE standard sixth order sub-transient model<sup>20</sup>. The parameters of the generator used as a baseline for the evaluation of the interface converter harmonic performance are listed in Table 1. As it can be noted, the generator rating is higher than the engine power rating as it includes provision for reactive power capability (up to 0.8 power factor at full load) which is required common practice for directly-connected CHP.

Parameters	Value	Parameters	Value
Rating (MVA)	2.5	d-axis time constant (s)	1.17
Rated voltage (V)	480	d-axis sub-transient time constant (s)	0.027
Frequency (Hz)	60	q-axis synchronous reactance (pu)	0.99
Leakage reactance (p.u.)	0.062	q-axis transient reactance (pu)	0.99
Resistance (p.u.)	0.008	q-axis sub-transient reactance (pu)	0.122
d-axis synchronous reactance (p.u.)	1.94	q-axis time constant (s)	1.17
d-axis transient reactance (p.u.)	0.191	q-axis sub-transient time constant (s)	0.099
d-axis sub-transient reactance (p.u.)	0.122	Inertial constant (s)	0.4

**Table 1:** Parameters of the baseline generator for the harmonic evaluation

The key function of an excitation system is to provide direct current to the synchronous machine field winding to regulate the generator terminal voltage. The exciter model used in this analysis is the IEEE standard excitation system “AC7B”<sup>21</sup> representing one of the industry mainstream excitation and automatic voltage regulator (AVR) systems for small to medium size generators.

For the harmonic analysis, the dynamics of the prime mover and governor control can be neglected. The generator is assumed to be operated at the rated speed and the grid-side inverter is a rated at 2.5MVA to match the reactive power capability of the directly-connected generator.

### 3.1.1 Harmonics analysis

For the different rectifier solutions analyzed the generator terminal voltages and currents are monitored and compared in both time domain and frequency domain. Per IEEE Std. 519-2014, the voltage distortion limits for bus voltage lower than 1 kV is that individual harmonic should be no more than 5% and total harmonic distortion (THD) should be no

<sup>20</sup> IEEE Guide for Synchronous Generator Modeling Practices and Applications in Power System Stability Analyses," in IEEE Std 1110-2002 (Revision of IEEE Std 1110-1991) , vol., no., pp.0\_1-72, 2003.

<sup>21</sup> IEEE Power Engineering Society, “IEEE Recommended Practice for Excitation System Models for Power System Stability Studies,” 3 Park Avenue, New York, NY.

more than 8%; for system short-circuit ratio lower than 20, the current harmonics limitations are listed in Table 2.

Harmonic Order ( $h$ )	3-10	11-16	17-22	23-34	TDD
Harmonics Limits (%)	4	2	1.5	1	8

**Table 2:** Current Distortion Limits for system rated 120 V Through 69 kV and  $I_{sc}/IL < 20$

#### *Case I: Six-Pulse Diode Rectifier*

The first case studied uses a six-pulse diode rectifier and the generator is oversized to 3.2MVA (1.6 times the CHP power rating). In the simulation model, the generator rating in Table 1 is increased to 3.2 MVA and the rest of parameters remain the same, assuming such oversizing will not cause significant physical design changes to the generator. The simulation results are shown in Figure 4. They reveal that the generator output currents are highly distorted due to the diode rectifier. The current harmonics and high sub-transient reactance of the generator result in distorted generator output voltages. The Fast Fourier Transform (FFT) results show the spectrum of the generator output voltages and currents. The harmonics percentages are higher than the limits of IEEE Std. 519-2014<sup>18</sup>.

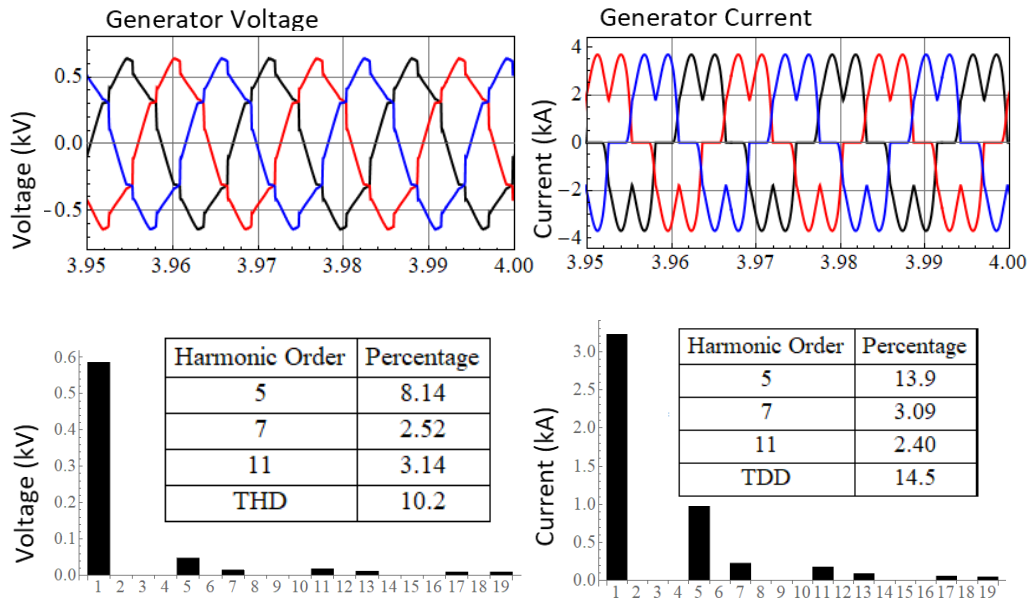


**Figure 4:** Time-domain waveforms(upper) and frequency-domain spectrum (lower) of generator output voltage and current with 6-pulse diode rectifier

#### *Case II: Twelve-Pulse Diode Rectifier*

The second case studied uses twelve-pulse diode rectifier with 2.8MVA generator. The three-winding phase-shift transformer is assumed to have a rating of 2.5MVA with leakage inductance of 6%. The simulation results are shown in Figure 5. Without additional

harmonic filters, the harmonics distortion induced by the twelve-pulse diode rectifier is, as expected, reduced compared to the six-pulse diode rectifier. The FFT analysis of the generator output voltages and currents shows that harmonics are below IEEE Std. 519-2014 limits<sup>18</sup>.

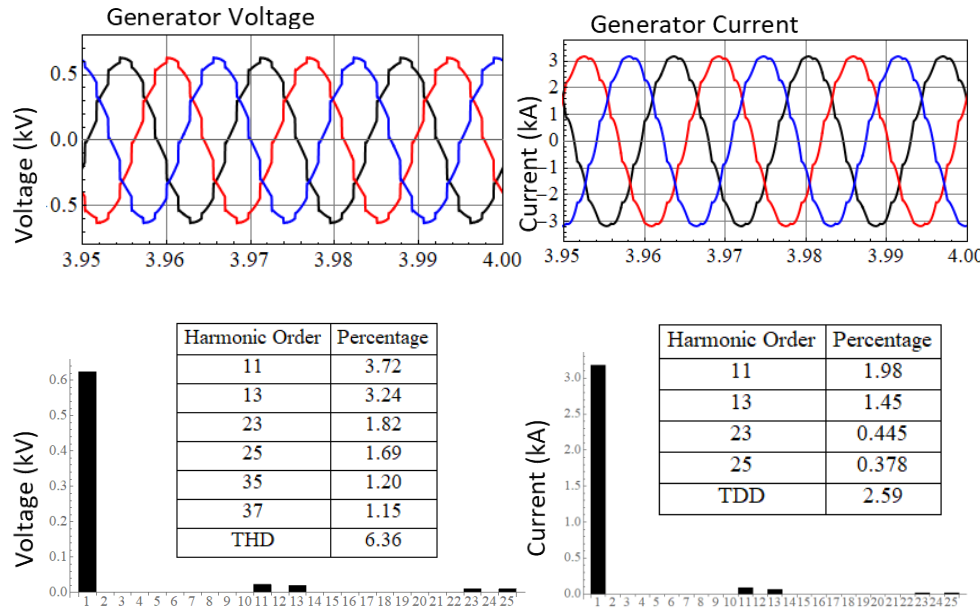


**Figure 5:** Time-domain waveforms(upper) and frequency-domain spectrum (lower) of generator output voltage and current with 12-pulse diode rectifier.

### Case III: Six-Pulse Diode Rectifier with Active Harmonic Filter

In this case study, a six-pulse diode rectifier is used with an additional active harmonic filter which is a two-level VSC with hysteretic current control. The generator rating is kept at the size it would be with the converter-interfaced i.e., downsized to 2.1MW (1.05pu of the engine rating) as no reactive power oversize will be required. The simulation results are shown in Figure 6. They indicate that the generator output voltages and currents contain fewer harmonic components compared to in cases I and II and the harmonics levels are below IEEE 519-2014 limits<sup>18</sup>, even though the voltages are distorted during the commutation instants. In addition, the input current of the active filter is calculated to be 315 A (RMS) which provides the guideline for determining the rating of the filter.

### Case IV: VSC Rectifier

In this case, a two-level VSC is used as rectifier. To absorb the high frequency switching harmonics, an LCL filter is added at its ac terminal. However, the size and capacity of these filters are relatively small (reactive power generation is less than 10% of the converter rating). This leads to a VSC back-to-back configuration for the interface converter, topology that is widely used in wind turbine applications. In addition, the rectifier control is designed to regulate the generator output power factor to be unity so that the instability issues and oversizing requirement caused by leading power factor operation can be avoided. This allows to downsize the generator to 2.1MVA. The simulation results are presented in Figure

7. With a VSC rectifier, the generator output currents and voltages contain the least harmonic levels among all four cases that were analyzed. The voltage and current harmonics remain far below the limits of IEEE Std. 519-2014<sup>18</sup>.

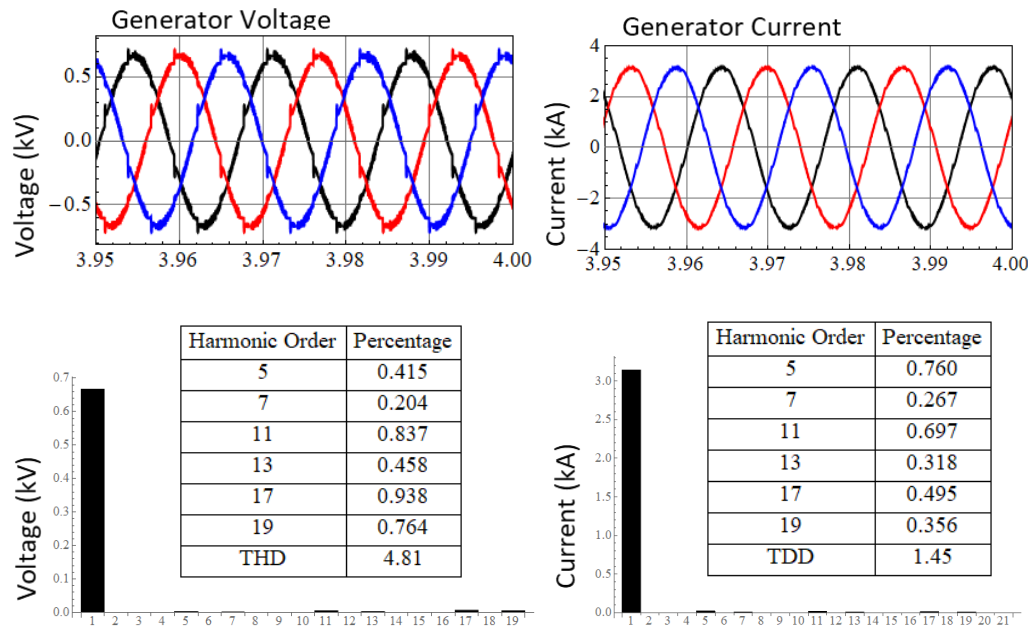


**Figure 6:** Time-domain waveforms(upper) and frequency-domain spectrum (lower) of generator output voltage and current with 6-pulse diode rectifier and active harmonic filter

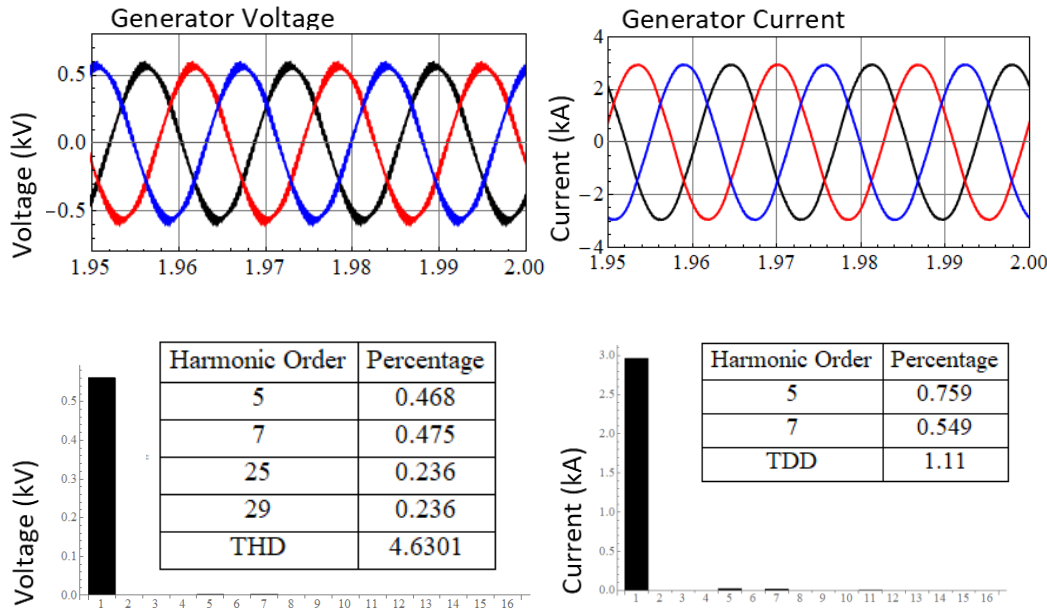


**Figure 7:** Time-domain waveforms(upper) and frequency-domain spectrum (lower) of generator output voltage and current with VSC rectifier.

### 3.1.2 Cost trade-off analysis of the interface converter

The harmonic analysis revealed that the VSC rectifier solution has the best performance among the four analyzed and meets IEEE Std. 519-2014<sup>18</sup>. The overall electrical system cost of the four cases has been also investigated. The analysis is based on the costs of the major components of the electrical interface including the inverter, rectifier, generator, and any other ancillary equipment required such as an active filter or a phase shift transformer. The cost breakdown is listed in Table 3. It shows the cost of the diode rectifier is ~70% of a VSC rectifier unit. The cost of the generators is based on a Magna Power listing, 480V 1800RPM Generators, Class H<sup>22</sup>. As it can be noted, the unit price (\$/kVA) of a 3.2 MVA generator is significantly higher than that of a 2.1 MVA generator, due to the increased number of leads.

Converter option	Rated power (Grid side) (kW)	Minimum PF at rated power output	Inverter			Rectifier			THD	Additional Filter requirements		IEEE 519 compliance	Generator			Total System Cost
			Rating (kVA)	Unist cost (\$/kVA)	Cost	Rectifier type	Rating (kVA)	Unit Price (\$/kW)		Filter Components	Cost		Rating (kVA)	Unit cost (\$/kVA)	Cost	
Case 1	2000	0.8	2500	35	\$ 87,500	6-Pulse Diode	2100	25	\$ 52,500	16.9%	N/A	Fail	3360	65	\$ 218,400	\$ 358,400
Case 2	2000	0.8	2500	35	\$ 87,500	12-Pulse Diode	2100	25	\$ 52,500	6.4%	2.5 MVA Phase-shift Xfrm	Pass	2940	65	\$ 192,129	\$ 394,629
Case 3	2000	0.8	2500	35	\$ 87,500	6-Pulse Diode	2100	25	\$ 52,500	4.8%	>315A RMS Active Filter Included in VSC	Pass	2205	48	\$ 105,840	\$ 320,840
Case 4	2000	0.8	2500	35	\$ 87,500	VSC	2100	35	\$ 73,500	4.6%		Pass	2205	48	\$ 105,840	\$ 266,840

**Table 3:** Electrical System Cost Analysis of Four Different Rectifier Units

From Table 3, it can be concluded that the VSC rectifier configuration offers the least capital cost among the cases analyzed. Although the VSC rectifier is more expensive, the total balance of plant cost is lower because of smaller size of generators or filters. Compared to directly-coupled CHP, the VSC back-to-back converter-interfaced CHP also allows to reduce the cost of interconnection equipment such as breakers and relays.

In summary Figure 8 shows the minimum sizing requirements for directly-coupled and converter-interfaced CHP.

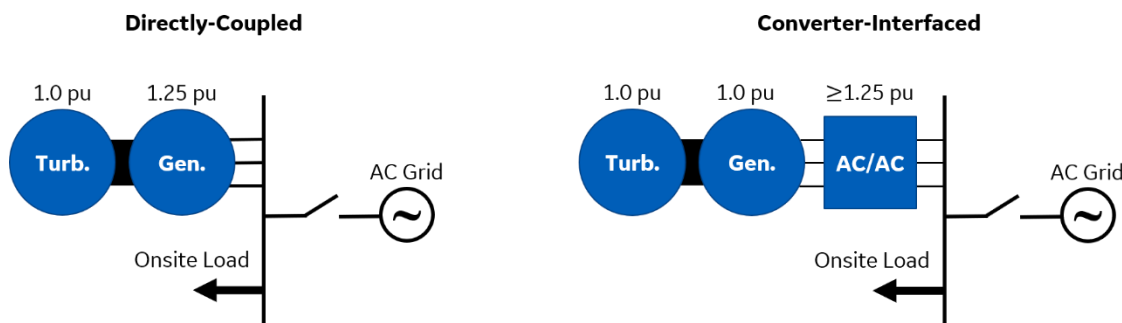


**Figure 8:** Schematics of directly-coupled and converter-interfaced CHP

<sup>22</sup> Generators Selection and Pricing Catalog, Marathon. Available online: <https://www.marathongenerators.com/generators/docs/manuals/GPN006.pdf>

In the directly-coupled scenario, the generator must be oversized by 25% to account for reactive power requirements while in the converter-interfaced case, no oversizing of the generator is required. For the interface converter, the grid-side inverter will be sized similarly to the directly-coupled generator to match the reactive power capability but the rectifier, i.e., the generator VSC, can be sized at 1.0pu. However, it would be more practical to size both VSC of the interface converter at 1.25pu.

### 3.1.3 Stability assessment of the back-to-back VSC system

For impedance-based stability analysis, the VSC back-to-back CHP system is separated into the load and source subsystems as shown in Figure 9.  $Z_{inv}(s)$  represents the dc impedance of the grid-side inverter which regulates dc bus voltage.  $Z_{rec}(s)$  represents the dc impedance of generator-side rectifier. For the impedance-based stability criterion, the system is stable if and only if the impedance ratio  $Z_{inv}(s)/Z_{rec}(s)$  meets the Nyquist stability criterion.

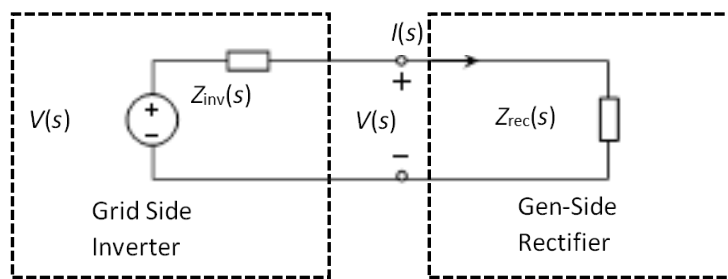
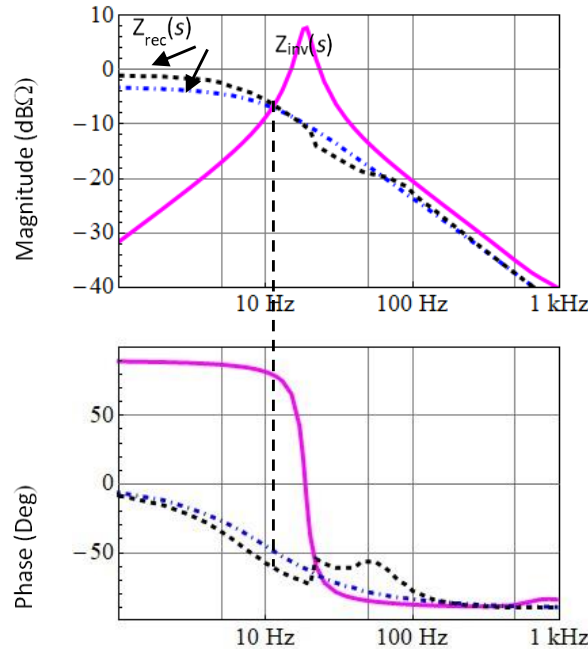


**Figure 9:** Small-signal impedance representation of VSC back-to-back system.

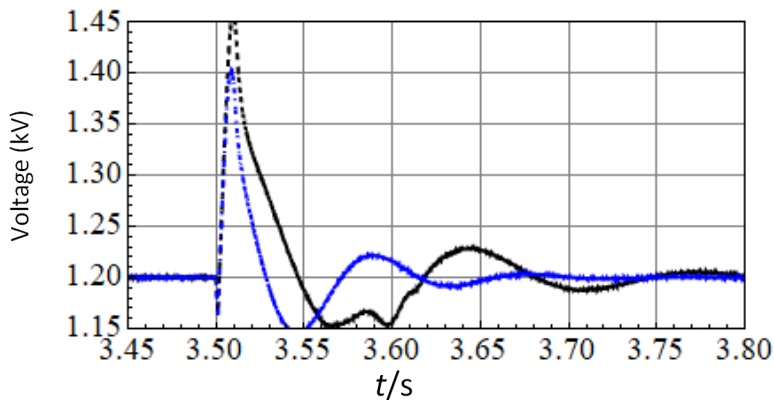
The converter dc impedances are obtained through point-by-point impedance scan in numerical simulation.

Figure 10 depicts dc impedance responses of the inverter and rectifier. The inverter dc impedance  $Z_{inv}(s)$  has a resonance peak at around 20 Hz which is close to the dc bus voltage control bandwidth. The rectifier dc impedances are obtained with two different AVR designs to evaluate the effects of AVR control on dc link stability. From Figure 10, it can be observed that with fast AVR, the phase of  $Z_{rec}(s)$  decreases below 20 Hz. The phase margin at the intersection frequency where the magnitude of  $Z_{inv}(s)$  equals to that of  $Z_{rec}(s)$  also decreases. The impedance analysis indicates that fast AVR design could lead to a less damped dc bus dynamics.

Figure 11 shows the numerical simulation results of dc link dynamics with fast and slow AVR designs. The generator outputs 1.6MW power at steady state before 3.5s. At 3.5s, the active power command steps up to 2.0MW. It can be found that with slow AVR control, the peak value and settling time of the dc bus voltage is lower showing better damped system dynamics. This correlates to the impedance analysis.



**Figure 10:** Impedance responses of grid side inverter  $Z_{\text{inv}}(s)$  and generator side rectifier  $Z_{\text{rec}}(s)$ . Solid lines:  $Z_{\text{inv}}(s)$ ; dashed lines:  $Z_{\text{rec}}(s)$  with slow AVR; dot-dashed lines:  $Z_{\text{rec}}(s)$  with fast AVR



**Figure 11:** Time-domain responses of dc link bus voltage when the active power command steps from 1.6 MW to 2.0 MW. Dashed lines: dc voltage with slow AVR; dot-dashed lines: dc voltage with fast AVR.

The impedance-based stability analysis shows that the AVR is critical to the dc link stability of the VSC back-to-back interface converter.

### 3.2 Review of distributed energy resources (DER) interconnection standards

The dominant standard for DER grid interconnection and operation is the IEEE standard 1547<sup>5</sup>. It was originally established (in 2003) for inverter-based generators such as residential and commercial photovoltaic (PV) solar systems but is now widely adopted as minimum interconnection requirements for any DER into the distribution grid. For the

converter-interface CHP controls it is important to identify and establish the minimum criteria that will apply for performance validation.

### 3.2.1 Steady-state performance requirements

In its latest version, the IEEE standard 1547<sup>5</sup> assigns categories to DER based on their performance requirements for steady-state and for transients. For steady-state operation, DER can be in two categories, A and B as shown in Figure 12 following a suggested decision-tree shown in Figure 13.

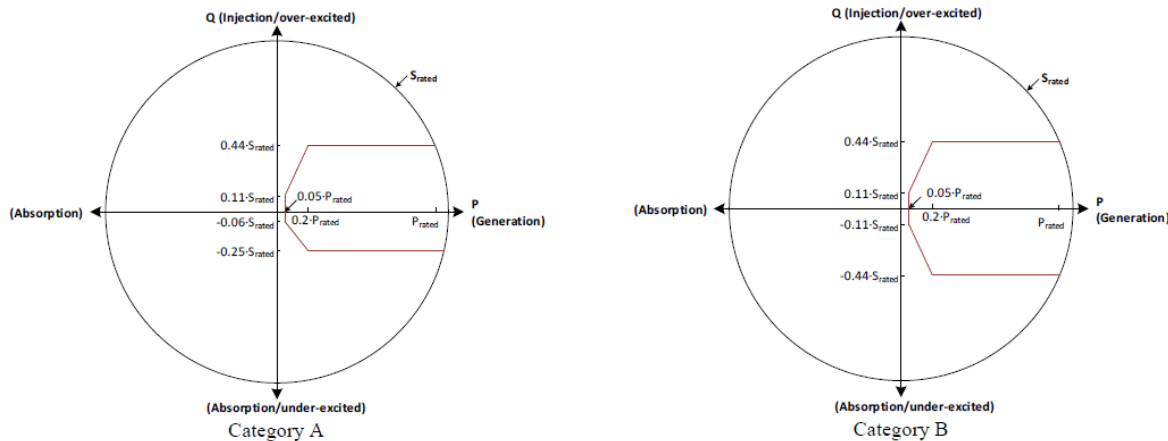


**Figure 12:** Comparison of minimum reactive power requirements for Categories A and B DER.

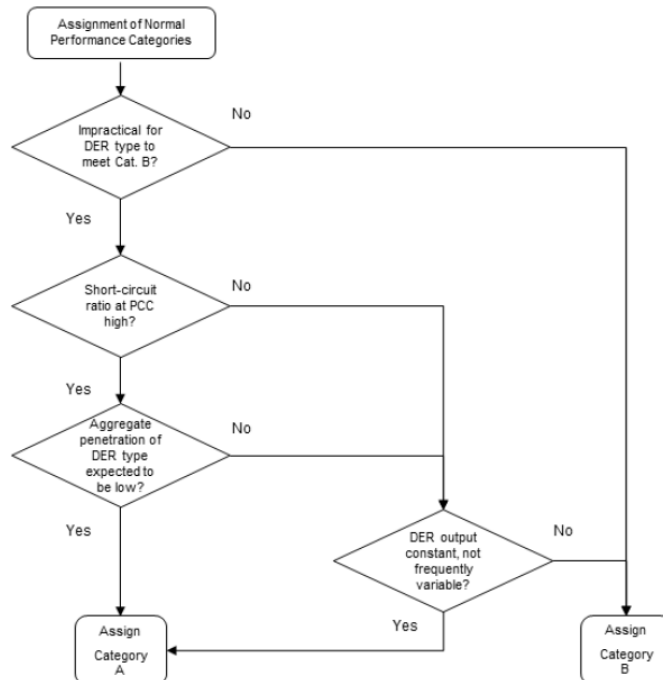


**Figure 13:** Decision-tree for steady-state performance category assignment of DER

### 3.2.2 Dynamic performance requirements

There are three categories for the transients performances. The DER needs to be assigned one category for steady-state and one for transients and meet the requirements for those. For the category assignment of a converter-interface CHP plant it was evaluated that Category B-II (B for steady-state operation and II for transients) will apply. Figure 14 shows as reference the transient category assignment table per IEEE standard 1547-2018.

DER type	DER application purpose						
	Retail self generation	Combined heat and power	Waste fuel recovery	Renewable energy	Merchant generation <sup>a</sup>	Critical backup <sup>b</sup>	Peak shaving
	A	B	C	D	E	F	G
1 Engine or turbine driven synchronous generator	Category I	Category I	Category I	Category I	Category I	Category I	Category I
2 Wind turbines (all types)	Category II	N/A	N/A	Category II	Category II	N/A	N/A
3 Inverters sourced by solar PV	Category II <sup>c</sup>	N/A	N/A	Category II <sup>c</sup>	Category II <sup>c</sup>	N/A	N/A
4 Inverters sourced by fuel cells	Category I	Category I	Category I	Category I	Category II	Category I	N/A
5 Synchronous hydrogenerators	Category I	N/A	N/A	Category I	Category I	Category I	N/A
6 Other inverter applications	Category II	Category II	Category II	Category II	Category II	Category II	N/A
7 Inverters sourced by energy storage	Category II	N/A	N/A	N/A	Category II	Category II	Category II
8 Other synchronous generators	Category I	Category I	Category I	Category I	Category I	Category I	N/A
9 Other induction generators	Category II	Category II	Category II	Category II	Category II	Category II	Category II

**Figure 14:** Transient performance category assignment for DER

The category assignment leads to the specific requirements for reactive power rating, voltage and frequency ride-through limits as well as requirements for islanding. Figure 15 shows for comparison the voltage and frequency ride-through limits assigned to Category I and II.

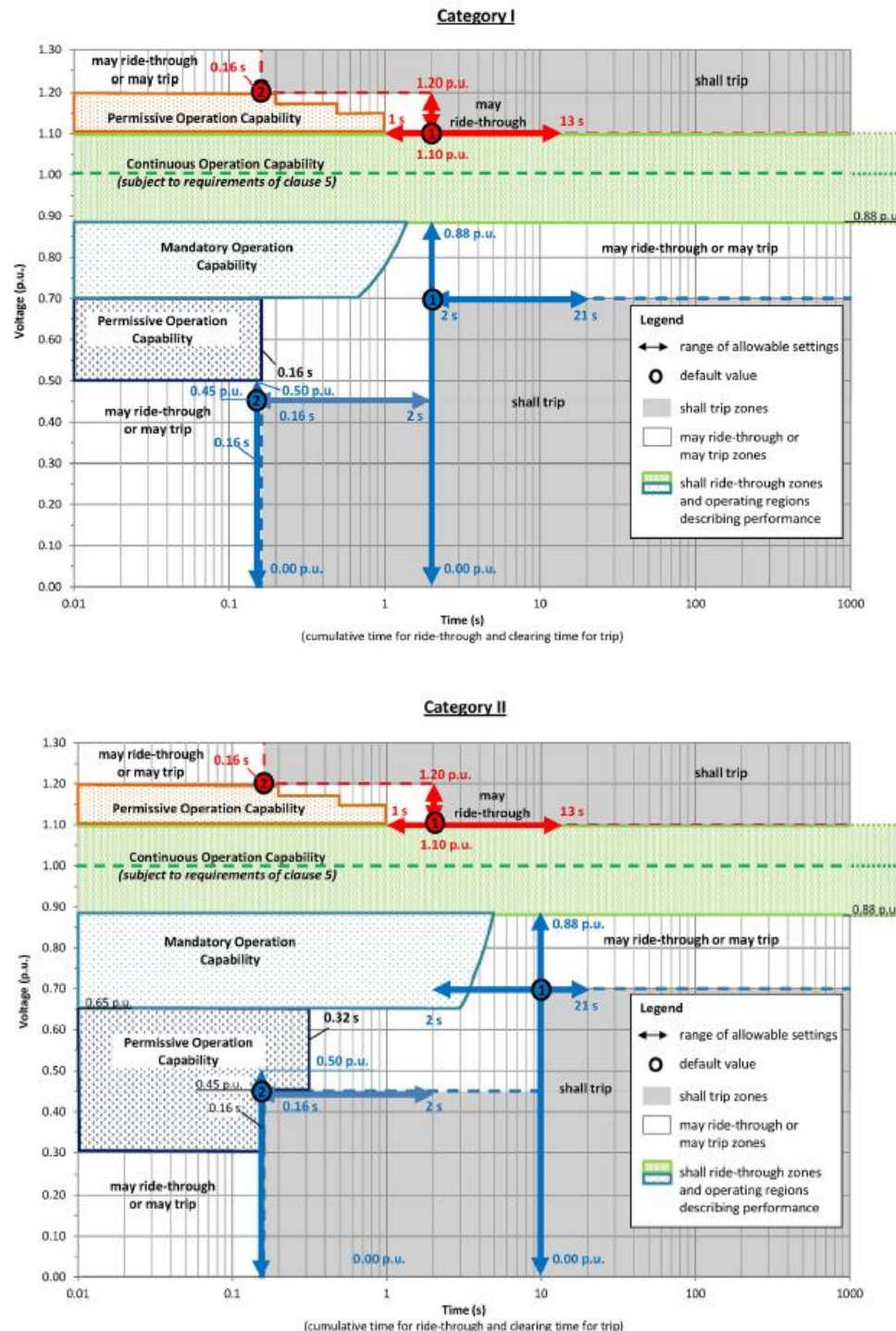


Figure 15: Comparison of category I and II transient performance requirements<sup>5</sup>

### 3.2.3 Microgrid operation and controller functions

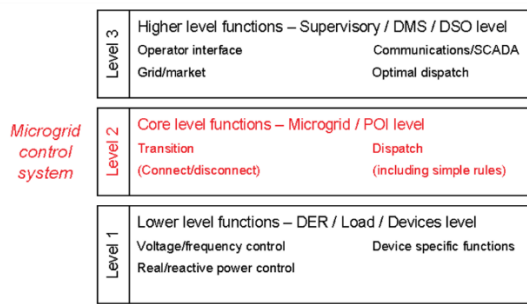
The IEEE standard 2030.7<sup>23</sup> relative to the specifications for microgrids controllers has also been analyzed. This standard defines the minimum requirements for power dispatch and

<sup>23</sup> [https://standards.ieee.org/standard/2030\\_7-2017.html](https://standards.ieee.org/standard/2030_7-2017.html)

energy management as well as transition operations supervised by microgrid controller. Figure 16: shows a summary of the key requirements. For the converter-interface CHP it will be demonstrated the plant controller can meet these requirements.

**Microgrid Controller:**

1. Transition: supervises the transitions between connected and disconnected states, and ensures the dispatch is appropriate for the given state
2. Dispatch: dispatch individual devices in given operating modes and with specified setpoints



*Transition Function of Microgrid:*

1. DSO interconnection requirement and agreements
2. Microgrid owner/operator requirements
3. Distribution system requirements for the microgrid
4. Other standards and requirements: a) IEEE std 1547; b) UL 1741; c) IEEE Std 1453

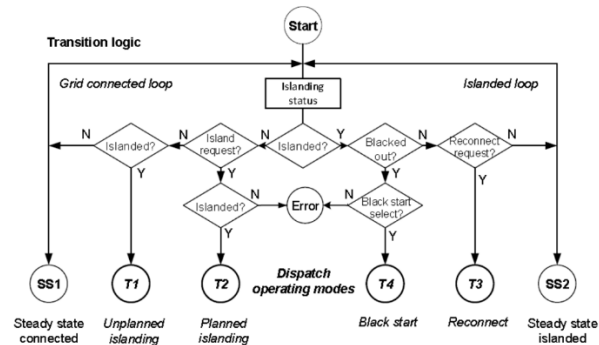


**Figure 16:** Minimum functional requirements of microgrid controllers

#### 4. ECONOMIC FEASIBILITY ANALYSIS OF CONVERTER-INTERFACED CHP

As established by DOE the major barrier for a broader adoption of CHP in commercial and small to medium-sized industrial applications are: 1) a high initial investment, 2) a lengthy interconnection process involved in satisfying utility standards and grid codes and 3) lack of technical sophistication of small entities to deal with the technical complexity related to CHP deployment<sup>2</sup>. The interface converter solution proposed has a significant potential to reduce those barriers however, a detailed analysis is required to validate its economic advantages over directly-coupled systems. As the traditional directly-coupled CHP system has proven its profitably in many applications<sup>24,25,26</sup>. Converter-interfaced CHP system needs to demonstrate equal or higher profitably, in order to be widely adopted by the industry. A platform to analyze in the details the revenue from the CHP system both on active power and heat as well as on grid support services has been developed. It includes hourly timeseries simulations that allows to estimate based on the plant load profile the energy consumption, the energy exported to the grid as well as the charges of operating (Opex) the CHP. Then the financial parameters such as capital expenditures (Capex) & Taxes are included to calculate the annualized ROI evaluation. Five user case scenarios selected for the U.S Technical Potential database and representative of most typical

<sup>24</sup> Mone, C. D., D. S. Chau, etc. "Economic feasibility of combined heat and power and absorption refrigeration with commercially available gas turbines." *Energy Conversion and Management* 42, no. 13 (2001): 1559-1573

<sup>25</sup> X. Q. Kong, R. Z. Wang, etc. "Energy efficiency and economic feasibility of CCHP driven by stirling engine." *Energy Conversion and Management* 45, no. 9-10 (2004): 1433-1442

<sup>26</sup> Wood, S. R., and P. N. Rowley. "A techno-economic analysis of small-scale, biomass-fuelled combined heat and power for community housing." *Biomass and Bioenergy* 35, no. 9 (2011): 3849-3858

applications of CHP as DER are analyzed. The user cases are also selected such each of the five leading US in CHP potential is represented. The location of the application is in fact an important parameter as it allows to determine load profile and the energy price as well as the grid support services entitlement for the CHP application. Indeed, both the plant operation and the location weather condition will affect the heat and power demand. Additionally, not all Independent System Operator (ISO) territories apply the same energy rate neither the same rules for DER participation in grid support services.

In traditional directly-coupled CHP systems, sizing of generator is commonly 25% more than engine capacity for providing reactive power and harmonics mitigation. As shown in Figure 1, the converter-interfaced CHP is connected through a rectifier and a grid-ready inverter to support local loads and export excess power into the grid (the diagram for directly-coupled CHP is similar with removing the components located in the dashed box). The converter-interfaced CHP system does not need to oversize generator from two reasons: 1) it is equipped with a comprehensive control system which enables to limit the Total Harmonic Distortion at both the generator and grid sides to below 5%; 2) the grid-side inverter provides the required reactive power to the load. Thus, the power factor at the generator terminals will stay consistently at unity regardless of the load, and while conventional synchronous generators used with CHP systems are designed to provide their rated power at a minimum 0.8 power factor, converter-interfaced CHP will be able to operate at a lower power factor (e.g., 0.6) depending on the sizing of the inverter and the generator. Nevertheless, the converter-interfaced CHP limits the short-circuit contribution of the CHP, hence reducing the cost of interconnection equipment (e.g., breakers, busbars, relays) and design iterations required by the utility to be granted a “Permission-to-operate” approval. It facilitates compliance with major interconnection standards such as IEEE 1547 and 2030.7 since many commercial grid-ready inverters already comply with those standards.

#### **4.1 Analysis of the U.S Technical Potential of CHP**

As reported by the DOE, more than 240 GW of cogeneration potential, distributed across 291,000 sites, exists in the U.S<sup>2</sup>. Around 35% of that capacity i.e., 82.7 GW are consisted of CHP systems ranging between 1 MWe (MW electricity) and 20 MWe. Those, so-called small to medium-sized CHP systems include over 4,400 industrial and commercial facilities across the country, which represents ~7% of today's U.S. power generation capacity<sup>2</sup>.

The small to medium-sized CHP systems are usually used for facilities in the industrial or commercial sectors. These facilities, by the type of loads they host have a coincidental need of power and heat which fits well the performance of CHP systems. The typical applications targeted include food processing plants, chemicals, refining, metal manufacturing in the industrial sector and hospitals, hotels, multifamily or professional services buildings, colleges and universities, wastewater treatment plants in the commercial sector. In those applications, the engineering practice of CHP owners is to serve the on-site electricity and

thermal loads first with limited interaction with the grid. This is due to numerous technical and non-technical issues such as limited net metering program support at utility companies' service jurisdiction, limited understanding of the economic potential from CHPs to provide energy and service to grid, limited infrastructures at the CHP site or others. For some industrial facilities with a fairly lower power to thermal ratio, CHP systems reveal high technical potentials for electricity export. A total of ~91GW electricity export potential was estimated nationwide from all CHPs categories in the U.S. Industrial facilities such as petroleum refining, paper, chemicals, food and lumber and wood have a high potential for electricity export because of the high thermal loads relative to on-site electric demand<sup>2</sup>. This technical export potential is not evenly distributed nationwide in the U.S. and is highly correlated with industrial levels and size of industry in question at each state. For instance, Texas, as a leading state with chemical and petrochemical facilities, has the most export potential. Followed are other large industrial states like California, Louisiana, Illinois, and New York.

As the DOE has already recognized, the penetration of small to medium-sized CHP still lags far behind that of large CHP. Indeed, only ~7.6GW of the estimated ~82.7GW of this category of CHP, representing 9.2% of the small to medium-sized CHP potential have been installed. Therefore, it remains substantial opportunity for small to medium sized CHP to be installed in the grid. This section gives an overview of the population of small to medium-sized CHPs in the U.S.

#### ***4.1.1 Analysis of the population of small to medium sized CHP installed in the U.S.***

Figure 17 shows the geographic distribution of existing small to medium-sized CHPs as installed in 47 states and the District of Columbia<sup>27</sup>. It reveals that a large number of CHPs are installed in the leading industrial states such as California, New York, Illinois, New Jersey and Pennsylvania. The number of CHP units installed in each state are depicted in Figure 18. It can be noted that around 304 and 109 small to medium-sized CHP are installed in the two leading states of California and New York, respectively. Other leading states by number of units installed include Arkansas, Illinois, Massachusetts, New Jersey and Pennsylvania. A few CHPs are installed in the middle west states such as Idaho, Nevada, and Utah

---

<sup>27</sup> U.S. Department of Energy, Combined Heat and Power Installation Database. Available online: <https://doe.icfwebservices.com/chpdb/>

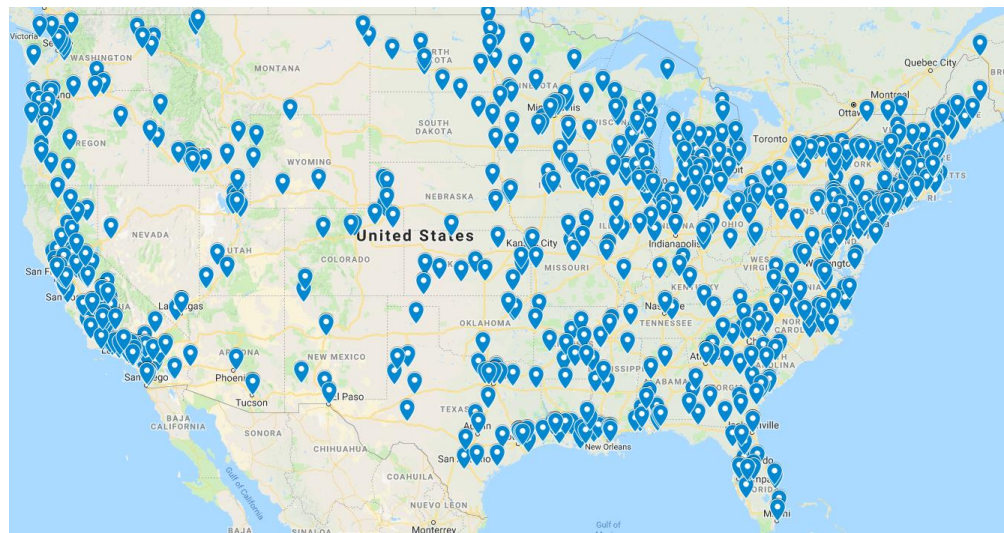


**Figure 17:** Geographic distribution of the small to medium-sized CHP in the U.S



**Figure 18:** Distribution of the small to medium-sized CHP in the U.S per state

Analyzed also by size, Figure 19 shows that six states including California, New York, Texas, Illinois, Arkansas, and New Jersey concentrates 42% of the total installed capacity of small to medium-sized CHP with 18% for California alone.

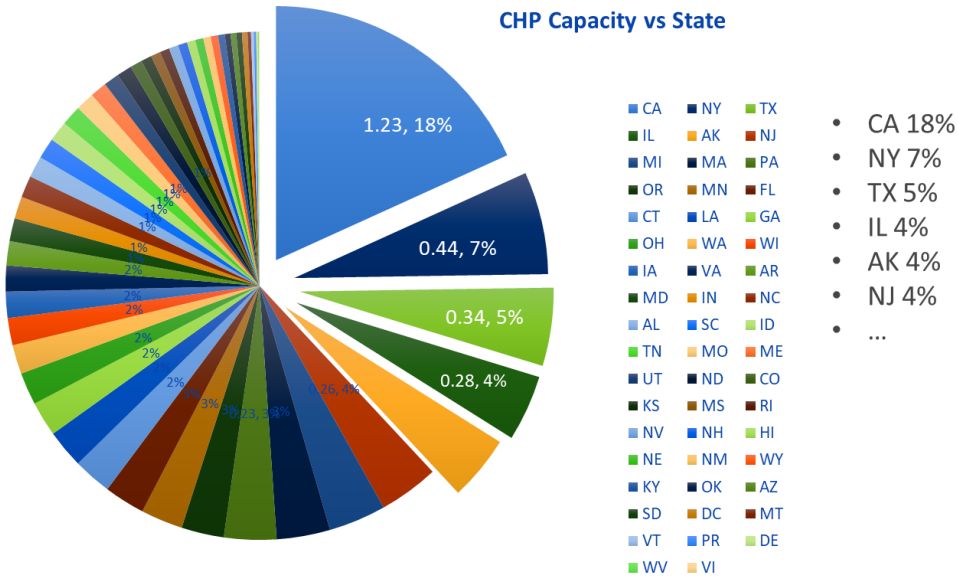


**Figure 19:** Small to medium-sized CHP installed capacity by state

Additionally, Figure 20 shows that ~70% of the small to medium-sized CHP are below 5MWe and as expected the largest units (>10MWe) are more predominant in the industrial states. The segment of 1MWe to 2MWe alone represents ~33% of the entire small to medium-sized CHP population.



**Figure 20:** Distribution of the small to medium-sized CHP in the U.S per MW size

Analyzed by application, Figure 21 and Figure 22 reveal that ~40% of the total small to medium-sized CHP installations are for colleges/universities, hospital/healthcare, chemicals, food processing, and wastewater treatment facilities. A further analysis suggests as shown in Table 4 that the installations sizes are more equally distributed between the leading applications.



**Figure 21:** Distribution of the small to medium-sized CHP across the U.S by application

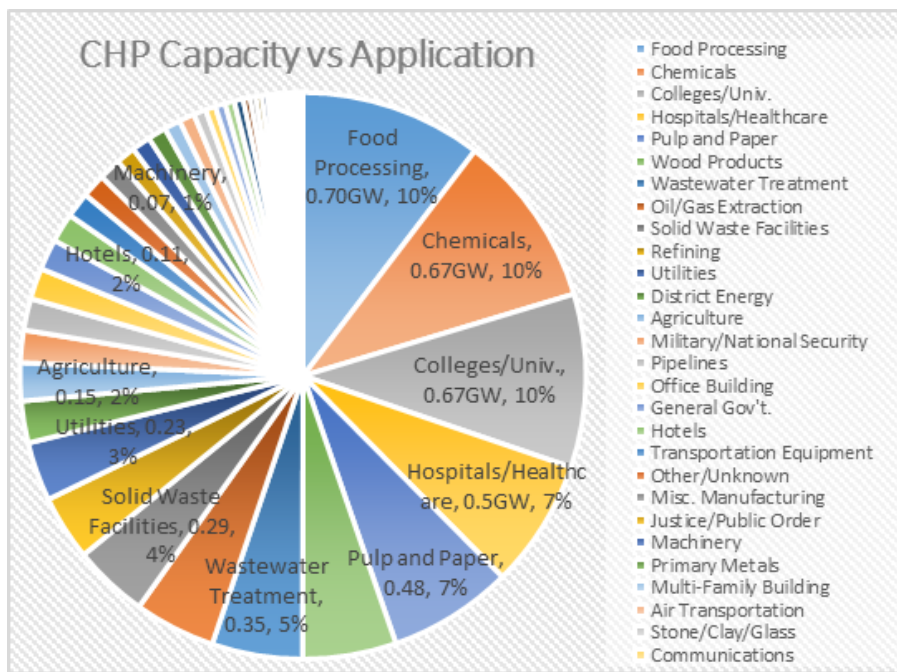


**Figure 22:** Repartition of small to medium-sized CHP applications by installed capacity

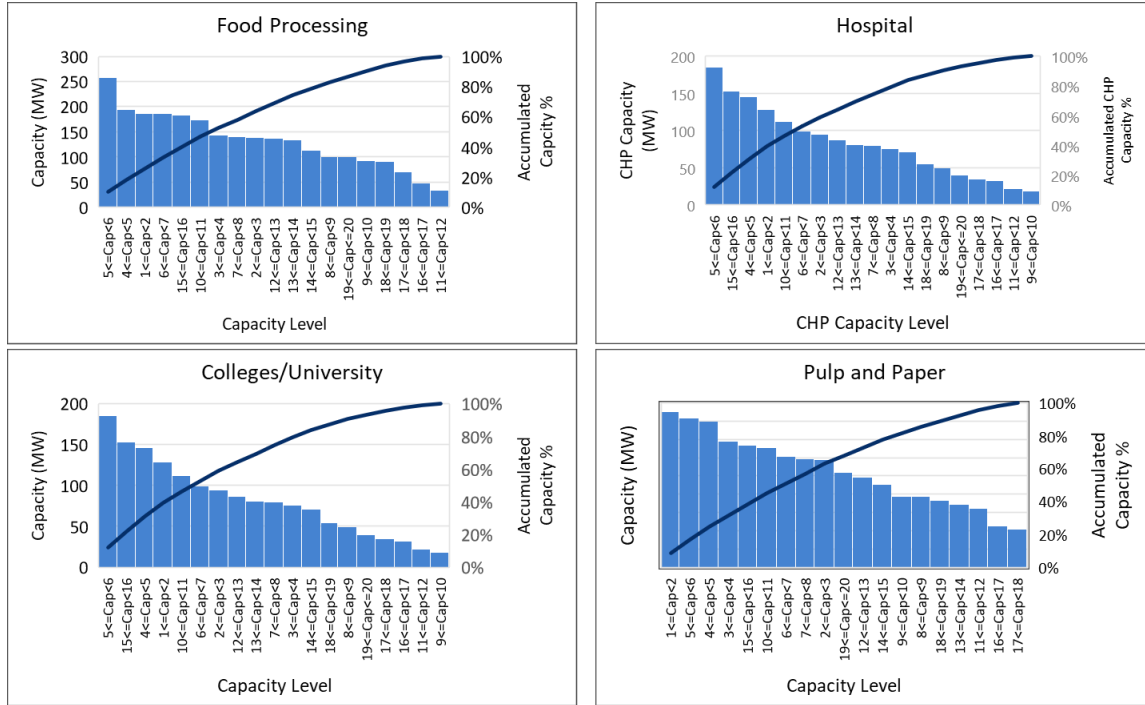


**Table 4:** Repartition of system sizes in leading small to medium-sized CHP applications

The repartition of the prime movers used by the small-to medium sized installed CHP in the U.S<sup>27</sup> is shown in Figure 23.

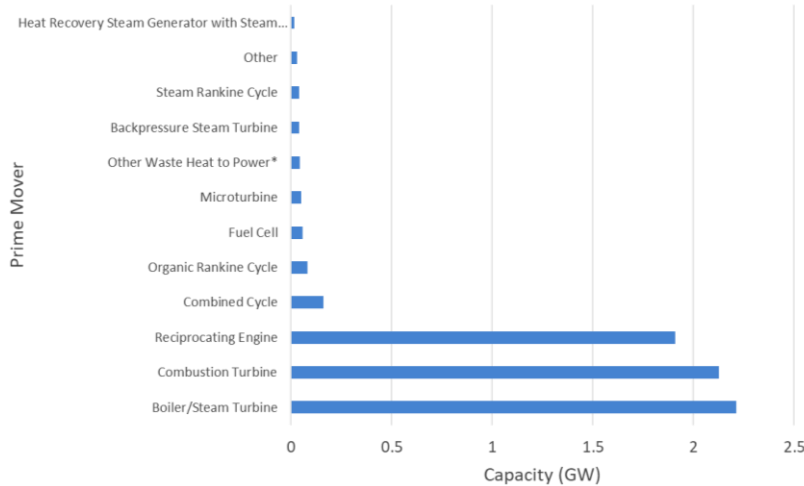


**Figure 23:** Repartition of prime movers used in small to medium-sized CHP U.S installations

It can be noted that reciprocating engine, combustion turbine, and steam turbine dominate the prime movers adopted in the existing CHP population with each having an installation base of ~2GW. Reciprocating engines and combustion engines with their high efficiency and lower costs at smaller sizes are usually more favorable for small to medium-sized CHP applications. The high representation of steam turbines despite their lower efficiency at small to medium size is mainly due to the legacy industrial facilities with CHP in the U.S.

For new installations, steam turbines will not be selected due to cost and the low efficiency of such an engine at small sizes. Other prime movers such as microturbines or fuel cell are also adopted in the 1 MWe to 20 MWe CHP installations however those engines are usually more favorable in the kW range.

#### 4.1.2 The U.S technical potential of small to medium-sized CHP

The U.S Technical Potential for CHP is defined as the potential, subject only to technological constraints, i.e., not including economic considerations. Estimates of TP for 1MWe to 20MWe CHP exceed 65 GW at more than 23,000 existing commercial and industrial sites nationwide. This reveals that over ~65.3 GW additional CHP can be installed at the distribution grid by industrial and commercial facilities in the U.S as opposed to the ~7.6GW existing<sup>28</sup>. Figure 24 shows the distribution by total estimated capacity in each state<sup>28</sup>. It is important to note that the CHP technical potential only consider the ability of the CHP technology to fit the site's energy need. If other factors such as availability of fuel supply are considered, the potential market size of CHPs will be lowered.

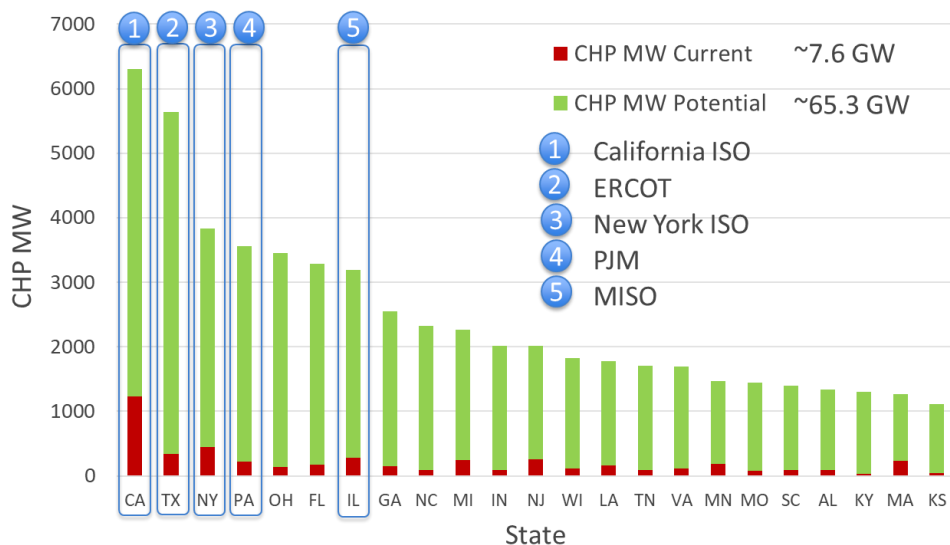


**Figure 24:** Distribution of the small to medium-sized technical potential CHP by state capacity

The analysis of the technical potential in the leading states suggest that applications such as college campuses, hospitals, office buildings, food processing and water treatment plants hold the largest potential in capacity for new small to medium-sized CHP installations<sup>28</sup>. Figure 25 through Figure 34 show the distribution of the small to medium-sized CHP technical potential in California, Texas, New York, Pennsylvania, and Illinois respectively. The analysis reveals that the industrial potential is in general larger than the commercial potential. However, looking into the application sizes the 1MWe to 5MWe

<sup>28</sup> U.S. Department of Energy, Combined Heat and Power (CHP) Technical Potential in the United States: [https://betterbuildingssolutioncenter.energy.gov/sites/default/files/attachments/CHP\\_Technical\\_Potential\\_Study.pdf](https://betterbuildingssolutioncenter.energy.gov/sites/default/files/attachments/CHP_Technical_Potential_Study.pdf)

category is well represented in both sectors. It also noticeable that in some states up to 40% of the technical potential of small to medium-sized CHP are for colleges/universities

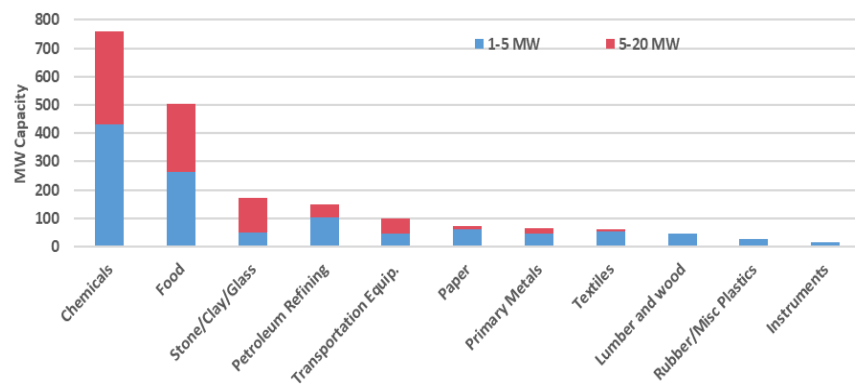


**Figure 25:** Distribution of the technical potential of small to medium-sized CHP for industrial applications in California

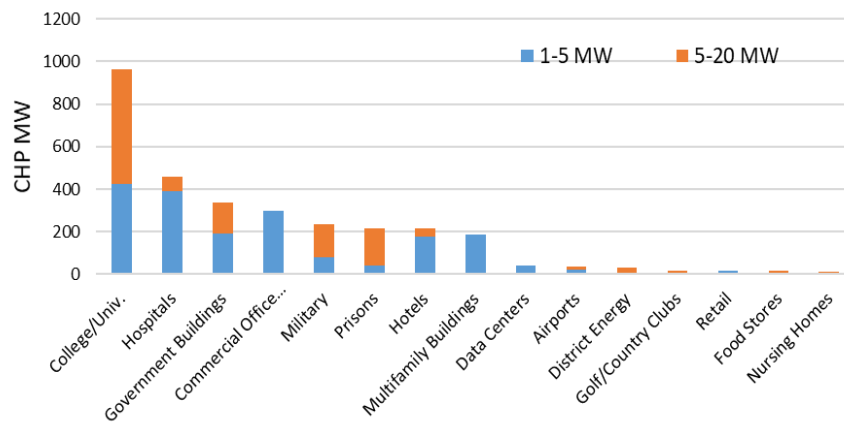


**Figure 26:** Distribution of the technical potential of small to medium-sized CHP for commercial applications in California

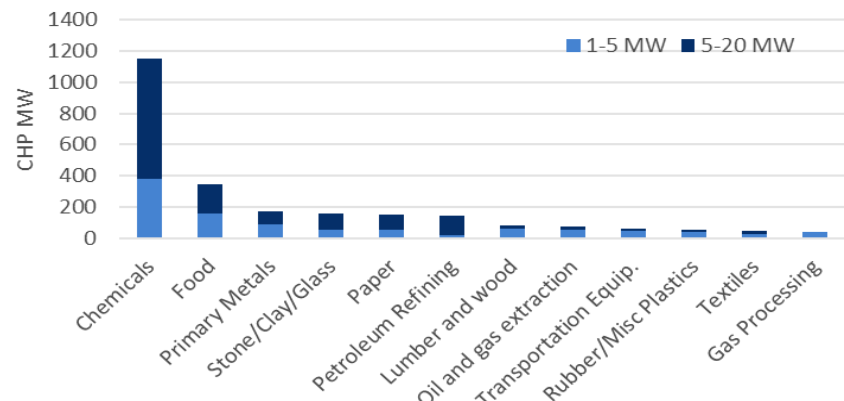


**Figure 27:** Distribution of the technical potential of small to medium-sized CHP for industrial applications in Texas

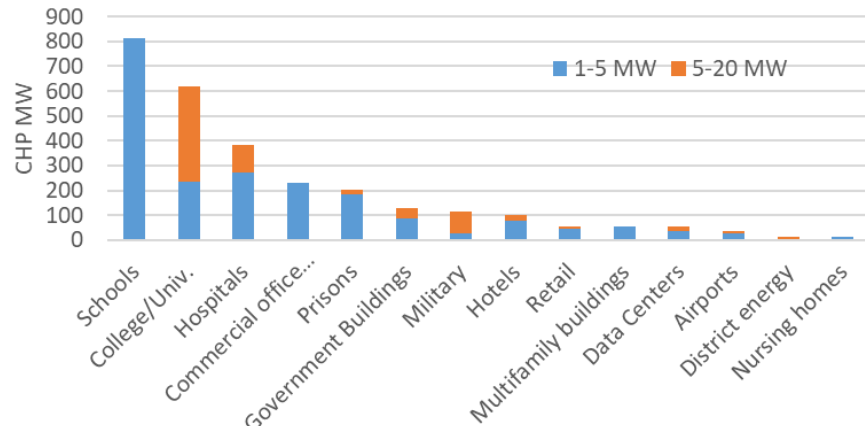


**Figure 28:** Distribution of the technical potential of small to medium-sized CHP for commercial applications in Texas

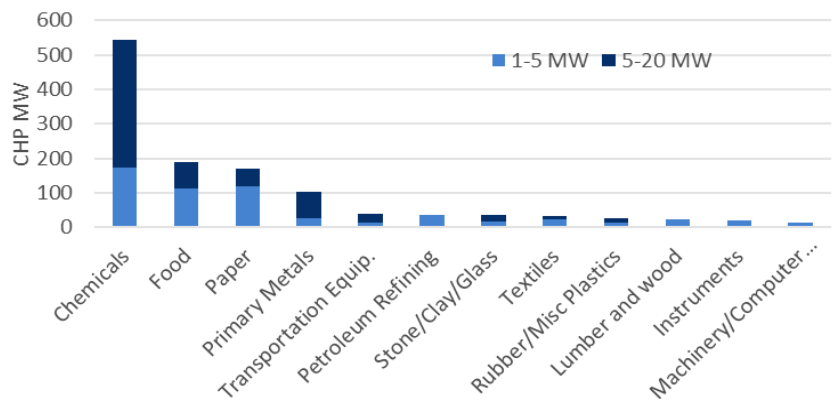


**Figure 29:** Distribution of the technical potential of small to medium-sized CHP for industrial applications in New York

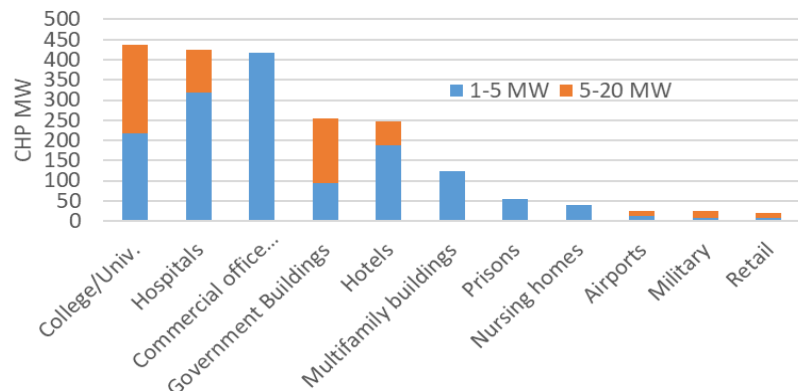


**Figure 30:** Distribution of the technical potential of small to medium-sized CHP for commercial applications in New York

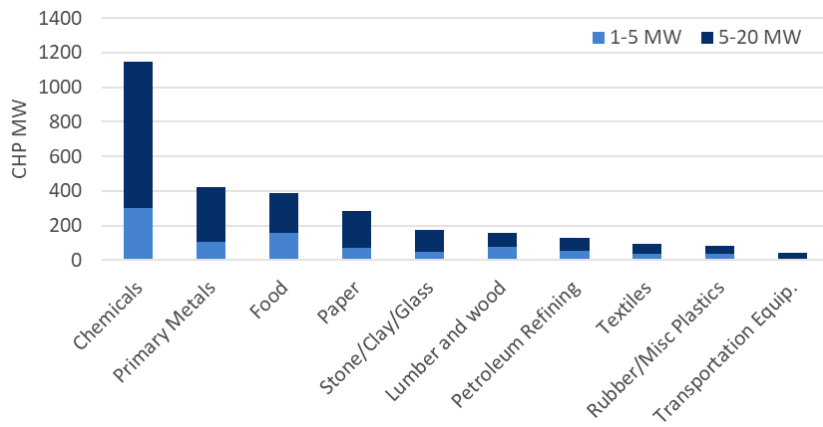


**Figure 31:** Distribution of the technical potential of small to medium-sized CHP for industrial applications in Pennsylvania

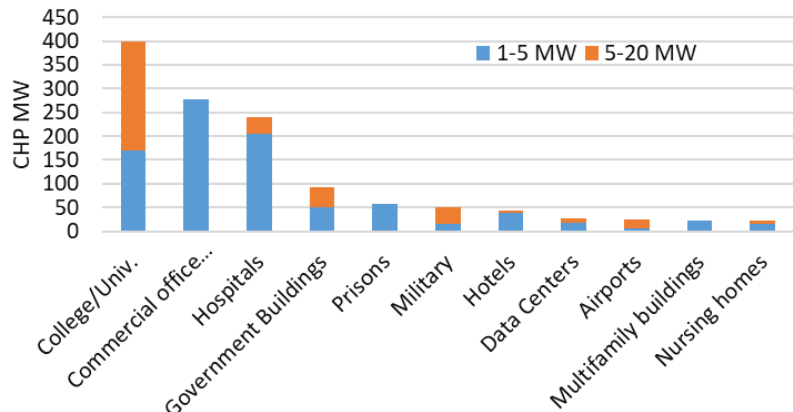


**Figure 32:** Distribution of the technical potential of small to medium-sized CHP for commercial applications in Pennsylvania

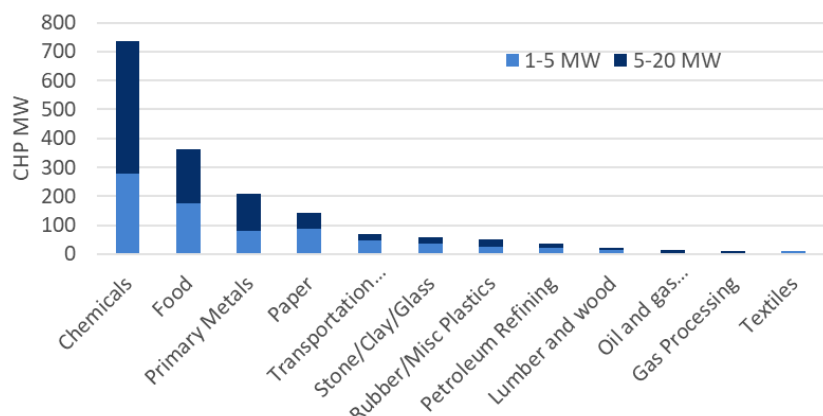


**Figure 33:** Distribution of the technical potential of small to medium-sized CHP for industrial applications in Illinois

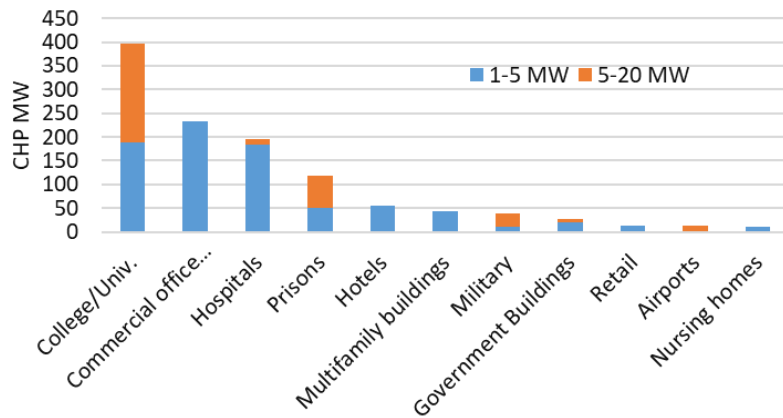


**Figure 34:** Distribution of the technical potential of small to medium-sized CHP for commercial applications in Illinois

#### 4.1.3 User cases selected for the feasibility analysis of converter-interfaced CHP

Based on the technical potential distribution of small to medium-sized CHP, five user cases presented in Table 5 are selected for the economic feasibility analysis of converter-interfaced CHP. Each of the user case represents a predominant application in each of the five leading ISO territories for small to medium-sized CHP potential. As indicated in Figure 24 the leading ISO territories include CAISO, ERCOT, NYISO, PJM and MISO. The Southeast electricity market which encompasses Florida through the Florida Reliability Coordinating Council (FRCC) is excluded from this ranking as it runs a traditional bilateral power transactions system and does not support a competitive energy and ancillary markets for DER like in the other ISOs precited<sup>29</sup>. The different ISO territories allow to evaluate the impact of the energy costs, seasonal variation of the thermal and electrical load profiles and grid code requirements

Application	ISO	System size	Primary Mover
College/Univ.	CAISO	4.4 MW	Combustion Turbine
Water Treatment plant	ERCOT	5.2 MW	Combustion Turbine
Hospital	NYISO	2.2 MW	Reciprocating Engine
Commercial Building	PJM	1.5 MW	Reciprocating Engine
Hotel	MISO	2.6 MW	Reciprocating Engine

**Table 5:** Selected five user cases for the economic feasibility analysis

<sup>29</sup> Electric Power Markets <https://www.ferc.gov/electric-power-markets>

#### 4.1.4 Challenges facing the interconnection of CHP systems in the distribution grid

Integration of small to medium-sized CHPs are typically governed by utilities grid codes or standards for DER interconnection due to the significant impact a +1MW CHP can potentially have on the hosting feeder's operation. Depending on the connection configuration i.e., directly coupled with the grid or through a converter, different guidelines will be imposed to the plant owner. In existing engineering practices CHP systems are directly connected to the electric networks. Such an option leads to thorough studies and validation that can extend readiness for parallel grid operation to years. In the evaluation process, expenses such as engineering studies, finance charges if debt for Capex is already contracted may occur. Additionally, any modification to the hosting facility or neighboring circuit such as new protection device, voltage regulator or any ancillary grid equipment required by the utility will need to be completed before "Permission to Operate can be granted". This imposes a financial burden that can eventually lead to the project failure. Figure 35 shows as an example the typical interconnection process for DER and the preferred aimed for by all owners of new CHP plants.

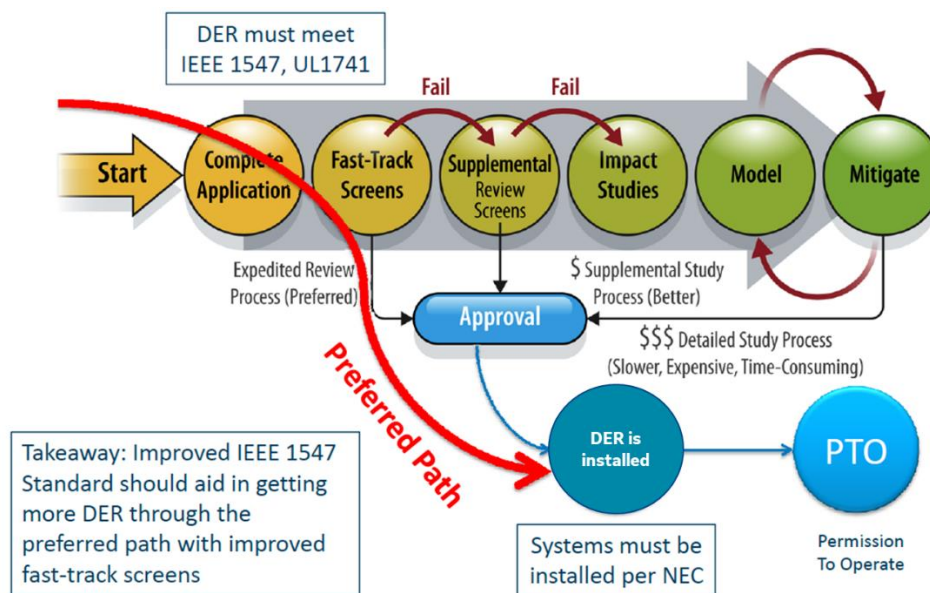


Figure 35: Typical interconnection process of DER<sup>30</sup>

Unlike in the directly-coupled scenario, small to medium-sized converter-interfaced CHP have significant chances to get to the preferred path thanks to the opportunity provided by the grid-ready inverter for easier and fast compliance to grid codes requirements<sup>31</sup> and

<sup>30</sup> U.S. Department of Energy (DOE). 2017. "Energy Transition Initiative: Islands—Sun Screens Maintaining Grid Reliability and Distributed Energy Project Viability through Improved Technical Screens" (DOE/GO-102017-4946). <https://www.nrel.gov/docs/fy17osti/67633.pdf>

<sup>31</sup> National Grid, Requirements for Parallel Generation Connected to National Grid Owned EPS, December 2019 [https://www9.nationalgridus.com/non\\_html/shared\\_constr\\_esb756.pdf](https://www9.nationalgridus.com/non_html/shared_constr_esb756.pdf)

DER standards IEEE 1547 and UL 1741<sup>32</sup>. The example of the National Grid interconnection requirements allows to observe the technical and economic benefits that the interface converter can provide to a small to medium-sized CHP project. It can be observed that inverter based generation requires less complex protection system including no breaker or current sensors and wires as compared to directly-coupled generation. Those features are indeed already included in commercial grid-ready inverters.

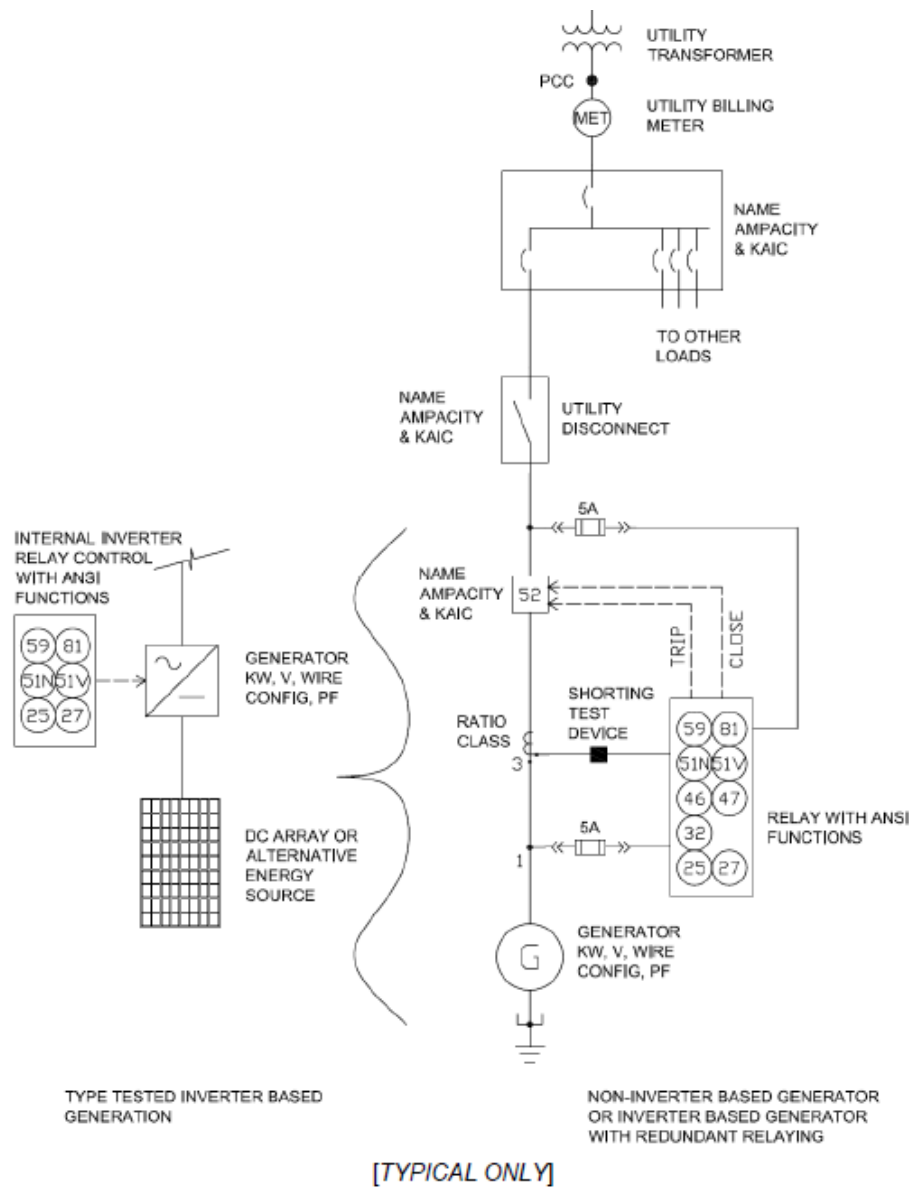


**Figure 36:** Typical interconnection equipment required for DER (National Grid)

<sup>32</sup> UL 1741, UL standard Inverters, Converters, Controllers and Interconnection System Equipment for Use With Distributed Energy Resources <https://standardscatalog.ul.com/ProductDetail.aspx?productId=UL1741>

#### 4.1.5 Federal and States incentives for CHPs

CHP project needs a high capital investment from the owner. While depending on factors such as the CHP capacity, the fuel type and its availability, the adopted prime mover, and the system configuration, the actual cost of a CHP project may vary between \$1,000 and \$5,000 per kW of the installed capacity while operational and maintenance costs of CHP systems can range from \$0.005 per kWh to \$0.015 per kWh<sup>33</sup>. In addition, preliminary feasibility studies and obtaining permits can cause tens of thousand dollars for potential CHP investors. To help promote the CHP system, the U.S. federal government together with state governments and utility companies has rolled out various financial incentive programs. The U.S. federal incentive for CHP systems is named “the federal Business Energy Investment Tax Credit (ITC)” and it provides 10% corporate tax credit for CHP projects placed in service after October 3, 2008 and before the end of Year 2021 as shown in Table 6<sup>34</sup>. For a CHP system with 15MW or less in capacity and with more than 60% energy efficiency, the full credit equal to 10% of expenditures with no maximum limit stated can be received while a larger CHP system up to a maximum of 50MW can qualify for a reduced tax credit equal to the ratio between the actual system capacity and 15MW. The efficiency requirement does not apply to CHP systems that use biomass for at least 90% of the system’s energy source but the credit may be reduced for less efficient systems<sup>34</sup>.

Technology	12/31/16	12/31/17	12/31/18	12/31/19	12/31/20	12/31/21	Future years
CHP Systems	10%	10%	10%	10%	10%	10%	N/A

**Table 6:** Federal government clean energy program

Along with the federal tax credit, financial incentives from state governments or local utilities are offered including rebates, grants, tax credits, and net metering. Some leading states with financial incentives are summarized in Table 7. States like California, New York, Pennsylvania and Rhode Island provide full or partial net metering program which supports the electricity export from DER like CHPs. For the self-generation incentive program (SGIP) in California, the state government provides grants and loans to CHP project with generation from a variety of sources. Specifically, from 2017, it is required that a minimum of renewable fuel is blended with the gas fueling CHP project to be qualified for the SGIP program. In 2018, the amount of renewable fuel is required to be at least 25% of the total fuel input, rising each year to 100% in 2020<sup>35</sup>.

<sup>33</sup> U.S. Department of Energy, Combined Heat and Power (CHP) Technical Potential in the United States : <https://betterbuildingssolutioncenter.energy.gov/sites/default/files/attachments/CHP%20Technical%20Potential%20Study%203-31-2016%20Final.pdf>

<sup>34</sup> U. S. Department of Energy, Business Energy Investment Tax Credit (ITC) <https://www.energy.gov/savings/business-energy-investment-tax-credit-itc>.

<sup>35</sup> California Public Utilities Commission, Self-Generation Incentive Program: <http://www.cpuc.ca.gov/sgip/>

State	Financial Incentive Program	Net Metering entitlement for CHP
California	Self-Generation Incentive Program	✓
Illinois	Public Sector CHP Pilot Program	
New York	NYSERDA'S Program	✓
Pennsylvania	Pennsylvania Energy Department Authority and Commonwealth Financing Authority's Alternative Clean Energy Program	✓
Rhode Island	National Grid's CHP Program	✓ only to renewable energy systems

**Table 7:** State incentives for CHP Systems<sup>36</sup>

For public sector CHP pilot program in Illinois, cash incentives are provided for CHP projects that increase energy efficiency of local governments, municipal corporations, public school districts, community college districts, public universities, and state/federal facilities. The program is structured to provide performance-based incentives during various stages of public sector projects, including after the design phase (\$75/kW), commissioning (\$175/kW), and after 12 months of measured operational performance (\$0.08/kWh or \$0.06/kWh depending on system efficiency)<sup>37</sup>.

In New York, the New York State Energy Research and Development Authority (NYSERDA) provides financial incentives of up to \$2.5 million for the installation of CHP systems with a capacity up to 3 MW in New York State. Customers can choose from a range of pre-approved, pre-packaged CHP systems, or if a system greater than 1 MW is desired, a custom-engineered option is also available. Typical CHP customers include industrial, commercial, institutional, and multifamily facilities<sup>38</sup>.

In Rhode Island, the utility company National Grid provides capacity incentives ranging from \$900/kW to \$1,250/kW, depending on the efficiency of the CHP system design and the host customer's commitment to implement other energy efficiency measures that reduce onsite energy consumption while the incentives will not exceed 70% of the total project costs<sup>39</sup>. Other states such as Taxes, North Carolina, and New Hampshire provide financial incentives for qualified CHP programs.

In summary, the government or utility companies' incentive programs can be categorized into three kinds:

<sup>36</sup> U.S. Environmental Protection Agency, Combined Heat and Power (CHP) Partnership- dCHPP (CHP Policies and Incentives Database). Available online: <https://www.epa.gov/chp/dchpp-chp-policies-and-incentives-database>

<sup>37</sup> Illinois Energy Resources Center, DCEO CHP Pilot Program. Available online: <http://www.erc.uic.edu/energy-efficiency/illinois-energy-now-programs/dceo-chp-pilot-program/>

<sup>38</sup> New York State Energy Research and Development Authority, Combined Heat and Power Program. Available online: <https://www.nyserda.ny.gov/All-Programs/Programs/Combined-Heat-and-Power-Program>

<sup>39</sup> National Grid, Cogeneration Program. Available online: <https://www.nationalgridus.com/RI-Business/Energy-Saving-Programs/Cogeneration>

- performance contracting such as the program in Illinois: local governments contract with CHP owners based on the energy performance to purchase, install, maintain CHP systems. These contracts with a promised performance guarantee to ensure the investment's success, are typically financed with money saved through reduced utility costs but the systems may also be financed using tax exempt lease-purchasing agreements
- State government programs such as in NY and California: these programs offer financial incentives for CHP projects which may include tax credits, rebates, and low-interest loans.
- utilities programs such as with National Grid in Rhode Island: some utilities offer financial assistance or rebates for CHP projects to help cover the costs of purchasing and installing CHP systems.

## 4.2 Evaluation of the economic benefits of interface converter for CHP coupling

### 4.2.1 *Return of Investment (ROI) calculations for CHP applications*

From a financial perspective, ROI evaluation is very critical in determining a project economic viability and performing a comparison among competing technologies. Thus, the formula of annualized ROI<sup>40</sup>, as shown in (15), is utilized to assess the economic feasibility of a converter-interface CHP system as opposed to its directly-coupled counterpart.

$$\text{Annualized ROI} = \frac{\text{total yearly net cash flow}}{\text{year 0 equity investment}} / \text{project life} \quad (1)$$

The calculation of yearly net cash flow is shown in Figure 37. It involves detailed parameters such as the Capital Expenditure (Capex) i.e., the cost of purchasing and installing the CHP system; the Operational Costs (Opex) i.e., the cost of operating the system including fuel costs, maintenance and insurance costs; the Revenues, i.e., from energy savings and export to the grid as well as participation in grid support services; the taxes and tax credits, the finance charges, etc. Some parameters for the ROI calculation are straightforward while some others are more complex to determine. A simplified proforma calculation which estimates the complex parameters was adopted, the main objective of this analysis being to establish a baseline for comparison between two competing technical solutions rather to establish the ROI for a given project and enter financial negotiations. Since the same financial assumptions are applied to the two competing scenarios (directly-coupled vs converter-interfaced) the ROI comparison is expected to be valid. Table 8 and Table 9 show respectively the financial parameters considered for the ROI calculation and the Capex & Opex costs. In Table 9, the data for directly-coupled CHP is from EPA's CHP catalog<sup>41</sup>; while the cost breakdown for converter-interfaced CHP is adjusted based on manufacturing data and engineering judgment. The converter is manufactured as a package, including the

<sup>40</sup> Investopedia. "A Guide to Calculating Return on Investment-ROI". [Online available]:

<https://www.investopedia.com/articles/basics/10/guide-to-calculating-roi.asp>

<sup>41</sup> U.S. EPA, "Catalog of CHP Technologies", September 2017. [https://www.epa.gov/sites/production/files/2015-07/documents/catalog\\_of\\_chp\\_technologies.pdf](https://www.epa.gov/sites/production/files/2015-07/documents/catalog_of_chp_technologies.pdf)

power electronics hardware, the control systems, and the switchgear. The interconnection costs are significantly reduced with a grid-ready converter, as well as the soft costs required for compliance with the grid code. When compared to the directly-coupled CHP system, the O&M cost for converter-interfaced CHP is slightly higher, due to the additional maintenance cost of the converter. More detailed information on the Capex, Opex, revenues, taxes, credits, and finance charges results can be found in parameters of each of the user cases studied.

### Yearly net cash flow:

**Revenue** (Avoided cost for purchasing electricity from grid + revenue from selling energy and ancillary service to grid + avoided cost for thermal )

Minus O&M (CHP O&M cost) (OPEX)

Minus Insurance premium (~0.5% CAPEX/yr)

Minus Property tax (~ 0.22% CAPEX/yr, OPEX)

Minus Property fuel cost for CHP (OPEX)

= **EBITDA (Earnings before interest, tax, depreciation and amortization)**

PLUS ITC (subsidy for CHP is 10% until year 2021)

Minus State tax Liability

Minus Federal tax Liability

Minus Debt payment (principal + interest)

= **Yearly net cash flow**

State tax Liability = (EBITDA – Debt interest – Depreciation) \* state tax rate

Federal tax Liability = (EBITDA – Debt interest – Depreciation - State tax Liability) \* federal tax rate

**Figure 37:** Proforma calculation of yearly net cash flow of CHP investment

<b>Equity hurdle rate [%]</b>	9%	<b>Federal Tax</b>	21%
<b>Insurance rate [% of CAPEX/yr]</b>	0.005	<b>Property Tax [% of CAPEX/yr]</b>	0.22%
<b>Project life [yr]</b>	20	<b>Debt rate [%/yr]</b>	4.50%
<b>Depreciation schedule</b>	15	<b>Debt tenor [yr]</b>	15
<b>ITC<sup>42</sup></b>	10%	<b>Debt [%]</b>	80%
<b>State Tax</b>	4%	<b>Equity [%]</b>	20%

**Table 8:** Financial parameters for the ROI calculations

<sup>42</sup> Business energy investment tax credit.

	Directly-coupled	Converter-interfaced
<b>CHP-primary mover [\$/kW]</b>	262.5	262.5
<b>CHP-gen [\$/kVA]</b>	112.5	112.5
<b>CHP-converter [\$/kVA]</b>	/	70
<b>Heat Recovery [\$/kW]</b>	500	500
<b>Interconnect/Electrical [\$/kW]</b>	100	20
<b>Exhaust Gas Treatment [\$/kW]</b>	500	500
<b>Engineering and Fees [\$/kW]</b>	175	87.5
<b>Labor/Materials [\$/kW]</b>	369	376.4
<b>soft cost [\$/kW]</b>	347	294.9
<b>O&amp;M cost [\$/MWh]</b>	19	19

**Table 9:** Capex and Opex parameters

One of the major components of the ROI calculation is the revenue, obtained from energy cost savings and transaction export with the grid. To estimate the annual revenue, the yearly energy output from the CHP needs to be calculated. This requires the plant loads profile and the energy prices data. The hourly thermal and electrical load profiles baseline used for the five selected user cases are obtained from the NREL database which lists examples of commercial loads<sup>43</sup>. For each user case, in addition to collecting the hourly electrical and thermal load data, the utility rate, the hourly energy and ancillary service prices, financial parameters, fuel price, and installed costs of CHP are also collected<sup>41</sup>. Timeseries simulations are performed in MATLAB™ 2017b for an entire year to calculate the annual revenues from the CHP system. The obtained results are used to calculate the yearly net cash flow and furthermore the annualized ROI. The summary of the approach used for the ROI calculation is shown Figure 38.

In this analysis, it is assumed that the excess power from CHP system will be for grid export and to provide grid ancillary services. The ancillary services entitlements of CHP systems from the selected user cases ISOs are summarized in Table 10. For regulation reserve, the service provider should be able to immediately increase or decrease output to follow Automatic Generator Control (AGC) signal (4s or 6s setpoints update). For 10 minutes (/30 minutes) spinning reserves, the provider should be synchronized to the grid and respond within 10 minutes (/30 minutes). For 10 minutes (/30 minutes) non-spinning reserve, the resource should be able to connect, synchronize and respond within 10 minutes (/30 minutes). Small to medium-sized CHP systems, in particular reciprocating engines, have fast response time that qualifying them for the ancillary services listed in Table 10.

<sup>43</sup> NREL database for commercial load.

[https://openei.org/datasets/files/961/pub/COMMERCIAL\\_LOAD\\_DATA\\_E\\_PLUS\\_OUTPUT/](https://openei.org/datasets/files/961/pub/COMMERCIAL_LOAD_DATA_E_PLUS_OUTPUT/)

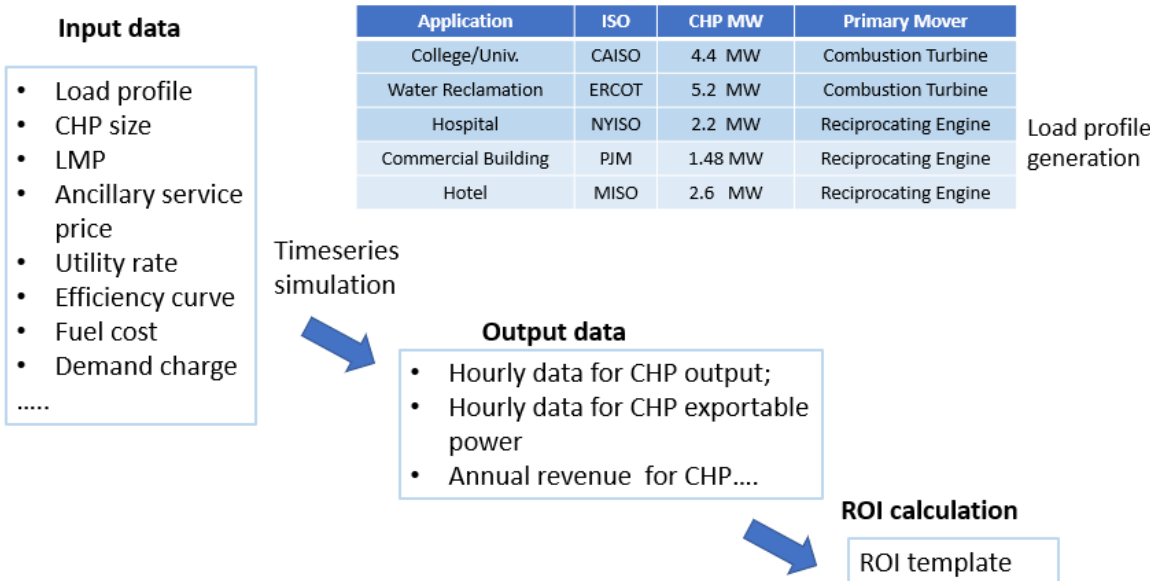


**Figure 38:** Summary of the approach for the evaluation of the economic performance of CHP systems

	Regulation		Contingency Reserve/ Operating Reserve			
	Reg Up	Reg Down	10min Spin	10min N-Spin	30min Spin	30min N-Spin
<b>CAISO</b>	√	√	√	√	--	--
<b>MISO</b>	√		√	√	--	--
<b>ISO-NE</b>	√		√	√	--	√
<b>NYISO</b>	√		√	√	√	√
<b>PJM</b>	√		√	√	--	--
<b>ERCOT</b>	√	√	√	--	--	√
<b>SPP</b>	√	√	√	√	--	--

**Table 10:** Summary CHP eligibility for ancillary services in different ISO territories

It is important to note that Table 10 focuses on regulation and contingency reserve only. However, CHP can provide additional services such as voltage support by exporting or importing reactive power to or from the grid. This is considered as a potential revenue source for CHP. The ROI calculation also includes production loss resulting from the delay in the interconnection process. The production loss from interconnection delays for directly-coupled CHP system is estimated to be approximately one year's net profits.

#### 4.2.2 Time-series simulations for the evaluation of revenue generation of CHP plants

The timeseries simulations are to evaluate hourly thermal and electrical energy outputs provided to the local loads, the performance of CHP system, capacity factor, fuel consumption as well as determining the amount of exportable energy to the grid. Most

previous similar studies only focus on active power generation. However, to better assess the CHP performance, particularly with the presence of the interface converter, reactive power operation needs to be included.

An hourly profile for a full calendar year is considered to capture daily and seasonal variations of local loads and therefore the dynamic amount of exportable energy to the grid. For each simulated hour, the operating region of CHP is determined first, then the output and exportable power from CHP based on the load demand, load power factor and ratings of the CHP unit. With additional calculations, the thermal output, system losses and fuel consumption are also obtained. All the CHP output data are used in the ROI calculations. The timeseries simulations are performed with MATLAB. As described in Figure 39, the CHP will fall in one of the three operating regions depending on its loading level. If the load ranges between the CHP maximum power output ( $kW_{CHP,max}$ ) and its minimum stable power output ( $kW_{CHP,min}$ ), the system will be able to satisfy the load; this regime is defined as operating region 1. If the plant load is above  $kW_{CHP,max}$  the CHP system will operate at its maximum power output; this regime is defined as operating region 2. If the load is below  $kW_{CHP,min}$ , the CHP will be shut down. CHP systems have lower efficiencies and uneconomic performance in small part loads in addition to an unstable operation. In this regime defined as operating region 3, the plant load is fully supplied by the grid except during islanding mode which is not considered in the ROI calculation.

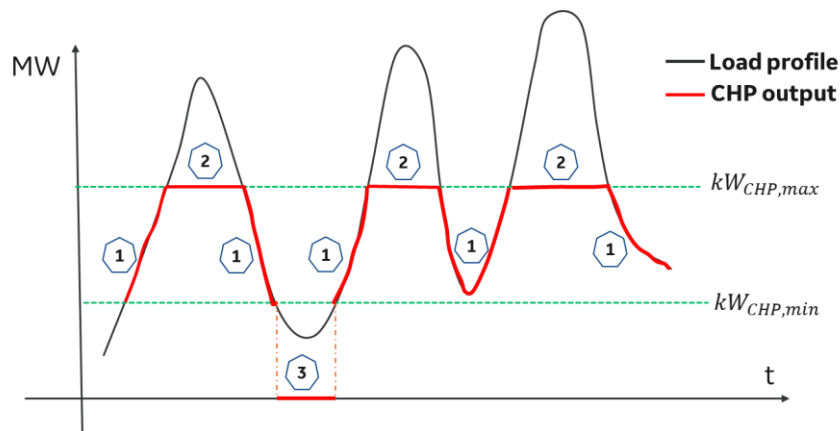


**Figure 39:** Operating regions of a CHP system used as DER

$kW_{CHP,max}$  and  $kW_{CHP,min}$  are the most critical constraints for operating CHP systems.  $kW_{CHP,max}$  is determined by the engine rated power while  $kW_{CHP,min}$  is imposed by economic and technical factors. The operating region is determined by the relationship between load requirement and CHP maximum and minimum output  $kW_{CHP,max}$ ,  $kW_{CHP,min}$ . In general,  $kW_{CHP,min}$  is set to 30% of  $kW_{CHP,max}$ <sup>44</sup>. An additional constraint is the power factor of generator. Synchronous generators have typically a

<sup>44</sup> Kesley Horowitz et al., "An Overview of Distributed Energy Resource (DER) Interconnection: Current Practices and Emerging Solutions". <https://www.nrel.gov/docs/fy19osti/72102.pdf>

minimum power factor  $\sim 0.8$  they can operate with a full load. At lower loads particularly in leading mode their power factor capability is also constrained above  $\sim 0.3$  for stable operation. For those reasons, the formulas governing directly-coupled CHP and converter-interfaced CHP system in each operating region are slightly different. The directly-coupled CHP generator is oversized by 25% to accommodate 0.8 power factor at rated active power (the engine size). However, with a converter interfacing CHP the generator does not need to be oversized as it always operates at unity power factor regardless of the load conditions. The grid-side inverter responsible to provide the required reactive power to the load is sized to accommodate at the minimum 0.8 power factor at full load. The inverter can be in fact sized for much lower power factor at full load if proven to be economically viable. The technical formulas for each operating region in each configuration are detailed as follows:

- **Operating region 1:**  $kW_{CHP,min} \leq kW_{load} \leq kW_{CHP,max}$

For Directly-coupled CHP system

In this region, the CHP system can satisfy all the load requirements on active power. The performance on reactive power depends however on the load power factor. If the power factor is low ( $< 0.6$ , which is uncommon), grid support is required for injecting additional reactive power. Thus, the formulas summarizing the CHP behavior are shown in equations (1) to (4). Specifically, for equation (2), when the power factor of load is no less than  $PF_{CHP,max-min}$ , the minimum operating power factor limit when CHP outputs the maximum active power, it indicates that CHP unit itself can satisfy load requirement on the reactive power. Thus, there is zero support necessary from the grid.

$$kW_{CHP}(t) = kW_{load}(t) \quad (2)$$

$$\text{If } PF_{load} \geq PF_{CHP,max-min}$$

Then

$$\begin{cases} kVar_{CHP}(t) = kVar_{load}(t) \\ kW_{grid}(t) = 0, kVar_{grid}(t) = 0 \end{cases} \quad (3)$$

$$\text{If } PF_{load} < PF_{CHP,max-min}$$

Then

$$\begin{cases} kVar_{CHP}(t) = \min \left( kVar_{load}(t), \sqrt{\min \left( \frac{kW_{CHP}(t)}{PF_{CHP,min}}, kVA_{CHP,max} \right)^2 - kW_{CHP}(t)^2} \right) \\ kW_{grid}(t) = 0 \\ kVar_{grid}(t) = kVar_{load}(t) - kVar_{CHP}(t) \end{cases} \quad (4)$$

The exportable active and reactive power to the grid are:

$$\begin{cases} kW_{CHP,exp}(t) = kW_{CHP,max} - kW_{load}(t) \\ kVar_{CHP,exp}(t) = \max\left(0, \sqrt{kVA_{CHP,max}^2 - kW_{CHP,max}^2} - kVar_{load}(t)\right) \end{cases} \quad (5)$$

*For converter-interfaced CHP*

The active power output of converter-interfaced CHP is similarly governed by equation (2). For the reactive power the maximum is only constrained by the rating of the grid-side inverter,  $kVA_{cvt,max}$ . The formulas for the converter-interfaced CHP are shown in equations (2), (6) and (7). The grid contribution is still 0.

$$\begin{cases} kVar_{CHP}(t) = 0 \\ kW_{grid}(t) = 0 \\ kVar_{grid}(t) = \max\left(0, kVar_{load} - \sqrt{kVA_{cvt,max}^2 - kW_{CHP}(t)^2}\right) \end{cases} \quad (6)$$

The exportable active and reactive power to the grid are as follows:

$$\begin{cases} kW_{CHP,exp}(t) = kW_{CHP,max} - kW_{load}(t) \\ kVar_{CHP,exp}(t) = \max\left(0, \sqrt{kVA_{cvt,max}^2 - kW_{CHP,max}(t)^2} - kVar_{load}(t)\right) \end{cases} \quad (7)$$

- **Operating region 2:  $kW_{load} > kW_{CHP,max}$**

In this region, the CHP system outputs its maximum active power:

$$kW_{CHP}(t) = kW_{CHP,max} \quad (8)$$

As previously, the reactive power depends on the interconnection method. The grid active and reactive power contributions are also indicated.

*For a directly-coupled CHP*

The reactive power output is the smaller between the maximum reactive power capable by the generator and the load requirement as shown in equation (9).

$$\begin{cases} kVar_{CHP}(t) = \min\left(kVar_{load}(t), \sqrt{\min\left(\frac{kW_{CHP}(t)}{PF_{CHP,min}}, kVA_{CHP,max}\right)^2 - kW_{CHP}(t)^2}\right) \\ kW_{grid}(t) = kW_{load}(t) - kW_{CHP}(t) \\ kVar_{grid}(t) = kVar_{load}(t) - kVar_{CHP}(t) \end{cases} \quad (9)$$

The exportable active and reactive power to the grid are:

$$\begin{cases} kW_{CHP,exp}(t) = 0 \\ kVar_{CHP,exp}(t) = \max\left(0, \sqrt{kVA_{CHP,max}^2 - kW_{CHP,max}^2} - kVar_{load}(t)\right) \end{cases} \quad (10)$$

For a converter-interfaced CHP

The reactive power is provided by the grid-side inverter, which is limited by its kVA rating.

$$\begin{cases} kVar_{CHP}(t) = 0 \\ kW_{grid}(t) = kW_{load}(t) - kW_{CHP}(t) \\ kVar_{grid}(t) = \max\left(0, kVar_{load}(t) - \sqrt{kVA_{cvt,max}^2 - kW_{CHP}(t)^2}\right) \end{cases} \quad (11)$$

The exportable active and reactive to the grid are :

$$\begin{cases} kW_{CHP,exp}(t) = 0 \\ kVar_{CHP,exp}(t) = \max\left(0, \sqrt{kVA_{cvt,max}^2 - kW_{CHP,max}(t)^2} - kVar_{load}(t)\right) \end{cases} \quad (12)$$

- **Operating region 3:  $kW_{load} < kW_{CHP,min}$**

In this operating region, the CHP system is shut down. The load request in active and reactive power is entirely fulfilled by the grid. Formulas are as follows:

$$\begin{cases} kW_{CHP}(t) = 0, kVar_{CHP}(t) = 0 \\ kW_{grid}(t) = kW_{load}(t), kVar_{grid}(t) = kVar_{load}(t) \end{cases} \quad (13)$$

If the CHP system is reconnected to the grid, the exportable active and reactive power to the grid are as (14) and (15) respectively for the directly-coupled and the converter-interfaced configurations:

For a directly-coupled CHP,

$$\begin{cases} kW_{CHP,exp}(t) = kW_{CHP,max} - kW_{load}(t) \\ kVar_{CHP,exp}(t) = \max\left(0, \sqrt{kVA_{CHP,max}^2 - kW_{CHP,max}^2} - kVar_{load}(t)\right) \end{cases} \quad (14)$$

For a converter-interfaced CHP,

$$\begin{cases} kW_{CHP,exp}(t) = kW_{CHP,max} - kW_{load}(t) \\ kVar_{CHP,exp}(t) = \max\left(0, \sqrt{kVA_{cvt,max}^2 - kW_{CHP,max}(t)^2} - kVar_{load}(t)\right) \end{cases} \quad (15)$$

#### 4.2.3 Results of the ROI calculations for the different user cases

Table 11 shows the results of the timeseries simulations and annualized ROI calculations for the NYISO hospital. This user case pictures a hospital located in Utica, NY hosting a 2,200kW reciprocating engine-based CHP system. The peak load of the hospital is 2,190kW, and the average hourly electrical load is 1,470kW. The average hourly thermal load is 2,573MBtu and the availability of CHP is 98%. Demand charge is \$3.52/kW/month and the hourly electricity rates are obtained from National Grid, the utility serving the hospital. Exportable active power of CHP can be monetized for one of the candidate services (energy, regulation reserve and 10-min spinning reserve). The 10-min non-spinning reserve is only applicable when CHP is shut down. Exportable CHP reactive power is utilized for voltage support at a price of \$2.792/kVar/year. The gas price is assumed to be \$4/MMBtu. For the two competing CHP architectures (directly-coupled and converter-interfaced) the engine is at the same size, however, the generator is oversized by 25% for the directly-coupled scenario. For the converter-interfaced configuration, although the converter eliminates the need for oversizing the generator the grid-side inverter needs to be rated at least similarly than the generator in directly-coupled to match the reactive power capability in both scenarios. Even if the cost of the full converter (rectifier + grid-side inverter) gets higher than that of the generator price, significant savings from interconnection costs, reduced production loss due shorter interconnection delays can be accounted for by the converter-interfaced configuration.

In the timeseries simulations, the energy efficiency of engine, generator, and converter is considered and quantified. The efficiency of the generator is affected by the loading level as well as by the power factor at its terminals<sup>45</sup> while for the converter only the loading level affects its efficiency.

As shown in Table 11, the converter-interfaced CHP system has a better ROI than the directly-coupled for the NYISO's hospital user case. Indeed, despite a slightly higher fuel cost due to the additional losses in the converter and less export revenue again impacted by the overall system efficiency, its Capex is lower thanks to the reduced generator size and interconnection costs. Additionally, its loss of production is reduced as the interface converter earns it up 1 year operation ahead of the directly-coupled with a streamlined interconnection process.

---

<sup>45</sup> FKI Energy Technology. Data sheets-three phase synchronous generators.

<http://www.powertechengines.com/MarelliData/Data%20Sheet/COMM.DSG.001.6%20GB.pdf>

User case parameters	Directly-coupled	Converter-interfaced
Engine size, kW	2,200	2,200
Generator size, kVA	3,000	2,310
Converter size, kVA	/	2,500
Capacity to peak ratio 1	1.005	1.005
Annual CHP output, kWh	12,607,529.34	12,732,548.99
Annual exportable CHP, kWh	5,671,091.46	5,508,267.01
% CHP usage	97.88%	97.86%
Annual Fuel consumption, MBTU	67,412,891.71	68,001,741.99
Table Annual Energy Cost Savings, \$	\$555,714.07	\$555,620.44
Annual Demand Charge Savings, \$	\$87,802.08	\$87,802.08
Annual Thermal Savings, \$	\$90,195.29	\$90,195.29
Annual Profit from exporting kW, \$	\$178,146.27	\$172,918.23
Annual Profit from exporting kVar, \$	\$1,498.14	\$699.44
Annual Revenue (no fuel cost), \$	\$913,355.85	\$907,235.48
CAPEX, \$	\$5,295,200.00	\$5,100,801.00
<b>ROI</b>	<b>7.04%</b>	<b>8.61%</b>

**Table 11:** Results of the timeseries simulations and ROI calculations for the hospital in NYISO

The fact sheets of the other four user cases are summarized in Figure 40 through Figure 43 and in Table 12. The ROI calculation results which includes the annual revenue, Capex and ROI for each user case are compiled in Table 13.

## College in CA



### Fact sheet

Location	SF, CA
Market sector	Education
Scenario of observation	Average Thermal
Engine size, kW	4400
Engine type	Combustion
Peak load, kW	18227
Capacity to peak ratio 1	0.241
Average electric load, kW	9703
Average thermal load, MBTU	15013
Availability of CHP	95%

- Demand charge is \$19.6/kW/month
- Exportable kW CHP is distributed between LMP, regulation reserve, 10 min spinning reserve in an optimized way; 10 min non-spinning reserve is applicable when CHP is shut down
- Exportable kVar CHP is eligible for resource adequacy: \$6/kW/year
- Gas price : \$7.24/MMBTU

	directly-coupled CHP	converter-interfaced CHP
Engine size, kW	4400	4400
Generator size, kVA	5500	4620
Converter size, kVA	/	5000
Annual CHP output, kWh	35,470,617.60	35,470,617.60
Annual exportable CHP, kWh	0.00	0.00
% CHP usage	41.73%	41.31%
Annual Fuel consumption, MBTU	136603513.70	137983347.17
Annual Energy Cost Savings, \$	\$1,953,380.81	\$1,908,591.88
Annual Demand Charge Savings, \$	\$1,415,462.36	\$1,379,839.91
Annual Thermal Savings, \$	\$723,709.14	\$731,019.33
Annual Profit from exporting kW, \$	\$0.00	\$0.00
Annual Profit from exporting kVar, \$	\$0.00	\$0.00
Annual Revenue (no fuel cost), \$	\$4,092,552.31	\$4,019,451.12

### ROI Results

	directly-coupled CHP	converter-interfaced CHP
CAPEX, \$	\$10,534,150.00	\$10,201,602.00
ROI	17.89%	18.80%

**Figure 40:** Fact sheet of a college user case in CAISO

## Water Reclamation in TX

Fact sheet		directly-coupled CHP	converter-interfaced CHP
Location	Dallas, TX	5200	5200
Market sector	Chemical	6500	5460
Scenario of observation	/	/	6250
Engine size, kW	5200	41,919,820.80	41,919,820.80
Engine type	Combustion	0.00	0.00
Peak load, kW	12500	51.30%	50.79%
Capacity to peak ratio	0.416	161440516.19	163071228.47
Average electric load, kW	9328	\$1,970,822.10	\$1,932,194.58
Average thermal load, MBTU	10718	\$232,917.55	\$226,879.07
Availability of CHP	95%	\$307,014.05	\$307,014.05
		Annual Profit from exporting kW, \$	\$0.00
		Annual Profit from exporting kVar, \$	\$0.00
		Annual Revenue (no fuel cost), \$	\$2,510,753.70
			\$2,466,087.70

- Demand charge is \$4/kW/month
- Exportable kW CHP is distributed between LMP, regulation reserve, 10 min spinning reserve in an optimized way; 30 min non-spinning reserve is applicable when CHP is shut down
- Gas price : \$ 3.27/MMBTU

### ROI Results

	directly-coupled CHP	converter-interfaced CHP
CAPEX, \$	\$12,449,450.00	\$12,104,166.00
ROI	10.28%	10.41%

**Figure 41:** Fact sheet of a water reclamation plant user case in ERCOT

## Large office building in PJM

Fact sheet		directly-coupled CHP	converter-interfaced CHP
Location	Pittsburg, PA	1480	1480
Market sector	Large office	1950	1625
Scenario of observation	Average thermal	/	2500
Engine size, kW	1480	12,245,662.08	12,245,662.08
Engine type	Reciprocating	0.00	0.00
Peak load, kW	20147	16.50%	16.33%
Capacity to peak ratio	0.073	47160173.15	47636538.53
Average electric load, kW	8474	\$609,758.60	\$570,970.66
Average thermal load, MBTU	1480	\$88,230.84	\$79,407.40
Availability of CHP	98%	\$314,125.48	\$317,298.46
		Annual Profit from exporting kW, \$	\$0.00
		Annual Profit from exporting kVar, \$	\$0.00
		Annual Revenue (no fuel cost), \$	\$1,012,114.92
			\$967,676.53

- Demand charge is \$4/kW/month
- Exportable kW CHP is distributed between LMP, regulation reserve, 10 min spinning reserve in an optimized way; 10 min non-spinning reserve is applicable when CHP is shut down
- Gas price : \$9.09/MMBTU

### ROI Results

	directly-coupled CHP	converter-interfaced CHP
CAPEX, \$	\$3,554,555.00	\$3,553,980.90
ROI	9.96%	6.02%

**Figure 42:** Fact sheet of a large office building user case in ERCOT

# Hotel in MN



## Fact sheet

Location	Minneapolis, MN
Market sector	Large hotel
Scenario of observation	Average Thermal
Engine size, kW	2600
Engine type	Reciprocating
Peak load, kW	2859
Capacity to peak ratio	0.909
Average electric load, kW	1664
Average thermal load, MBTU	8872
Availability of CHP	98%

- Demand charge is \$4/kW/month
- Exportable kW CHP is distributed between LMP, regulation reserve, 10 min spinning reserve in an optimized way; 10 min non-spinning reserve is applicable when CHP is shut down
- Gas price : \$6.56/MMBTU

	directly-coupled CHP	converter-interfaced CHP
Engine size, kW	2600	2600
Generator size, kVA	3565	2990
Converter size, kVA	/	3750
Annual CHP output, kWh	14,025,402.07	14,165,097.39
Annual exportable CHP, kWh	7,352,805.88	7,228,492.96
% CHP usage	96.22%	96.21%
Annual Fuel consumption, MBTU	80,301,992.89	81,337,841.29
Annual Energy Cost Savings, \$	\$674,452.98	\$674,088.22
Annual Demand Charge Savings, \$	\$316,461.68	\$316,469.70
Annual Thermal Savings, \$	\$386,006.00	\$390,985.25
Annual Profit from exporting kW, \$	\$211,124.57	\$208,040.61
Annual Profit from exporting kVar, \$	\$2,992.75	\$8,314.61
Annual Revenue (no fuel cost), \$	\$1,591,037.98	\$1,598,206.83

	ROI Results	
	directly-coupled CHP	converter-interfaced CHP
CAPEX, \$	\$4,783,925.00	\$4,928,230.00
ROI	15.42%	15.53%

Figure 43: Fact sheet of a hotel user case in MISO

	College in CAISO	Water Reclamation in ERCOT	Large office in PJM	Hotel in MISO
<b>Location</b>	SF, CA	Dallas, TX	Pittsburg, PA	Minneapolis, MN
<b>Market sector</b>	Education	Chemical	Large office	Large hotel
<b>Engine size, [kW]</b>	4,400	5,200	1,480	2,600
<b>Engine type</b>	Combustion	Combustion	Reciprocating	Reciprocating
<b>Peak load, [kW]</b>	18,227	12,500	20,147	2,859
<b>Capacity to peak ratio</b>	0.241	0.416	0.073	0.909
<b>Average electric load, [kW]</b>	9,703	9,328	8,474	1,664
<b>Average ther load, [MBTU]</b>	15,013	10,718	1,480	8,872
<b>Availability of CHP</b>	95%	95%	98%	98%

Table 12: Summary of the factsheets of the CAISO, ERCOT, PJM and MISO user cases

	Colledge in CAISO		Water Reclamation in ERCOT		Large Office in PJM		Hotel in MISO	
	Directly-coupled CHP	Converter-interfaced CHP	Directly-coupled CHP	Converter-interfaced CHP	Directly-coupled CHP	Converter-interfaced CHP	Directly-coupled CHP	Converter-interfaced CHP
<b>Annual Revenue</b>	\$4,092,552	\$4,019,451	\$2,510,753	\$2,466,087	\$1,012,114	\$967,676	\$1,591,037	\$1,598,206
<b>CAPEX</b>	\$10,534,150	\$10,201,602	\$12,449,450	\$12,104,166	\$3,554,555	\$3,553,980	\$4,783,925	\$4,928,230
<b>ROI</b>	17.89%	18.80%	10.28%	10.41%	9.96%	6.02%	15.42%	15.53%

Table 13: Summary of the ROI results for the five user cases analyzed

It can be observed that except for the PJM's large office building user case, the ROI for converter-interfaced is consistently higher than that of directly-coupled CHP. The driving reason is the same as in the NYISO hospital user case; the Capex for converter-interfaced CHP is lower than that of the directly-coupled thanks to the reduced size of generator and reduced interconnection costs. Production loss is also reduced. Therefore, despite slightly lower revenues due to the penalty in the converter efficiency, the annualized ROI of converter-interfaced CHP outperforms that of directly-coupled in most of the cases. In the PJM's large office building user case exception, the converter is heavily oversized acknowledging that only discrete ratings of inverters (for instance 1,250kVA and 2,500kVA are used) will be commercially available. That high Capex combined with the efficiency-penalized revenues do not allow the ROI to be superior to directly-coupled in this case.

In summary, results show that for majority of the user cases (4 out of 5) analyzed, a converter-interfaced CHP system outperforms a directly-coupled CHP system on annualized ROI. The converter-interfaced option trades generator size for reactive power with grid-ready inverter. As such, it allows the generator to consistently operate at unity power factor and the plant to benefit from higher reactive power support. The presence of the interface converter largely simplifies the interconnection process, allowing the CHP to be in production significantly faster than the directly-coupled option. This reduces the interconnection costs and delays which ultimately make the converter-interface CHP economically feasible and more profitable in many cases than a directly-coupled CHP. As compared to active power, reactive power is not currently highly valued by utilities. Upon increase of voltage support price, the converter-interfaced option is expected to be even more competitive than the directly-coupled. Another aspect that is not also well monetized is the increase reliability and resiliency of the plant in the presence of the converter. Because this configuration offers a more stable operation in islanding it's expected that more loads will be able to stay in operation in the event of grid loss. All these factors allow to consider the converter-interfaced CHP a better option than the directly-coupled. Section 4.3 evaluates the robustness of the calculated ROI against the variation of the many parameters that can affect the economics of CHP including size, costs, interconnection delays, energy price, load seasonal variations, and grid support services entitlements.

#### **4.3 Sensitivity analysis on the ROI of converter-interfaced CHP**

The dominant drivers making interfacing converter for CHP an economically viable option include: 1) trading generator size (25%) for converter which allows to streamline the interconnection process and achieves greater reactive power capability for grid support; 2) reduction of the costs of interconnection and production loss due to quicker approval to operate by the utility. This section further investigates the economics of converter-interfaced CHP and analyzes its sensitivity against the critical parameters that affect its profitability over directly-coupled. Such study is performed using an automatic toolkit for CHP ROI evaluation, which is built to enhance computation capability.

#### 4.3.1 Automatic toolkit for CHP ROI evaluation

As shown in section 4.2, the platform of the economic analysis consists of two major parts: the timeseries simulations and 2) the annualized ROI evaluation considering the Capex, Opex and financial parameters of the user case under evaluation. A sensitivity study requires to run tens to hundreds of scenarios for analyzing the impact of critical parameters, requiring a significantly high computation capability. Therefore, an automatic toolkit which automates the entire process of the ROI calculation is developed to efficiently run large number of case studies by varying any of the critical parameters listed. As shown in Figure 44, the process starts with assembling the input files. Based on the given parameters of the user case, such as location, CHP unit size and financial parameters, the toolkit fetches the corresponding load profile, utility rate, Locational Marginal Pricing (LMP) and ancillary service prices from the pre-established database pool, to generate the required input files and prepare the results file based on the template pool. The input files are then passed to the timeseries simulations platform which generates hourly energy outputs of the CHP system including with directly-coupled and interface converter configurations. The process continues with annualized ROI calculation and post-processing to output for the given scenario and user case, the calculated ROI.

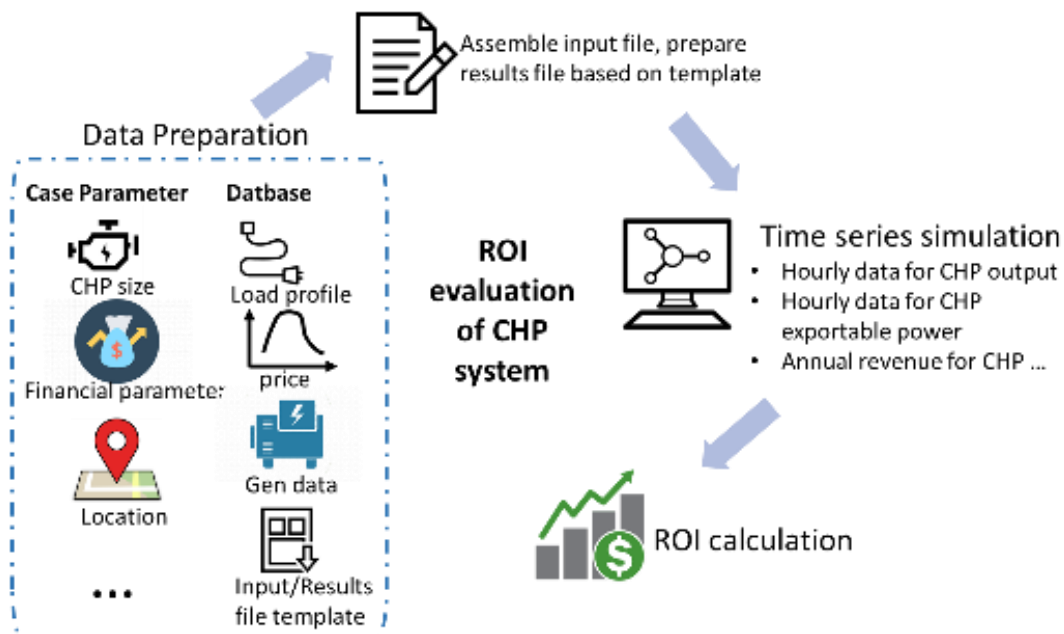


Figure 44: Automated simulation toolkit for CHP ROI evaluation

#### 4.3.2 Approach for the sensitivity analysis

The sensitivity analysis on the converter-interfaced CHP ROI is performed on user case location, CHP sizing scenario and other critical parameters including energy price, generator cost, converter cost, voltage support price, converter to engine size ratio and interconnection delay. Specifically, the converter to engine size ratio is calculated as the installed capacity of converter divided by the installed capacity of the prime mover. It

indicates the level of reactive power capability that can be monetized for grid support. The parameter of interconnection delay is the time consumed from the project initiation until “Permission to Operate” is granted by the hosting utility after all standard interconnection requirements (such as IEEE 1547) have been satisfied. The interconnection processing time for the directly-coupled CHP system is longer than that of the converter-interfaced configuration and the relative difference is considered as loss of production for the directly-coupled CHP system.

For this analysis the five representative user cases selected for ROI calculations and shown in Table 5 are extended to 25 scenarios. Basically, each of the user case is now studied in the 5 ISO territories leading to 5 applications across 5 ISO/RTO territories. This forces the change in load profile to correlate with customer behaviors (e.g., heating and cooling needs and season are different in CAISO and NYISO).

Power to Heat ratio, calculated as annual power consumption divided by annual thermal consumption, is a representative parameter for characterizing the various applications. Figure 45 describes the power to heat ratio for the 25 user cases. It can be observed that the ratio varies by location and application.

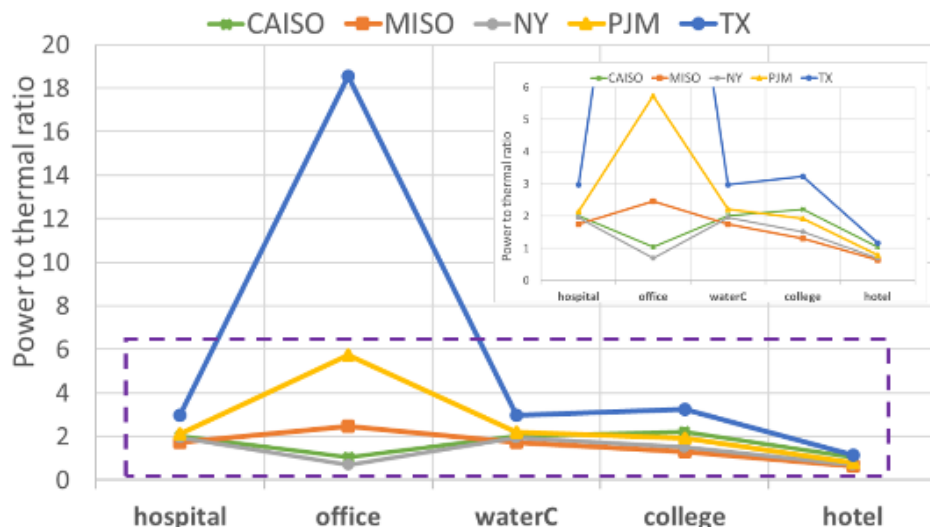


**Figure 45:** Power to thermal loads ratio in the investigated user cases

The factor of location bundles multiple sub-factors, such as fuel price, energy price and ancillary service price. Figure 46 shows the hourly LMP in the 5 ISOs in question from their market clearing price data in 2018. The dataset is available at each ISO’s official website. CAISO has a relatively higher LMP while NYISO and ERCOT have relatively the lowest. Table 14 summarizes the rest of the parameter settings for the baseline cases.

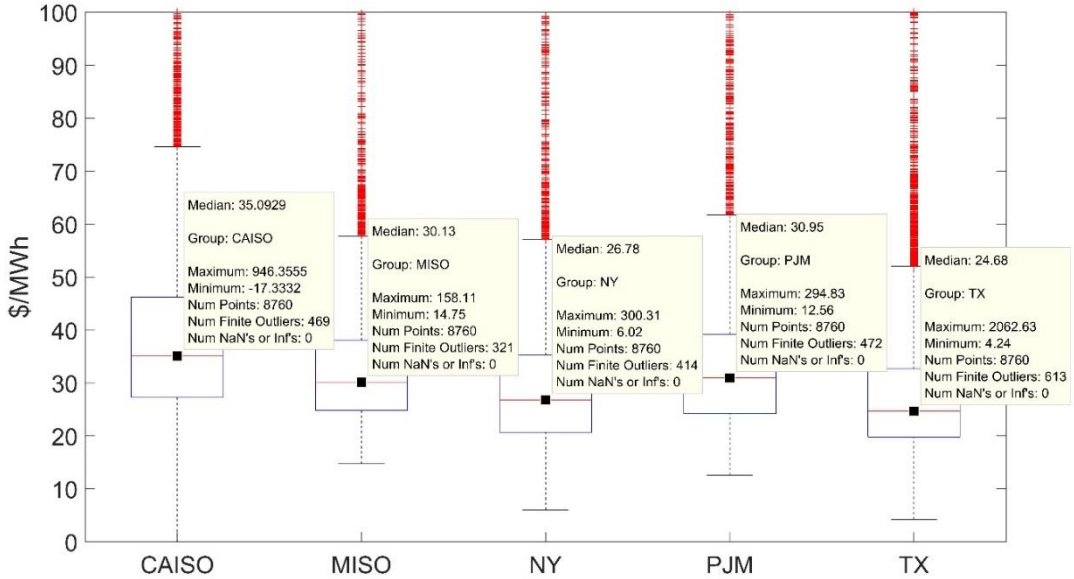


**Figure 46:** Box plot for hourly LMP in different ISO territories (2018 data)

Table 15 shows the ROI results calculated for the extended 25 user cases using the automatic toolkit. The number in each cell represents  $\Delta ROI$  (relative value) calculated as in equation (16). A positive number indicates that converter-interfaced CHP has a higher ROI in this application than directly-coupled. The numbers in parentheses indicate the ROI value for directly-coupled CHP.

$$\Delta ROI = \frac{(ROI_{converter} - ROI_{direct})}{ROI_{direct}} \quad (16)$$

	Gen. Cost, \$/kVA	Converter to engine size ratio	ISO	Voltage support price, \$/kVar
<b>Hospital</b>	44	1.7	<b>CAISO</b>	6
<b>Large office</b>	47	1.69	<b>MISO</b>	6
<b>Water Reclamation</b>	115	1.25	<b>NYISO</b>	2.79
<b>College/University</b>	117	1.42	<b>PJM</b>	3
<b>Hotel</b>	44	1.44	<b>ERCOT</b>	4

**Table 14:** Parameter settings for the baseline case

As shown in Table 15, for 19 out of 25 cases, the converter-interfaced CHP has a relatively higher annualized ROI with an average increase of 2.3% at  $\Delta ROI$ . From the perspective of locations, CAISO, MISO and ERCOT are highly favorable for converter-interfaced CHP as its comparative ROI is consistently higher than that of directly-coupled. Conversely, PJM and NYISO will be challenging territories. From the perspective of application, hospitals and hotels will be regularly more favorable for converter-interfaced CHP while college campuses will be the least favorable. The specific load profiles of colleges due to the

reduced summer loads and similar conditions for winter break are not favorable for installing the converter-interface CHP as the efficiency of interfaced converter drops for operating at partial-load condition and this reduces its profitability. Resizing the CHP system for smaller capacities might help improve the competitiveness of converter-interfaced CHP in those applications but this might defeat the overall benefits of installing the CHP. Indeed, the baseline results suggest that colleges are one of the most favorable application for CHP with an average ROI of ~ 13.94% across the five ISOs.

Application	CAISO	MISO	NYISO	PJM	ERCOT
Hospital	3.98% (18.73%)	3.51% (13.64%)	0.82% (10.26%)	1.25% (9.56%)	2.69% (10.08%)
Large office	9.15% (12.44%)	5.73% (12.87%)	1.94% (11.12%)	<b>-0.62%</b> (9.62%)	3.89% (10.08%)
Water Reclamation	3.48% (12.95%)	2.51% (11.21%)	<b>-4.78%</b> (10.52%)	<b>-9.68%</b> (9.68%)	0.70% (10.60%)
College/University	3.06% (14.78%)	1.30% (15.62%)	<b>-5.39%</b> (13.67%)	<b>-8.47%</b> (11.39%)	<b>-1.15%</b> (14.27%)
Hotel	4.67% (18.33%)	5.06% (15.63%)	1.12% (13.61%)	0.85% (13.49%)	2.23% (14.33%)

**Table 15:** ROI evaluation results for the extended 25 user cases

#### 4.3.3 *Impact of the CHP sizing scenario*

CHP has load following capability and can be set to track either the electrical or the thermal facility load. Three CHP sizing scenarios are typically adopted<sup>46</sup>: average thermal load, the most common sizing (denoted as “AvrgThem”) which gives results as in Table 15, average electric load (denoted as “AvrgElec”) and peak electric load (denoted as “PeakElec”). To analyze the impact of the CHP sizing on the profitability of converter-interfaced CHP, the “AvrgElec” and the “PeakElec” sizing were also analyzed which led to 50 additional user cases. Results are summarized in Table 16 and Table 17.

Application	CAISO	MISO	NYISO	PJM	ERCOT
Hospital	6.12%	5.78%	3.50%	1.52%	1.17%
Large office	9.10%	2.65%	2.39%	<b>-88.72%</b>	<b>-1.36%</b>
Water Reclamation	3.83%	4.35%	5.98%	<b>-9.11%</b>	9.70%
College/University	1.84%	1.88%	<b>-2.10%</b>	<b>-6.90%</b>	<b>-1.27%</b>
Hotel	6.38%	7.85%	3.86%	6.52%	3.98%

**Table 16:** ROI evaluation results (“AvrgElec”)

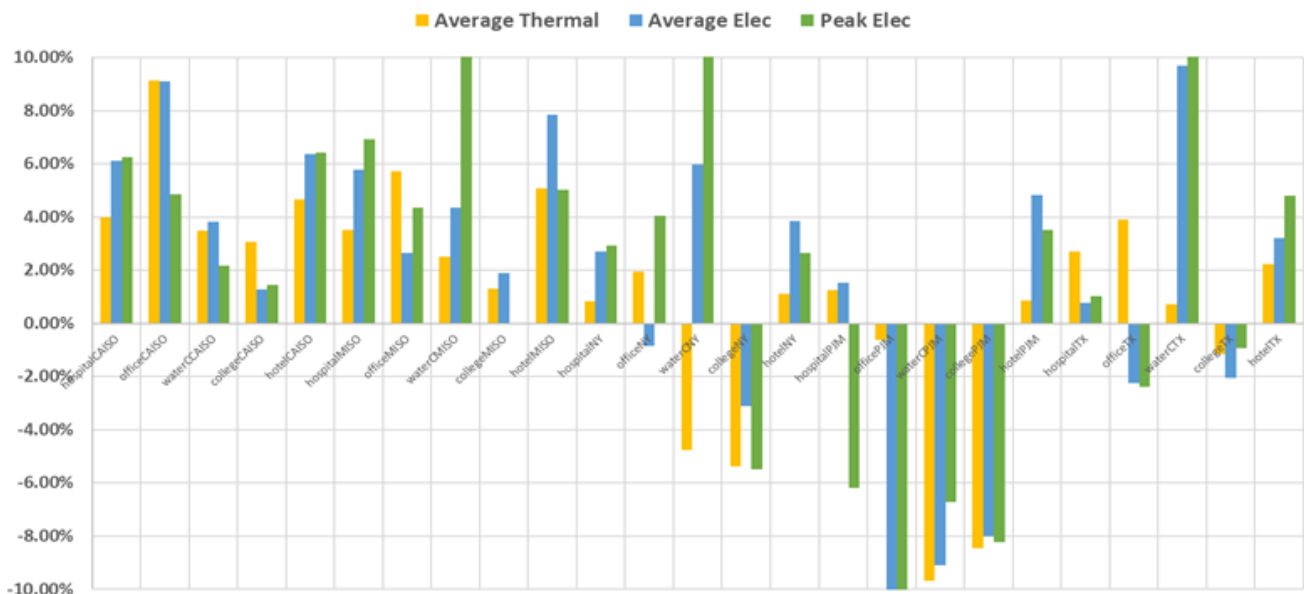
<sup>46</sup> Centrica Buisness Solutions. A guide to CHP unit sizing.

[https://www.centricabusinesssolutions.ie/sites/g/files/qehiga126/files/CBS\\_TECH\\_CHP\\_Unit%20sizing%20guide\\_A4\\_RGB.pdf](https://www.centricabusinesssolutions.ie/sites/g/files/qehiga126/files/CBS_TECH_CHP_Unit%20sizing%20guide_A4_RGB.pdf).

Application	CAISO	MISO	NYISO	PJM	ERCOT
Hospital	6.26%	6.92%	2.93%	<b>-6.20%</b>	1.02%
Large office	4.85%	4.34%	4.03%	<b>-18.24%</b>	<b>-2.39%</b>
Water Rec.	2.17%	22.34%	157.02%	<b>-6.73%</b>	49.66%
College/Univ.	1.43%	<b>-0.03%</b>	<b>-5.49%</b>	<b>-8.24%</b>	<b>-0.93%</b>
Hotel	6.41%	5.02%	2.65%	3.52%	4.81%

**Table 17:** ROI evaluation results (“PeakElec”)

Winning rate is defined as the proportion of user cases with positive  $\Delta\text{ROI}$  to the total number of user cases investigated. The winning rate for “AvrgElec” and “PeakElec” is 72% and 68%, respectively. Figure 47 describes the  $\Delta\text{ROI}$  of each user case among the three CHP sizing scenarios (overall 75 user cases). There are 19 cases in which the standard deviation of  $\Delta\text{ROI}$  is less than 3%, which indicates that CHP sizing scenario does not significantly impact the performance on relative profitability of converter-interfaced CHP to directly-coupled. For “WaterCNY”, “HospitalPJM” and “OfficeTX”, the best performance varies with CHP sizing scenario; while for “WaterCMISO”, “OfficePJM”, and “WaterCTX”, there is no change induced by the sizing scenario but the standard deviation of  $\Delta\text{ROI}$  is larger than 3%.

**Figure 47:**  $\Delta\text{ROI}$  for each use case by different CHP sizing scenarios

The varying factor behind CHP sizing scenario is in fact the prime mover size. For instance, in the “HospitalPJM”, the prime mover size is 2,200 kW, 4,800 kW and 6,800 kW for “AvrgThem”, “AvrgElec” and “PeakElec”, respectively, while the corresponding  $\Delta\text{ROI}$  is 1.25%, 1.52% and -6.2%. A possible explanation is the tradeoff between increased revenue by increasing engine size and energy outputs as compared to increased Capex. If the increase in revenue dominates (as in changing from “AvrgThem” to “AvrgElec”), the

converter-interfaced CHP will win more largely. On the other hand, if the increase in Capex dominates (as in changing from “AvrgElec” to “PeakElec”), the converter-interfaced loses in profitability and eventually becomes not competitive. However, this observation may not be generalized (example of hospital cases in PJM), since the profitability of converter-interfaced CHP over directly-coupled is impacted by multiple factors including the load profile. This analysis on the sizing impact can conclude that for most investigated user cases, CHP sizing scenario does not have a statistically significant effect on the profitability of converter-interface CHP over directly-coupled. However, it is recommended that the decisions on the CHP installation size should be made after evaluating all three CHP sizing scenarios, for a particular use case

#### **4.3.4 Evaluation of the most critical parameters impacting the economic feasibility of converter-interfaced CHP**

The ROI evaluation is a complex process, and many parameters contribute to it. This required narrowing the sensitivity analysis to six of the most critical parameters for the converter-interfaced configuration. Those parameters include the energy price, the voltage support price, the converter and generator cost, the converter to engine size ratio and the interconnection delay. CHP sizing by average thermal load is adopted to study the impact of these parameters since this sizing is the most common in CHP applications<sup>46</sup>. With the parameters listed in Table 18 a total of 325 scenarios have been processed. Results obtained are summarized in Table 19. They are shade-coded for better legibility. Darker shades indicate that the relative profitability of converter-interfaced CHP to directly-coupled is more sensitive to the variation of that parameter.

Critical parameters	Varying scenario	Critical parameters	Varying scenario
Energy price	Up 50%; Dn 50%	Generator cost	Up 25%; Dn 25%
Voltage support price	Up 50%; Dn 50%	Converter to engine size ratio	Up 25%; Dn 25%
Converter cost	4 cent/W; 8 cent/W	Interconnection delay	6 months; 18 months

**Table 18:** Critical parameters and varying scenarios

The overall conclusion is that the profitability of converter-interfaced CHP is highly sensitive to energy price, interconnection delay, converter cost and almost insensitive to generator cost and voltage support price.

Critical Parameter	Change in winning rate	Average change of $\Delta ROI$	Standard deviation of change in $\Delta ROI$
Energy price up 50%	<b>24.00%</b>	<b>2.75%</b>	<b>-2.40%</b>
Energy price dn 50%	<b>-36.00%</b>	<b>-21.33%</b>	<b>57.33%</b>
Converter cost at 8¢/W	<b>-36.00%</b>	<b>-2.61%</b>	<b>0.41%</b>
Converter cost at 4¢/W	8.00%	2.68%	-0.27%
Converter to engine size ratio up 25%	<b>-36.00%</b>	<b>-3.10%</b>	<b>1.92%</b>
Converter to engine size ratio dn 25%	8.00%	1.65%	0.08%
Interconnection delay as 18 months	8.00%	2.34%	0.89%
Interconnection delay as 6 months	-36.00%	-2.22%	-0.78%
Generator cost up 25%	0.00%	0.23%	-0.03%
Generator cost down 25%	0.00%	-0.23%	0.02%
Voltage support price up 50%	0.00%	0.17%	0.11%
Voltage support price dn 50%	0.00%	-0.17%	-0.08%

**Table 19:** Impact of critical parameters on the profitability of converter-interfaced CHP

#### *Impact of the generator cost*

Converter-interfaced CHP trades generator cost for converter cost therefore an increase of the generator cost (e.g., due to the class) is favorable for this option. Conversely a reduction in generator cost is unfavorable for the converter-interfaced CHP competitiveness but not as much as one could expect. Indeed, as in the NYISO's water reclamation case shown in Table 20, with generator cost declines by 25%, the Capex for converter-interfaced CHP decreases only by \$34k while for directly-coupled CHP it's \$38k reducing the Capex gap from \$32k to \$28k. This relative difference in Capex does not influence the comparison outcome, therefore generator cost does not significantly change the win position of converter-interfaced CHP.

#### *Impact of the converter cost*

As previously mentioned, it is required for directly-coupled CHP to size the generator to at least 125% of engine size for reactive power provision, while for converter-interfaced CHP the generator can be at same size of the engine. does not need to provide reactive power and therefore can be sized exactly to the engine. The saving on generator cost allows to partly offset the cost of the converter as observed in the Capex of most of the investigated cases. When converter cost increases by 50% from 6 ¢/W , the converter-interfaced CHP becomes less profitable, resulting in a 36% lower winning rate as shown in Table 19. When converter price is decreased to 4 ¢/W, the converter-interfaced CHP has a slightly better profitability with its winning rate going up by 8%. A significant decrease in converter cost

does not increase equally increase the winning rate since the 6 \$//W baseline converter price is already favorable.

	Base case		Generator cost down by 25%	
	<i>Directly coupled</i>	<i>Converter interfaced</i>	<i>Directly coupled</i>	<i>Converter interfaced</i>
Engine size, kW	1000	1000	1000	1000
Generator size, kVA	1320	1175	1320	1175
Converter size, kVA	/	1250	/	1250
Annual CHP output, kWh	6,165,883.50	6,194,046.43	6,165,883.50	6,194,046.43
Annual exportable CHP, kWh	1,714,235.37	1,672,884.92	1,714,235.37	1,672,884.92
% CHP usage	35.19%	35.00%	35.19%	35.00%
Annual Fuel consumption, MBTU	29,592,200.43	29,560,361.07	29,592,200.43	29,560,361.07
Annual Energy Cost Savings, \$	\$270,170.54	\$268,678.05	\$270,170.54	\$268,678.05
Annual Demand Charge Savings, \$	\$40,423.68	\$40,019.44	\$40,423.68	\$40,019.44
Annual Thermal Savings, \$	\$87,016.48	\$86,930.82	\$87,016.48	\$86,930.82
Annual Profit from exporting kW, \$	\$54,756.87	\$53,461.15	\$54,756.87	\$53,461.15
Annual Profit from exporting kVar, \$	\$0.00	\$0.00	\$0.00	\$0.00
Annual Revenue (no fuel cost), \$	\$452,367.56	\$450,414.87	\$452,367.56	\$450,414.87
<b>CAPEX, \$</b>	<b>\$3,032,224.47</b>	<b>\$3,000,476.82</b>	<b>\$2,994,274.47</b>	<b>\$2,966,695.57</b>
<b>ROI</b>	<b>10.52%</b>	<b>10.02%</b>	<b>10.96%</b>	<b>10.42%</b>

**Table 20:** Example of the water reclamation user case in NYISO

#### *Impact of the energy price*

The profitability of converter-interfaced CHP changes in the same direction as energy price. The winning rate increases by 24% when energy price goes up by 50% from the baseline value. Table 21 gives the example of the water reclamation case in ERCOT.

As previously mentioned, converter-interfaced CHP has relatively less efficiency due to additional energy loss in the converter particularly during part load conditions. The difference in yearly revenue between directly-coupled and converter-interfaced CHP can be estimated by:

$$(\eta_{direct} - \eta_{converter}) \times LMP \times 8760 \quad (17)$$

$\eta$  is the overall system efficiency. When the energy price increases two effects take place: 1) the revenue gap increases from \$2k to \$4k in favor of the directly-coupled option; and 2) the production loss due to the interconnection delay also increases; in this case by ~\$140k. Thus, higher energy prices significantly favor the converter-interfaced configuration.

	Base case		Energy price goes up 50%	
	Directly coupled	Converter interfaced	Directly coupled	Converter interfaced
Engine size, kW	1000	1000	1000	1000
Generator size, kVA	1320	1175	1320	1175
Converter size, kVA	/	1250	/	1250
Annual CHP output, kWh	6,165,883.50	6,194,046.43	6,165,883.50	6,194,046.43
Annual exportable CHP, kWh	1,714,235.37	1,672,884.92	1,714,235.37	1,672,884.92
% CHP usage 1	35.19%	35.00%	35.19%	35.00%
Annual Fuel consumption, MBTU	29,602,414.03	29,567,867.96	29,602,414.03	29,567,867.96
Annual Energy Cost Savings, \$	\$283,347.00	\$281,907.04	\$425,020.50	\$422,860.57
Annual Demand Charge Savings, \$	\$45,936.00	\$45,476.64	\$45,936.00	\$45,476.64
Annual Thermal Savings, \$	\$71,149.38	\$71,071.33	\$71,149.38	\$71,071.33
Annual Profit from exporting kW, \$	\$69,976.91	\$68,314.30	\$104,965.37	\$102,471.45
Annual Profit from exporting kVar, \$	\$0.00	\$0.00	\$0.00	\$0.00
Annual Revenue, \$	\$470,409.30	\$468,179.40	\$647,071.26	\$643,995.12
<b>CAPEX, \$</b>	<b>\$3,032,224.47</b>	<b>\$3,000,476.82</b>	<b>\$3,032,224.47</b>	<b>\$3,000,476.82</b>
<b>Cost of interconnection delay</b>	<b>\$90,832.22</b>	<b>/</b>	<b>\$230,339.34</b>	<b>/</b>
<b>ROI</b>	<b>10.60%</b>	<b>10.67%</b>	<b>25.60%</b>	<b>26.42%</b>

**Table 21:** Example of the water reclamation user case in ERCOT

#### *Impact of the voltage support price*

Voltage support price is attached to the revenue that can be obtained from exporting or absorbing reactive power to or from the grid. With higher voltage support price, converter-interfaced CHP will relatively earn more revenue and is expected to have a higher winning

rate. However, only 8 out of 25 use cases (5 application across 5 locations) have non-zero revenue from exporting reactive power, and in all these cases the converter-interfaced CHP is already more competitive. Higher voltage support prices just make the converter-interfaced CHP be more profitable as it would cost less to oversize the grid-side inverter than the directly-connected generator to earn more voltage support revenue. Table 19 confirms this statement however the impact is marginal as voltage support is still not highly monetized by utilities.

*Impact of the converter to engine size ratio*

As commercially available inverters come in discrete sizes, 1,250kVA is used as the increments for varying the size of the grid-side inverter. Discretely sized available products aggravate the oversizing. For instance, PJM's Hotel user case, when the converter to engine size ratio increases by 25%, there are two factors that take place. On one side the Capex increases by \$75k and the other side the capacity of the converter to provide voltage support to grid increases. A revenue increase from providing voltage support is noted even if this is only ~\$4.5k/year. Accrued for 20 years (project lifetime) it is ~\$90k that add to the revenue stream. However, larger Capex has multiple effects, such as rising debt payment, tax, insurance and other related payments, making the net yearly net cash flow increase to lower than \$4.5k. The compound impact is that the annualized ROI decreases and the converter-interfaced loses profitability against the directly-coupled. Thus, oversizing the interface converter (grid-side inverter only) is unfavorable for converter-interfaced CHP despite the potential increased revenue from voltage support.

Downsizing the inverter to the minimum acceptable does not change the winning rate as for most of the user cases, the grid-side inverter size is already close to the minimum required (1.25 p.u of the engine size).

*Impact of the interconnection delay*

A longer interconnection delay indicates a larger production loss for directly-coupled CHP and a more competitive converter-interfaced solution because energy revenues can be collected sooner. Thus, when the interconnection delay is reduced to 6 months from 1 year, the winning rate of converter-interfaced CHP declines by 36%. However, when the loss of interconnection delay increases from 1 year to 18 months, the winning rate of converter-interfaced CHP only increases by 8%, which indicates that at 1 year delay a converter-interfaced solution is already highly favorable for the CHP.

*Other observations*

To achieve more general conclusions about the winning rate of a predefined cases, the critical parameters variations are repeated for CHP sizing scenarios as in "AvrgElec" and "PeakElec". Thus, a total of 975 user cases are evaluated and the results are summarized in Figure 48. They reveal that for MISO and CAISO, converter-interfaced CHP is largely favorable regardless of the application; for ERCOT and NYISO it is typically favorable while for PJM it is rarely favorable and a case by case analysis should be conducted. In terms of

application, except for office buildings and college campuses, a converter-interfaced CHP is likely to be more profitable than a directly-coupled installation. Figure 48 provides the winning rate for each individual case which could serve as a reference when making selections on CHP interconnection solution.

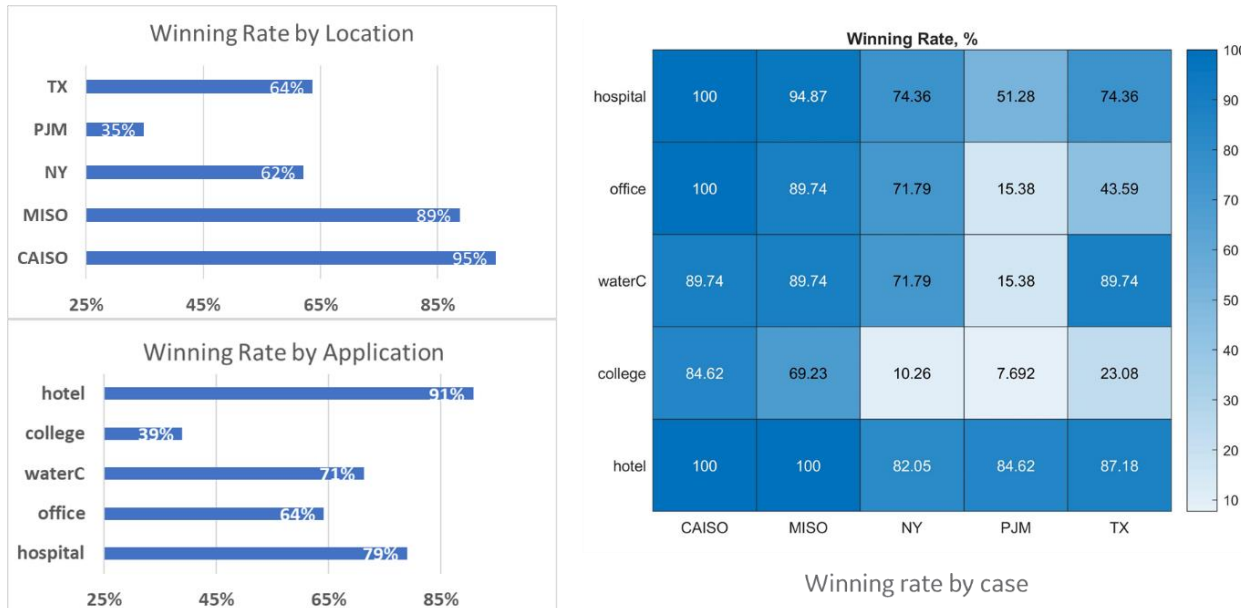


**Figure 48:** Converter-interfaced CHP winning rate by location, application and user case

#### 4.4 Analysis of the U.S Technical Potential of converter-interfaced CHP

Based on the promising results of the competitiveness of converter-interfaced CHP and the sensitivity analysis performed it is possible to estimate the U.S technical potential<sup>47</sup> of small to medium-sized CHP that would be more economically viable with a converter interface. This consist of determining whether an interface converter would improve the economics of a CHP plant at each of the 23,000+ identified sites by the U.S technical potential. To make such a determination, a simple model is built to capture the major economic factors in the tradeoff between a directly grid-coupled and converter-interfaced CHP plant. Each site is evaluated by the model yielding the more profitable topology. The sites favoring the converter-interfaced (C-I) solution over the directly-coupled (D-C) are totaled to estimate the size of the U.S technical potential of converter-interfaced CHP. This approach is obviously optimistic. However, the results can be interpreted similarly to those in the DOE U.S Technical Potential<sup>47</sup>, i.e., an estimation by state of the potential penetration of converter-interfaced CHP and extrapolation of the number facilities that can install CHP

<sup>47</sup> U.S. Department of Energy, Combined Heat and Power (CHP) Technical Potential in the United States: [https://betterbuildingssolutioncenter.energy.gov/sites/default/files/attachments/CHP\\_Technical\\_Potential\\_Study.pdf](https://betterbuildingssolutioncenter.energy.gov/sites/default/files/attachments/CHP_Technical_Potential_Study.pdf)

because of this new solution. The provided data is broken down by plant size, facility type, and location (state).

This analysis is different from the sensitivity study in 4.3 in that the sensitivity analysis examined in detail five sites in five ISOs to identify the parameters with the strongest effects on the converter interface profitability. This U.S technical potential analysis attempts to estimate of the future population of converter-interfaced CHP including inverters connected to the distribution grid that could provide grid support services (for instance voltage

#### 4.4.1 Basic comparison model

The model built for this analysis compares the major revenues and costs that differentiate the converter-interfaced and the directly-coupled solutions. Many otherwise important factors can be neglected because the addition of a converter has no effect on them, for instance the engine size or type. The factors that do vary between the converter-interfaced and the directly-coupled cases include revenue from energy sales, revenue from voltage support, generator cost, converter cost, and interconnection cost and delay. The economic model in equation (18) captures these quantities and evaluates the favorability of the converter-interfaced solution.

$$P_{\text{turb}} \left\{ 175200C_{\text{MWh}}\eta_{\text{conv}} + 20C_{\text{MVAR}} \left[ \sqrt{\left( \frac{S_{\text{conv}}}{P_{\text{turb}}} \right)^2 - 1} - 0.75 \right] - C_{\text{gen},1}^{\text{conv}} \right\} - S_{\text{conv}}(C_{\text{conv}} + C_{\text{IC}}^{\text{conv}}) - C_{\text{gen},0}^{\text{conv}} \geq P_{\text{turb}} [8760(20 - T_{\text{IC}})C_{\text{MWh}}\eta_{\text{DC}} - 1.25C_{\text{gen},1}^{\text{DC}} - 1.25C_{\text{IC}}^{\text{DC}}] - C_{\text{gen},0}^{\text{DC}} \quad (18)$$

where  $P_{\text{turb}}$  is the power rating of the turbine;  $C_{\text{MWh}}$ ,  $C_{\text{MVAR}}$  are the energy price per MWh of and the cost of MVAR of reactive power, respectively;  $\eta_{\text{conv}}$ ,  $\eta_{\text{DC}}$  are the overall electrical efficiencies of the converter-interfaced and the directly-coupled solutions, respectively.  $S_{\text{conv}}$  is the power rating of the converter and  $C_{\text{gen},1}^{\text{conv}}$ ,  $C_{\text{gen},0}^{\text{conv}}$ ,  $C_{\text{gen},1}^{\text{DC}}$ ,  $C_{\text{gen},0}^{\text{DC}}$  are the coefficients of the generator cost using a linear functions respectively for the converter-interfaced and the directly-coupled solutions.  $C_{\text{conv}}$ ,  $C_{\text{IC}}$  are respectively the converter cost per MVA and cost of interconnection.  $T_{\text{IC}}$  is the interconnection delay (in years) between the directly-coupled and the converter-interfaced solution. To use the above model, both sides of equation (18) must be calculated. If the inequality holds, then the converter-interfaced solution is considered superior. Inversely, if the inequality does not hold, then directly-coupled solution is considered superior.

Examining the terms individually, the first term represents the revenue from selling energy hourly to the grid in the converter-interfaced case. The coefficient represents the number of hours in 20 years. The second term represents the increased revenue from voltage support (selling reactive power) in the converter-interfaced case over the directly-coupled case. This can be seen from the definition of reactive power  $Q$ :

$$Q_{\text{conv}} = P_{\text{turb}} \sqrt{(S_{\text{conv}}/P_{\text{turb}})^2 - 1}, \quad Q_{\text{DC}} = \sqrt{S_{\text{gen}}^2 - P_{\text{turb}}^2}, \quad S_{\text{gen}} = 1.25P_{\text{turb}} \quad (19)$$

$$\Rightarrow Q_{\text{DC}} = 0.75P_{\text{turb}} \quad (20)$$

Therefore, the term in square brackets simply represents the difference in reactive power capacity of the converter-interfaced solution over the directly-coupled solution. Because voltage support is priced for annual capacity, the coefficient accounts for the 20-year lifetime of the project. Table 23 shows the average wholesale electricity prices and voltage support prices, respectively, for the different ISO in the U.S.

The third term and the last term on the LHS of equation (18) together represent a linear cost function for the generator in the converter-interfaced case  $C_{\text{gen}}^{\text{conv}}$ . The fourth and fifth terms represent the cost of the converter and of the interconnection in the converter-interfaced case.

$$C_{\text{gen}}^{\text{conv}} = P_{\text{turb}} C_{\text{gen},1}^{\text{conv}} + C_{\text{gen},0}^{\text{conv}} \quad (21)$$

On the RHS of equation (18), the first term represents the revenue from selling energy to the grid in the directly-coupled case. The term  $8760(20 - T_{\text{IC}})$  represents the number of hours that the turbine is operational accounting for the interconnection delay of the directly-coupled solution. Similarly, to equation (21), the second and last terms on the RHS together represent a linear cost function for the generator in the directly-coupled case  $C_{\text{gen}}^{\text{DC}}$ . The third term on the RHS represents the interconnection cost in the directly-coupled case. The 1.25 coefficients for the second and third terms on the RHS capture the higher generator size required in the directly-coupled as compared to the converter-interfaced solution.

Table 22 below contains values for certain model parameters. The efficiency values are averages obtained from the timeseries simulations in section 4.2.3.

$\eta_{\text{conv}}$	93.1%	$\eta_{\text{DC}}$	93.2%
$T_{\text{IC}}$	12 months	$C_{\text{conv}}$	6 ¢/VA

**Table 22:** Known parameters for the U.S technical potential estimation

ISO/RTO	Average Energy Price [\$/MWh]
CAISO	\$39.46
MISO	\$33.19
ISO-NE	\$32.21
NYISO	\$31.05
NW	\$30.25
PJM	\$35.57
SE	\$26.96
SW	\$49.70
SPP	\$25.02
ERCOT	\$33.47
AK	\$85.50
HI	\$130.50

(a): Average cost of electricity for each ISO/RTO<sup>48,49,50,51,52,53</sup>

ISO/RTO	Voltage Support Price [\$/MVAR/year]
CAISO	\$6000.00
MISO	\$6000.00
ISO-NE	\$2190.00
NYISO	\$3919.00
NW	-
PJM	\$3000.00
SE	-
SW	-
SPP	-
ERCOT	\$4000.00
AK	-
HI	-

(b): Voltage support prices for each ISO/RTO<sup>49</sup>

**Table 23:** Average cost of electricity and price for reactive power in different ISO

The coefficients of the linear function of generator cost were found as shown in Figure 49.(a) by performing a piecewise linear regression of the generator price versus its size.

<sup>48</sup> ISO New England, “Monthly LMP Indices,” 2019 [Online]. Available: <https://www.iso-ne.com/transform/csv/monthlylmpindex?year=2019>

<sup>49</sup> Northwest Power and Conservation Council, “Seventh Northwest Conservation and Electric Power Plan: Chapter 8,” 2016 [Online]. Available: [https://www.nwcouncil.org/sites/default/files/7thplanfinal\\_chap08\\_priceforecast\\_1.pdf?sm\\_au=iVVNFSjfDDH16kDsML8tvK34L00HF](https://www.nwcouncil.org/sites/default/files/7thplanfinal_chap08_priceforecast_1.pdf?sm_au=iVVNFSjfDDH16kDsML8tvK34L00HF)

<sup>50</sup> Southwest Power Pool, “LMP By Location,” 2018 [Online]. Available: <https://marketplace.spp.org/file-browser-api/download/da-lmp-by-location?path=%2F2018%2F12%2FDA-LMP-MONTHLY-SL-201812.csv>

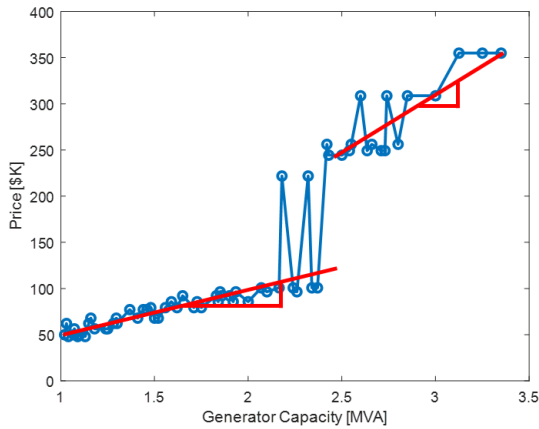
<sup>51</sup> Southern Company, “Auction Clearing Prices,” 2019 [Online]. Available: [https://www.southerncompany.com/about-us/energy-auction/auction-clearing-prices.html?sm\\_au=iVVNFSjfDDH16kDsML8tvK34L00HF](https://www.southerncompany.com/about-us/energy-auction/auction-clearing-prices.html?sm_au=iVVNFSjfDDH16kDsML8tvK34L00HF)

<sup>52</sup> U.S. Energy Information Administration, “Electric Power Annual 2018,” 2018 [Online]. Available: <https://www.eia.gov/electricity/annual/pdf/epa.pdf>

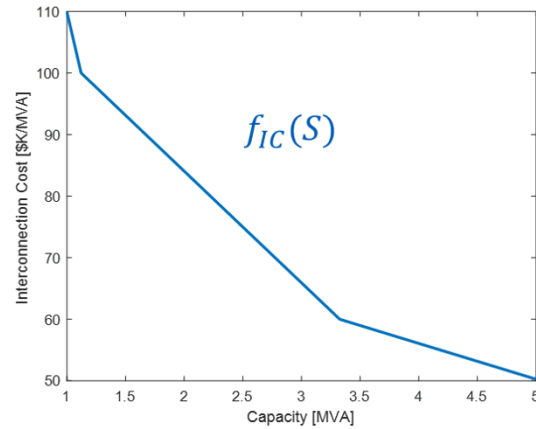
<sup>53</sup> Arizona Public Service, “Rate Schedule E-32 L,” 2017 [Online]. Available: [https://www.aps.com/-/media/APS/APSCOM-PDFs/Utility/Regulatory-and-Legal/Regulatory-Plan-Details-Tariffs/Business/Business-NonResidential-Plans/e32\\_Large.ashx](https://www.aps.com/-/media/APS/APSCOM-PDFs/Utility/Regulatory-and-Legal/Regulatory-Plan-Details-Tariffs/Business/Business-NonResidential-Plans/e32_Large.ashx)

Manufacturer listed prices<sup>54</sup> were increased by 40% to account for installation costs. The resulting model for generator cost  $C_{\text{gen}}$  as a function of capacity  $S_{\text{gen}}$  follows:

$$C_{\text{gen}} = \begin{cases} \$12K + S_{\text{gen}} \left( \frac{\$41K}{\text{MVA}} \right), & S_{\text{gen}} < 2.5 \text{ MVA} \\ -\$68K + S_{\text{gen}} \left( \frac{\$128K}{\text{MVA}} \right), & S_{\text{gen}} \geq 2.5 \text{ MVA} \end{cases} \quad (22)$$



(a): Linear regression of generator cost as function of capacity



(b): Linear interpolation of interconnection cost as function of system size

**Figure 49:** Cost of generator and interconnection for CHP applications

As shown in Figure 49.(b), the cost of interconnection was determined via linear interpolation of the data shown in Table 24<sup>55</sup>. The parameters  $C_{\text{IC}}^{\text{conv}}, C_{\text{IC}}^{\text{DC}}$  are then determined as follows:

$$C_{\text{IC}}^{\text{conv}} = 0.5f_{\text{IC}}(S_{\text{conv}}), \quad C_{\text{IC}}^{\text{DC}} = f_{\text{IC}}(1.25P_{\text{turb}}) \quad (23)$$

where the coefficient of 0.5 is added to the converter-interfaced case to reflect the reduced interconnection cost as compared to directly-coupled.

<b>Nominal capacity (kVA)</b>	100	633	1121	3326	9341
<b>Interconnection cost (\$/kVA)</b>	\$250	\$140	\$100	\$60	\$25

**Table 24:** CHP interconnection costs as function of the generator size

<sup>54</sup> Marathon Generators, “Generators Selection and Pricing Catalog,” 2015:

<https://www.marathongenerators.com/generators/docs/manuals/GPN006.pdf>

<sup>55</sup> U.S. Environmental Protection Agency Combined Heat and Power Partnership, “Catalog of CHP Technologies,”

2014. Available: [https://www.epa.gov/sites/production/files/2015-07/documents/catalog\\_of\\_chp\\_technologies.pdf](https://www.epa.gov/sites/production/files/2015-07/documents/catalog_of_chp_technologies.pdf)

Unlike generators that are available in nearly every possible relevant capacity, converters are only available in discrete capacities. For this analysis, it is assumed that converters are available in integer multiples of 1.25 MVA. To also account for the reactive power requirements, the converters are sized as:  $S_{\text{conv}} = 1.25 \times \text{ceil}(P_{\text{turb}})$  where the  $\text{ceil}(\cdot)$  function represents rounding up to the next integer.

The final variable in the model is the turbine capacity  $P_{\text{turb}}$ . The values for  $P_{\text{turb}}$  are determined from the U.S Technical Potential<sup>47</sup> which identifies the number of potential CHP sites in each of the 50 states as well as the total capacity of all the sites in each state. However, the specific individual capacity of each site is not provided. To cope with the lack of detailed site data, a simple statistical approach was adopted. The average site capacity  $P_{\text{turb}}^{\text{avg}}$  is determined for each category as shown in Table 25 for the state of New York as an example. Then, a linear probability density function (pdf) is estimated for each category in each state. For example, the coefficients  $\alpha, \beta$  of the pdf for 1MWe to 5MWe New York industrial sites  $f(x) = \alpha x + \beta$  are determined from the following conditions:

$$\int_1^5 f(x) dx = 1, \int_1^5 x f(x) dx = P_{\text{turb}}^{\text{avg}} \quad (24)$$

where  $P_{\text{turb}}^{\text{avg}} = 2.17$  MW and  $x$  is a random variable that represents site capacity for that category. The first condition is the definition of a pdf, and the second condition ensures that the mean value of the distribution is equal to the average capacity for that category from the data. Similarly, a pdf is constructed for 1MWe to 5MWe New York commercial sites using equation (24) where  $P_{\text{turb}}^{\text{avg}} = 1.55$  MW.

	Number of Sites	Total Capacity (MW)	Avg. Capacity (MW)
1-5 MW	177	384	2.17
5-20 MW	46	448	9.74

(a): industrial technical potential CHP

1-5 MW	143	222	1.55
5-20 MW	22	191	8.68

(b): commercial technical potential CHP

**Table 25:** New York state industrial and commercial technical potential for CHP<sup>47</sup>

The 5MWe to 20MWe New York industrial sites pdf  $g(y)$  is determined from similar conditions to equation (25):

$$\int_5^{20} g(y) dy = 1, \int_5^{20} y g(y) dy = P_{\text{turb}}^{\text{avg}} \quad (25)$$

where  $P_{\text{turb}}^{\text{avg}} = 9.74 \text{ MW}$  and  $y$  is a random variable that represents site capacity for that category. Similarly, a pdf is constructed for the 5MWe to 20MWe New York commercial sites using equation (25) where  $P_{\text{turb}}^{\text{avg}} = 8.68 \text{ MW}$ .

Sampling from these distributions yields individual site capacities for each category. In the case of New York, the 1MWe to 5MWe industrial pdf is sampled from 177 times, the 1MWe to 5MWe commercial pdf is sampled from 143 times, the 5MWe to 20MWe industrial pdf is sampled from 46 times, and the 5MWe to 20MWe commercial pdf is sampled from 22 times. For each individual site with an estimated capacity  $P_{\text{turb}}$ , equation (18) is evaluated to determine whether the converter-interfaced or the directly-coupled solution is superior. This process is repeated for all 50 states. Because the 5MWe to 20MWe sites are rarely implemented as a single large genset, this analysis assumes that these sites are staged with multiple smaller gensets in parallel. It is assumed that the site capacity is achieved using the minimum number of stages where each stage is between 1 and 3.5MWe. For the multistage sites, the LHS and RHS of equation (18) is applied to each stage, and then summed to determine whether all stages in aggregate favor the converter-interfaced or the directly-coupled solution.

#### 4.4.2 Comparison model with MVA demand charge

Rather than applying demand charge on the active power (MW) as in today's general practices, it is possible that in the future, with the revalorization of reactive power, utilities apply demand charge to the total MVA demand. This section explores the effects of a demand charge for MVA on the comparative economics of converter-interfaced and directly-coupled CHP. An MVA demand charge adds two terms to equation (18) and modifies the voltage support term. The added terms account for the cost of the demand charge for the C-I solution  $C_{\text{dem}}^{\text{conv}}$  and the D-C solution  $C_{\text{dem}}^{\text{DC}}$ :

$$C_{\text{dem}}^{\text{conv}} = 240S_{\text{pd}}^{\text{conv}}C_{\text{MVA}}, \quad C_{\text{dem}}^{\text{DC}} = 12(20 - T_{\text{IC}})S_{\text{pd}}^{\text{DC}}C_{\text{MVA}} \quad (26)$$

where  $C_{\text{MVA}}$  is the demand charge per MVA and  $S_{\text{pd}}^{\text{conv}}, S_{\text{pd}}^{\text{DC}}$  are the peak apparent power demands from the grid of the converter-interfaced and directly-coupled systems, respectively. The coefficients also take into account that demand charge is billed monthly. In the converter-interfaced case, there are 240 months in 20 years while in the directly-coupled case, the  $20 - T_{\text{IC}}$  accounts for the interconnection delay. Equation (26) can be rewritten in terms of real power and power factor:

$$C_{\text{dem}}^{\text{conv}} = \frac{240P_{\text{pd}}C_{\text{MVA}}}{\text{PF}_{\text{conv}}}, \quad C_{\text{dem}}^{\text{DC}} = \frac{12(20 - T_{\text{IC}})P_{\text{pd}}C_{\text{MVA}}}{\text{PF}_{\text{DC}}} \quad (27)$$

where  $P_{\text{pd}}$  is the plant demand from the grid that is the same in both cases converter-interfaced and directly-coupled. Indeed, the presence of the converter does not affect the power capacity of the CHP.  $\text{PF}_{\text{conv}}, \text{PF}_{\text{DC}}$  are the power factors at the point of common

coupling (PCC) of the converter-interfaced and directly-coupled solutions, respectively. Referring to Figure 8, it can be seen that:

$$P_{pd} = P_{pl} - P_{turb} \quad (28)$$

where  $P_{pl}$  is the load maximum power. It is assumed for this study that CHP turbines are sized as  $P_{turb} = 0.4P_{pl}$ . Therefore, the final demand charge terms can be written as:

$$C_{dem}^{conv} = \frac{360P_{turb}C_{MVA}}{PF_{conv}}, \quad C_{dem}^{DC} = \frac{18(20-T_{IC})P_{turb}C_{MVA}}{PF_{DC}} \quad (29)$$

The voltage support term of equation (18) becomes more complicated in this model because the differing power factors of the two solutions must be accounted for. From the definition of power factor, the peak reactive power demand from the grid  $Q_{pd}$  is:

$$Q_{pd}^{conv} = 1.5P_{turb} \tan[\arccos(PF_{conv})] = \frac{1.5P_{turb}\sqrt{1-PF_{conv}^2}}{PF_{conv}} \quad (30)$$

$$Q_{pd}^{DC} = 1.5P_{turb} \tan[\arccos(PF_{DC})] = \frac{1.5P_{turb}\sqrt{1-PF_{DC}^2}}{PF_{DC}} \quad (31)$$

where  $P_{pd} = 1.5P_{turb}$ . Similarly, the peak plant reactive power  $Q_{pl}$  can be written:

$$Q_{pl} = \frac{2.5P_{turb}\sqrt{1-PF_1^2}}{PF_1} \quad (32)$$

where  $P_{pl} = 2.5P_{turb}$  and  $PF_1$  is the power factor of the onsite load. Therefore, the site reactive power supplied by the CHP in the converter-interfaced case  $Q_{pl}^{conv}$  and the directly-coupled case  $Q_{pl}^{DC}$  are:

$$Q_{pl}^{conv} = Q_{pl} - Q_{pd}^{conv} = P_{turb} \left\{ \frac{2.5\sqrt{1-PF_1^2}}{PF_1} - \frac{1.5\sqrt{1-PF_{conv}^2}}{PF_{conv}} \right\} \quad (33)$$

$$Q_{pl}^{DC} = Q_{pl} - Q_{pd}^{DC} = P_{turb} \left\{ \frac{2.5\sqrt{1-PF_1^2}}{PF_1} - \frac{1.5\sqrt{1-PF_{DC}^2}}{PF_{DC}} \right\} \quad (34)$$

Using equation (19), the reactive power available for voltage support in the converter case  $Q_{avail}^{conv}$  and the directly-coupled case  $Q_{avail}^{DC}$  can be determined:

$$Q_{\text{avail}}^{\text{conv}} = Q_{\text{conv}} - Q_{\text{pl}}^{\text{conv}} = P_{\text{turb}} \left\{ \sqrt{\left(\frac{S_{\text{conv}}}{P_{\text{turb}}}\right)^2 - 1} - \frac{2.5 \sqrt{1 - \text{PF}_1^2}}{\text{PF}_1} + \frac{1.5 \sqrt{1 - \text{PF}_{\text{conv}}^2}}{\text{PF}_{\text{conv}}} \right\} \quad (35)$$

$$Q_{\text{avail}}^{\text{DC}} = Q_{\text{DC}} - Q_{\text{pl}}^{\text{DC}} = P_{\text{turb}} \left\{ 0.75 - \frac{2.5 \sqrt{1 - \text{PF}_1^2}}{\text{PF}_1} + \frac{1.5 \sqrt{1 - \text{PF}_{\text{DC}}^2}}{\text{PF}_{\text{DC}}} \right\} \quad (36)$$

Subtracting equation (36) from equation (35) yields the difference in the amount of reactive power available for voltage support. Using this result along with equation (26) yields the following comparison model including an MVA demand charge:

$$\begin{aligned} P_{\text{turb}} \left\{ 175200 \eta_{\text{conv}} C_{\text{MWh}} + 20 C_{\text{MVAR}} \left[ \sqrt{\left(\frac{S_{\text{conv}}}{P_{\text{turb}}}\right)^2 - 1} + \frac{1.5 \sqrt{1 - \text{PF}_{\text{conv}}^2}}{\text{PF}_{\text{conv}}} - 0.75 - \frac{1.5 \sqrt{1 - \text{PF}_{\text{DC}}^2}}{\text{PF}_{\text{DC}}} \right] - C_{\text{gen},1}^{\text{conv}} \right. \\ \left. - \frac{360 C_{\text{MVA}}}{\text{PF}_{\text{conv}}} \right\} - S_{\text{conv}} (C_{\text{conv}} + C_{\text{IC}}^{\text{conv}}) - C_{\text{gen},0}^{\text{conv}} \\ \geq P_{\text{turb}} \left[ 8760(20 - T_{\text{IC}}) \eta_{\text{DC}} C_{\text{MWh}} - 1.25 C_{\text{gen},1}^{\text{DC}} - 1.25 C_{\text{IC}}^{\text{DC}} - \frac{18(20 - T_{\text{IC}}) C_{\text{MVA}}}{\text{PF}_{\text{DC}}} \right] - C_{\text{gen},0}^{\text{DC}} \end{aligned} \quad (37)$$

Table 26 show the average demand for all the U.S states<sup>56</sup>. The values shown are per kW. They will be used in this analysis as demand charge per kVA as no value for demand charges per kVA is currently available.

State	Demand Charge [\$/kW]								
AL	7.72	HI	10.75	MA	6.75	NM	6.26	SD	8.24
AK	5.91	ID	3.37	MI	5.57	NY	9.52	TN	10.69
AZ	9.32	IL	5.40	MN	6.10	NC	8.65	TX	3.87
AR	5.36	IN	6.44	MS	5.86	ND	8.27	UT	6.86
CA	11.93	IA	5.01	MO	4.20	OH	5.83	VT	9.08
CO	5.91	KS	3.99	MT	5.41	OK	4.62	VA	6.90
CT	9.94	KY	6.59	NE	7.04	OR	5.37	WA	3.58
DE	7.43	LA	3.23	NV	9.18	PA	5.49	WV	5.65
FL	6.10	ME	8.67	NH	7.97	RI	7.95	WI	4.89
GA	2.86	MD	4.22	NJ	7.91	SC	6.37	WY	6.28

**Table 26:** Average demand charge across the U.S states

<sup>56</sup> National Renewable Energy Laboratory, "A Survey of U.S. Demand Charges," 2017 [Online]. Available <https://www.nrel.gov/solar/assets/pdfs/2017-us-demand-charges-webinar.pdf>

Regarding the power factor, IEEE standard 1547 and typical grid codes require the site to maintain at the point of interconnection (POI) a power factor equal or greater than 0.9 to avoid penalties. Therefore, it is assumed that  $PF_{DC} = 0.9$ . However, with the converter-interfaced, it is possible to set the power factor arbitrarily between 0.9 and 1. Results are presented in section 4.4.3 for multiple values within that range.

#### 4.4.3 *Estimation of the U.S technical potential of converter-interfaced CHP*

Results of the U.S technical potential of converter-interfaced CHP, using the basic comparison model of equation (18), are presented in Figure 50 and Figure 51 for the industrial and commercial, respectively.

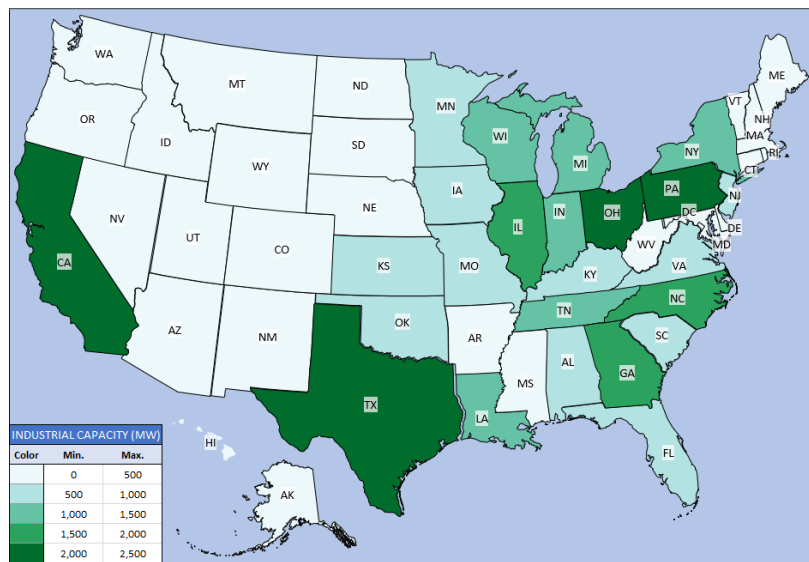


**Figure 50:** Portrait of the U.S technical potential of industrial converter-interfaced CHP

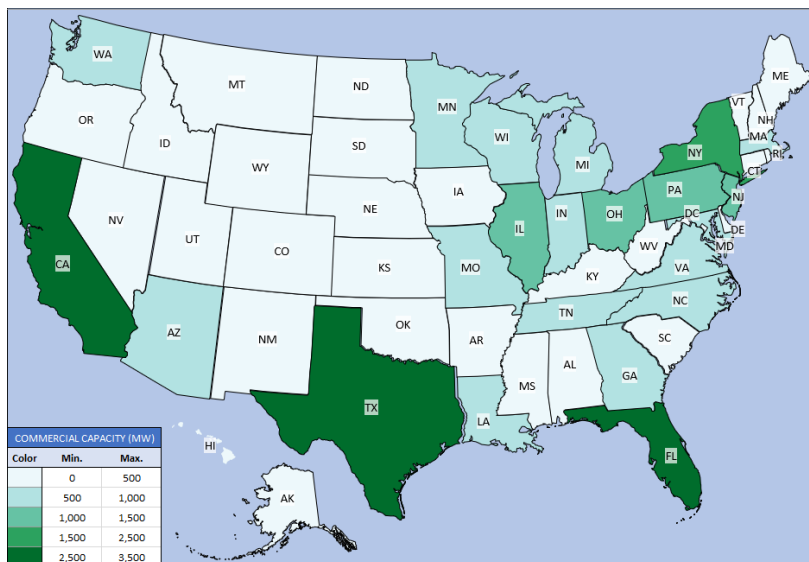


**Figure 51:** Portrait of the U.S technical potential of commercial converter-interfaced CHP

Figure 52 and Figure 53 show the breakdown of the technical potential of converter-interfaced CHP by size. The 1MWe to 5MWe and the 5MWe to 20MWe are estimated to account for 36+ GW and 28+ GW respectively nationwide in the technical potential of converter-interfaced CHP. Figure 52 and Figure 53 are qualitatively similar to Figure 50 and Figure 51 because in what is considered the small to medium-sized CHP technical potential (1MWe to 20MWe), the majority of the commercial sites are in the 1MWe to 5MWe range while the potential industrial sites tend to be in the 5MWe to 20MWe range.

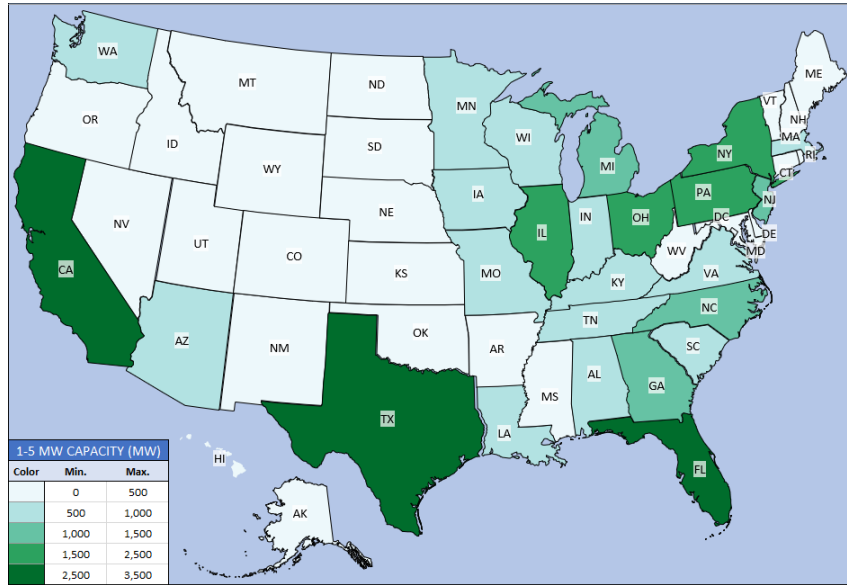


**Figure 52:** Nationwide technical potential of converter-interfaced CHP ranging from 1MWe to 5MWe

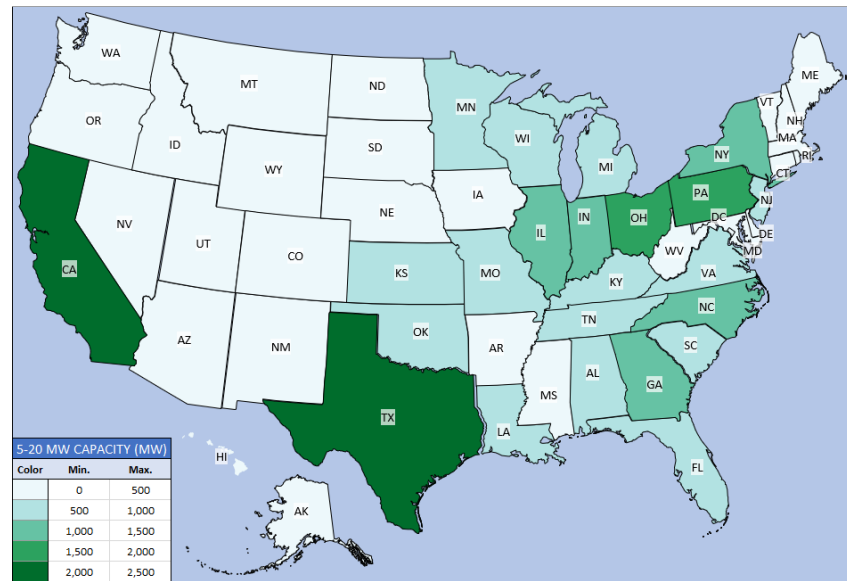


**Figure 53:** Nationwide technical potential of converter-interfaced CHP ranging from 5MWe to 20MWe

Unsurprisingly, states such as California and Texas with large commercial and industrial potential for CHP have more sites for which a converter-interfaced interconnection would be more favorable. Nationwide, there is 35+ GW and 30+ GW of technical potential for respectively industrial and commercial converter-interfaced CHP. In other words, the converter-interfaced solution is preferred for all sites of the U.S Technical Potential.

To account for uncertainty in the assumptions, the impact of critical parameters that can affect the winning rate of converter-interfaced and therefore the number of sites at which it will be more favorable than directly-coupled is also analyzed. Figure 54 shows the number of technical potential sites at which the converter-interfaced solution remains more favorable upon variation of certain critical parameters. Each plot in Figure 54 includes four curves representing the number sites favorable to the converter-interfaced for interconnection delay of 12, 9, 6 and 3 months shorter than with the directly-coupled. The sensitivity analysis results discussed in section 0 already showed that the longer the interconnection delay of directly-coupled the more competitive the converter-interfaced solution is. Figure 50 and Figure 51 already revealed that at 12-months interconnection delay all the sites listed in the U.S Technical Potential (23,000+) will be more viable with the converter-interfaced solution. Figure 54 shows how significant the impact of the interconnection delay is. Indeed, it reveals that at 12 months interconnection delay, all the sites of the U.S Technical Potential are favorable to the converter-interfaced solution and this is insensitive to the variation of system efficiency and the costs of converter, generator or interconnection within the ranges analyzed. This is a major result as one of the main benefits provided by the interface converter is to streamline the grid interconnection of small to medium-sized CHP and significantly reduces the delays to operation approval. Results of Figure 54 prove that the economic performance of the converter-interfaced over the directly-coupled is very robust and will hold despite the relative volatility of energy price, converter, or generator costs.

Figure 54 also shows that if 12 months interconnection delay gives 100% of the Technical Potential sites favorable to the converter-interfaced solution, a more conservative delay of 6 months still grants it most sites. However, parameters such as the system efficiency will start having non-negligible effects. For instance, Figure 54.a suggests that at 6 month interconnection delay a difference in system efficiency of 1.5 point will reduce the number of sites favorable to the converter-interfaced solution from 100% to ~73%. At 3 months interconnection delay the converter-interfaced solution still wins a good majority of the sites but parameters such as converter cost or interconnection cost will need to be very competitive. Figure 54.b and Figure 54.c suggest that a variation in any of those two parameters would significantly reduce the number of favorable sites. It is important to note as shown in Figure 54.d that the generator cost does not seem to have any influence on the number of sites favorable to the converter-interfaced solution. This is despite generator cost is traded for converter cost in the converter-interfaced solution. This

observation suggests that the converter-interfaced solution can be profitable regardless of the price of the cost of the generator.

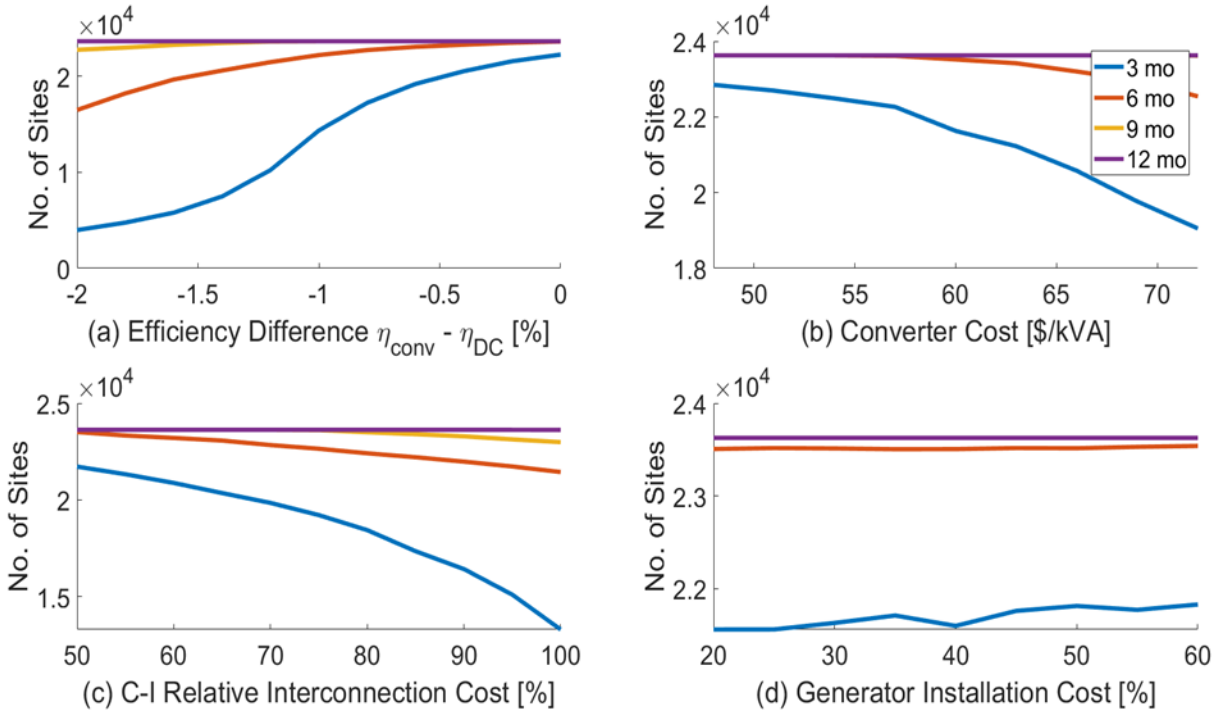


**Figure 54:** Estimation of U.S. technical potential sites favorable to the converter-interfaced solution.

(a) as a function of interconnection delay and system efficiency  $\eta_{conv} - \eta_{DC}$ . (b) as a function of interconnection delay and converter cost. (c) as a function of interconnection delay and interconnection cost. (d) as a function of interconnection delay and generator cost

As previously mentioned, reactive power is still not highly monetized by utilities. However, the situation can change in the future with higher penetration of DER and inverter-based resources. This can also lead to new tariff trends including billing demand charge per MVA instead of MW. The economic benefits of oversizing converter (the grid-side inverter only) in anticipation of an increase in reactive power value can be examined analytically by focusing on the terms including  $S_{conv}$  in equation (18):

$$20P_{turb}C_{MVAR} \left[ \sqrt{\left( \frac{S_{conv}}{S_{turb}} \right)^2 - 1} - 0.75 \right] \geq S_{conv}(C_{conv} + C_{IC}^{conv}) \quad (38)$$

$$\Rightarrow S_{conv}^2 \geq \frac{625P_{turb}^2C_{MVAR}^2}{400C_{MVAR}^2 - C_{conv}^2 - (C_{IC}^{conv})^2} \quad (39)$$

$$\Rightarrow 400C_{MVAR}^2 > C_{conv}^2 + (C_{IC}^{conv})^2 \quad (40)$$

Equation (40) provides a condition under which it is preferable to oversize the converter. In California for instance, a 3 MVA excess capacity at  $C_{MVAR} = \$6K/MVA$ ,  $C_{conv} = \$60K$ ,

$C_{IC}^{\text{conv}} = \$66\text{K/MVA}$  will yield greater revenue than cost based on equation (40), therefore oversizing the converter would be profitable.

By applying equation (37), the comparison model with an MVA demand can be evaluated. Equation (37) introduces the power factor of the two solutions. However, that there are competing effects regarding power factor. A  $\text{PF}_{\text{conv}}$ .  $\text{PF}_{\text{conv}} = 1$  at POI results in the minimum demand charge while  $\text{PF}_{\text{conv}} = 0.9$  results in largest potential for reactive support revenue. Essentially, there is a tradeoff between commitment of available reactive power for minimizing monthly MVA demand charges or maximizing annual reactive power revenue. Figure 55 shows as comparison the number of technical potential sites at which the converter-interfaced solution is more favorable as a function of the interconnection delays varying from 3 to 12 months for different POI power factor settings assuming demand charge is on MVA. It can be observed that if demand charge is applied to the MVA the converter-interfaced solution is more favorable at ~98% of the technical potential sites regardless of the interconnection delay. Applying the reactive power to reduce demand charge ( $\text{pf} = 1$ ) would be more valuable than providing voltage support ( $0.9 < \text{pf} < 1$ ).

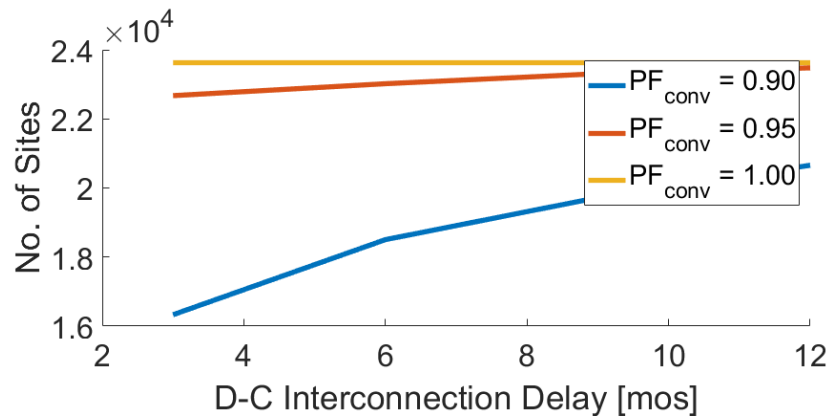


**Figure 55:** Estimation of U.S technical potential sites favorable to the converter-interfaced solution if MVA demand charge applies

The results also suggest that if demand charge is applied to MVA, setting the POI power factor to 1 is the most valuable strategy. In that situation the converter-interfaced solution will be more favorable to all the technical potential sites even interconnection delays just shorter by 3 months relative to directly-coupled.

#### 4.5 Evaluation of the economic benefits of converter-interfaced CHP combined with battery energy system (BESS)

In the analysis, the economic feasibility of CHP combined with Battery Energy and Storage System (BESS) is evaluated with focus given to the benefits provided by the interface converter for the battery interconnection. Both AC and DC-coupled BESS battery system are investigated. Figure 56 shows the architecture of the two configurations. It can be noted that the DC-coupled BESS is directly connected to the DC link of the interface

converter. Such a configuration only requires a DC/DC converter for the battery voltage regulation. The AC-coupled BESS in the other hand needs a separate battery inverter and interconnection equipment e.g transformer if need, to connect to the plant distribution system. Thus, relatively lower Capex and higher roundtrip efficiency are expected with the DC-coupled BESS. For the same reasons, it is expected that the converter-interfaced configuration will be more advantageous than the directly-coupled. Indeed, directly-coupled CHP will require AC coupling and therefore higher Capex.

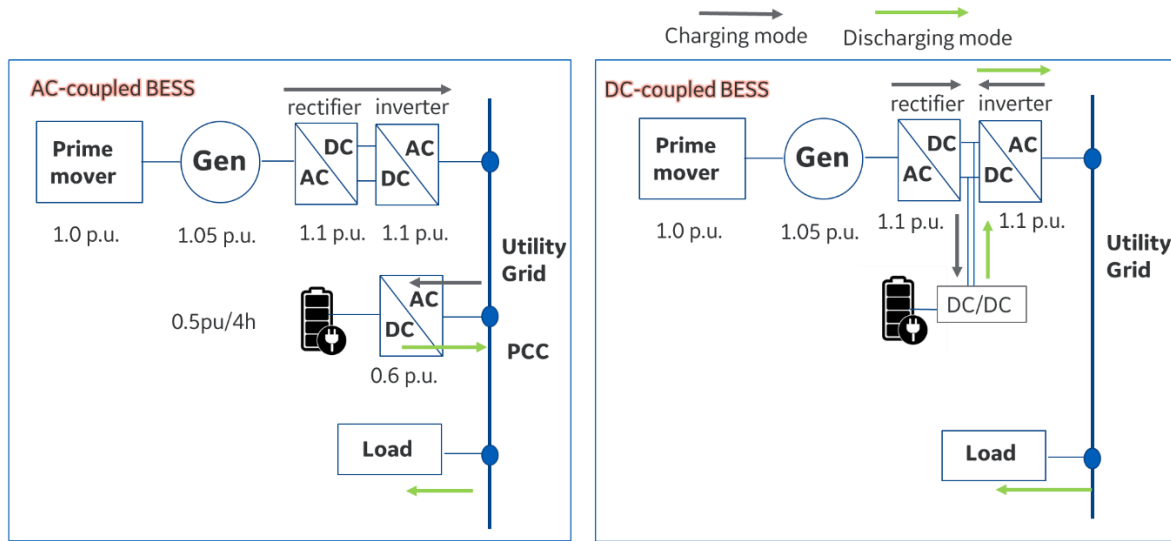


**Figure 56:** System architecture of BESS combined with converter-interfaced CHP

Regarding the operation modes as defined in section 4.2.2, the battery charges in operating region 1 and 3 if full capacity i.e., 100% State of Charge SOC is not reached. The battery discharges in operating region 2 if commanded to help support the plant load. The detailed charging/discharging logic is as follows:

#### *Charging mode*

The BESS charging rate,  $kW_{BESS}(t)$ , is described by equation (41):

$$kW_{BESS}(t) = \min(kW_{BESS,max}, kW_{CHP,max} - kW_{load}(t), kW_{100SOC}) \quad (41)$$

Where,  $kW_{BESS,max}$  is the maximum charging/discharging rate in current mode and  $kW_{100SOC}$  the charging rate in voltage mode i.e., kW required to reach 100% SOC for BESS within the next hour.  $kW_{100SOC}$  is calculated as follows.

$$kW_{100SOC} = \frac{kWh_{BESS,max} - kWh_{BESS}(t-1)}{\Delta t} \times \eta \quad (42)$$

Where  $kWh_{BESS,max}$  is the energy capacity of the BESS,  $\eta$  the battery roundtrip efficiency and  $\Delta t$  the operating interval.

### Discharging mode

Multiple discharging strategies can be applicable however, for this analysis it is considered that the BESS will be primarily used for peak-shaving to reduce demand charge. This means the BESS will be only discharged when the load exceeds a certain threshold set for demand charge. Demand charge is the amount paid every month for the highest power consumed from the grid during the month. Equation (43) details the discharging rule.

$$kW_{BESS}(t) = \min(kW_{BESS,max}, kW_{CHP,max} - kW_{load}(t), kW_{100SOC}, kW_{totarget}) \quad (43)$$

Where,  $kW_{totarget}$  is the discharging power required to stay within the desired peak load (expressed as the percentage-  $\alpha_{peak\_month}$  of the original monthly net peak load). ,  $kW_{totarget}$  can be calculated as follows:

$$kW_{totarget} = \max(0, kW_{load}(t) - kW_{CHP}(t) - (kW_{peak\_month} - kW_{CHP,max}) \times \alpha_{peak\_month}) \quad (44)$$

The ROI evaluation form presented in Figure 44 is modified to include the BESS Capex and the input/output templates are adjusted to reflect the power and energy transactions as described above and then the ROI is calculated. The same previous five user cases evaluated in section 4.2 are selected for BESS evaluation. Results are shown in Table 27. For reference, the battery system is a 4-hour battery with 4MWh capacity. The discharge threshold for demand charge management  $\alpha_{peak\_month}$  is set to 85%.

Case Name	Hospital	WaterC	Hotel	WaterC	College
	CAISO AvgElec	CAISO AvgThem	MISO PeakElec	TX PeakElec	PJM PeakElec
Exportable CHP output	8.26	21.43	40.64	91.94	48.38
% operation in region 2	43.66	46.03	0.62	0.02	0.13
No BESS, ROI	16.63	13.43	11.23	12.46	13.72
ROI, AC-BESS	14.36	13.49	8.98	11.27	11.68
ROI, DC-BESS	15.15	13.81	9.37	11.34	11.71
AC round-trip $\eta$	95.56	96.25	95.10	95.37	95.27
DC round-trip $\eta$	96.60	97.27	96.10	96.49	96.30

**Table 27:** ROI calculations of converter-interfaced CHP combined with BESS

Table 27 reveals that the level of exportable output is not significantly correlated with ROI of converter-interfaced combined with BESS. Not the higher exportable energy cases get the higher ROI but the cases with high percentage of CHP operation in region 2. Indeed, it seems the longer the CHP is in operating region 2, i.e., CHP running at its maximum capacity, the higher the ROI of combination with BESS is. The dominant reason is that BESS

is set to only discharge in operating region 2, where it plays a major role to compensate load for peak reduction. Therefore, what matters is not how big is the load excess but rather how long the BESS can be utilized. It is evaluated that operating in region 2 40% to ~60% of the time would be the most economical for BESS in combination with the CHP. This percentage should not be too high since the CHP still needs to run in the other operating regions to get BESS charged for the next load excess. As observed in Table 27, in most of the cases, the BESS for the applications does not allow to improve the ROI except for the waterCCAISO (AvrgThem) which has a CHP running in operating region 2 ~40% of the time. Table 27 also shows the ROI and round-trip efficiency comparison between AC-coupled and DC-coupled BESS. For all the cases examined, DC-coupled BESS outperforms the AC-coupled thanks to presence of the grid-ready inverter of the interface converter that can be leveraged by BESS to reduce Capex and system losses.

To further analyze the impact of the BESS discharging strategy on the ROI of converter-interfaced CHP coupled with BESS, the HospitalCAISO (AvrgElec) and waterCCAISO<sup>57</sup> cases were evaluated for different discharge thresholds  $\alpha_{peak\_month}$  and BESS capacities. Figure 57 and Figure 58 show the results obtained for BESS installed cost of 400\$/kWh. Results showed that with BESS cost ~400\$/kWh it's unlikely that adding BESS to CHP installation will be profitable. Indeed, in both the hospital and the water reclamation cases, when varying the discharge threshold from 95% of the previous month peak (discharge only during high loads) to 10% (discharge anytime that the load exceeds the CHP capacity by 10%) the ROI in the presence of the BESS is consistently lower than that of the CHP alone. In other words, the prohibitive Capex of BESS will outweigh the benefits generated e.g in demand charge reduction. Although larger battery can significantly reduce the peak load provide large savings in demand charge, the BESS at 400/kWh is just too prohibitive

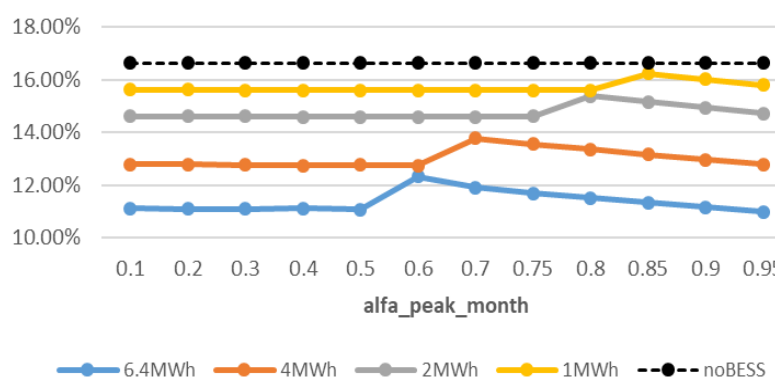


**Figure 57:** ROI of converter-interfaced CHP coupled with BESS for a hospital case in CAISO: BESS installed cost 400\$/kWh

<sup>57</sup> Peak load of hospital in CAISO is 6.1MW with peak to average load ratio as 1.4, while peak load of water reclamation in CAISO is 14.8MW with peak to average load ratio is 7.4.

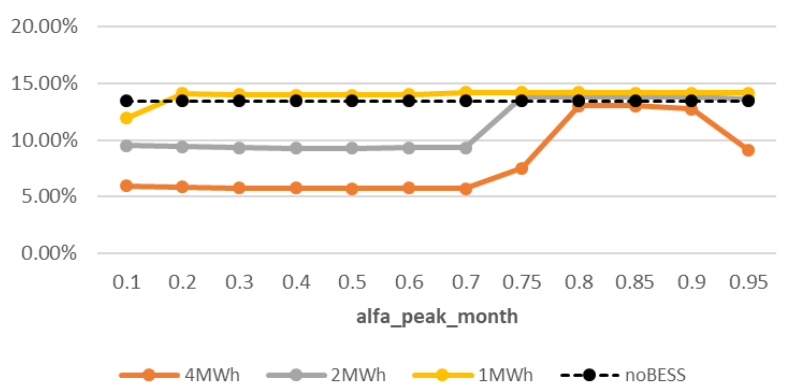


**Figure 58:** ROI of converter-interfaced CHP coupled with BESS for a water reclamation plant case in CAISO: BESS installed cost 400\$/kWh

Another observation is also the optimal discharge thresholds  $\alpha_{peak\_month}$  seems to be attached to size of the BESS. Larger BESS will be optimized with higher discharging threshold. This is due to the combination effects of demand charge reduction and energy cost savings. With too small  $\alpha_{peak\_month}$ , the battery tends to fully discharge its energy before the peaking hours, making the peak shaving less effective. Thus, selecting a reasonable BESS size and discharge threshold  $\alpha_{peak\_month}$  is critical in operating optimally CHP coupled with BESS. For instance, for the hospital case in CAISO, a BESS size of 1MWh with a discharge threshold of 85% of the peak appears to be the most economical combination with a 16.24% ROI while for the water reclamation case a 4MWh battery and discharge threshold of 80% seems to be more optimal yielding a ROI of 18.03%. With a BESS cost of 250\$/kWh as projected in near future<sup>58</sup> BESS coupling with CHP can yield ROI higher than with CHP alone as shown in Figure 59 and Figure 60.

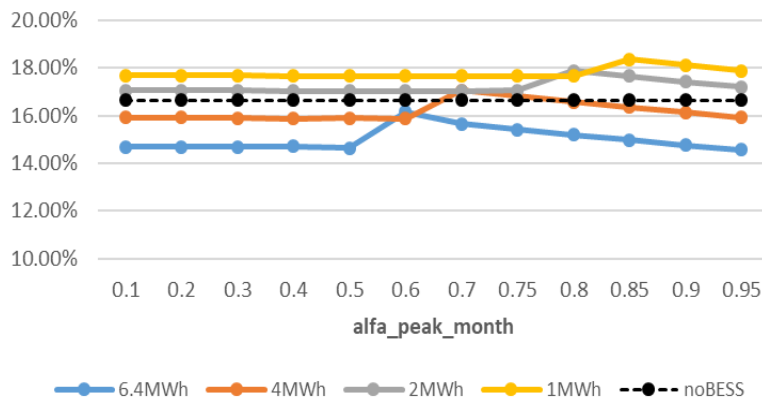


**Figure 59:** ROI of converter-interfaced CHP coupled with BESS for a hospital case in CAISO: BESS installed cost 250\$/kWh

<sup>58</sup> PNNL. Energy Storage Technology and Cost Characterization Report, July 2019.

[https://www.energy.gov/sites/prod/files/2019/07/f65/Storage%20Cost%20and%20Performance%20Characterization%20Report\\_Final.pdf](https://www.energy.gov/sites/prod/files/2019/07/f65/Storage%20Cost%20and%20Performance%20Characterization%20Report_Final.pdf)

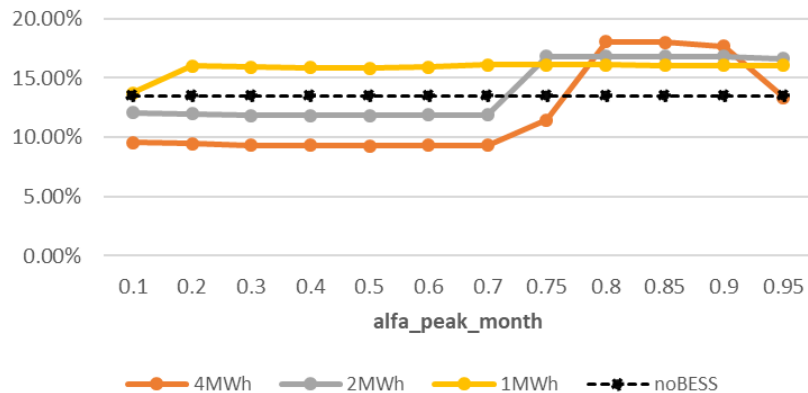


**Figure 60:** ROI of converter-interfaced CHP coupled with BESS for a water reclamation plant case in CAISO: BESS installed cost 250\$/kWh

#### 4.6 Evaluation of CHP coupled with BESS and solar photovoltaic (PV) system

As discussed in the previous section, the converter-interfaced CHP provides the possibility of interconnecting DER such as BESS and PV system without procuring inverters. As shown in Figure 61, only a separate DC/DC converter is required to regulate for each DER the DC voltage for an optimal operation. This allows to reduce the overall system Capex and improve the economic feasibility of the CHP and the additional DER.

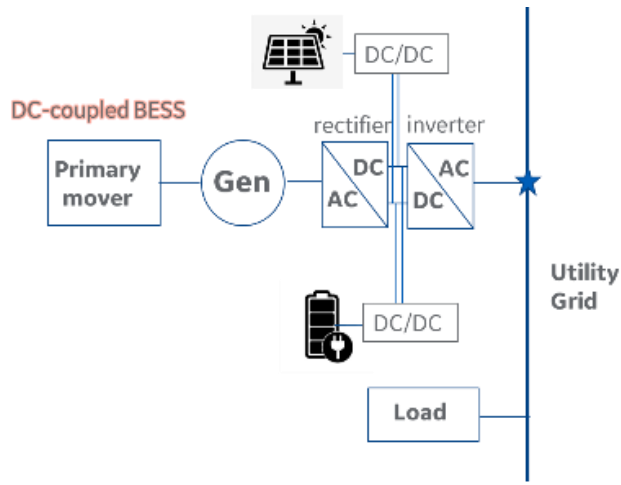


**Figure 61:** Architecture of a hybrid CHP system with PV and BESS coupling

In the dispatch logic for the hybrid CHP system, it is assumed that since electricity produced from the PV has the least cost, the priority for supplying on-site load is given to the PV first, then CHP follows and ultimately the BESS. Thus, two conditions are applicable which are detailed as follows:

- If  $kW_{load}(t) \leq kW_{PV}(t)$ , then it's not necessary to operate CHP system and the excess power can be used to charge the battery. The different power outputs are indicated as equation (45).

$$\begin{cases} kW_{CHP}(t) = 0 \\ kW_{BESS}(t) = \begin{cases} 0, & \text{if } kWh_{BESS}(t-1) = kWh_{BESS,max} \\ \min(kW_{BESS,max}, kW_{PV}(t) - kW_{load}(t), kW_{100SOC}), & \text{if } kWh_{BESS}(t-1) < kWh_{BESS,max} \end{cases} \\ kWh_{BESS}(t) = kWh_{BESS}(t-1) + kW_{BESS,act}(t) \times \Delta t \end{cases}, \quad (45)$$

- If  $kW_{load}(t) > kW_{PV}(t)$ , the net power that needs to be supplied by the CHP is  $kW'_{load}(t) = kW_{load}(t) - kW_{PV}(t)$ .  $kW'_{load}(t)$  will therefore substitute  $kW_{load}(t)$  in the ROI calculation form evaluation without integrating PV system.

The hospital user case in CAISO was selected for the ROI evaluation of the hybrid CHP. A 1MWh BESS was considered as the benchmark case and nine scenarios including three PV sizes 250kWac, 500kWac, 1000kWac and three BESS discharge threshold settings ( $\alpha'_{peak\_month} = 0.8, 0.85, 0.9$  in respect to net load  $kW'_{load}(t)$ ) were evaluated. The annual hourly PV profile is generated from NREL System Advisor Model tool (SAM)<sup>59</sup>. Results obtained are shown in Figure 63. They revealed that integrating PV with CHP and BESS increase the ROI compared to CHP coupled with BESS only. However, higher PV capacities tend to decrease the ROI, due to the increased Capex outweighing by the electricity savings generated by PV system. Therefore, the sizing and operation of the hybrid need to be evaluated for the optimal ROI. For the hospital user case analyzed, a PV size of 250kWac (1.25 DC to AC ratio) with a BESS discharge threshold of 80% to 85% of the net peak load would provide the highest ROI (~21.5%).

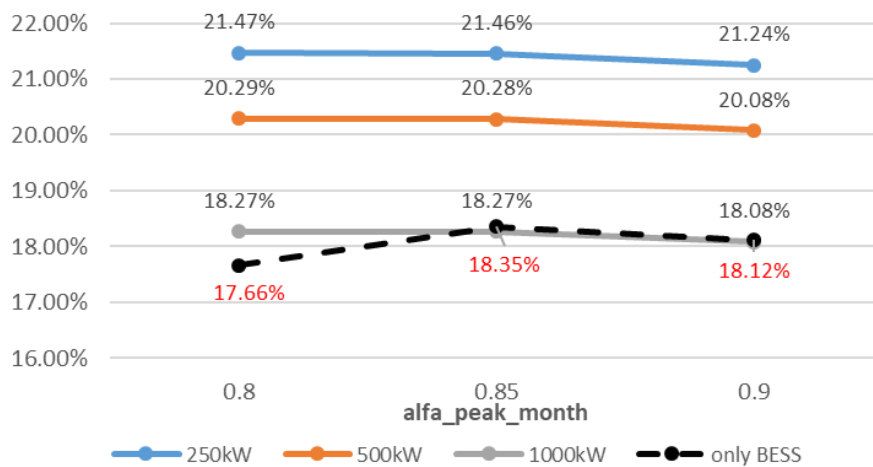


**Figure 62:** ROI evaluation of hybrid CHP using the hospital in CAISO user case

<sup>59</sup> NREL PVWatts model <https://pvwatts.nrel.gov/pvwatts.php>

## 5. DEVELOPMENT AND VALIDATION OF THE CONVERTER-INTERFACED CHP CONTROLS PLATFORM

In addition to its economic merit, the converter-interfaced solution needs to provide enough technical benefits to be rapidly adopted by the industry. Challenges associated with existing CHP control system include:

- the control system needs to be customized and tuned for different grid-integration requirements and operation environment, such as the frequency of operation (50Hz vs 60Hz), generator types and ratings, voltage, and frequency ride-through capability, etc. This translates to longer product development cycle and high cost of commissioning.
- the microgrid operation requires fast islanding detection, seamless transition between grid-tie and islanding modes, and re-synchronization, which require a fast and precise control system to prevent large voltage and frequency oscillation and protection trips.

It is important to highlight that as most small and medium sized commercial and industrial facilities typically interconnect to the grid at distribution voltage levels, CHP in those facilities must comply with grid codes applicable to DER. The control system of the converter-interfaced CHP is developed to meet IEEE 1547<sup>5</sup>, IEEE 2030.7<sup>9</sup> and UL 1741<sup>32</sup> requirements, improve operation flexibility for microgrid operation and to enable grid services such as demand response, voltage support and participation into ancillary services. To further evaluate the benefits of the interface converter for the interconnection of CHP into distribution grids, a comprehensive integration study was conducted. Specifically, a short-circuit analysis is conducted to compare the exposed equipment stress level during faults; the power factor of the CHP plant is analyzed to compare voltage support ability between the two configurations. In addition, the transient dynamics study is conducted in both grid-tie mode and islanding mode to compare the system stability for these two configurations.

### 5.1 Grid integration study of converter-interfaced CHP plants

Figure 63 shows the platform built in PSCAD to study the grid performance of the converter-interfaced CHP in comparison with directly-coupled CHP. The CHP system model includes a ~2MW round-rotor synchronous generator, a 1.65MW reciprocating gas engine, and an automatic voltage control (AVR). For the converter-interfaced configuration, a back-to-back voltage source converter is also included. Figure 64 shows the details of the directly-coupled and the converter-interfaced configuration.

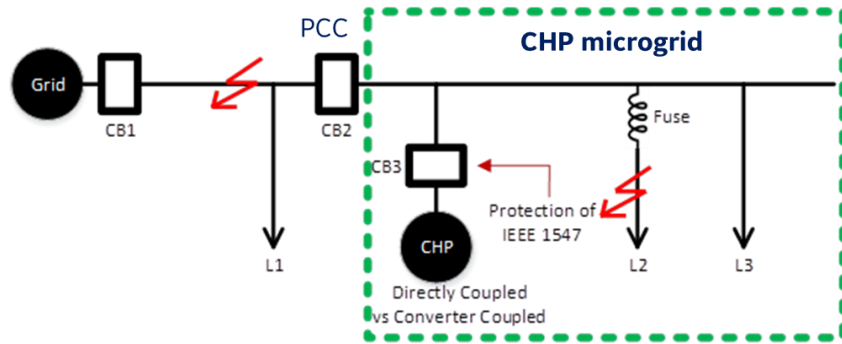


**Figure 63:** One-line diagram of the system for grid integration studies

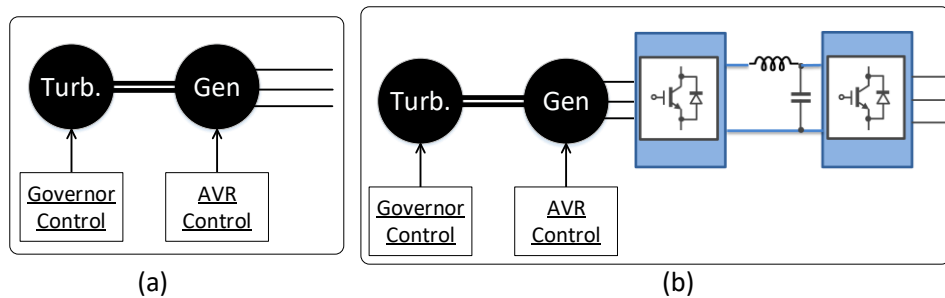


**Figure 64:** Different interconnection scenarios for grid-tied CHP system

### 5.1.1 Details of the system model

The CHP generator is represented by a seventh-order set of ordinary differential equations in a stationary direct-quadrature (dq0) reference frame. A 2MW Jenbacher engine system<sup>60</sup> is considered for this analysis with typical parameters of synchronous generators given in Table 28.

Parameters	Unit	Value
xd direct axis synchronous reactance	p.u.	2.301
xd' direct axis transient reactance	p.u.	0.117
xd'' direct axis sub transient reactance	p.u.	0.097
x2 negative sequence reactance	p.u.	0.12
Td'' sub transient reactance time constant	ms	40
Ta Time constant direct-current	ms	20
Tdo' open circuit field time constant	s	1.55
Capacity	MW	2.0625
Terminal Voltage	kV	0.48

**Table 28:** Parameters of the CHP generator for the grid study

<sup>60</sup> Jenbacher Gas engines <https://www.clarke-energy.com/gas-engines/>

The generator AVR is modeled using an IEEE type AC7B excitation system<sup>61</sup>. The control input of the AVR is a voltage reference setpoint provided by the CHP control system. If the generator is running in a voltage regulation mode, also known as PV mode, the setpoint as denoted by  $V_{ref}$  is set as a constant.  $V_{ref}$  can be varied for power factor control or reactive power control by implementing a controller attached to the AVR. Figure 65 shows the proposed power factor control scheme at the Point of Interconnection (POI). The control is based on a dead band and a proportional-integral (PI) block that uses the exchanged power at POI to calculate the desired reactive power from the generator to meet the power factor request. If the monitored reactive power at POI deviates from the desired value and the mismatch is greater than the dead band, the regulator is activated to adjust  $V_{ref}$  so that the power factor requirement is met.

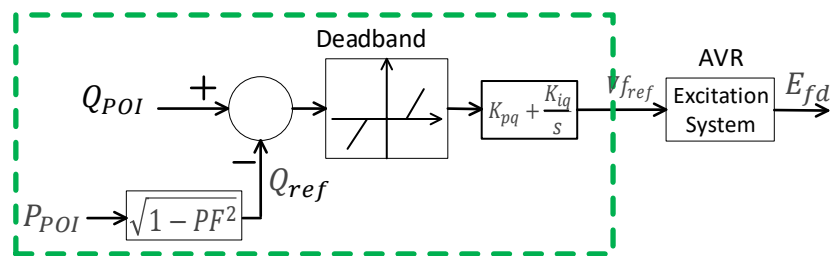


**Figure 65:** Power factor control logic of the AVR

Figure 66 shows the block diagram that represents the prime mover and the governor composed of a speed/load control, a fuel actuator, and the engine equivalent<sup>62</sup>. Inputs to the model are either the load reference setpoint and/or the engine-generator rotor speed depending on the operating mode of the CHP, i.e., grid-tied mode or islanding mode. As there is no industry-grade governor model specifically designed for reciprocating engines the generic governor model “GGOV1”<sup>63</sup> was used in this study with some minor changes to accommodate islanding operation. The output of the governor model is the expected fuel intake to maintain the desired operation of CHP either for maintaining the rotating speed in the islanding mode or regulating the output in the grid-tied mode. The fuel actuator is regulated to open or close the valve to adjust the mechanical torque to the generator.

The feeder connecting the CHP plant to the substation was modeled using line conductors and tower spacing from the IEEE 34 bus system which was considered as a representative

<sup>61</sup> IEEE Std 421.5-2016 “IEEE Recommended Practice for Excitation System Models for Power System Stability Studies,” [https://standards.ieee.org/standard/421\\_5-2016.html](https://standards.ieee.org/standard/421_5-2016.html)

<sup>62</sup> Farid Katiraei, Aidan Foss, Chad Abbey, and Benjamin Strehler, “Dynamic analysis and field verification of an innovative anti-islanding protection scheme based on directional reactive power detection,” Proceeding of the 2007 IEEE Canada Electrical Power Conference (EPC), Montreal, Canada

<sup>63</sup> North American Electric Reliability Corporation (NERC), “Gas Turbine Governor Modeling,” August 2017: [https://www.nerc.com/comm/PC/NERCModelingNotifications/Gas\\_Turbine\\_Governor\\_Modeling.pdf](https://www.nerc.com/comm/PC/NERCModelingNotifications/Gas_Turbine_Governor_Modeling.pdf)

U.S. distribution feeder<sup>64</sup>. The characteristics of the feeder section modeled as connecting the CHP plant are given in Table 29.

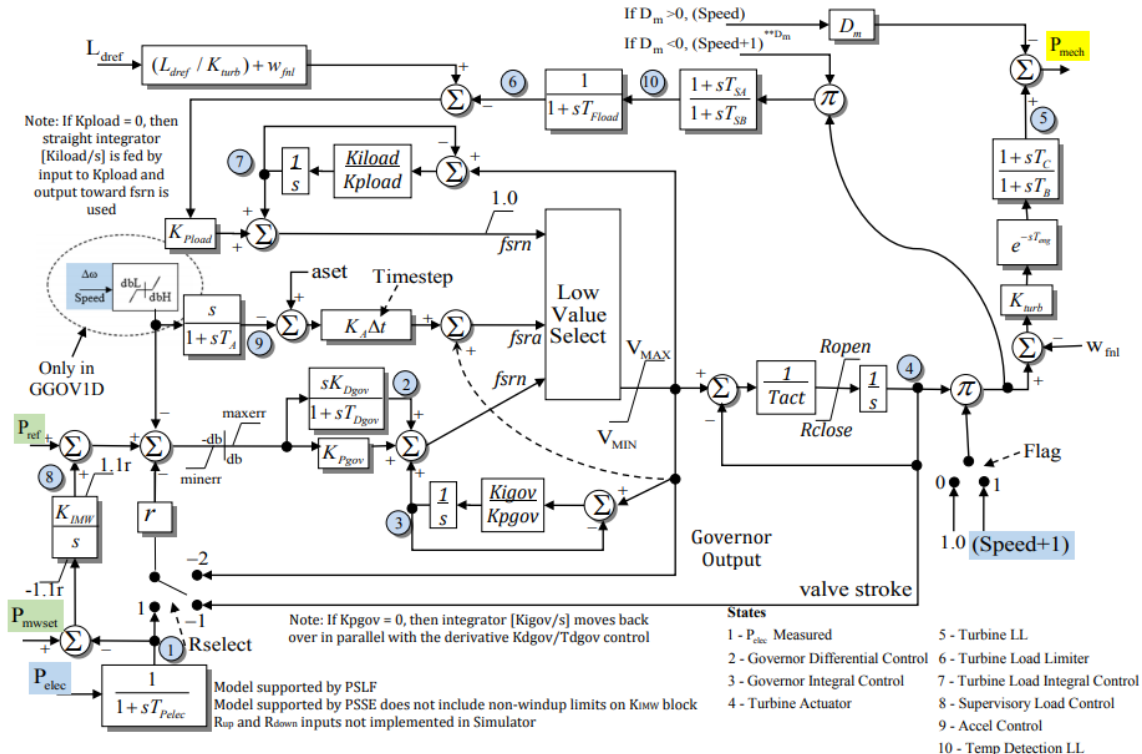


**Figure 66:** Governor and engine controls

The length of the section is varied to study different grid strengths and their impact on the interface converter performance. Table 30 shows the grid strength at the POI as function of the feeder section

Config.	Phasing	Phase	Neutral	Spacing ID
300	BACN	ACSR 1/0	ACSR 1/0	500

**Table 29:** Typical distribution feeder configuration in the U.S

	Distance to Substation	Short Circuit Ratio (SCR)
Strong Grid	0.3645 miles	77.9
Medium Grid	2.595 miles	11.3
Weak Grid	3.645 miles	7.8

**Table 30:** Different grid strengths at POI as function of the feeder length

The interface converter is modeled, using back to back inverters. As shown in Figure 67 the control includes a cascaded control loop for both active and reactive power. Active power

<sup>64</sup> IEEE Power & Energy Society, IEEE PES AMPS DSAS Test Feeder Working Group, "34-bus feeder." Available online: <http://sites.ieee.org/pes-testfeeders/resources>

control is performed through the DC voltage regulation which provides the active d-axis current command. Reactive power control is performed through the Volt/Var controller which gives the reactive q-axis current command. Included is also a reactive current curve to override the current command during Low Voltage Ride Through (LVRT) and High Voltage Ride Through (HVRT) events.

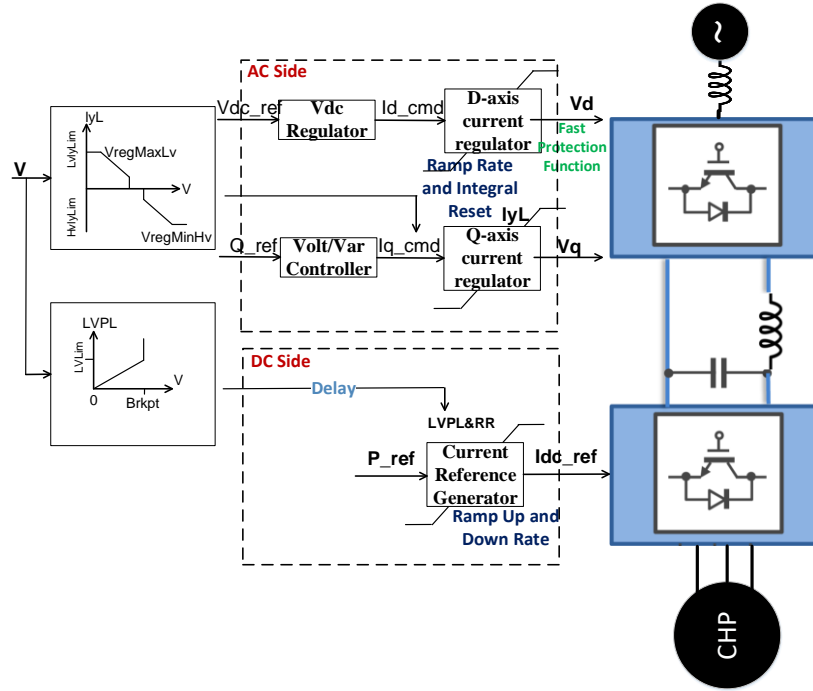


**Figure 67:** Diagram of the interface converter with its control loops

As explained in section 3.2, different control modes are recommended for DER by IEEE 1547, e.g., constant power factor and voltage-reactive power, etc. When the system is experiencing abnormalities including but not limited to voltage and frequency disturbances, the standard provides recommendation for detection thresholds and clearing time. The ride-through and protection settings applied for this analysis are summarized in Table 31.

Protection	Pickup Range	Clearing Time (sec)
Under Freq. 2	$f \leq 56.5 \text{ Hz}$	0.16
Under Freq. 1	$f \leq 58.5 \text{ Hz}$	300
Over Freq. 1	$61.2 \text{ Hz} \leq f \leq 62 \text{ Hz}$	300
Over Freq. 2	$f \geq 62 \text{ Hz}$	0.16
Under Volt. 1	$V \leq 50\% \text{ of Nominal}$	1.1
Under Volt. 2	$50\% < V \leq 80\% \text{ of Nominal}$	2
Over Volt. 1	$110\% \leq V < 120\% \text{ of Nominal}$	2
Over Volt. 2	$120\% \leq V \leq V$	0.16

**Table 31:** Selected ride-through settings for the grid integration study

### 5.1.2 Results of the grid integration study

Based on the CHP system model, the facility load and grid conditions, system simulations including short-circuit analysis, power factor analysis, and dynamic analysis are performed. The simulation results for directly-coupled and converter-interfaced configurations are compared.

#### Short-circuit analysis

For the directly-coupled and converter-interfaced configurations, different fault scenarios, including line to ground (L-G), line to line (L-L), line to line to ground (L-L-G), 3-phase fault, and a remote fault, are simulated to evaluate the stress level of generators during these events. The results are summarized in Table 32 and Table 33 where  $I_{fault\ peak}$  denotes the peak fault current and  $I_{fault}@0.18s$  represents the fault current at 180ms after the fault initiation. For reference, the 2MW, 480V generator used in this study has a rated current of 2.4kA.

	$I_{fault\ pre}^{Pre}$ (kA)	$I_{fault\ peak}^{Peak}$ (kA)	$I_{fault}$ (kA) @0.18 s	$V_{fault}$ (p.u.)	Event Duration	Tripped Protection
3 phase fault (bolted)	0.365	20.7	13.89	0.034	1.1 s	Under Volt 50%
L-G fault (bolted)	0.364	11.48	5.81	0.058	1.1 s	Under Volt 50%
L-L fault	0.365	15.45	10.95	0.104	1.1 s	Under Volt 50%
L-L-G fault	0.363	16.47	10.62	0.067	1.1 s	Under Volt 50%
Fault at utility side	0.365	19.22	10.62	0.012	1.1 s	Under Volt 50%

**Table 32:** Fault simulation results for the directly-coupled CHP

Fault Scenario	Generator terminal			Converter terminal		Event Duration	Tripped Protection
	$I_{fault\ pre}^{Pre}$ (kA)	$I_{fault}$ (kA) @0.18 s	$V_{fault}$ (kV)	$I_{fault\ peak}^{Peak}$ (kA)	$V_{fault}$ (p.u.)		
3-phase fault	0.365	0.367	0.257	3.33	0.10	0.18 s	Under Freq. <56.5 Hz
L-G fault	0.367	0.504	0.156	3.00	0.11	0.73 s	Under Freq. <56.5 Hz
L-L fault	0.364	0.377	0.285	3.73	0.10	0.80 s	Under Freq. <56.5 Hz
L-L-G fault	0.366	0.363	0.380	4.71	0.09	0.68 s	Under Freq. <56.5 Hz
Fault at utility side	0.365	0.372	0.274	2.07	0.45	0.19 s	Under Freq. <56.5 Hz

**Table 33:** Fault simulation results for the converter-interfaced CHP

Results show that for the directly-coupled CHP, the fault current can peak at 20.29kA, ~8.2 times the generator rated current while the 10cycles fault magnitude ( $I_{fault}$  @0.18s) remains high, above 4 times the rated current suggesting the generator undergoes the high stress under fault. For all scenarios, the breaker is opened by the 50% under-voltage protection, faster than the over-current protection. Total fault duration is ~1.1s.

In contrast with the directly-coupled, the fault current for the converter-interfaced CHP is much lower and close to the generator rated current. Indeed, at the generator terminals the current does not vary during fault and is similar to the pre-fault current while at the converter terminals, the peak fault current does go beyond ~2pu. This suggests that the converter acts as an isolator between the grid and CHP generator. From the measurements at the terminal of the converter, it can be observed that the maximum fault current is 4.71kA; 23.2% of the highest fault current with directly-coupled CHP. It can be also noted that the faults are isolated by the under-frequency protection which in all the scenarios trips the breaker within 0.8s. Therefore, the interface converter allows to limit the CHP contribution to grid side faults and exposes the generator to much less mechanical (peak fault current) and thermal (fault level and event duration) stresses than with a directly-coupled CHP system. This ultimately minimizes the wear and tear of the generator, hence extending its service life and reducing its operating costs over its lifetime.

#### *Power factor analysis*

Different grid conditions and plant loads are simulated to emulate the potential grid integration scenarios of the CHP system. Three load levels representing three distinct operating conditions for the CHP are simulated as shown in Table 34.

Peak Load	2.5x CHP MW capacity with a power factor of 0.9
Medium Load	1.5x CHP MW capacity with a power factor of 0.9
Light Load	0.5x CHP MW capacity with a power factor of 0.9

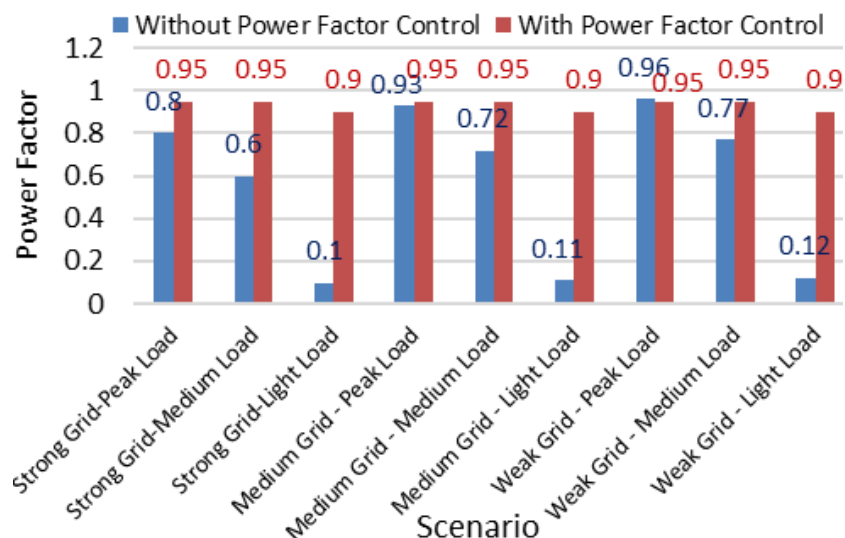
**Table 34:** Simulated CHP loading levels

For the directly-coupled CHP, if the generator is configured to run in the PV mode, results of the plant operation in that case are summarized in Table 35. The results show that in light load scenarios, the demand is supplied by the CHP locally and the grid provides the reactive power. Therefore, the power factor at POI is low. Compared with the strong grid case, the power factor at the POI under weak and medium grid conditions are slightly higher, which is expected. Under a weak grid, the voltage at the POI is lower than the reference value of the AVR due to the voltage drop along the feeder. To compensate for it the CHP generator outputs more reactive power to maintain its terminal voltage to the prescribed value. Nevertheless, the simulation results show that if the CHP is running at PV mode, the plant may violate the power factor requirement specified by the service utility. To ensure that the power factor requirement is met, the reactive power control scheme as shown in Figure 65 is integrated into the platform.

Grid strength	Load	CHP Output			P & Q at POI		PF of POI
		P(kW)	Q(kVar)	kVA	P(kW)	Q(kVar)	
Strong grid	Peak	1575	240	1593	2460	1850	0.80
	Medium	1565	125	1570	884	1191	0.60
	Light	777	8	777	42	416	0.10
Medium grid	Peak	1496	1179	1905	2224	898	0.93
	Medium	1570	507	1650	788	765	0.72
	Light	782	121	791	36	324	0.11
Weak grid	Peak	1504	1450	2089	2117	600	0.96
	Medium	1579	631	1700	757	629	0.77
	Light	793	143	806	36	296	0.12

**Table 35:** Power output of directly-coupled CHP in PV mode

In real-world applications, the proposed power factor controller can be embedded into any communication enabled plant level controller to dispatch the CHP in such a way that the power factor of the plant is met in real time while respecting its operational constraints. With the designed power factor control implemented, results of the plant operations under different grid and load scenarios are shown in Figure 68. The results demonstrate that the controller can effectively regulate the power factor (PF) of the CHP plant to meet the utility requirement.

**Figure 68:** Power factor at the POI with directly-coupled CHP

For the converter-interfaced CHP, the generator side converter operates at a unity power factor in any load or grid scenario. The reactive power for POI power factor is provisioned by the grid side inverter. For the cases without the power factor controller, the reactive power command to the grid-side inverter is proportional to the active power command to the CHP with a constant power factor of 0.9. Due to the losses from the controller, the power factor of the CHP plant is in fact slightly lower than the desired value at POI, which is observed from simulation results in Figure 69.

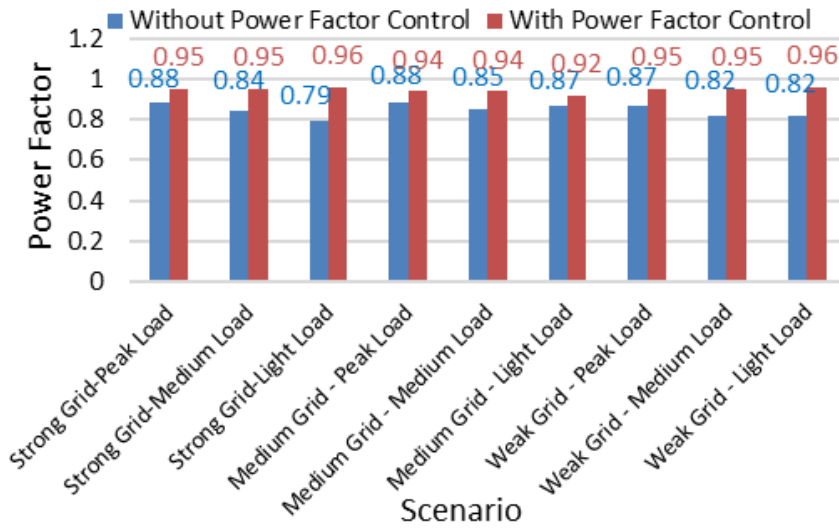


**Figure 69:** Power factor at the POI with converter-interfaced CHP

After implementing the power factor control logic, the active and reactive power obtained from the CHP engine and inverters are summarized in Table 36. Results show that the power factor of the CHP plant can be maintained at ~0.95 in all conditions with a 2MVA grid-ready inverter and a 1.6MVA generator. Compared to the directly-coupled CHP a ~2.1MVA generator would be required to achieve the same performance. Therefore, the presence of the interface converter allows to reduce the required size of the generator by ~25%. The cost difference can be used to subsidize the cost of the converter.

Grid strength	Load	CHP Output			Converter			P&Q at POI		Power Factor of POI
		P(kW)	Q(kVar)	kVA	P(kW)	Q(kVar)	kVA	P(kW)	Q(kVar)	
Strong Grid	Peak	1628	-7	1628	1472	1234	1921	2403	792	0.95
	Medium	1628	-7	1628	1479	1000	1785	907	298	0.95
	Light	824	0	824	772	419	878	55	17	0.96
Medium Grid	Peak	1628	-7	1628	1471	1140	1861	2112	736	0.94
	Medium	1628	-7	1628	1478	942	1753	866	319	0.94
	Light	827	1	827	776	415	880	49	21	0.92
Weak Grid	Peak	1628	-7	1628	1470	1188	1890	1903	621	0.95
	Medium	1628	-7	1628	1477	989	1777	796	253	0.95
	Light	824	0	824	772	418	878	46	14	0.96

**Table 36:** Power output of the converter-interfaced CHP with pf control

The interface not only allows to reduce the short-circuit contribution of the CHP system, but the stress exposed to the generator in addition to improving the power quality at POI.

#### *Dynamic performance*

The dynamic performance of the directly-coupled and converter-interfaced CHP systems is compared in islanding mode. Scenarios including a 3-phase fault, an L-G fault, and a load

step change are simulated for the two configurations and the results obtained are summarized in Table 37. These results show that for the converter-interfaced CHP, the impact of transient events is smaller than for the directly-coupled CHP. This is mainly due to the DC capacitor of back to back inverters which acts as a buffer to mitigate the transient response of the CHP generator

CHP interconnection	Scenario	Max $\Delta f$ (p.u.)	Max $\Delta v$ (p.u.)
Directly-coupled	3 Phase fault (bolted)	0.012	0.964
	L-G fault (bolted)	0.330	0.933
	100kW load step change	0.046	0.104
Converter-interfaced	3 Phase fault (bolted)	0.022	0.027
	L-G fault (bolted)	0.062	0.033
	100kW load step change	0.003	0.005

**Table 37:** Results of transient simulations in islanding

This analysis of the grid performance of converter-interfaced CHP as compared to directly-coupled CHP confirmed that the interface converter allows to significantly reduce fault contributions of the CHP plant and the short-circuit stress level that the generator is exposed to. Moreover, it allows to reduce the size of the generator by 25% while providing better power quality at POI and more stability in islanding operation with reduced frequency and voltage deviation during transient events. Hardware-in-the-loop (HIL) simulations with a grid-ready controller hardware and a microgrid controller were performed to confirm the ability of the converter-interface CHP to meet IEEE standards 1547 and 2030.7 and typical grid codes requirements for DER. As summarized in section 3.2 category B-II will be the assignment of the converter-interfaced CHP.

## 5.2 Development of the hardware-in-the-loop simulation platform

The hardware-in-the-loop (HIL) simulations platform was built using GE's Brilliance inverter<sup>65</sup> control hardware and GE's C90+ microgrid controller<sup>66</sup>. The converter-interfaced CHP model including the engine, the converter hardware, the plant loads, and hosting grid was modeled in RSCAD/RTDS<sup>67</sup>, an industry standard power system modeling and real-time simulation tool. The conceptual diagram of the microgrid system with converter-interfaced CHP as DER simulated in RTDS is shown in Figure 70 while Figure 71 describes the functional blocks of the system built in the HIL simulation platform.

<sup>65</sup> GE Brilliance inverter specifications

[https://www.caiso.com/Documents/GEEnergyStoragePresentation\\_ReactivePowerRequirements\\_FinancialCompliance\\_WorkingGroup.pdf](https://www.caiso.com/Documents/GEEnergyStoragePresentation_ReactivePowerRequirements_FinancialCompliance_WorkingGroup.pdf)

<sup>66</sup> GE Grid Solutions C90+ microgrid controller <https://www.gegridssolutions.com/multilin/catalog/c90plus.htm>

<sup>67</sup> Real-Time Digital Simulator software and platform <https://www.rtds.com/>

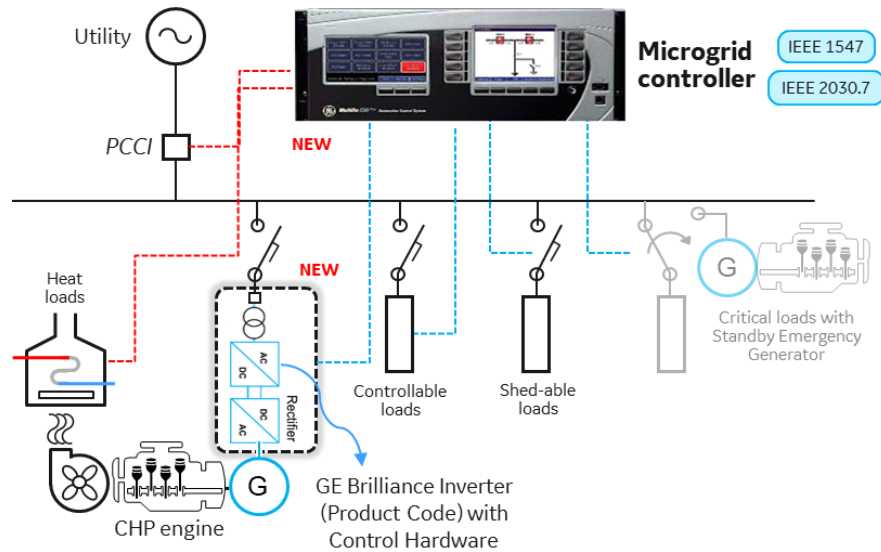


**Figure 70:** Conceptual diagram of the simulated microgrid with converter-interfaced CHP

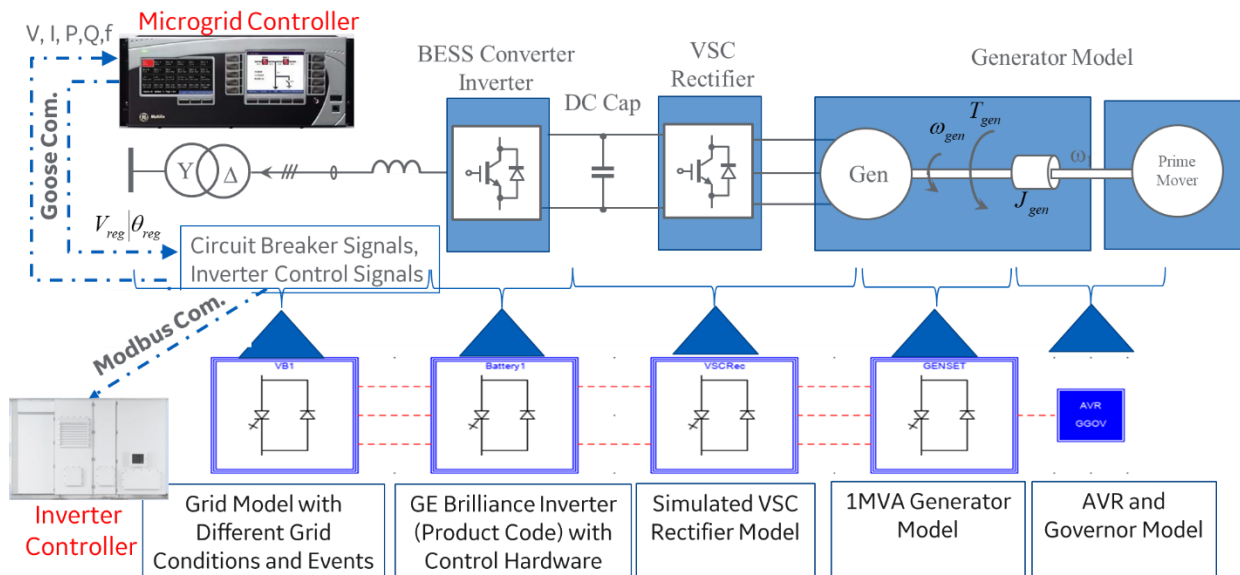


**Figure 71:** Functional blocks of the converter-interfaced CHP system built in the hardware-in-the-loop (HIL) simulation platform

Figure 71 shows the interface converter as constituted with two blocks: a grid-ready inverter and a rectifier. If for the rectifier a generic voltage source converter (VSC) model is used, for the grid-ready inverter, it's an actual GE Brilliance control hardware product code and model (1250 kW) that is used. Therefore, the inverter included in this model and test is using the real control software and commercially available product which reinforce the confidence in the simulation results. The engine model was developed separately using PSCAD then implemented in RTDS to complete the converter-interfaced CHP model. The

Jenbacher JMS 320 GS-N.LC<sup>68</sup> product specifications were used as the model baseline. The specifications of the engine are shown below



JMS 320 GS-N.LC

Electrical output 1065 kW el.  
Thermal output 4559 MBTU/hr  
Emission values Nox < 500mg/Nm<sup>3</sup>

		100%	75%	50%
Power input	[2]	MBTU/hr 9,199	7,138	5,105
Gas volume	*)	scf/hr 10,032	7,784	5,567
Mechanical output	[1]	bhp 1,468	1,101	735
Electrical output	[4]	kW el. 1,065	796	527
<b>Recoverable thermal output</b>				
~ Intercooler 1st stage	[9]	MBTU/hr 610	215	48
~ Lube oil		MBTU/hr 388	351	286
~ Jacket water		MBTU/hr 1,297	1,204	1,000
~ Exhaust gas cooled to 248 °F		MBTU/hr 2,265	1,841	1,380
Total recoverable thermal output	[5]	MBTU/hr 4,559	3,611	2,714
<b>Heat to be dissipated</b>				
~ Intercooler 2nd stage		MBTU/hr 181	150	103
~ Lube oil		MBTU/hr 80	72	59
~ Surface heat	ca. [7]	MBTU/hr 314	~	~
Spec. fuel consumption of engine electric	[2]	BTU/kWel.h 8,637	8,969	9,694
Spec. fuel consumption of engine	[2]	BTU/bhp.hr 6,265	6,484	6,946
Lube oil consumption	ca. [3]	gal/hr 0.10	~	~
Electrical efficiency		39.5%	38.0%	35.2%
Thermal efficiency		49.6%	50.6%	53.2%
Total efficiency	[6]	89.1%	88.6%	88.4%

**Figure 72:** Specifications of the Jenbacher engine used as reference for the engine emulator and for the relationship between power and heat.

Details of the simulation model built in RTDS is shown in Figure 73.

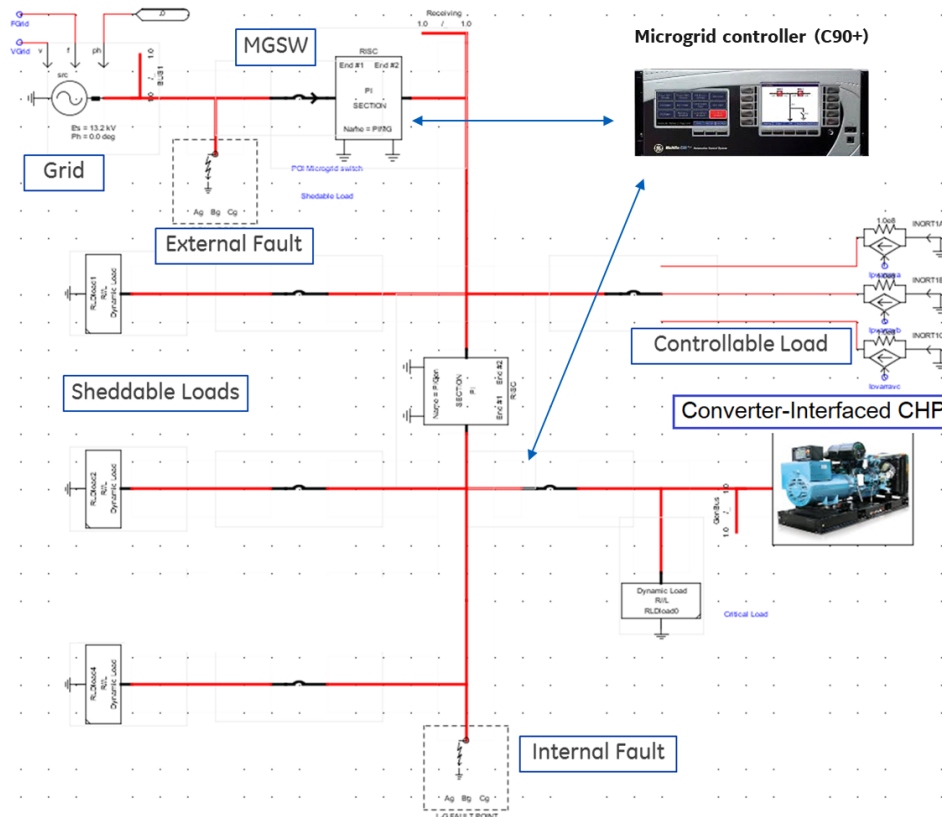


**Figure 73:** One-line diagram of the simulation model built in RTDS

<sup>68</sup> Jenbacher J320 <https://www.clarke-energy.com/gas-engines/type-3-gas-engines/>

It can be observed that it reflects the microgrid described in Figure 70 and includes features to simulate dynamic steady-state operation (load variation) and fault scenario at different locations of the plant to the steady-state, dynamic and transient performance of the converter-interfaced CHP.

The microgrid controller used in the HIL simulations is the GE's C90Plus microgrid controller. It is configured to contain several routines so it can achieve the supervisory functions recommended by IEEE 2030.7 including monitoring, energy dispatch, protection, power quality i.e., voltage support and power factor control as well as commands for seamless connection or disconnection to or from the grid. Additional capabilities such as economic dispatch, load, or price forecasting, not required for the controls validation of the compliance to standard, can also be implemented to support the technical and financial operation of the plant. The controller is compatible with IEC 61850 and support Modbus and Ethernet as well as GOOSE messaging. An example of timeline of the IEC61850/GOOSE message<sup>69</sup> response in a protection event is shown in Figure 74. It indicates that controller will react within 17 milli seconds.

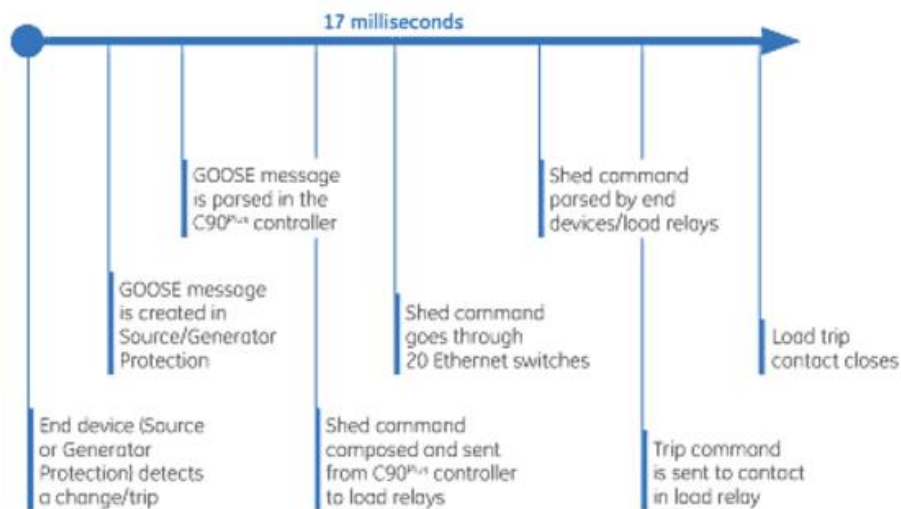


**Figure 74:** Example of the GE's C90+ communication with IEC61850/GOOSE messaging

The rate of communication to the HMI/SCADA shall be nominally 1/sec. Signals include:

- RMS voltages and currents on either side of the POC
- RMS voltage and currents on either side of the PCC
- RMS voltage and currents out of the generator
- instantaneous frequency on either side of the PCC
- power production from the generator, status of the POC breaker
- power transaction between the grid and the microgrid, status of the PCC breaker
- RMS currents through the controllable loads
- RMS currents through the shippable loads

<sup>69</sup> IEC 61850 - Communication Networks and Systems in Substations <https://webstore.iec.ch/publication/6007>

### 5.2.1 Performance objectives of the HIL simulations

Specifically, the HIL simulations allow to validate the ability of the converter-interfaced CHP to:

- meet typical load and VAR commands in steady-state operation
- ride-through abnormal conditions as required by IEEE 1547-2018
- operate in islanding conditions and,
- seamlessly transition from grid-tie to islanding and the opposite.

The performance objectives of the HIL are listed in Table 38 will focus on validating the ability of the integrated control system of the converter-interfaced CHP and the microgrid controller to meet minimum requirements of IEEE standard 1547 and 2030.7.

Performance Objective	Metric	Data Requirements	Success Criteria
Disconnection	disconnection times	measurements of POI opening response	IEEE 1547 compatible
Reconnection	Frequency, Voltage and phase angle difference	measurements of voltage & frequency and phase angle (at both sides of PCC)	IEEE1547 compatible
Power Quality	Voltage, frequency, harmonics and power factor values	measurements of voltage & frequency, THD, and power factor at the PCC and POC	IEEE 1547 and IEEE 2030.7 compatible
Protection	response to faults and voltage and frequency ride-through capabilities	measurements of voltages, currents and frequency at the PCC and POC following fault events	IEEE 242 (Buff Book) and IEEE 1547 compatible
Dispatch	generation outputs following heat and power commands	Meter measurements, response time	IEEE 2030.7 compatible
Islanding	Stable frequency and voltage after grid isolation	Voltage and frequency at the CHP and response to faults events	IEEE 2030.7 compatible

**Table 38:** Performance objectives of the microgrid controller and integrated control system of converter-interfaced CHP

#### *Disconnection*

A seamless transition from grid-tied to island mode of operation is required to avoid any major disturbance, damage to the plant component or interruption of critical loads. The disconnection procedure will require for instance to control the power (kVA) at the PCC near 0 before opening the PCC breaker. A control routine that will ensure a seamless disconnection following a command to disconnect is implemented into the microgrid controller and tested. During the disconnection process, the microgrid controller brings the power at POI to near 0kVA in controlled before opening the breaker. This allows to reduce transients and ensure a seamless transition from the grid connected to the island mode. To bring the power transit at POI to ~0kVA, the loads are prioritized as critical, controllable

and sheddable loads. The microgrid will dispatch the CHP for loads critical loads first and then adjust the controllable to as sustainable level by the CHP.

The disconnection routine also makes distinction between normal disconnection and rapid disconnection. Indeed, unlike the seamless transition from grid-tied mode to islanding, the rapid disconnection applies when abnormal conditions such as under/over voltage and/or frequency tends to persist beyond the ride-through clearing times. In the presence of those events, the protection functions integrated into the interface converter controls should disconnect the CHP as required by the IEEE 1547-2018. Backup protection functions with same pickup levels and clearing times will be implemented into the microgrid controller to force disconnection if the converter-interfaced CHP does not disconnect itself. A rapid disconnection command from the microgrid controller may be warranted under the following conditions:

- A trip request from the distribution system operator (RTDS signal in this case).
- When the voltage or frequency at the PCC (utility breaker) or at the POC (DER breaker) violates the requirements specified by IEEE 1547-2018.

Other protection functions (internal to the converter, generator, or engine) such thermal limit may also trigger the disconnection. Those scenarios are not tested with the microgrid controller as not specific to the converter-interfaced configuration.

When the condition for disconnection is met, the protection module of the interface converter and/or the microgrid controller sends a trip signal to the PCC breaker. The response time for disconnection, starting from the time of occurrence of the condition to the full opening of the breaker, is calculated as the disconnection time is compared with the IEEE 1547-2018 requirements.

#### *Resynchronization and reconnection:*

Resynchronization and reconnection are part of a transition from shutdown mode or islanding to grid-connected mode. Resynchronization is the process of aligning the frequency, phase angle and voltage magnitudes of the DER as closely as possible to that of the grid values before reconnection. However, in the case of the converter-interface, it is possible to close the POC without synchronization as no power (0kVA) will circulate through POC unless gating signals are sent to the power modules. The POC can be closed at any time after the DC bus is charged by the rectifier. This is a big advantage of the converter-interfaced over directly-coupled. Indeed, synchronization takes time and can be followed by transients which can reject the reconnection and delay further again the process. For the converter-interfaced, a resynchronization is not required unless except from islanding to grid-tied mode. In that case the decoupling of the reactive power and active power and the engine speed from the grid frequency will be very beneficial. Table 39 show the synchronization parameters as perter IEEE Std 1547-2018.

Aggregate rating of DER units (kVA)	Frequency difference ( $\Delta f$ , Hz)	Voltage difference ( $\Delta V$ , %)	Phase angle difference ( $\Delta \Phi$ , °)
0–500	0.3	10	20
> 500–1 500	0.2	5	15
> 1 500	0.1	3	10

**Table 39:** DER synchronization parameters as per IEEE Std 1547-2018

The resynchronization capability is embedded in the microgrid controller which will manage the procedure depending on the plant operating condition. If the CHP is coming from shutdown mode while the plant is still connected to the grid (PCC breaker is closed) no synchronization will be applied, inverter gating will begin after POC breaker is closed. If the CHP was operating in islanding mode, the synchronization requirements will be applied to the PCC (utility breaker). The synchronization procedure will be inhibited if the grid is down (PCC breaker is opened) is the CHP is coming from shutdown to power the plant loads (for instance in multiple units staging configuration).

#### *Power quality*

The converter-interfaced CHP is required to meet a minimum performance for voltage regulation, frequency control, harmonics injection, etc. depending on its operating mode. The microgrid controller allows to dispatch the required amount of active and reactive power to meet target voltage or power factor at the PCC in grid tied mode and to maintain reliable operation (power limit, frequency control) in islanding mode. In grid connected mode the voltage and frequency of the electrical network are set by the grid. However, the converter-interfaced CHP can help improve the voltage profile in the plant or the power factor at the PCC (utility breaker). In islanded mode, the converter-interfaced CHP will be responsible of maintaining the frequency and the voltage of the plant within prescribed values. The microgrid controller is then responsible of dispatching the active and reactive power within the voltage and frequency limits. It will have the ability to control or disconnect non-critical loads in that mode.

#### *Protection coordination*

For most electrical networks, protection of assets happens at the asset level due to the need for fast response and cost-effective solution. In a microgrid configuration, the microgrid controller acts as a supervisory layer for protection system, while the primary protection actions will be performed by existing local devices (fuse and breakers). The behavior of the microgrid controller for possible fault scenarios is described as follow:

- utility feeder fault (external): the PCC breaker trip unit is given a time overcurrent curve to react. The microgrid controller trips the POC and PCC depending on the voltage and frequency ride-through requirements.
- plant local fault (internal): All branch feeders including the POC breaker are given a time overcurrent curve. The microgrid controller will trip the faulty branch if the local breaker does not trip or PCC if breaker failure or communication issue with local breaker. The IEEE 1547 ride-through protection will trip the CHP before the

fault is cleared (PCC breaker open). The microgrid ensure then the fault is cleared before resynchronizing and reconnecting the CHP.

- fault during islanding: the microgrid controller gives priority to the local protection device to clear the fault. If the local protection fails to open (breaker or communication failure), then the microgrid controller will trip the CHP using overcurrent setting. Note the IEEE 1547-2018 voltage and frequency ride-thorough requirements are disabled during islanding operation.

### 5.2.2 Validation of the converter-interfaced CHP RTDS model

Figure 75 gives an overview of the CHP system model developed in RTDS showing the generator and engine models. The model is based on the Jenbacher engine J320<sup>68</sup> and represent a 1,065 kWe engine with a 1.32MVA generator. The technical data of the generator is shown in Table 40.

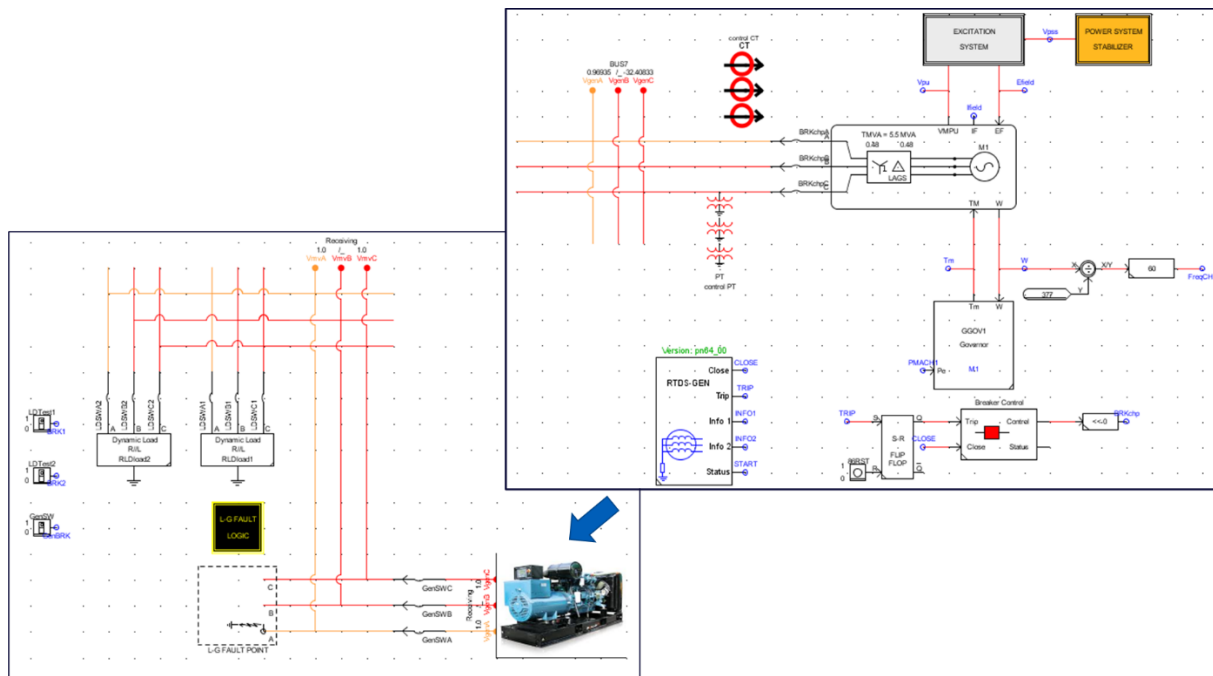


**Figure 75:** Overview of the RTDS model of the CHP system implemented with the interface converter

Ratings at p.f. = 1.0	kW	1,065
Ratings at p.f. = 0.8	kW	1,056
Rated output at p.f. = 0.8	kVA	1,320
Rated reactive power at p.f. = 0.8	kVAr	792
Rated current at p.f. = 0.8	A	1,588
Frequency	Hz	60
Voltage	V	480
Speed	rpm	1,800
Permissible overspeed	rpm	2,250
Power factor (lagging - leading)		0.8 - 1.0
Efficiency at p.f. = 1.0		97.3%
Efficiency at p.f. = 0.8		96.4%
Moment of inertia	lbs-ft <sup>2</sup>	1055.93
Mass	lbs	7,882
Radio interference level to EN 55011 Class A (EN 61000-6-4)		N
Ik" Initial symmetrical short-circuit current	KA	19.63
Is Peak current	KA	49.96
Insulation class		H
Temperature rise (at driving power)		F
Maximum ambient temperature	°F	104

#### Reactance and time constants (saturated) at rated output

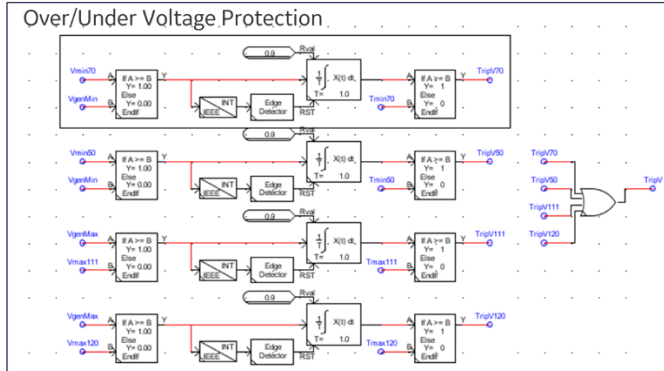
xd direct axis synchronous reactance	p.u.	1.84
xd' direct axis transient reactance	p.u.	0.11
xd" direct axis sub transient reactance	p.u.	0.08
x2 negative sequence reactance	p.u.	0.12
Td" sub transient reactance time constant	ms	20
Ta Time constant direct-current	ms	20
Tdo' open circuit field time constant	s	2.46

**Table 40:** Technical data of the ~1MW generator used as a reference for the generator model

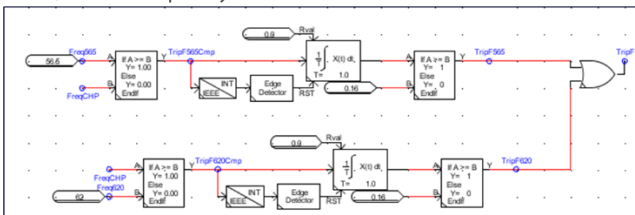
Figure 76 details the protection logic implemented showing compliance with IEEE std 1547-2018 requirements.

#### Protection settings

Protection	Pickup Range	Clearing Time (sec)
Under Freq. 2	f ≤ 56.5 Hz	0.16
Over Freq. 2	f ≥ 62 Hz	0.16
Under Volt. 1	V ≤ 50% of Nominal	1.1
Under Volt. 2	50% ≤ V ≤ 80% of Nominal	2
Over Volt. 1	110% ≤ V ≤ 120% of Nominal	2
Over Volt. 2	120% of Nominal ≤ V	0.16
Over Cur. 1	2.22 p.u.	Extreme Inverse
Over Cur. 2	17.78 p.u.	Instantaneous



#### Over/Under Frequency Protection



#### Over Current Protection

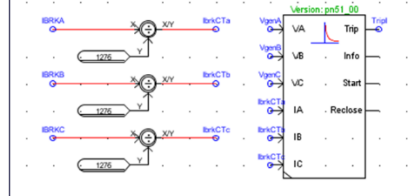


**Figure 76:** Overview of the protection logic implemented with the CHP system

Following the integration of the CHP model with the interface converter simulations were performed to evaluate the performance of the controls. The model validation results are shown in Figure 77. They indicate that the converter-interfaced CHP responds adequately to normal load dynamics comforting that the controls has been successfully integrated. The DC bus is regulated to  $\sim 800$ Vdc, and the generator output voltage, torque and speed are stable. It can be also noted that generator reactive power output is  $\sim 0$ kVAR.

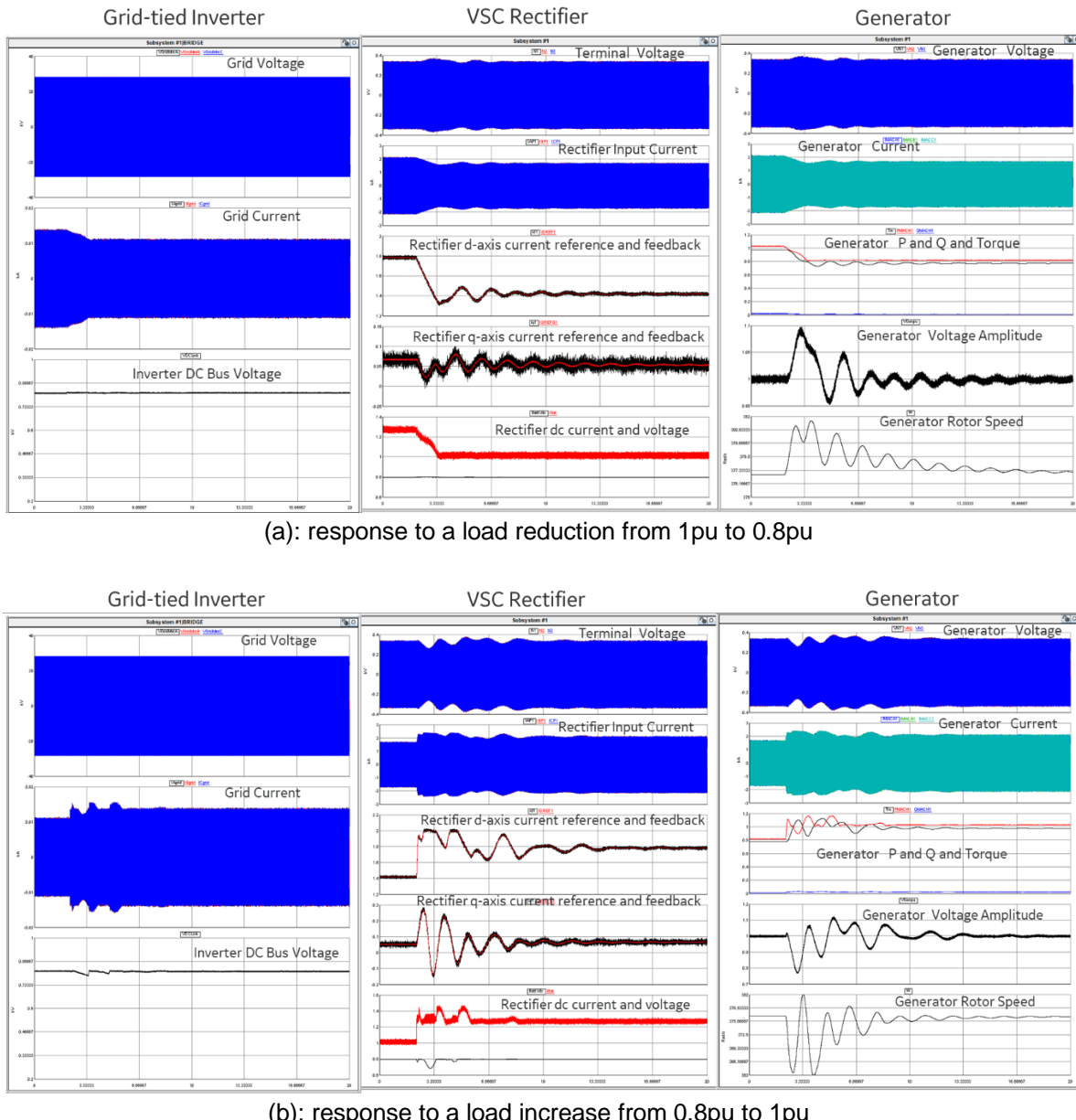
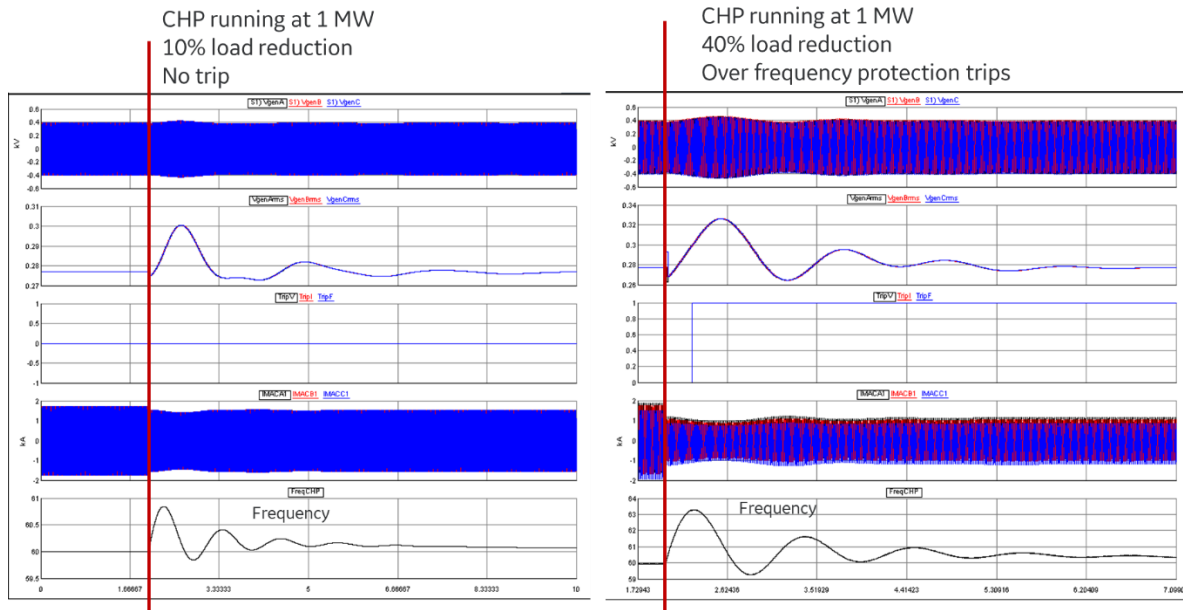


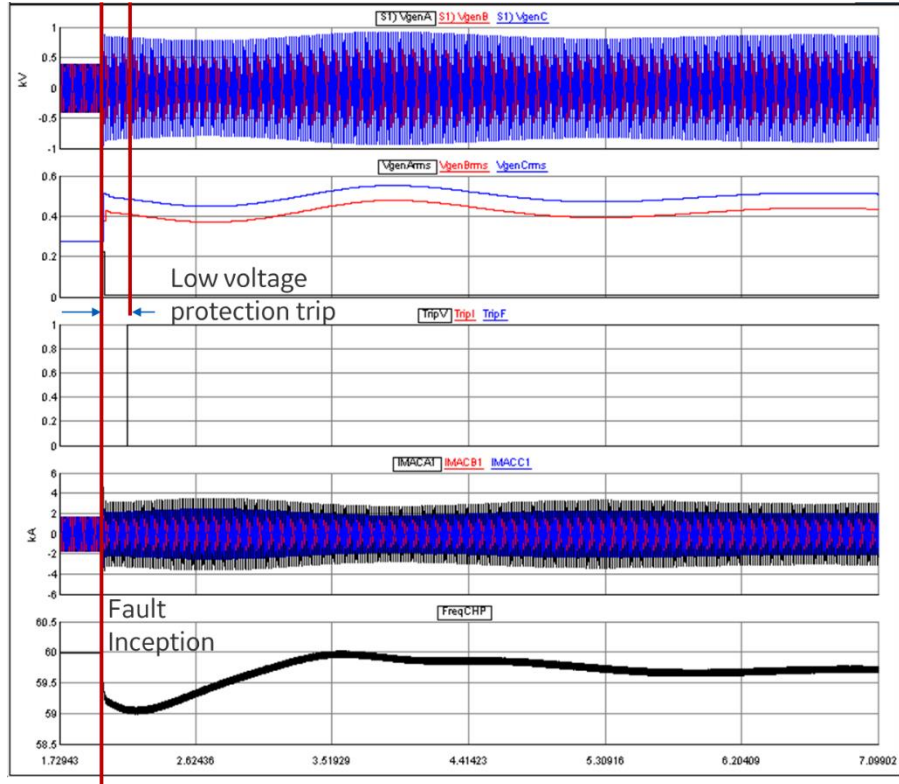
**Figure 77:** Validation of the voltage and frequency ride-through settings

Testing of the voltage and frequency ride-through requirements shows that both the controls and protection settings are compliant with IEEE std 1547-2018. Indeed, Figure 77 indicate that when frequency remains below 61Hz (10% load reduction) no trip occur while

at 63Hz (40% load reduction) the trip for over-frequency is instantaneous. Similarly, when the voltage on one phase reaches ~0Vrms due a line to ground fault as shown in Figure 77.(b) the trip for under-voltage is instantaneous.



(a): response to frequency transient event



(b): response to a voltage transient

**Figure 78:** Simulation results of the integrated converter-interfaced CHP

Figure 80 shows a screenshot of the control interface of the GE's Brilliance inverter and the GE's C90+ microgrid controller validating the data communication between RTDS, the microgrid controller and grid-side inverter. A screenshot of the C90+ logic editor showing some examples of algorithm implementation (UF detection -> C264; UV detection -> C77 and C84; Power import and export calculations -> C268 and C272, respectively) in presented in Figure 80.

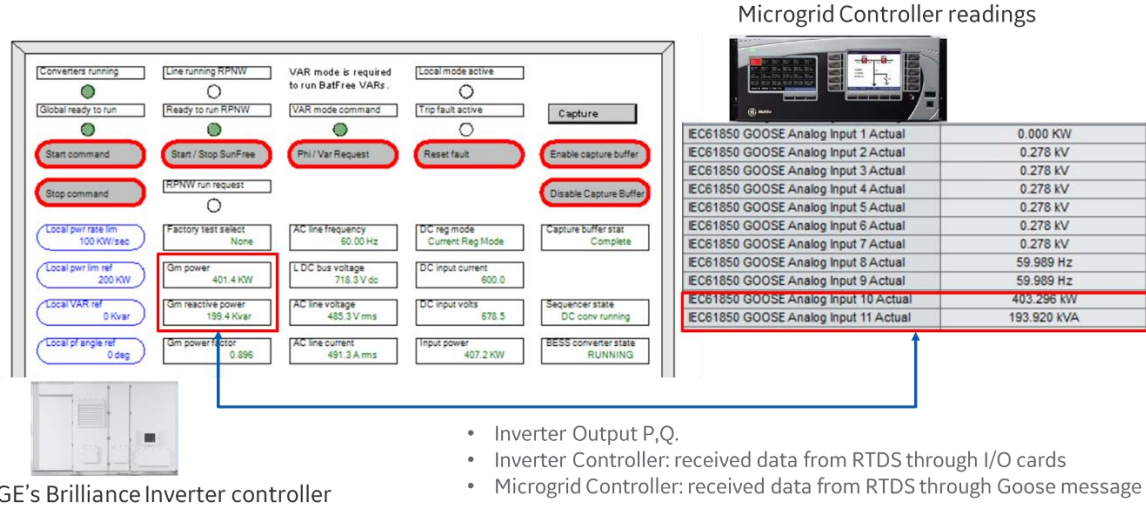


**Figure 79:** Validation of the communication of the HIL simulation platform

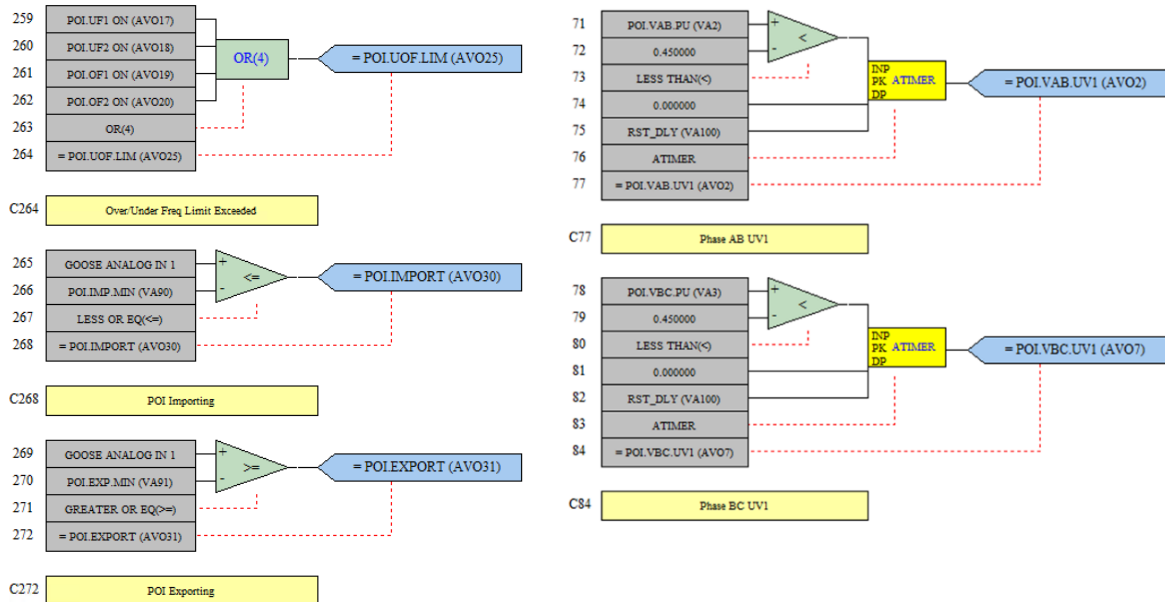


**Figure 80:** An overview of the C90+ logic editor for algorithms implementation

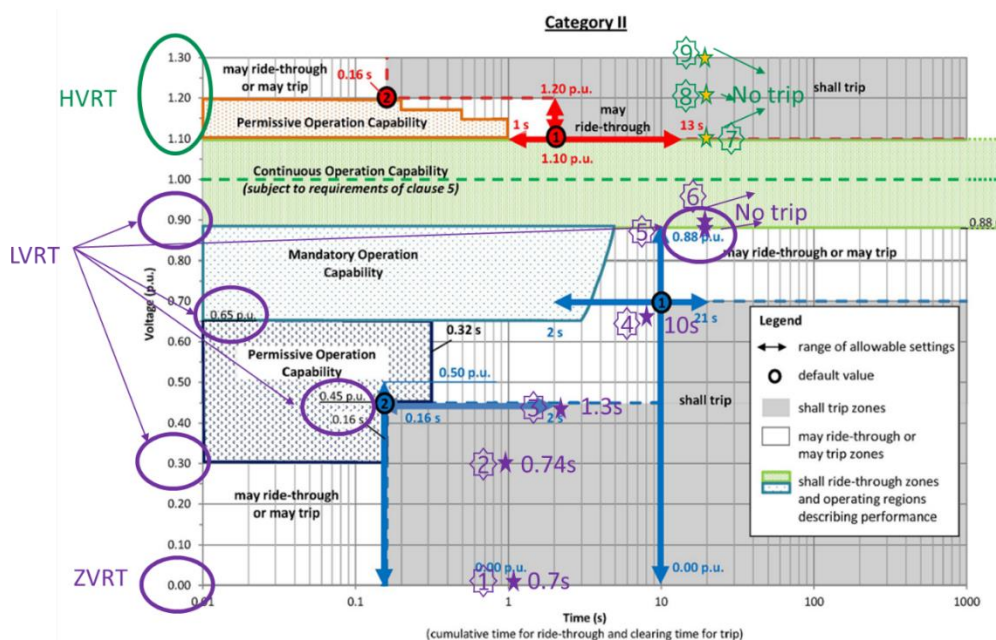
The results of the converter-interface CHP control performance are presented in the following section.

### 5.3 Validation of the control performance of converter-interfaced CHP

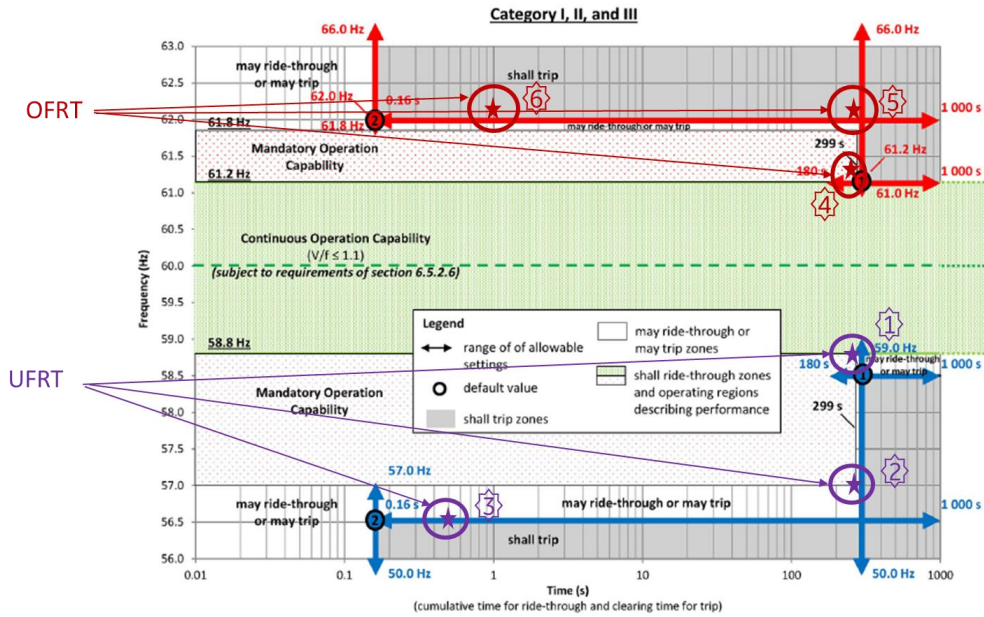
A test plan was developed to validate the compliance of the converter-interfaced CHP to governing standards IEEE 1547-2018<sup>5</sup> and IEEE 2030.7-2017<sup>6</sup>. In addition to the voltage and frequency transients simulations ride-through performance capabilities, multiple scenarios including steady-state and dynamic operating conditions, applicable to small and medium-sized industrial commercial and industrial plants have been tested using the HIL simulation platform. Results are summarized in Figure 81 and Figure 82, respectively for the voltage and frequency ride-through and in Table 41 for the steady-state and dynamic performances.

Figure 81 and Figure 82 show that the converter-interfaced comply to IEEE std 1547-2018 category II DER requirements for voltage and frequency ride-through. Indeed, the converter-interfaced CHP does not trip in “mandatory operation” zones and have enough capability in most cases to withstand transients deep inside the “shall trip” zones. This proves that the interface converter has margin to adapt to different grid conditions which provides flexibility in setting up clearing times.

Overall, 22 user cases including high load, low load, small and large abnormal conditions (seen on voltage and frequency), faults inside and outside the plant, active and reactive power dispatch have been tested. Table 41 show that all tests have passed according to the success criteria set forth and described in Table 38. Figure 83 through Figure 88 provide details on some user cases.



**Figure 81:** Summary of the voltage ride-through simulation results for the converter-interfaced CHP (category II DER per IEEE 1547-2018)

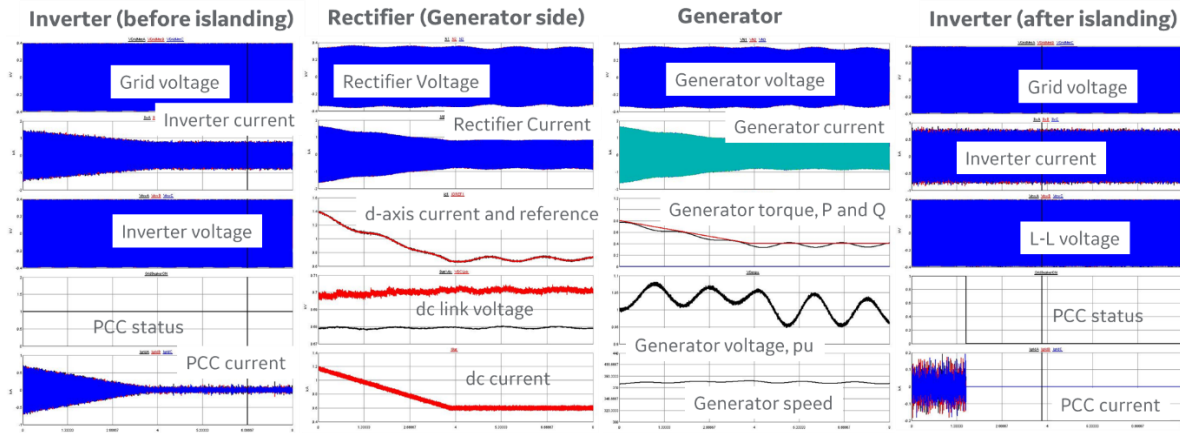


**Figure 82:** Summary of the frequency ride-through simulation results for the converter-interfaced CHP (category II DER per IEEE 1547-2018)

Performance Objective	Metric	Data Requirements	Success Criteria	Results
<b>C1. Disconnection</b> • Seamless disconnection • Abnormal condition	disconnection times	measurements of POI opening response	IEEE 1547 compatible	Passed
<b>C2. Reconnection</b> • Synchronization	Frequency, Voltage and phase angle difference	measurements of voltage & frequency and phase angle (both sides of PCC)	IEEE1547 compatible	Passed
<b>C3. Power Quality</b> • kW dispatch • kVAR dispatch and power factor control	Voltage, frequency, harmonics and power factor values	measurements of voltage & frequency, THD, and power factor at PCC/POC	IEEE 1547 and IEEE 2030.7 compatible	Passed Passed
<b>C4. Protection</b> • Internal faults • External faults	response to faults and voltage and frequency ride-through capabilities	measurements of voltages, currents and frequency at the PCC and POC following fault events	IEEE 242 (Buff Book) and IEEE 1547 compatible	Passed Passed
<b>C5. Dispatch</b> • Load following • Heat following	generation outputs following heat and power commands	Meter measurements, response time	IEEE 2030.7 compatible	Passed with PHIL
<b>C6. Islanding</b> • Served load beyond critical loads • Black start	Stable frequency and voltage after grid isolation	Voltage and frequency at the CHP and response to faults events	IEEE 2030.7 compatible	Passed Passed

**Table 41:** Summary of the HIL simulation results

Figure 83 shows the case of a seamless disconnection from the grid where the CHP was outputting 800kW (0.8 pu) with 400kW of local load while in grid-tie. When a dispatch signal is sent the inverter decreased its output to 400kW at a rate of 100 kW/s. After 10s at ~0kW the microgrid controller opens the PCC breaker, the CHP continues then its operation in islanding with 400kW output. Total time between initial request to full disconnection is less than 30s. The generator voltage oscillated between ~0.95pu and ~1.1pu during the transition but no reactive power was required, and the frequency was steadily maintained at 60Hz. No trip occurred during the transition.



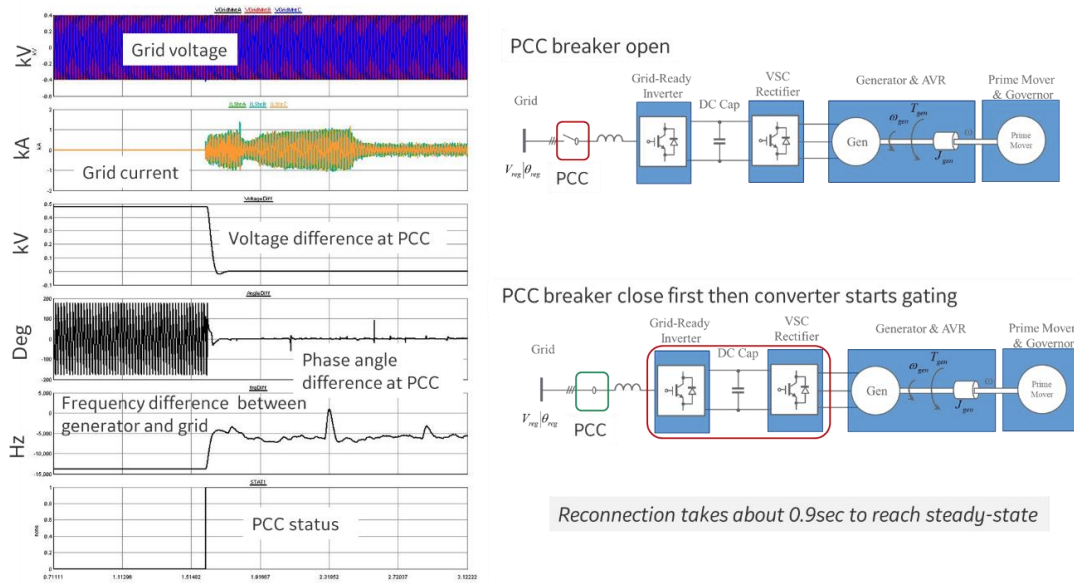
**Figure 83:** Simulation results for transition from grid-tie mode to island

Figure 84 shows the case of a grid reconnection. As previously explained, with the converter-interfaced CHP, the PCC breaker can be closed without resynchronization. An inrush current during the DC bus (link between the rectifier and the inverter) charging can be noted. After the transient, the CHP starts injecting power once the inverter starts gating as shown in the grid side current measurement. The time from reconnection request (PCC breaker close) to steady-state grid-tied takes about 0.9s. No trip occurred during the reconnection.

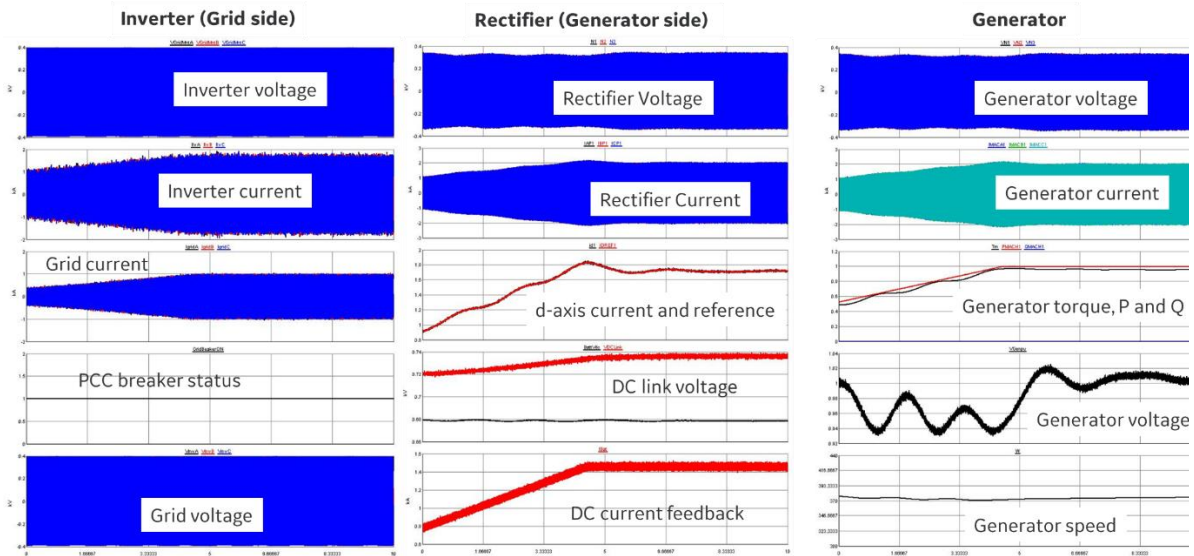
Figure 85 shows the case of an active power dispatch. A command is sent to the CHP to increase the grid export by ~0.5pu of the CHP capacity. It can be observed that the inverter and generator output currents have increased accordingly. During the transient the generator output voltage decreases first to 0.94pu and then recover and stabilized to 1.02pu due to the reaction of the AVR. As expected, the generator speed and reactive power remain almost unchanged to 370rad/s and ~0kVAR, respectively. The load request reaches steady-state within 4.5s. No trip occurred during the transition.

Figure 86 shows the case of reactive power dispatch to control the power factor at PCC. The first scenario (left) shows a power factor control a full load export where the CHP is exporting its rated power of ~1MW. Before the dispatch command, the pf at PCC was 0.8 and the reactive power ~435kVAR. The interface converter was injecting ~95kVAR. To regulate the pf at 1, the inverter injects ~340kVAR. It can be observed that the active power

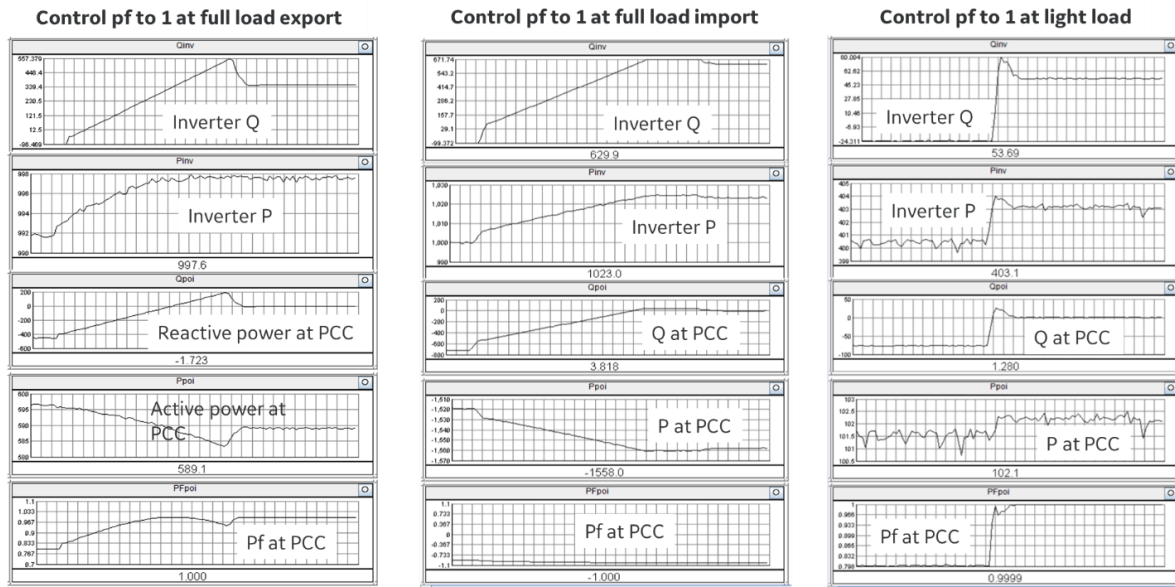
at PCC slightly decreases (from 597kW to 590kW) due to additional losses in the inverter induced by its increased reactive power. The second scenario in Figure 86 (middle) is similar to the previous one described except the power at PCC is in importing mode. Before the dispatch command the inverter was injecting ~1,000kW and absorbing ~100kVAR. The pf factor at PCC was 0.8. To regulate the pf at PCC to 1, the inverter injects ~672kVAR, a difference of 775kVAR. Losses at the inverter increased by 20kW. The last scenario (right) is a control of the pf at light load ~400kW. The pf at PCC can be improved from 0.8 to 1 by injecting 75kVAR additional.



**Figure 84:** Simulation results for reconnection to utility grid

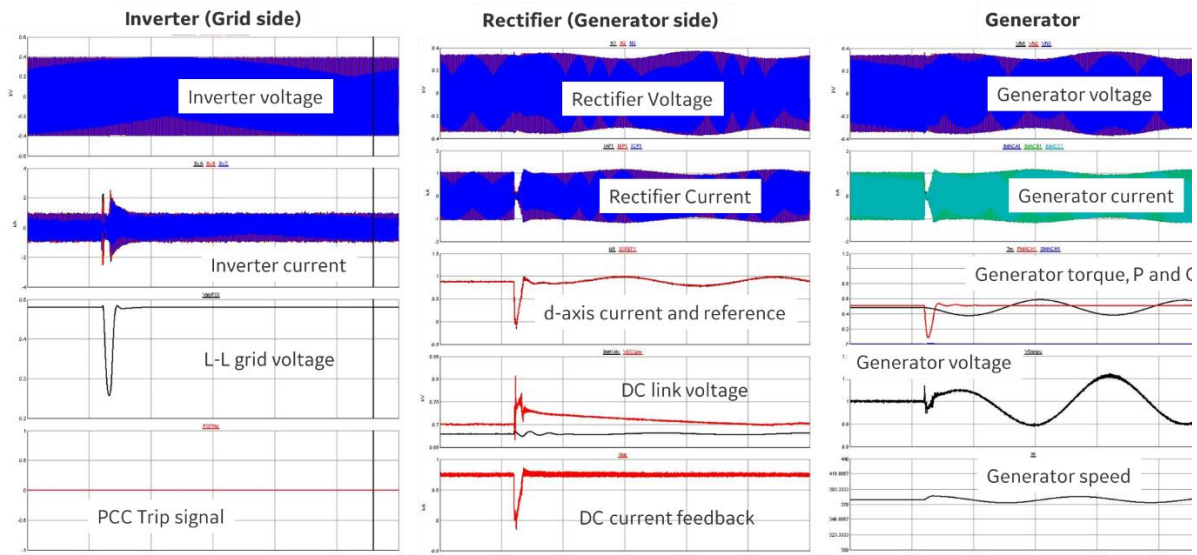


**Figure 85:** Simulation results for active power dispatch with increase of grid-export



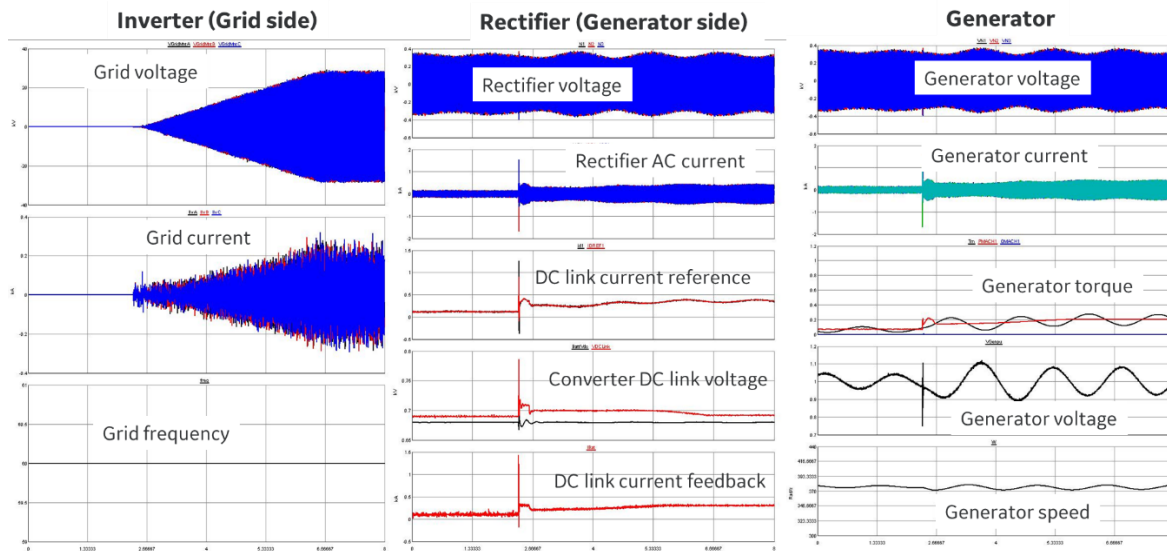
**Figure 86:** Simulation results for power factor control at PCC

Figure 87 shows the case of a temporary single phase-to-ground internal fault. The fault is applied at the distribution feeder of the plant and lasts for 80ms. It can be observed that no trip occurs thanks to the ride-through settings and capabilities of the interface converter. During the fault, the inverter injected around  $\sim 1.2\text{pu}$  of its rated current while the generator was almost shutdown ( $\sim 0\text{pu}$  current output). After the fault disappears the system gradually recovers with little oscillations in the generator voltage ( $\pm 10\%$ ) and speed ( $\pm 3\%$ ). The scenario shows that the interface converter allows to significantly limit the fault contribution of the CHP system while keeping the generator “invisible” to the fault.



**Figure 87:** Simulation results for temporary L-G fault inside the plant

Figure 88 shows the case of a black-start in islanding mode with 20% of CHP loading. When the black start command is sent, the inverter starts building up the voltage and current to satisfy the load. The generator shows an inrush current of 1.2pu of its rated current. However, the load is successfully established after ~4s with some oscillations in the generator voltage (+/- 10%) and speed (+/- 3%).



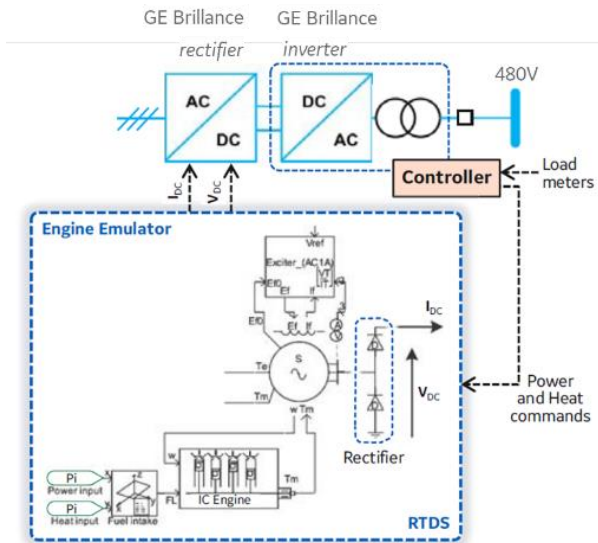
**Figure 88:** Simulation results for black-start in islanding operation

## 6. VALIDATION OF THE PERFORMANCE OF CONVERTER-INTERFACED CHP

### 6.1 Power hardware-in-the-loop test setup

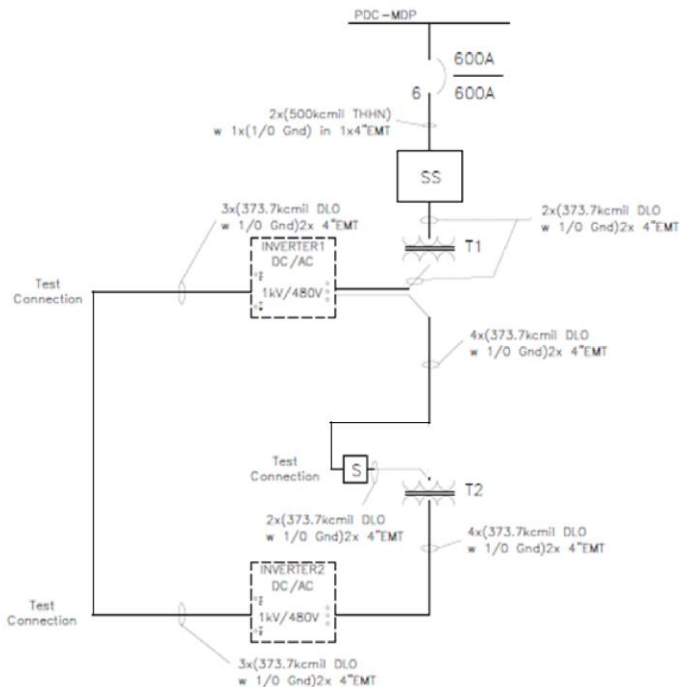
Following a successful control HIL (CHIL) testing, a power hardware-in-the-loop (PHIL) testbed was built to validate the performance in steady-state operation of the converter-interface CHP. Real buildings electric and heat loads in the GE Research facilities were used to emulate the real-time operation of a CHP in an industrial or commercial plant. The PHIL testbed consisted of the interface converter, an engine emulator and the microgrid controller. Two GE's Brilliance inverters configured in back-to-back operation were used to form the interface converter. The grid-side inverter was rated 1,275kW, and the VSC rectifier 700kW. An engine emulator built in a RTDS Novacor<sup>70</sup> rack was developed to represent the CHP engine, generator and controls and its interaction with the interface converter DC bus voltage and current. The PHIL is completed with the GE's C90+microgrid controller previously used in the CHIL simulations which embeds the algorithms for ride-through requirements, protection, heat, active and reactive power dispatch. Figure 89. shows schematically the diagram of the PHIL testbed including the CHP.

<sup>70</sup> RTDS Novacor, a real-time power simulator hardware <https://knowledge.rtds.com/hc/en-us/articles/360034290474-NovaCor->

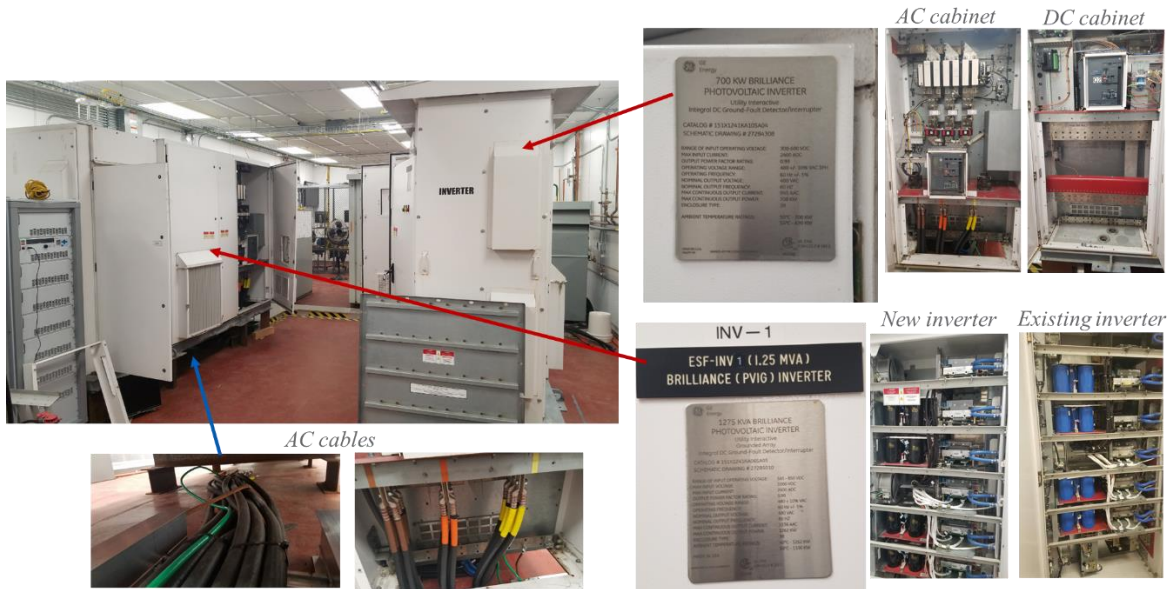


**Figure 89:** Schematic diagram of the power hardware-in-the loop (PHIL) testbed

The single line diagram (SLD) of the of the PHIL testbed is shown in Figure 90. It indicates a 480V/480V transformer for each inverter which allows to further isolate the “generator” side and the grid side in this testbed setup. Figure 91 shows the two inverters after installation including their AC and DC cabinets as well as their power electronics modules cabinet.



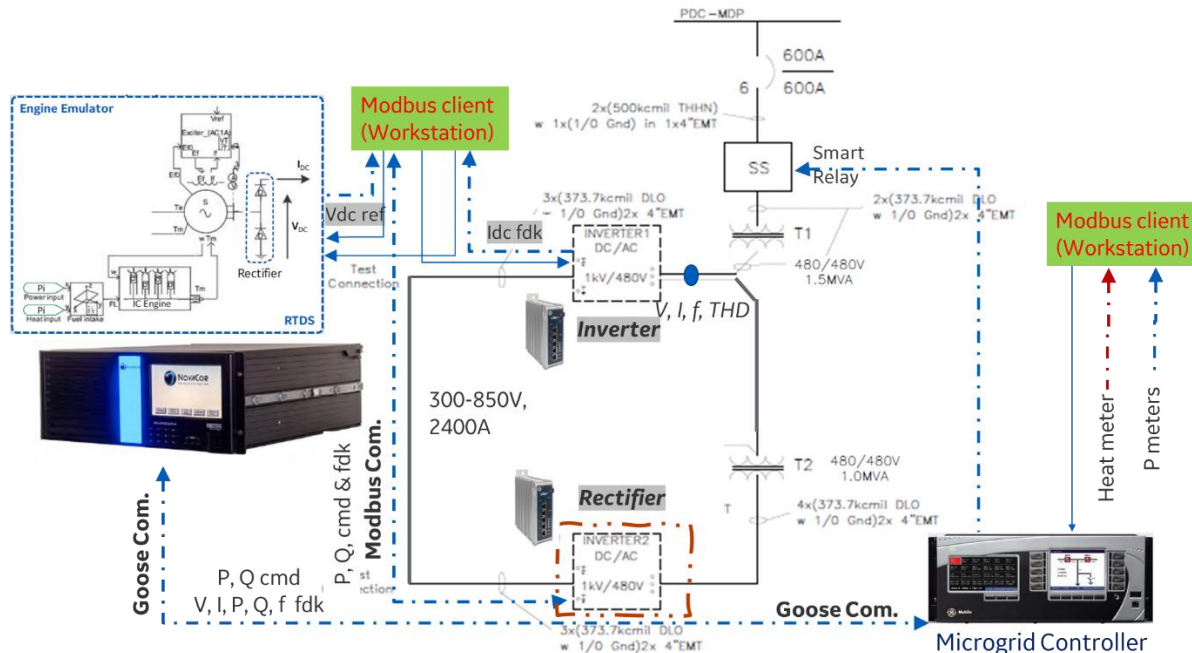
**Figure 90:** Single Line Diagram of the test layout



**Figure 91:** Installation of the two GE Brilliance inverters used as back-to-back VSC for the validation of the performance of the converter-interfaced CHP

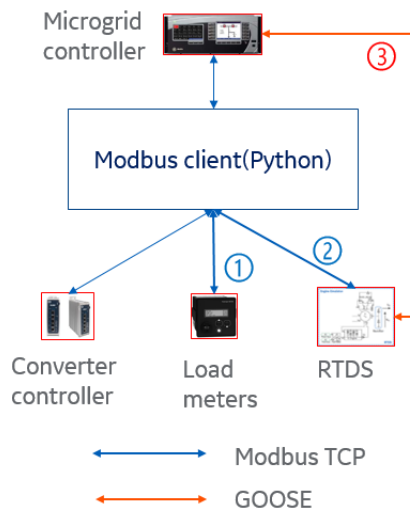
### 6.1.1 Development of the PHIL testbed communication architecture

Figure 92 shows the architecture of the testbed including the power and communication loops. It can be noted that the RTDS Novacor rack hosting the CHP engine emulator acts as the communication bridge of almost all the Intelligent Electronic Devices (IED) involved in the testbed including the C90+ microgrid controller, the Brilliance controllers and the Modbus workstation. It also enables GOOSE communication (IEC 61850) between the C90+ and the Novacor rack.



**Figure 92:** Control and communication architecture of the PHIL testbed

While the RTDS Novacor provides critical support by handling some of the required data exchange in GOOSE (for instance between the engine emulator and microgrid controller); most of the devices in the testbed use only Modbus as communication protocol and can behave as a Modbus server. As with typical Modbus server a Modbus client is required to initiate the communication. Therefore, a Modbus workstation was necessary to serve as a “bridge” between the devices in the testbed including the Novacor rack, the C90+ microgrid controller, the Brilliance controllers and the load meters. Figure 93 shows the summarized communication architecture with the GOOSE and Modbus links.



**Figure 93:** Load meter <-> RTDS <-> Microgrid controller.

Both Modbus TCP and GOOSE needed to be enabled. Firstly, Modbus workstation reads data from the load meters, then writes them to RTDS. RTDS broadcasts in GOOSE messages (IEC 61850) the analog values to be subscribed by the microgrid controller and collect back the commands to send to the Brilliance controllers through the Modbus workstation. The python script created to collect and process the data for command, controls and monitoring periodically sends “read” requests to IEDs and then forward the data collected from one to the other. One single full data exchange cycle involves client reading RTDS registers, client writing controller registers, client reading controller registers and client writing RTDS registers. Two approaches to determine the best option for the communication were tested: option 1 – sequential operation and option 2 – parallel operation. In the sequential operation the Modbus client was tested to sequentially repeat the following 4 steps: 1) read Voltage from RTDS, 2) write Voltage to controller, 3) read Current from controller, 4) write Current to RTDS. In the parallel operation the same test is performed while parallelizing the data request actions with multiprocessing i.e., to have two Modbus clients to process the data requests in parallel. Figure 94 shows the results of the time intervals between two contiguous writing actions for the two approaches. In both cases results indicate that the average time needed for a complete iteration is about 50ms. Although the parallel operation was more stable, it did not provide major benefit for

communication speed, therefore the sequential was adopted as simpler. Figure 95 show the results of the communication testing between RTDS and the Brilliance controller using a sequential operation.

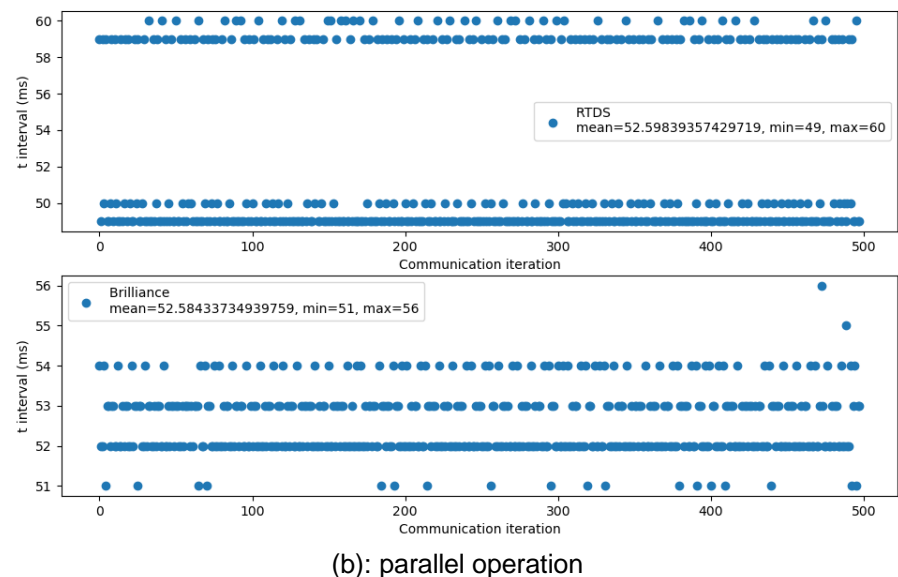
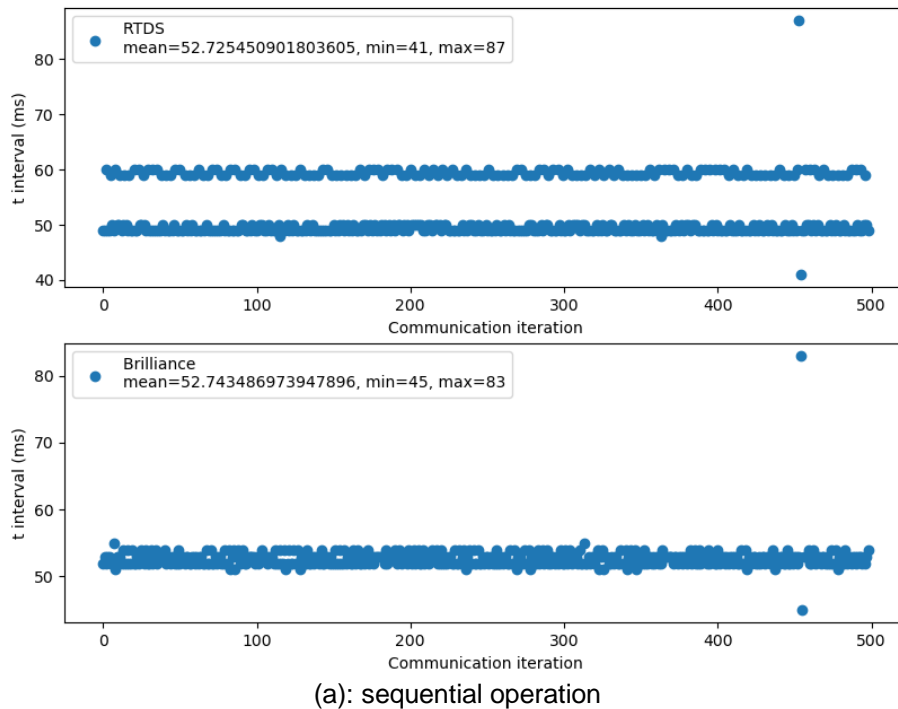


**Figure 94:** Requests intervals during communication RTDS and Brilliance controllers.

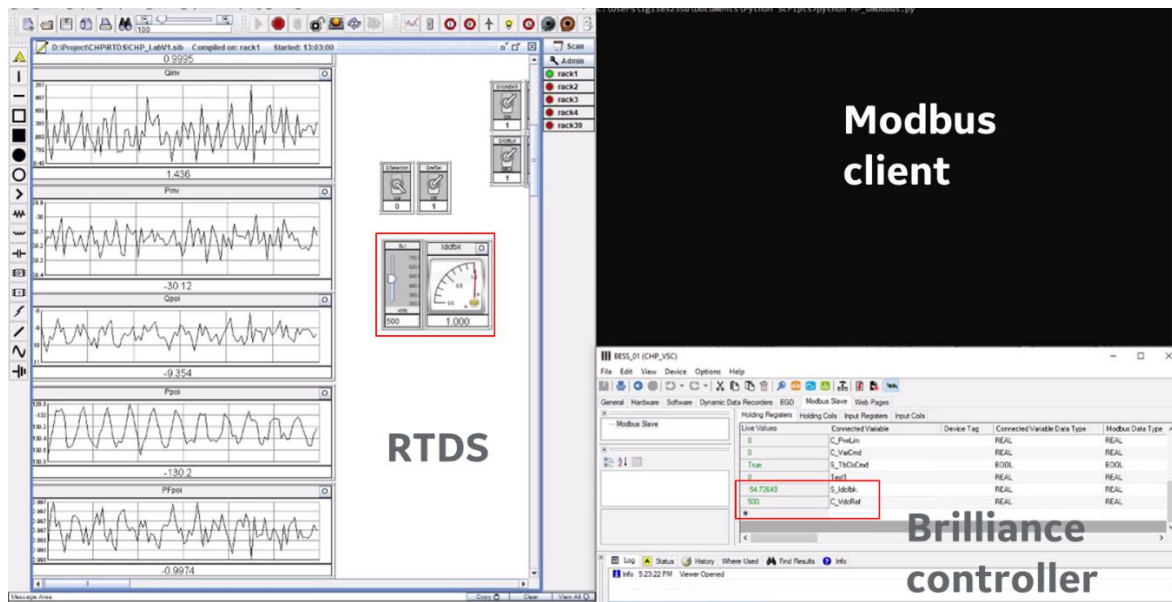


**Figure 95:** Test results of the communication between RTDS and the Brilliance controller.

Data exchange between RTDS (engine emulator) and the rectifier controller (engine side inverter; Brilliance #1) allows to regulate DC bus voltage. The Novacor rack passes the DC bus voltage command to the rectifier controller, collect as a feedback the DC current before sending it to the inverter controller. Timing performance of communication in this scenario is critical. Ideally, a single cycle of loop-back data exchange is expected to be completed within 10ms to fully capture the converter dynamics. But considering the Brilliance controller only provides limited communication options, communication delay is inevitable. Figure 96 shows the impact of the communication delay on fast dynamic transients such as voltage step change (for instance for grid reconnection) or signal tracking (for instance for frequency response).

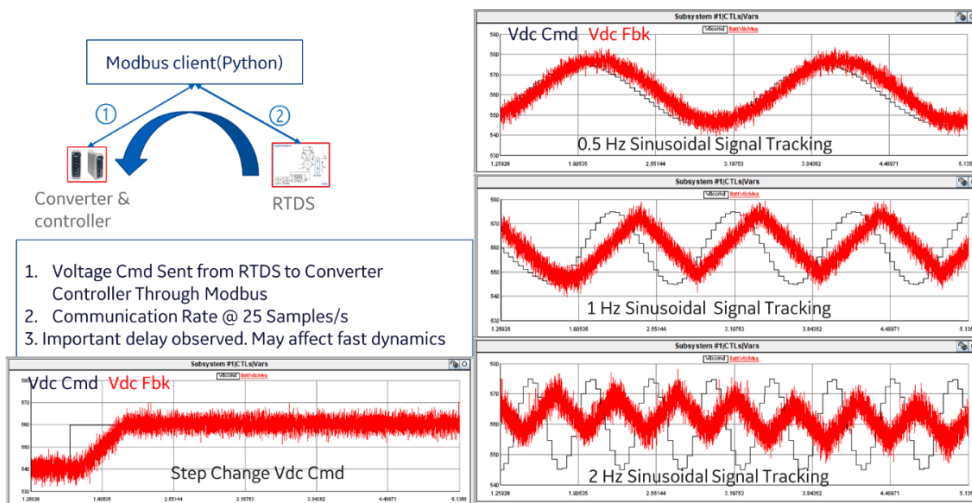


**Figure 96:** Evaluation of the impact of the communication delay between the Brilliance controller and RTDS.

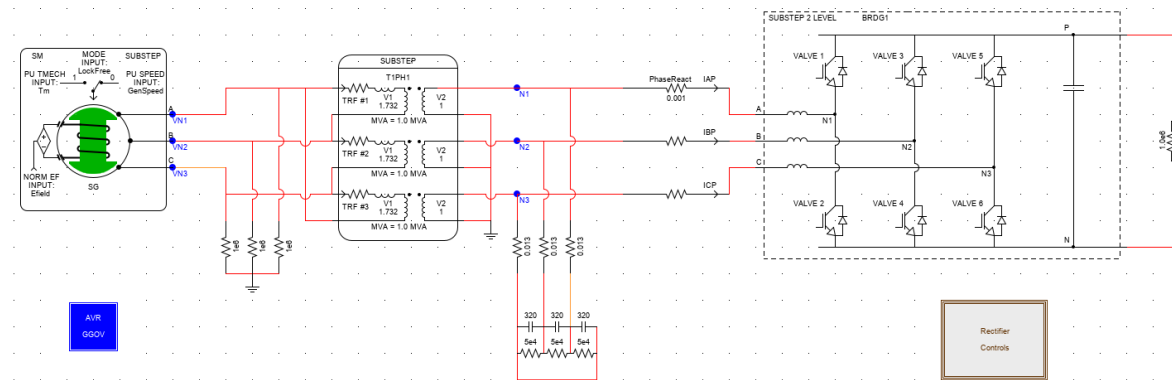
### 6.1.2 Validation of the functionality of the PHIL testbed

Figure 97 shows the fully functioning PHIL testbed as installed in the test lab. Inverter #1 is configured as a rectifier, here controlling the DC link voltage and inverter #2 is configured as the grid-ready inverter interfacing the CHP and rectifier to the grid.



**Figure 97:** Fully installed and configured PHIL testbed

Inverter#1 DC voltage reference is generated by the engine emulator which includes the CHP generator, AVR and rectifier models as shown in Figure 98. The generator was modeled based on the Jenbacher JMS 320 GS-N.LC<sup>68</sup> generator specifications which is a 1.32MVA generator with a rated active power of 1,065 kW.



**Figure 98:** Details of the engine emulator model as implemented in the RTDS Novacor rack

The configuration and setting of the inverters also consisted of identifying and installing the correct firmware and software version, integration of the controls (the RTDS Novacor, the C90+ microgrid controller) with the inverter controllers, establishing the communication between all IEDs involved and the workstation and troubleshooting the different errors messages until the inverters run properly. Figure 99 shows a screenshot of the rectifier control interface (inverter#2) confirming no error and readiness to operate. In this example ~52kW at power factor (pf) = 1 is generated by the “CHP” and injected to the

DC link (grid-side inverter input). The “generator” line voltage is 469Vrms, 60Hz. No reactive power is injected. The power injected to the inverter is ~48kW suggesting a ~3.7kW losses in the rectifier.

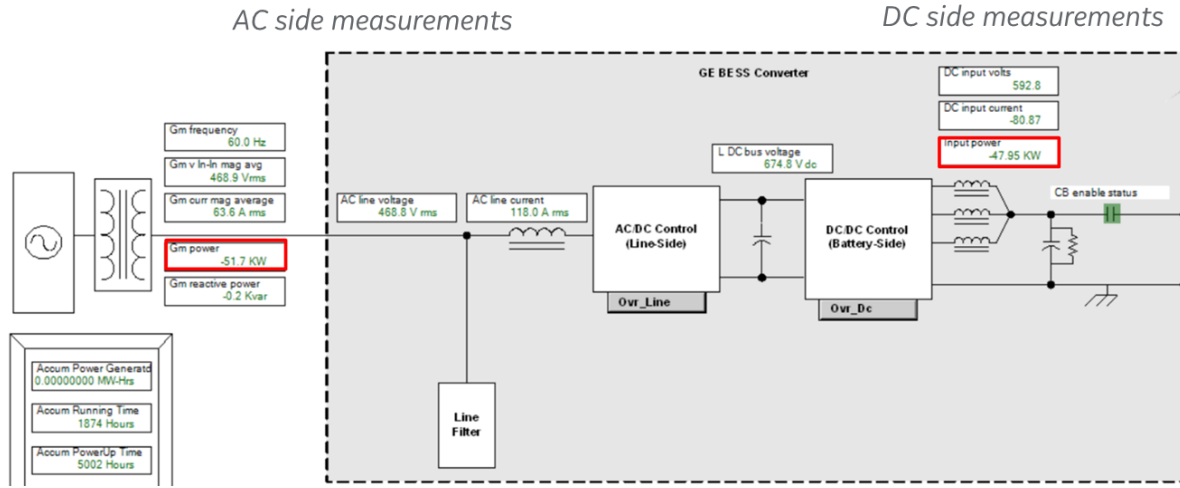


**Figure 99:** Confirmation of the inverters readiness to operate

Figure 100 shows the tests results of a power step change from 24kW to 48kW.

**Test case:** change power command from 24kW to 48kW in one step change

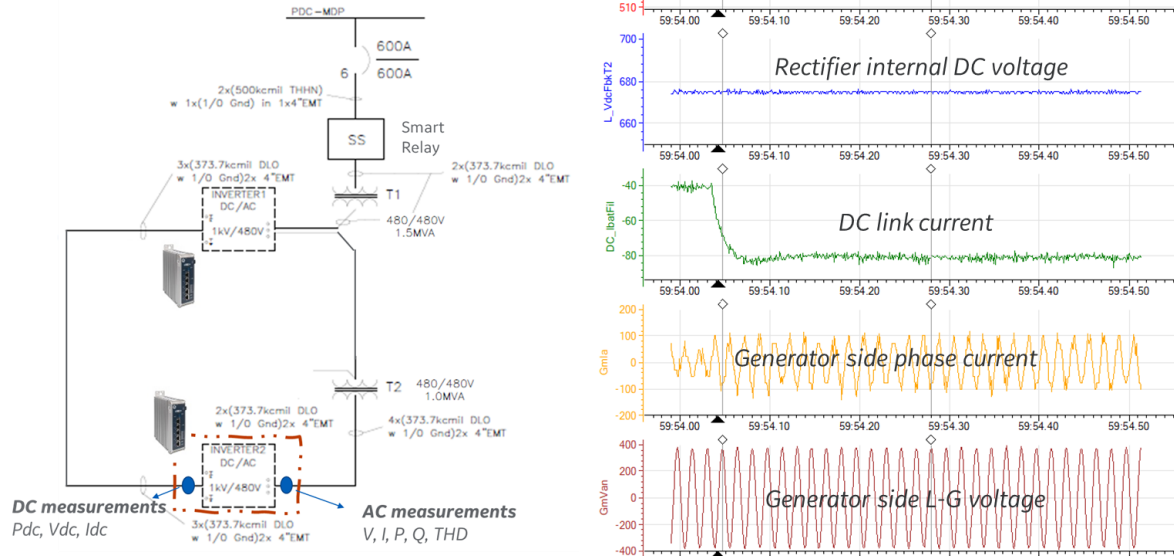


**Figure 100:** Steady-state operation following a power step change from 24kW to 48kW.

The functionality of the PHIL testbed is completed by the development and testing of the algorithms for power and heat dispatch, and for power factor control at the point of connection. The Jenbacher engine JMS 320 GS-N.LC<sup>68</sup> was used as reference for the heat and power relationship. Figure 101 shows the algorithms developed for the power-

following. In power following mode the CHP output can directly follow the electric loads if the power request is between 0.3pu and 1.0pu of the CHP rating. If the load is below 0.3pu the CHP is shut down due to a low fuel efficiency in that regime. If the load is above 1.0pu the excess will be supplied by the grid. However, in heat-following mode, because the heat output is a byproduct of the electric power, the equivalent power command needs to be extracted. Using the Jenbacher engine JMS 320 GS specifications the relationship between the electric power and the heat output can be described by equations (46) and (47). The electric power outputs  $P = f_1(H)$  if heat demand is between 30% and 75% of the maximum recoverable heat and  $P = f_2(H)$  if the heat demand is between 75% and 100% of the maximum recoverable heat.

$$f_1(H) = 0.293(0.9683H - 780.2) \quad (46)$$

$$f_2(H) = 0.293(1.023H - 979.0) \quad (47)$$

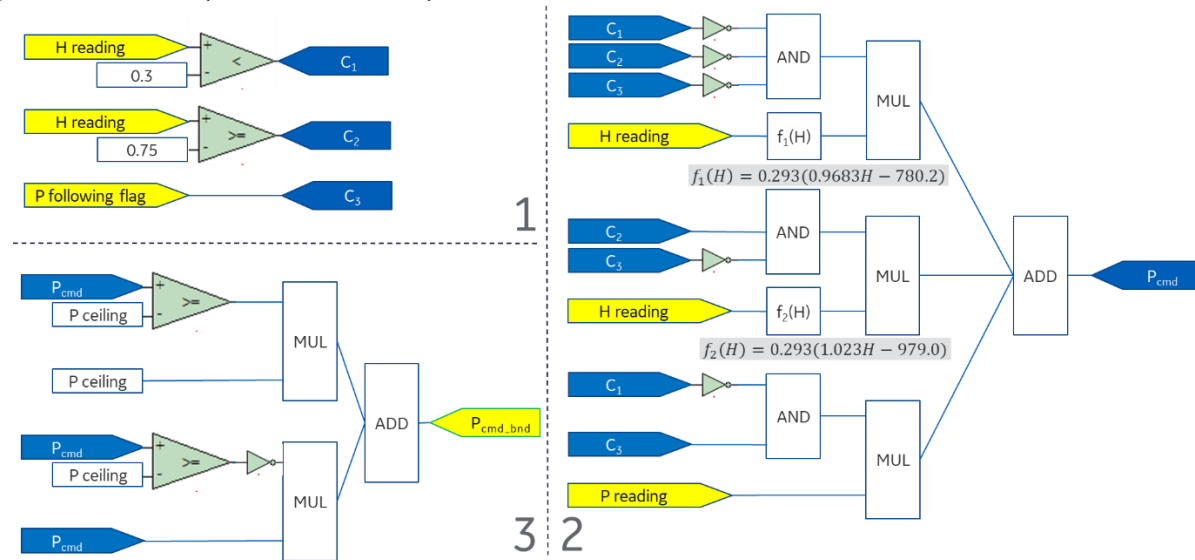


**Figure 101:** Algorithms implemented for the power and heat dispatch.

Figure 102 shows the algorithms developed for the power factor control. It suggests that if the pf control mode is enabled, the microgrid controller will generate the reactive power command necessary to meet the pf request. The reactive power command is calculated based on the inverter rating and the CHP power output. At 0kW, the grid-side inverter can output reactive power up to its power rating. Unlike in directly-coupled CHP, with the interface converter the reactive power capability is not limited by the CHP rating but by the inverter rating. Equations (48) and (49) show the implementation of the reactive power command calculation as function of the active power and power factor request at PCC.

$$f_{pf}(P) = \frac{\sqrt{1-PF^2}}{PF} \cdot P \quad (48)$$

$$f_q(P) = \sqrt{S^2 - P^2} \quad (49)$$

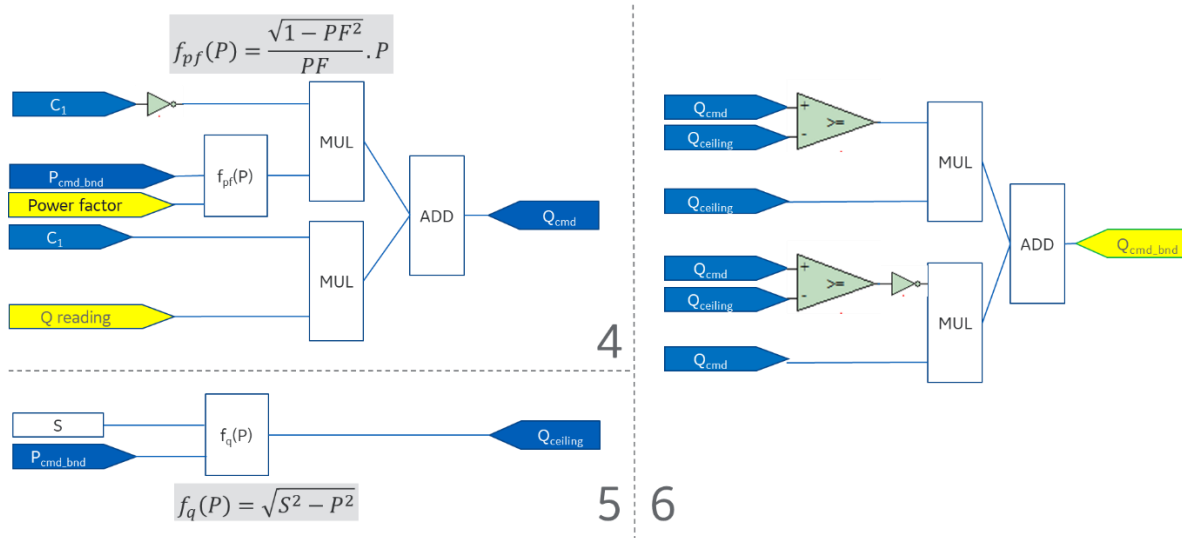


**Figure 102:** Algorithms implemented for the power factor control.

Figure 103 summarizes the test results obtained confirming the validity of the dispatch and power factor control algorithms. It shows dispatch strategy selection ( $P\_following=1$  corresponds to power following and  $P\_following=0$  corresponds to heat following), power factor settings (pf) and simulated  $P$  (power),  $Q$  (VAR),  $H$  (heat) load demands. In each scenario tested, the appropriate  $P$  and  $Q$  command issued by the microgrid controller ( $P_{cmd\_bnd}$  and  $Q_{cmd\_bnd}$ ) is captured. Results show that the dispatch algorithms perform as expected.

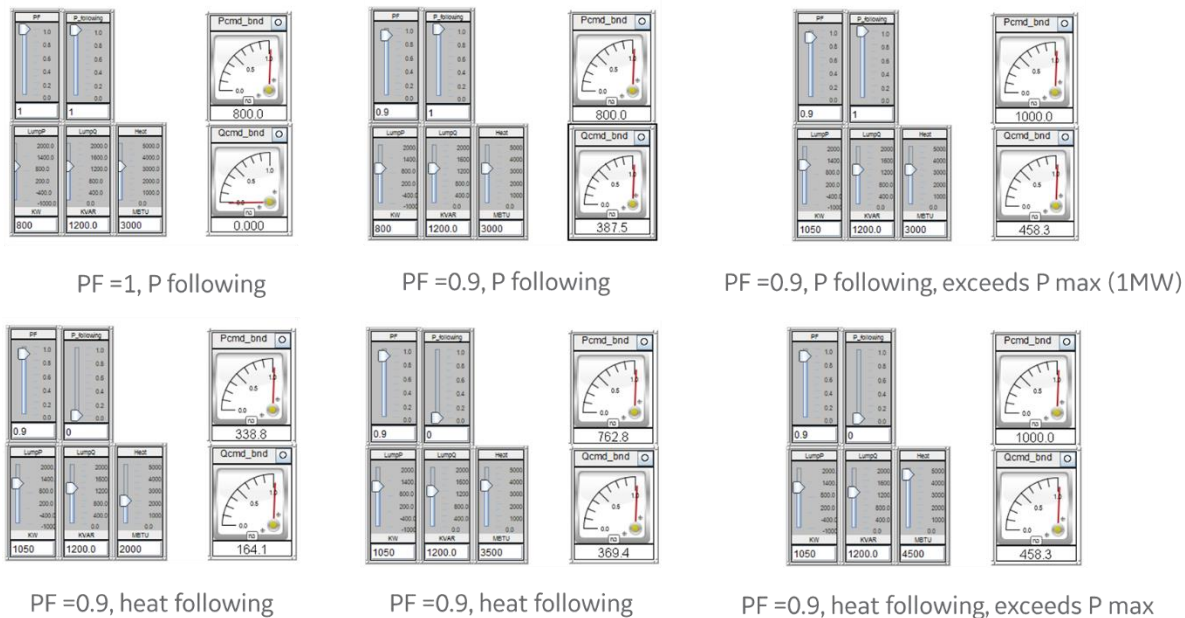


**Figure 103:** Tests results on the performance of the dispatch algorithms.

Table 42 details the different scenarios used to test the dispatch and power factor control algorithms. In these simulations the rated heat capacity is 4560MBTU/hr and the rated converter capacity is 1.1MVA and the CHP rating is 1MW.

Test Case	P follow	PF	Heat (MBTU/hr)	P (KW)	Q (KVar)	P <sub>cmd</sub> (KW)	Q <sub>cmd</sub> (KVar)
1	1	0.9	1370	600	-	600	290.6
2	1	0.9	1370	1010	-	1000	458.3
3	1	0.85	1370	600	-	600	371.8
4	1	-	1350 (<0.3)	600	300	0	300
5	1	-	1350 (<0.3)	600	1200	0	1100
6	0	0.9	2000 (>0.3, <0.75)	-	-	338.8	164.1
7	0	0.9	3500 (>0.75)	-	-	762.8	369.4
8	0	0.9	4500	-	-	1000	458.3
9	1	1	-	1000	-	1000	0
10	1	1	-	500	-	500	0

**Table 42:** Summary results of the dispatch and pf control algorithms testing

## 6.2 Power hardware test performance objectives

The performance objectives of the PHIL testing are summarized in Table 43. The testing focuses on validating the functional ability of the interface converter and integrated hardware (microgrid controller) control to meet minimum requirements of IEEE standard 1547-2018<sup>5</sup> and 2030.7-2017<sup>6</sup>.

Performance objectives	Metric	Data Requirements	Success Criteria
C1. Disconnection	disconnection times	measurements of V, I, P at the POC and breaker opening timeline	IEEE 1547 compatible
C2. Reconnection	POC breaker status	measurements of V, I, and P at the POC and breaker closing timeline	No trip after reconnection
C3. Power Quality	Voltage, frequency, harmonics and power factor values	measurements of V, f, THD, and power factor at the POC	IEEE 1547, IEEE 2030.7 and 2030.8 compatible
C4. Dispatch	generation outputs following heat and power commands	Loads meters P and H demand, measurement of P at POC and Heat from engine emulator	IEEE 2030.7 and 2030.8 compatible

**Table 43:** Performance objectives of converter-interfaced CHP testbed

The ride-through performance of the converter-interfaced CHP will be tested to validate that clearing times of the POC relay following abnormal voltage and frequency comply with the following tables, as listed in by IEEE 1547-2018 standard. In the PHIL testbed it is not possible to intentionally test response to grid disturbances (short-circuits, voltage or frequency variations, etc.) due to the limited capability of the testbed (for frequency and voltage change) and to the possible damaging consequences to the local grid and the test hardware. However, the fault protection and ride-through settings are implemented both in the inverters and in the microgrid controller to protect the testbed in the event of a disturbances generated outside of the testbed during testing.

#### *Seamless transition from grid-tied mode to islanding*

Due to the absence of an actual CHP unit, the PHIL testbed is not capable of islanding operations and as such is not fully operational as a microgrid. Therefore, the IEEE standard 2030.8 cannot be fully applied. However, the recommendations of IEEE standard 2030.7 and the steady-state guidelines of the IEEE standard 2030.8 can be applied.

#### *Rapid disconnection from the grid:*

Unlike the seamless transition from grid-tied mode to islanding, the rapid disconnection from the grid applies when abnormal conditions such as faults or under/over voltage and/or frequency events do persist beyond the ride-through clearing times. In the presence of such events, the protection functions integrated into the inverters will disconnect the test setup as required by the IEEE 1547-2018. Backup protection functions with same pickup levels and clearing times are implemented into the microgrid controller (tested in the HIL simulations) to force disconnection if the control of the inverters is delayed. Rapid disconnection command from the microgrid controller may be warranted under the following conditions: 1) a trip request from the system operator (signal from the workstation in this case); 2) when the voltage or frequency at the point of connection (testbed breaker) violates the requirements specified by IEEE 1547-2018; 3) other protection functions internal to the inverters (such as overload or other diagnostic functions) trigger the disconnection.

#### *Resynchronization and Reconnection:*

Resynchronization and reconnection is a transition from islanded or shutdown modes to grid connected mode. In the definition of the IEEE standard 1547-2018, resynchronization is the process of aligning the frequency, phase angle and voltage magnitudes of the DER at the POC (testbed breaker) or at the point of common coupling PCC (for microgrids) as closely as possible to those of the grid before reconnection to avoid or reduce any transients that may lead to disconnecting the DER following reconnection. To comply with IEEE 1547-2018 the differences in frequency, voltage and phase angle at both sides of the POC breaker should be within the limits shown in Table 39. However, in the case of the converter-interface CHP, the internal reconnection process of the grid-side inverter is deemed to be satisfactory to meet the IEEE 1547-2018 reconnection objectives. Indeed,

instead of synchronizing the AC output of the inverter, the reconnection process of Brilliance inverter includes: 1) closing the POC breaker and that of the inverter (located inside the inverter) while the gating command of the power modules (IGBT) is turned off. No power will be circulating (IGBT modules are blocked) therefore no voltage disturbance. 2) Once the AC voltage is sensed at the module side of the breaker, gating is initiated to enable DC bus charging and power circulation. Then the power output ramps up to meet the power command. Because this process does not involve transient other than for charging the interface converter DC bus, it is expected that objective of IEEE 1547-2018 will be met.

#### *Steady state power quality*

The converter-interfaced CHP testbed is required to meet a minimum performance for power dispatch, power factor control/voltage regulation, harmonics injection both at the grid and CHP sides. The microgrid controller will allow to dispatch the required amount of active and reactive power to meet target power, voltage and power factor at the POC. A snapshot of facilities electric loads measurements is shown in Figure 104 as example.

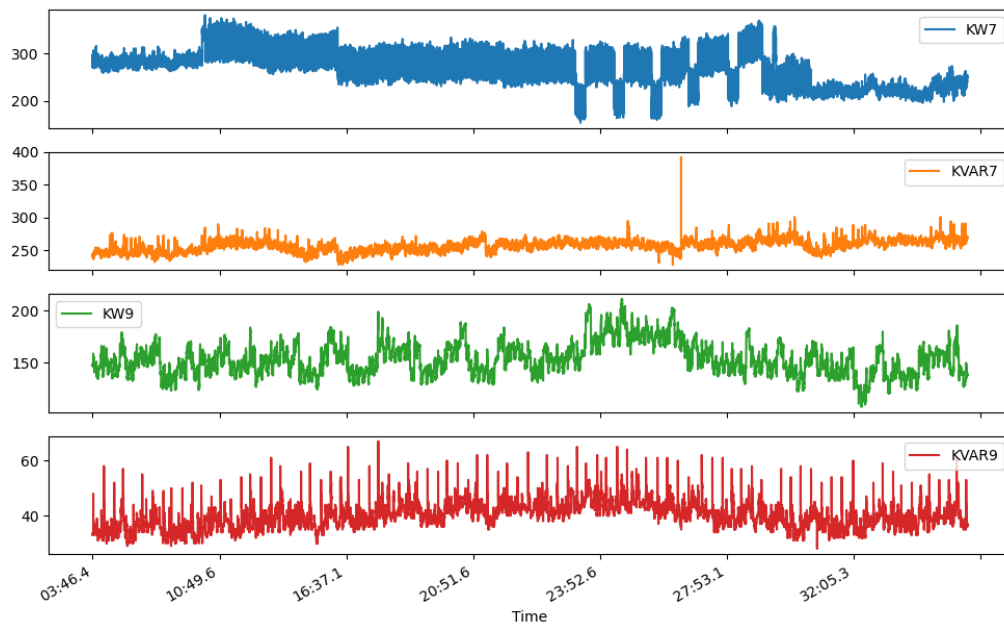


**Figure 104:** Snapshot of electric facilities loads measurement collected by the microgrid controller

The microgrid controller actions are described below.

- Power following: collect the electric load data and aggregate power and reactive power demands as well as the power factor target to send active power and reactive power commands to the interface converter. The testbed output should follow the load demand up to rating of the CHP engine and inverters. For load demand above the inverters rating, the testbed should output its maximum power.
- Heat following: collect the heat load data and convert the heat demand into power target using equations (46) and (47). Collect the power factor target to send active power and reactive power commands to the interface converter. The testbed

output should follow the heat demand up to the rating of the CHP engine. For heat demand above the engine rating, the testbed should output its maximum power. The microgrid controller should allow to switch between power following and heat following without tripping the testbed. Harmonics injection at the “generator” side inverter is carefully monitored as this intrinsically affects the sizing of the generator.

#### *Protection Coordination*

In the PHIL testbed, the microgrid controller acts as a backup supervisory protection, while the primary protection is performed by the main breaker relay (located at primary of isolation transformer T1 as shown in Figure 92). The relay is equipped with overcurrent (50), directional power (32) and undervoltage (27) protection functions. As mentioned previously no intentional fault will be created to test the protection system and the transient behavior under faults. In the event of a fault, the two inverters will be tripped by their local protection and the testbed will be isolated by the main breaker. Basic coordination settings are applied to trip the testbed with each inverter DC breaker if the fault is located within the DC bus (including the DC tie cable), then by the inverters local AC breakers if the fault is between the AC side and the DC side. If any of these two types of fault persist or the fault is located outside the inverters zone (from T1 and T2 secondary), the main breaker will trip first before any upstream breaker. The microgrid controller is not provided with the ability to issue a trip signal to either the inverters or main breakers.

### **6.3 Performance validation test results**

The summary of the PHIL validation tests is shown in Table 41.

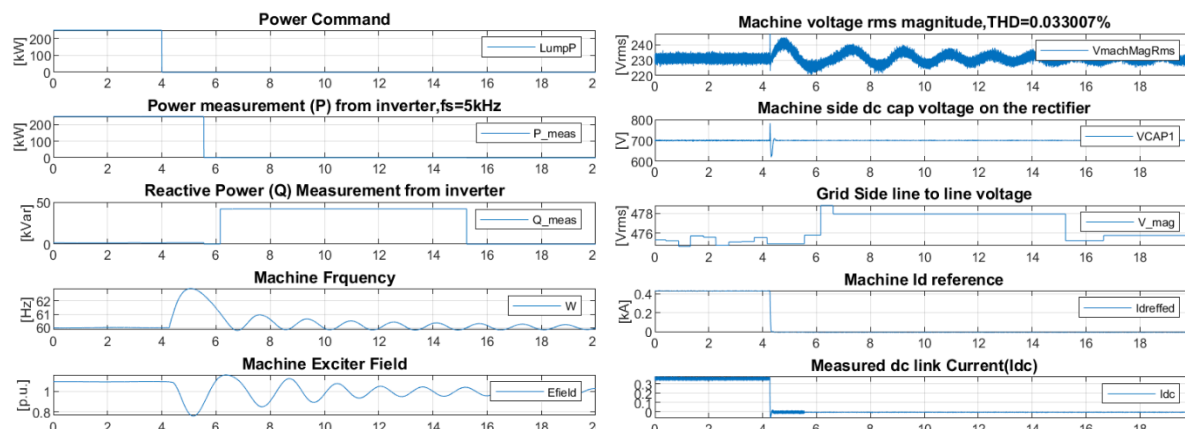
<b>Performance objectives</b>	<b>Metric</b>	<b>Data Requirements</b>	<b>Success Criteria</b>	<b>Results</b>
C1. Disconnection	disconnection times	measurements of V, I, P at the POC and breaker opening timeline	IEEE 1547 compatible	Passed
C2. Reconnection	POC breaker status	measurements of V, I, and P at the POC and breaker closing timeline	No trip after reconnection	Passed
C3. Power Quality	Voltage, frequency, harmonics and power factor values	measurements of V, f, THD, and power factor at the POC	IEEE 1547 and IEEE 2030.7 and 2030.8 compatible	Passed
C4. Dispatch	generation outputs following heat and power commands	Loads meters P and H demand, measurement of P at POC and Heat from engine emulator	IEEE 2030.7 and 2030.8 compatible	Passed

**Table 44:** Summary of the PHIL tests results

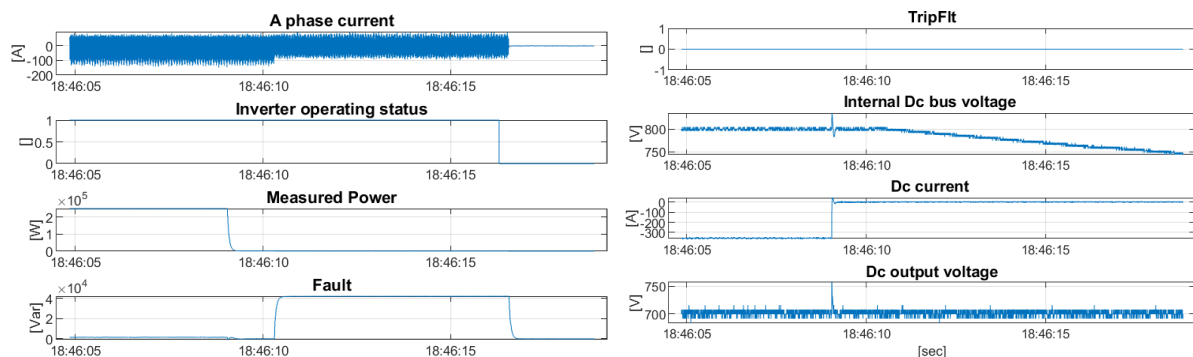
All the performance objectives planned to be validated with the PHIL have been met. Figure 105 to Figure 114 show the details of measurements for the different user cases. All the machine data i.e., generator including the active and reactive power, respectively *P machine* and *Q machine*; the frequency and voltage, respectively *Machine Frequency* and

*Machine Voltage*, were measured from the engine emulator shown in Figure 98. The harmonics level at the generator output THD and TDD was calculated based on the generator voltage and current in the engine emulator, *Machine voltage rms magnitude*, and *Machine current rms magnitude*, respectively. For all the tests the active power was limited to 250kW as the grid-side inverter was operating with one DC/DC module only. Two DC/DC modules were missing due to previous failures and needed replacement. However, the AC/DC modules as shown in Figure 99 were fully operational and therefore reactive power capability up to 700kVAr was available. The rectifier (inverter#2) was fully operational at 1,250kVAr.

Figure 105 summarizes a planned disconnection scenario where the power was ramped down from 250kW ( $pf = 1$ ) to 0kW before opening the POC breaker (grid-side inverter). As shown in the results no overstress was observed on the of engine or the converter. During the transition the generator voltage oscillates between 1.05pu and 0.95pu. Figure 106 gives a closer look at the transients captured from the Brilliance inverter interface. It shows a voltage surge of  $\sim 1.07$ pu at DC link. No trip was reported.

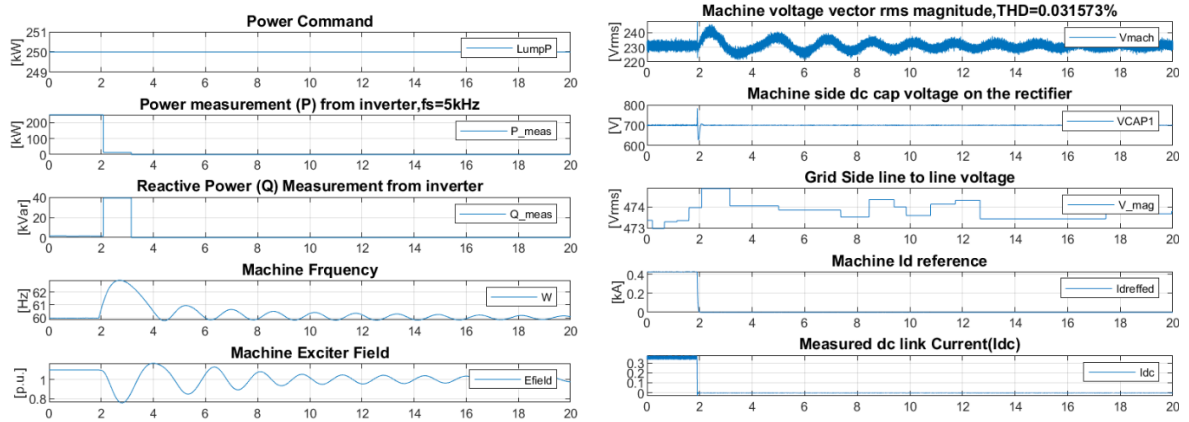


**Figure 105:** Planned disconnection at 250kW.

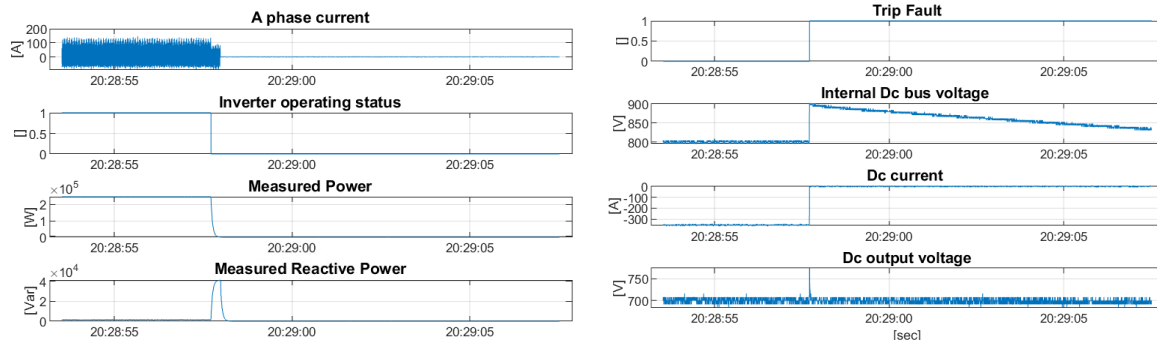


**Figure 106:** Transients captured at the Brilliance inverter control interface during a 250kW planned disconnection

Figure 107 and Figure 108 summarize a scenario of emergency disconnection where the system was instantaneously shut down while 250kW ( $\text{pf} = 1$ ) was flowing. The obtained results are very similar to the previous case even if the voltage surge at the DC link is slightly higher at  $\sim 1.12\text{pu}$ . It is however possible that an emergency shut down at higher power level would generate more transients. As the trigger of the emergency shutdown a trip fault is reported by the inverter control interface.

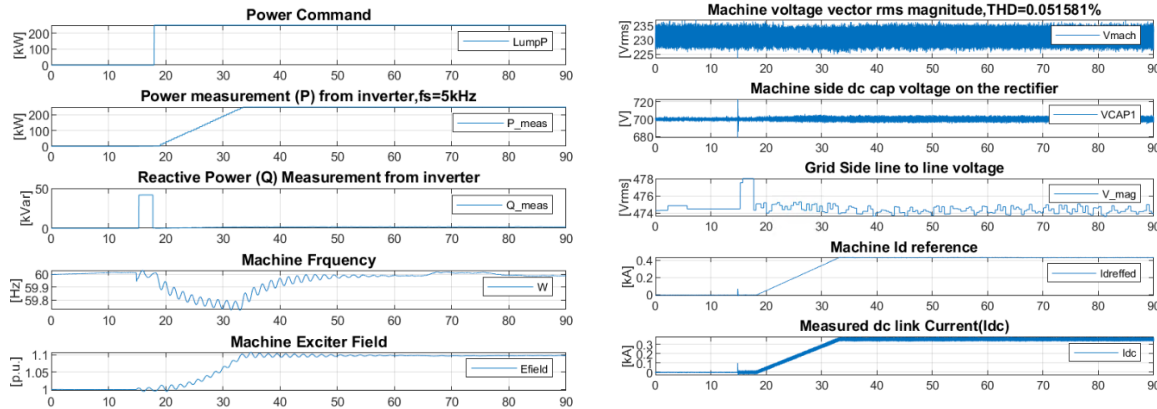


**Figure 107:** Emergency disconnection at 250kW.



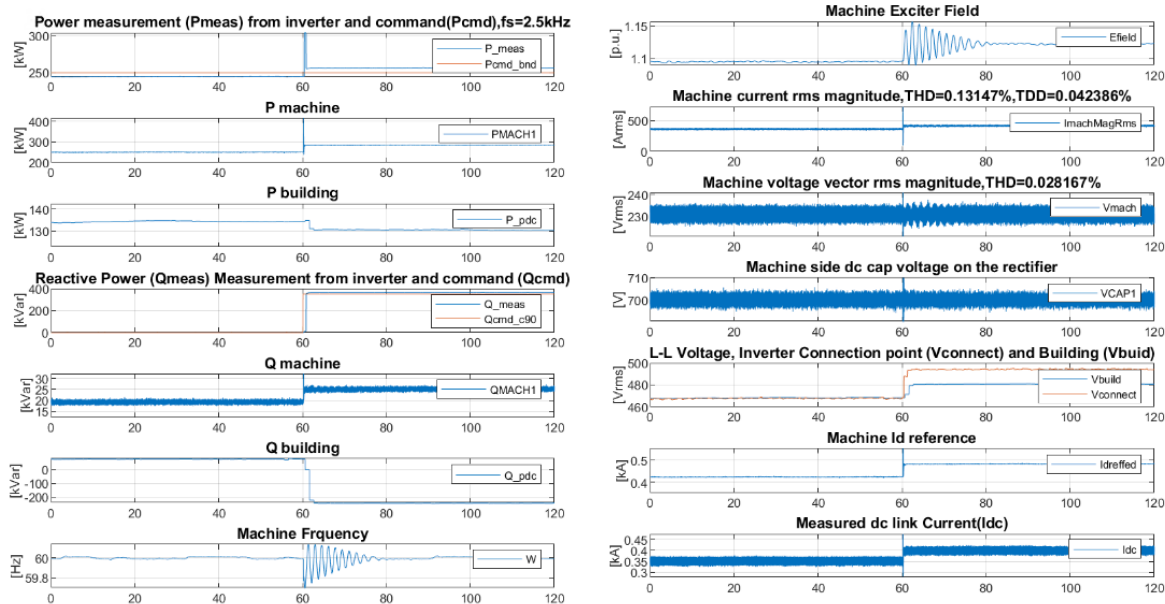
**Figure 108:** Transients captured at the converter during 250kW emergency disconnection.

Figure 109 summarizes a case of a reconnection to the grid followed by a power ramping. As shown the engine can ramp up power at rate of 1MW/min without limitation from the converter. As anticipated the generator frequency dips during power increase but recovers quickly to 60Hz once steady-state is reached. No overstress or trip was reported neither at the DC link nor at the generator side. Additionally, harmonics level calculated are largely below the limit prescribed by IEEE std 519.



**Figure 109:** Reconnection and power ramp up at 1000kW/min.

Figure 110 summarizes a case of voltage regulation at PCC (the building main breaker). The interface converter is requested to regulate the building voltage to 480V by injecting or absorbing reactive power while the system is running at 250kW. Results show that the voltage at the PCC can be maintained at 480V (L-L voltage  $V_{connect}$  and  $V_{build}$ ) with the converter injecting  $\sim 400$ kVAR (reactive power  $Q_{meas}$  and  $Q_{cmd}$ ) at 250kW while the generator still operates at  $\sim pf=1$  ( $Q$  machine  $\sim 25$ kVAR). This demonstrates that the generator operation is fully decoupled from reactive power support.



**Figure 110:** Voltage regulation at point of interconnection (building main breaker).

Figure 111 shows the case of power following. The CHP system is set to follow the electric load request aggregate from the building load meters (LumpP) while the converter is set to control the power factor at 1. As shown in the results, the inverter power output ( $P_{meas}$ ) is a mirror of the power command issued by the microgrid controller ( $P_{cmd\_bnd}$ ) which consistently follows the aggregated load meters readings (LumpP). During the time

window, the power limit set at 250kW was not met. Additionally, the reactive power command issued by the microgrid controller ( $Q_{cmd\_c90}$ ) and generated by the inverter is  $\sim 0$ kVAR confirming that the pf is being controlled to 1. The generator voltage and DC link voltage remain regulated at 470Vrms L-L and 700Vdc respectively while the generator current follows the load dynamics.

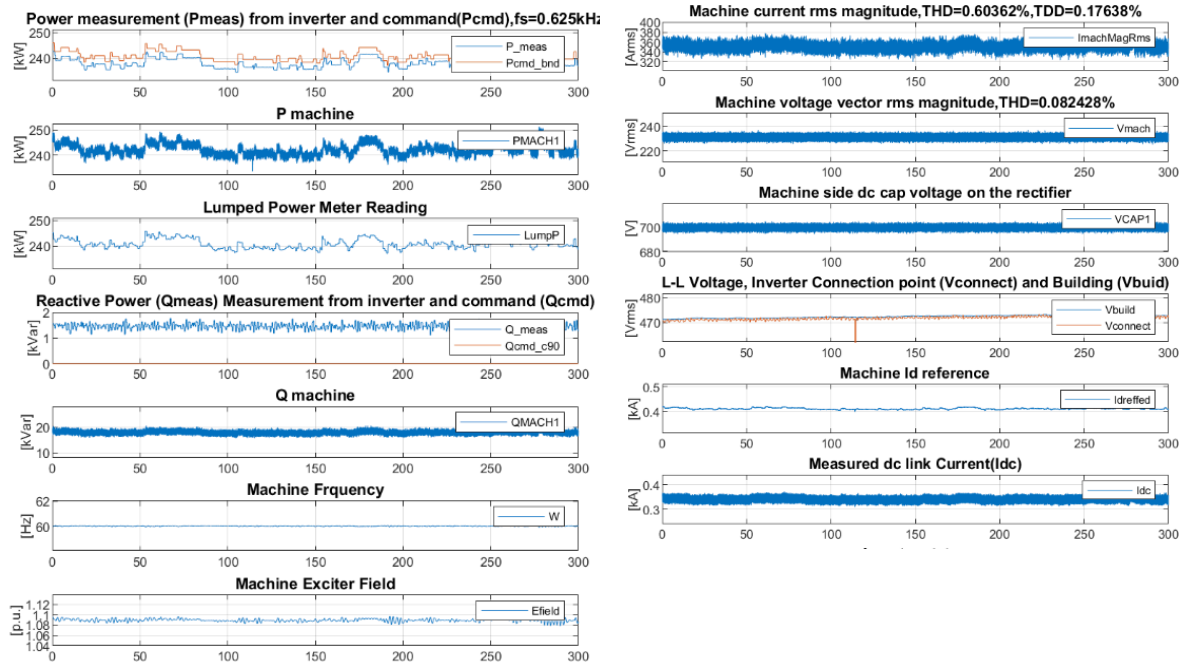
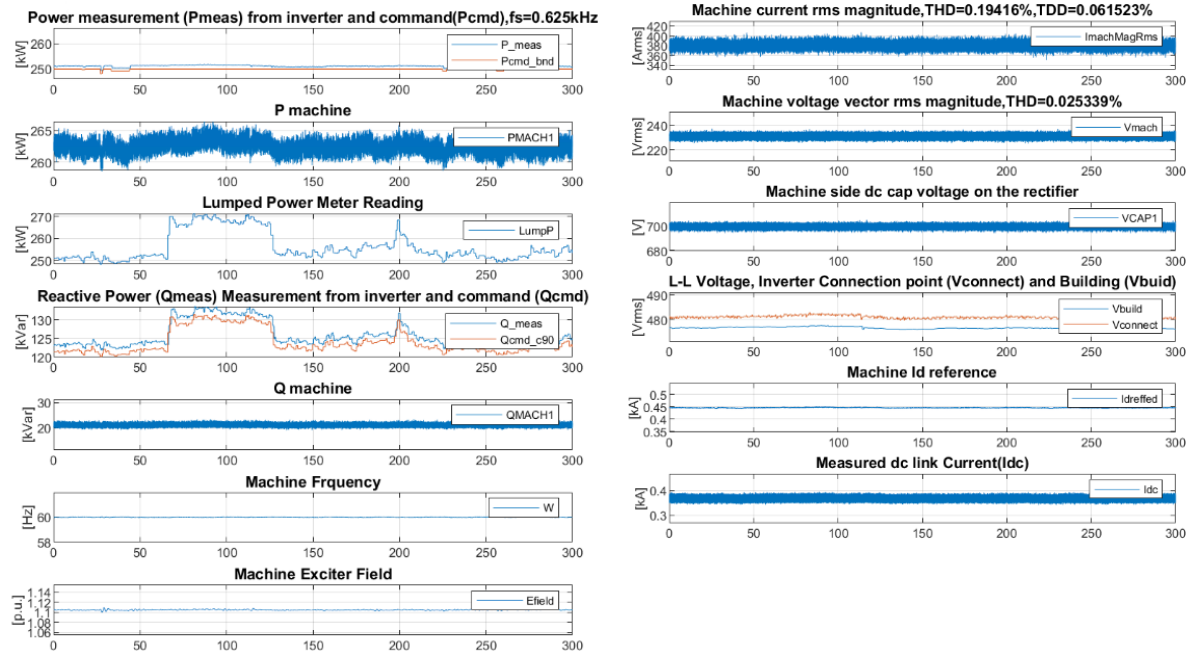


**Figure 111:** Power following dispatch while a  $pf = 1$  is maintained at POC (inverter).

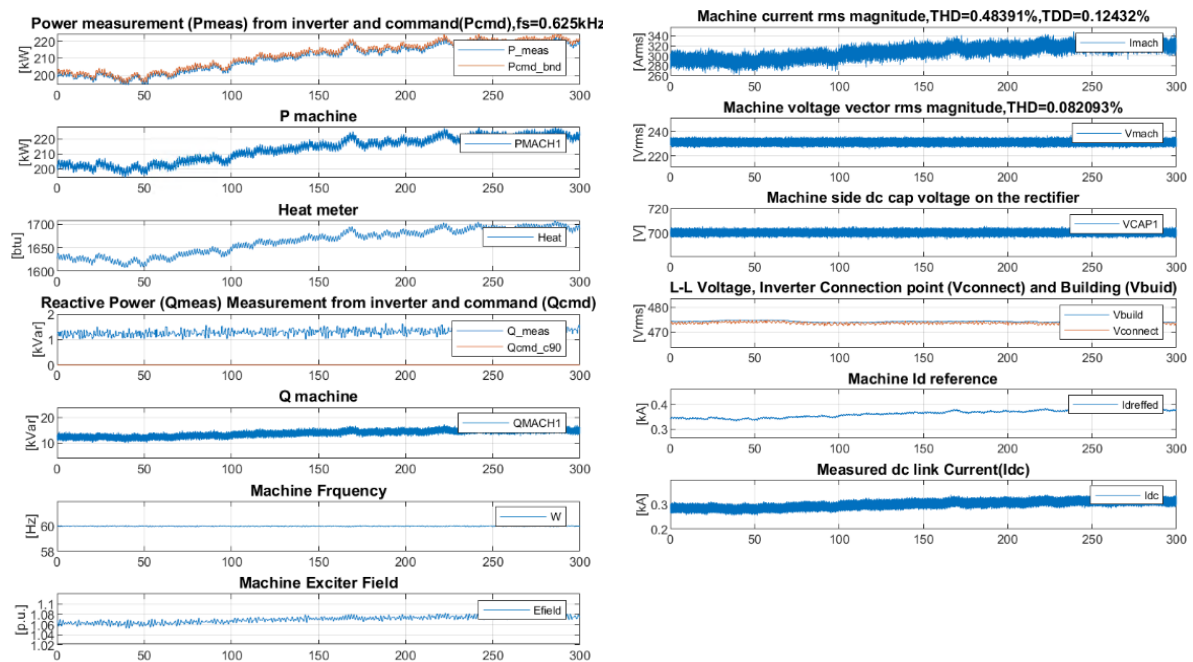
Figure 112 shows a scenario similar to the previous case except the power factor is controlled at 0.9 while following the electric load. This test shows that when the load demand exceeds the CHP capability (250kW in this case), the microgrid controller sends a command ( $P_{cmd\_bnd}$ ) equal to the maximum power which is generated by the grid-side inverter ( $P_{meas}$ ) and the generator ( $P$  machine). However, due to the relationship between the active and reactive power as expressed in equation (48) and (49), the reactive power output follows the load dynamics. This scenario also validates that the pf can be controlled at any value while following the active power. Indeed, despite the generator outputting  $\sim 0$ kVAR ( $Q$  machine), the grid-side inverter now generates reactive power ( $Q_{meas}$ ) following the microgrid controller command. This test validates that the generator successfully follows the electric load while the converter decouples  $P$  and  $Q$ .

Figure 113 shows the case of heat following. The CHP system is set to follow the heat load request aggregate from the building load meters (Heat meter) while the converter is set to control the power factor at 1. As shown in the results, the inverter power output ( $P_{meas}$ ) is a mirror of the power command issued by the microgrid controller ( $P_{cmd\_bnd}$ ) which consistently follows the aggregated heat load meters readings (Heat meter). During the time window, the power limit set at 250kW was not met. Additionally, the reactive power

command issued by the microgrid controller (Qcmd\_c90) and generated by the inverter is  $\sim 0$ kVAR confirming that the pf is being controlled to 1. The generator voltage and DC link voltage remain regulated at 475Vrms L-L and 700Vdc respectively while the generator and DC link current follow the load dynamics.



**Figure 112:** Power following dispatch while a pf = 0.9 is maintained at POC (inverter).



**Figure 113:** Heat following dispatch while a pf = 1 is maintained at POC (inverter).

Figure 114 shows a scenario similar to the previous case except the dispatch mode is being switched between heat following and power following while in both cases the factor at POC is maintained at 1.0. Results show that the engine (P machine) can follow the command issued by the microgrid controller (Pcmd\_bnd) alternately between the two dispatch modes without major transient on the generator or the interface converter while the grid-side inverter can consistently maintain the power factor setting ( $Q_{meas} = 0$ ). Indeed, during the heat following mode (from 0s to 150s), the power generated by the CHP (P machine) through the converter (Pmeas) closely follows the heat meter dynamics. At 150s, when the dispatch mode is switched to power following, now P machine and Pmeas follows the aggregated power loads meters (LumpP). When the power demand exceeded 250kW, the microgrid controller command (Pcmd\_bnd) limited the machine and converter outputs to 250kW. During the transition from heat following to power following, the generator speed (machine frequency) dropped momentarily because of the increase in the machine power request. However, the frequency recovered rapidly within 20s. No other transient was noted on the machine or the converter. This test successfully validates the flexibility of the converter-interfaced CHP for power dispatch and power factor control.

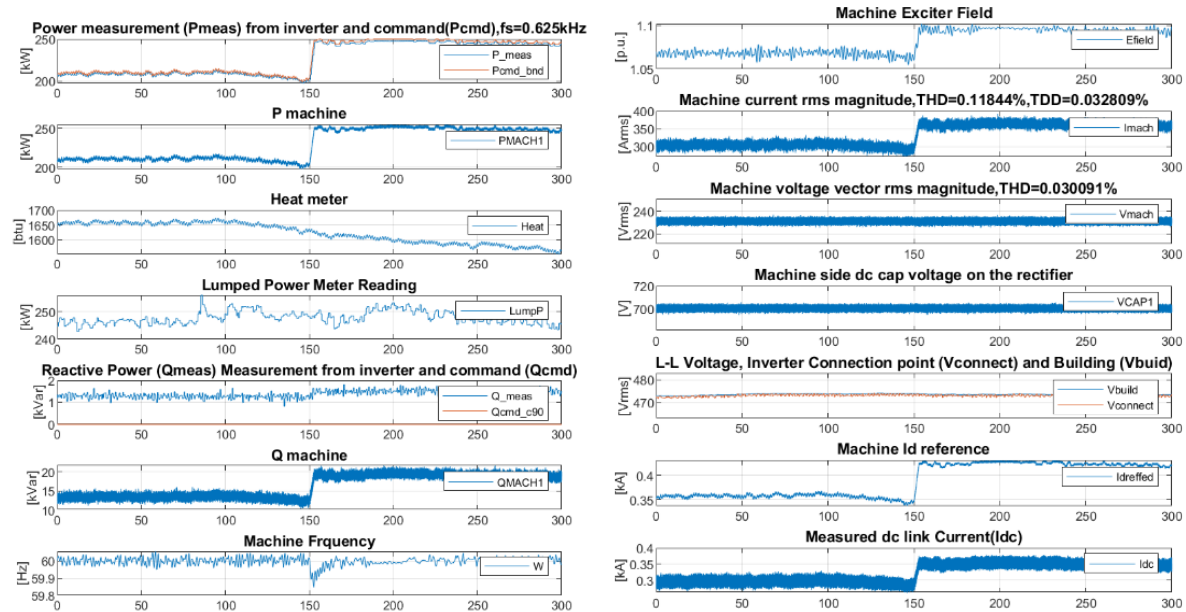


**Figure 114:** Varying command between heat and electric load following.

## 7. CONCLUSION

The overall objective of this project was to develop and validate a cost-effective solution to streamline the interconnection process of small-to medium sized CHP plants into utility distribution grids. An interface converter consisting of two back-to-back voltage source converters (VSC) was proposed. This solution holds indeed many benefits enabled by the presence of a grid-ready inverter which naturally complies with DER interconnection standards such as UL 1741, IEEE 1547, and IEEE 2030.7 and most utilities grid codes requirements. Additionally, the use of a VSC rectifier which helps to limit the harmonics level and reactive power requirement at the CHP side allows to reduce the generator size and cost which provides savings that can be applied to offset the cost of the converter.

Five user cases were selected to evaluate the economic feasibility of converter-interfaced CHP. Each represents a typical CHP application in the five leading states for CHP potential according to DOE. The return on investment (ROI) of each scenario was analyzed and compared with the equivalent conventional directly-coupled CHP configuration. The sensitivity of the ROI against critical parameters such as interconnection delay, converter to engine size ratio, generator and converter costs, energy and voltage support price were also analyzed.

Results showed that for most of the user cases analyzed, i.e., 4 out of 5, the annualized ROI of converter-interfaced CHP outperforms that of directly-coupled by 0.5 to 2 percentage points. By simplifying the interconnection process, the interface converter allows the CHP to be in production faster than the directly-coupled (>6 months). The savings in production loss, interconnection and generator costs traded with the converter cost ultimately make the converter-interface CHP economically feasible and in most of cases more profitable than the directly-coupled CHP. Looking into the specific results of the selected five user cases, the interface converter solution revealed to be largely more favorable than directly-coupled in MISO and CAISO and this regardless of the application. For ERCOT and NYISO, a converter-interfaced CHP will be typically favorable while for PJM it will be rarely favorable, suggesting for this last territory a case by case analysis before decision. In terms of application, except for office buildings and college campuses, a converter-interfaced CHP is likely to be more profitable than a directly-coupled installation. Results also revealed that the profitability of converter-interfaced CHP, despite being in general sensitive to energy price, interconnection delays and sizing of the converter, is extremely robust for the other parameters variation. The profitability of converter-interfaced CHP over directly-coupled CHP becomes more robust and insensitive to most parameters variations if interconnection delays between the two configurations is longer than 6 months, which can be expected. As an example, if the interface converter solution can guarantee a reduction of the interconnection delay by at least 12 months, all the +23,000 sites of the U.S Technical Potential will be more economically viable with a converter-interfaced installation, this regardless of the system efficiency, volatility of the energy price converter or generator costs within the ranges analyzed. This is a major result confirming that one of the main

benefits provided by the interface converter is to streamline the grid interconnection of small to medium-sized CHP and significantly reduces the delays to operation. The evaluation of the benefits of the interface converter also showed that it enables higher ROI when combined with other DER such as battery energy systems (BESS) or solar photovoltaic (PV). Indeed, by enabling DC-coupling, the grid-ready inverter included in the interface converter allows to avoid the installation of another inverter for the integration of those DER which reduces the overall system balance of plant.

On the technical performance, it has been verified that the presence of the interface converter allows to reduce the CHP short-circuit contribution by 70% to 80%. This leads to a significant reduction of the mechanical and thermal stress levels exposed to the generator which helps to extending its service life. Additionally, this lower short-circuit contribution also allows to increase the hosting capacity of the grid which ultimately enables higher penetrations of small to medium-sized of CHP. Another key benefit of the interface converter validated with hardware-in-the-loop simulations and testing is its superior capability for reactive power support. Indeed, a power hardware testbed using two +700kW inverters configured in back-to-back VSC, a microgrid controller and actual facilities loads allowed to demonstrate that the presence of the interface converter can help maintain at the point of common coupling (utility interface) a power factor near ~1 or regulate the voltage to ~1.0pu in almost all grid or load conditions. This benefit can be highly valuable if in the future, due higher penetration of renewable distributed energy resources (DER), utilities start billing demand charge based on kVA instead of kW as currently. Indeed, reactive power is not currently highly valued by utilities as compared to active power. Upon increase of voltage support price, the converter-interfaced solution is expected to be even more competitive than the directly-coupled. Another aspect that is not also well monetized is the increased reliability and resiliency of the plant in the presence of the converter. Because this configuration offers a more stable operation in islanding it's expected that more loads will be able to stay in operation in the event of grid loss. The power hardware tests also validated that converter-interfaced CHP can dispatch heat and power commands and seamlessly switch between the two modes while consistently controlling the power factor or voltage at the point of interconnection. Indeed, it was shown that grid-connected converter-interfaced CHP can follow either the power or heat demand while maintaining a unity power factor at converter output.

This research proved that the adoption of an interface converter for the interconnection of small to medium-sized CHP is a viable solution based on both the economic and technical performances. It also allows to greatly improve the plant power quality, increase the penetration of CHP into the distribution grid, extend their grid support capability, and facilitate the integration of renewables DER by streamlining the combination of CHP, solar PV and BESS in the same plant. This ultimately provides an opportunity for commercial and small industrial facilities in the U.S to accelerate their energy transition thanks to the high

energy efficiency of CHP systems and its reliable, flexible, and resilient microgrid operation when interconnected with an interface converter.

## **8. CERTIFICATE OF COMPLIANCE**

The Principal Investigator certifies that the information provided in the Final Technical Report is accurate and complete as of the date shown